BACTERIAL PROCESSING OF FLUORESCENT ORGANIC MATTER IN FRESHWATER

Bethany Gemma Fox MSci

A thesis submitted in partial fulfilment of the requirements of the University of the West of England, Bristol for the degree of Doctor of Philosophy.

Department of Applied Sciences, University of the West of England, Bristol

March 2018

Author's declaration

Abstract

Organic matter (OM) is ubiquitous to all aquatic environments and plays an essential role in global biogeochemical cycles and transportation of organic carbon throughout the hydrological continuum. Excitation-emission matrix (EEM) fluorescence spectroscopy has been used to characterise naturally occurring aquatic fluorescent OM (AFOM), classifying this AFOM as either humic-like, derived from terrestrial sources, or protein-like, of microbial origin. The research here explores *in situ* bacterial-OM interactions and AFOM evolution over time by employing fluorescence techniques, both within a freshwater body and by developing laboratory model systems.

Protein-like AFOM, with a particular focus on Peak T, has been linked to bacterial activity, with previous research suggesting Peak T as a bacterial enumeration proxy. To explore this further and understand the underpinning interactions, the work here employs model systems which use microbiological methods alongside fluorescence measurements, monitored over a variety of temporal scales. By culturing a range of bacterial species and communities, this study provides extensive evidence for the bacterial production of Peak T, confirming the suggestions within the literature. The universal presence of Peak T within the bacterial cultures studied here permits the conclusion that Peak T fluorescence cannot be used for bacterial enumeration but can provide information regarding microbial community presence and activity. The model systems utilised have also exposed the ability of bacteria to engineer a variety both protein- and humic-like AFOM *in situ*. This demonstrates the fast-acting dynamics of bacterial-AFOM production, challenging current understanding.

In addition to this, the application of *in situ* Peak T fluorescence sensing for monitoring microbial activity in freshwater systems is explored. This was undertaken by monitoring a water body, using a suite of *in situ* sensors to monitor a range of physicochemical parameters, alongside a discrete sampling monitoring program. This work, together with recent developments in the literature and the understanding gained from the laboratory model systems, has informed the development of a new generation multichannel fluorimeter.

Acknowledgements

I must thank everyone for their support, encouragement and patience over the past four years, without you this would not have been possible. I must say a special thanks to my supervisor, Prof. Darren Reynolds, for his guidance throughout the PhD and for creating a working environment that has allowed me to thrive and become an independent researcher. Special mention must also be given to Dr. John Attridge, Dr. Cathy Rushworth and the rest of my colleagues at Chelsea Technologies Group for their support and friendship during the PhD and placements. I would also like to extend my thanks to the rest of my supervisory team, Prof. Alex Anesio and Dr. Tim Cox for their support and direction throughout.

I would like to acknowledge NERC as the funders of this studentship, alongside the contribution from Chelsea Technologies Group. I am also forever grateful for to the technical and academic staff at the University of the West of England for their advice.

I would like to thank my colleagues, and friends, at UWE who have always been there with a friendly ear and invaluable advice, and often a beverage. As for my fellow PhD students, thank you for everything and for making this experience truly remarkable. I finish this thesis with an amazing group of friends, I could not have hoped for more.

As for my friends outside of UWE, thanks for still being my friends and for dealing with me through everything. Thanks for answering the numerous phone calls, making me laugh and just being there, always. Your constant hilarity and unwavering belief in me has got me through; I owe you one, maybe even two.

Last, but by no means least, I am eternally thankful for having such a wonderful family as my support network. My mum and dad have always believed in me and pushed me to be better. Without their never-ending love and encouragement I would not be where I am, fulfilling my dad's prophecy of me becoming an '-ologist' of some sort or, as my sister would say, "A Ross". I dedicate this thesis to you, the Fox family.

Contents Table

List of Figures

List of Tables

Abbreviations

Abbreviation	Definition
A.U.	Arbitrary Units
AFOM	Aquatic Fluorescent Organic Matter
ATCC	American Type Culture Collection, USA
BOD	Biochemical oxygen demand
BOD_5	5-day biochemical oxygen demand (BOD) test
BTEX	Benzene, toluene, ethylbenzene, xylene
CCD	Charged-coupled device
CDOM	Coloured dissolved organic matter
cfu	Colony forming units
CTG	Chelsea Technologies Group Ltd., UK
CV	Coefficient of variance
DBP	Disinfection by-product
DIC	Dissolved inorganic carbon
DO	Dissolved oxygen
DOC	Dissolved organic carbon
DOM	Dissolved organic matter
EC	Electrical conductivity
EEM	Excitation-emission matrix
FDOM	Fluorescent dissolved organic matter
FNU	Formazin nephelometric unit
FOM	Fluorescent organic matter
HDPE	High-density polyethylene
HPLC	High-performance liquid chromatography

IFE	Inner filter effect
LED	Light emitting diode
MPPC	Multi-pixel photon counter
NCIMB	National Collection of Industrial and Marine Bacteria, UK
NOM	Natural organic matter
NTU	Nephelometric turbidity unit
OD	Optical density
OM	Organic matter
PAH	Polycyclic aromatic hydrocarbons
PARAFAC analysis	Parallel factor analysis
PFA	Paraformaldehyde
PMT	Photomultiplier tube
POC	Particulate organic carbon
POM	Particulate organic matter
ppb	Parts per billion
ppm	Parts per million
ppt	Parts per trillion
QSU	Quinine sulphate units
RTU	Radio telemetry units
SiPM	Silicon photomultiplier
UV	Ultra-violet

This PhD was funded by NERC, in collaboration with Chelsea Technologies Group Ltd. (CTG), as a CASE Studentship award (Grant NE/K007572/1). CASE awards facilitate beneficial collaboration between academia and non-academic organisations, providing the doctoral student experience within both cutting-edge academia and the application of the research via business experience.

This NERC CASE studentship provided access to industry training through 3-month secondments working at CTG on the validation of a novel fluorimeter; this work is detailed in Chapter 6 of this thesis. The Technical Director of CTG was a member of the supervisory team, with frequent meetings held to discuss the research undertaken and the influence of this for the continuing development and testing of the novel sensor throughout the duration of studentship. The rest of the supervisory team, Professor Darren Reynolds (UWE Bristol, UK), Professor Alexandre Anesio (University of Bristol, UK) and Dr. Timothy Cox (Institute of Bio-Sensing Technologies, Bristol, UK), provided academic and pastoral support throughout the studentship.

Chapter 1 Introduction and literature review

1.1 Introduction

Freshwater accounts for only three percent of all water on planet Earth, with the majority of that inaccessible (Firth, 1999), and yet water is essential for all life on Earth (Postel, 2015). It has been internationally acknowledged that monitoring water quality is vital for human health and sustainable development, as well as aquatic ecosystem integrity (Postel, 2015; Firth, 1999). There is an ever increasing pressure on our limited available freshwater sources from population growth, climate change and anthropogenic activities, including rapid industrialisation, urbanisation and agricultural expansion (Khamis, Bradley and Hannah, 2017; Patil, Sawant and Deshmukh, 2012). Due to the increase in demand for, and therefore strain upon, freshwater resources, the ability to manage water sources is essential. The key to good water resource management stems from the ability to successfully monitor water quality (Postel, 2015). At present, most of the typical parameters are physicochemical, relying on discrete sampling and lengthy, and costly, laboratory testing (Peleato, Legge and Andrews, 2017; Blaen *et al.*, 2016). However, whilst these parameters provide information regarding the chemical properties of a water body, they do not provide adequate information for determining microbial dynamics and ecosystem interactions (Patil, Sawant and Deshmukh, 2012; Matilainen *et al.*, 2011). There is a need for novel monitoring parameters and technologies to enhance our understanding of water quality dynamics and processes that occur within natural water systems. This has led to extensive research into aquatic biochemistry, ecology and the composition of natural waters (Khamis, Bradley and

Hannah, 2017; Ruhala and Zarnetske, 2017; Carstea *et al.*, 2016; Coble *et al.*, 2014; Hudson, Baker and Reynolds, 2007).

Within this work there has been an emphasis on research into organic matter (OM) in aquatic systems. OM is ubiquitous in natural waters and its characteristics are influenced by the surrounding environment and the ecological dynamics and processes within the water body (Coble *et al.*, 2014). As such, understanding OM fluxes and composition provides information regarding the water quality and ecosystem health, alongside providing the ability to trace waters and contamination events (Peleato, Legge and Andrews, 2017; Zhou *et al.*, 2016; Tedetti, Joffre and Goutx, 2013). Naturally occurring aquatic fluorescent organic matter (AFOM) has been increasingly researched to determine OM distribution, composition, origin and dynamics within a variety of natural aquatic systems; for example lakes (Zhou *et al.*, 2016; Kellerman *et al.*, 2015; Kothawala *et al.*, 2014; Miller and McKnight, 2010; Cammack *et al.*, 2004; Tranvik, 1999), rivers (Baker *et al.*, 2003; Baker, 2002c) and marine waters (Timko *et al.*, 2015; Zhao, Lv and Miao, 2013; Romera-Castillo *et al.*, 2011; Stedmon, Markager and Bro, 2003; Determann *et al.*, 1998; Coble, 1996). Despite the vast amount of work conducted, further understanding of this is required for the exploitation of this phenomenon as a water quality parameter.

The majority of freshwater research has analysed AFOM in relation to anthropogenic activities, such as sewage treatment, agriculture and industry (Baker and Inverarity, 2004; Baker *et al.*, 2003; Baker, 2001, 2002a; Ahmad and Reynolds, 1999; Reynolds and Ahmad, 1997). This has exposed the Peak T region of the fluorescence spectrum as a potential tracer of source waters and contamination events, through the identification of

a link between microbial processes and Peak T fluorescence (Sorensen *et al.*, 2018b; Coble *et al.*, 2014; Hudson *et al.*, 2008). However, the exact nature of these interactions and the dynamics of this relationship through time and space are still unknown. Despite the requirement to understand the underpinning interactions of the phenomenon of microbially derived fluorescence, *in situ* fluorimeters for sensing this AFOM are currently available (Ruhala and Zarnetske, 2017; Khamis *et al.*, 2015). *In situ* fluorimeters have long been used to monitor anthropogenic pollution, such as hydrocarbons in marine waters and industrial effluent (Persichetti, Testa and Bernini, 2013). The use of Peak T fluorescence sensors has become popular over the past decade, due to the indication that this AFOM can provide information regarding microbial activity and act as a tracer within natural systems (Sorensen *et al.*, 2015a). However, without understanding the fundamental origin and interactions of AFOM, the application of these sensors, and adoption by water management policy, has been limited. Determining the microbial-AFOM relationship is essential in order to adapt this technology to fully exploit the phenomenon of microbial AFOM. This, in turn, is critical for the development and implementation of a novel biological water quality parameter, enhancing water quality monitoring and management through time and space.

1.1.1 Research aims

This research was carried out to further understand microbially derived AFOM, by employing fluorescence techniques, and to determine the potential application of this for monitoring microbial communities within freshwaters. To achieve this, the specific aims of this thesis were:

- To investigate the phenomenon of microbially engineered AFOM, and its evolution over time, by understanding the dynamics of bacterial consumption and production of AFOM at a high temporal resolution.
- To identify the specific relationship between Peak T fluorescence and bacterial growth and/or activity.
- To assess the performance of current *in situ* fluorescence sensing technologies for monitoring AFOM.
- To develop a new generation *in situ* fluorimeter for the continuous real-time sensing of fluorescence characteristics and inferred microbial activity.

1.1.2 Thesis overview

This thesis is comprised of seven chapters. The first chapter provides a general introduction to fluorescence, fluorescent organic matter and the current literature regarding the application of fluorescence techniques in natural waters. Chapter two details the experimental parameters of the methodologies employed throughout this research and outlines the development of bacterial model systems. Chapter three details the application of a laboratory model system which employs bacterial monocultures to determine the fast-acting dynamics of AFOM production with bacterial growth. Chapter four uses laboratory systems with isolated environmental bacteria and a standardised mixed culture to further explore the bacterial production and processing of AFOM over time. Chapter five presents a monitoring study of physicochemical and biological parameters of a freshwater system, alongside monitoring the fluorescence characteristics through the deployment of Tryptophan and CDOM UviLux sensors (Chelsea

Technologies Ltd., UK). This chapter also assesses the performance of these *in situ* sensors for observing microbial activity fluxes in freshwaters. Chapter six describes the development of a new generation portable *in situ* fluorescence sensor. Finally, chapter seven provides a summary discussion of the data presented in chapters three, four and five, overall conclusions and recommendations for future work.

1.2 Origins of fluorescence

Luminescence is defined as the emission of radiation from electronically, or vibrationally, excited species (Reynolds, 2014; Valeur and Berberan-Santos, 2011; Lakowicz, 2006). The various types of luminescence are classified by the excitation mode, such as chemiluminescence, bioluminescence and photoluminescence. Fluorescence is a form of photoluminescence; the emission of light from an excited species after the absorption of light (Valeur and Berberan-Santos, 2011; Lakowicz, 2006). Fluorescence effects have been observed throughout history but it was Sir George G. Stokes who first used the term fluorescence in 1852 (Stokes, 1852). Stokes also determined the phenomenon of the dispersed light universally being of longer wavelength, lower energy, than that of the original light for fluorescent molecules (fluorophores) in solution, termed Stokes' shift (Valeur and Berberan-Santos, 2011; Carstea *et al.*, 2010; Murphy *et al.*, 2008; Lakowicz, 2006; Stokes, 1852).

Molecule excitation occurs via absorbance, the process whereby a molecule absorbs radiation leading to an increase in its energy (Reynolds, 2014; Lakowicz, 2006). This increase in energy causes electronic transition of an electron from the ground state to an excited electronic state (Reynolds, 2014). The absorption of a photon of light by a molecule can stimulate the electron to an electronically excited state. The number of molecules in the light path is related to the radiation absorbed, through Beer-Lambert's Law (Equation 1.1):

$$I_t = I_0 \, exp^{-\epsilon c l} \qquad \text{(Equation 1.1)}$$

where I_t is light intensity transmitted, I_0 is the intensity of the incident light, $\in$ is the molar absorptivity (how well the chemical species absorbs light at a given wavelength), c is the concentration of the absorbing species, and l is the path length of the solution.

The processes of light absorption and emission by fluorophores are often illustrated using a Jablonski diagram (Coble *et al.*, 2014; Lakowicz, 2006). One form of a Jablonski diagram is shown in Figure 1.1, whereby fluorescence occurs when a molecule absorbs a photon of light, causing a valence electron to be excited to a higher energy level, e.g. S_2. The diagram shows a transition from S_2 to S_1; this is termed internal conversion. Internal conversion occurs rapidly, on a scale of picoseconds (10^{-12} s), and is often complete prior to emission as fluorescence lifetimes are typically close to a nanosecond (10^{-9} s) in length (Coble *et al.*, 2014; Lakowicz, 2006). Energy is also lost during vibrational relaxation, as shown in the figure. The molecule eventually returns from the electronically excited state, e.g. S_1, to the ground state, S_0 (Carstea, 2012; Murphy *et al.*, 2008; Hudson, Baker and Reynolds, 2007; Lakowicz, 2006; Baker, 2001). This can occur with the emission of fluorescence, as demonstrated by Figure 1.1. Loss of energy via other processes can also occur, such as non-radiative decay, energy transfer and collision (Carstea, 2012; Cory *et al.*, 2010). Loss of excitation energy as heat rather than light can also occur. These radiationless relaxation processes are known as external conversion, or quenching, such as collisional quenching where energy is transferred to other molecules via collisions (Coble *et al.*, 2014; Lakowicz, 2006). The potential impact of quenching on freshwater fluorescence signals is discussed in section 1.2.1.

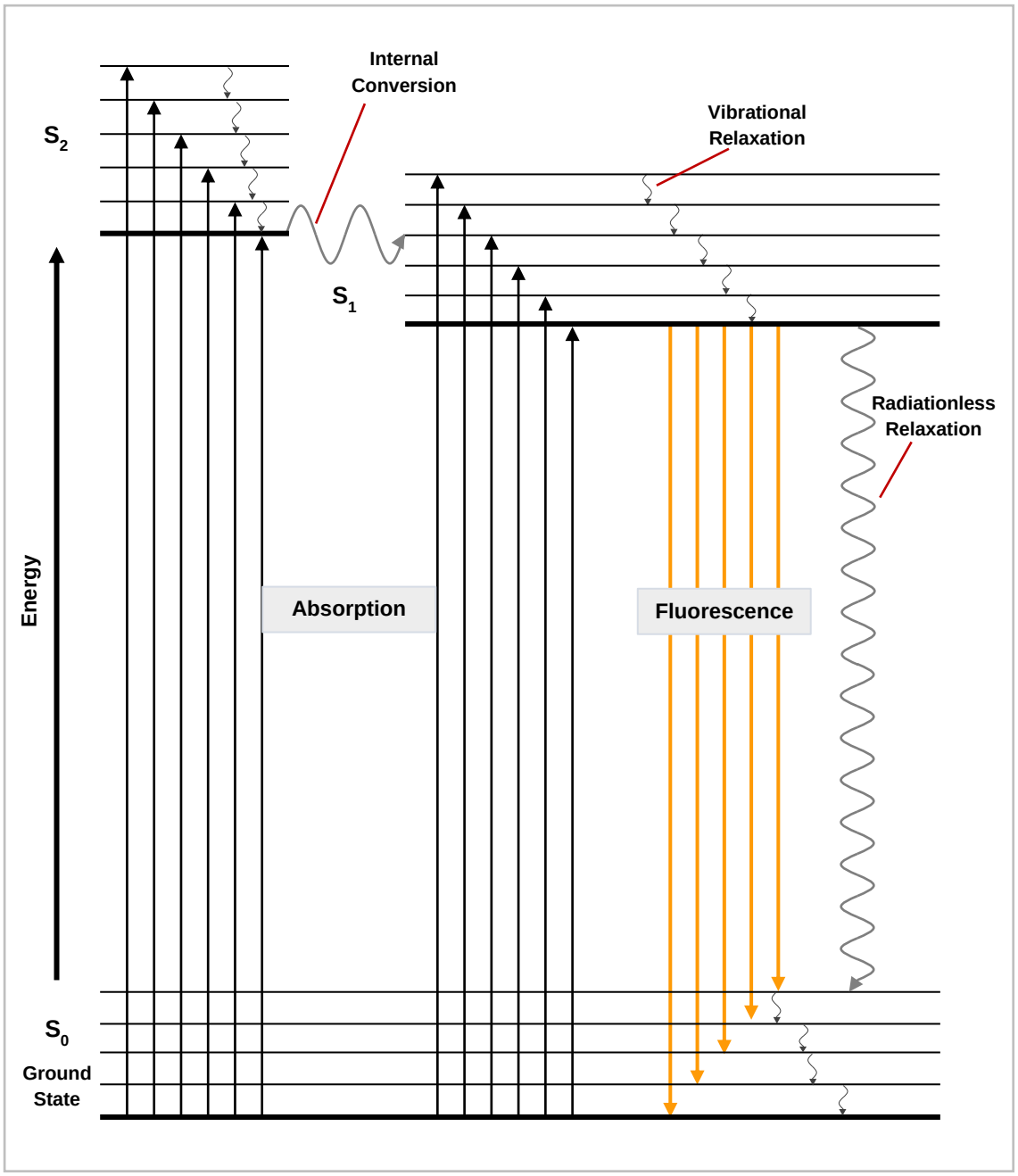

Figure 1.1: Jablonski diagram demonstrating the processes of fluorescence by fluorophores.

Scattering also occurs with the interaction of molecules and light. Elastic scattering, where little energy is transferred, occurs in the majority of fluorescence applications. The type of scattering is determined by the size of the scattering species in relation to the wavelength of the incident light. These radiation scattering phenomena are referred to as Rayleigh, Mie and Tyndall scattering, classified for entities smaller, equal to, and larger than the incident wavelength respectively (Reynolds, 2014). However, as this scattering does not provide a discernible signature specific to the scattering species, it is often cut, or 'masked', within fluorescence data.

Another notable scattering process is Raman scattering, whereby the scattering occurs at distinct wavelengths, determined by the size and symmetry of the scattering species (Reynolds, 2014; Lakowicz, 2006). Raman scatter is an inelastic process, involving energy transfer, meaning the scattered photons have different energy to that of the incident light (Lawaetz and Stedmon, 2009). The difference in energy is related to the difference between energy levels within a given molecule and, as such, can be detected as a constant frequency difference (Reynolds, 2014; Lawaetz and Stedmon, 2009). Although Raman scattering occurs at lower intensities than elastic scatter, such as Rayleigh, it has been used throughout much of the literature to normalise fluorescence spectra within aquatic fluorescence research (Mladenov *et al.*, 2017; Shutova *et al.*, 2014; Butturini and Ejarque, 2013; Murphy *et al.*, 2010; Para *et al.*, 2010; Baker, 2002a; Determann *et al.*, 1998). Alongside normalising spectra, Raman signals can also be used as an internal standard to correct for inner filter effects (IFE); IFE occurs where there is absorbance of the excitation or emission wavelength by something other than the fluorophore (Lakowicz, 2006).

1.2.1 Factors that affect fluorescence characteristics

Physicochemical properties of waters can impact the fluorescence of organic matter (OM), altering the characteristics of the fluorescence signal or by increasing or decreasing the fluorescence (Coble *et al.*, 2014). Fluorescence quenching, a reduction in the signal of fluorescent OM (FOM), is the most common outcome of these environmental effects (Coble *et al.*, 2014; Henderson *et al.*, 2009; Lakowicz, 2006; Baker, 2005). Quenching occurs due to reactions between the fluorophores and the environment, which reduces the fluorescence intensity by altering the excited state (Figure 1.1). This hinders the ability of the fluorophores to emit energy at lower energy, longer wavelength, than the absorbed energy (Coble *et al.*, 2014; Lakowicz, 2006). Alterations in chemical structure are also often considered to be a form of fluorescence quenching, although this does not directly involve a change in the excited state of the fluorophore.

The influence of the range of fluorescence quenching mechanisms has been well researched and discussed within the literature. There have been multiple studies exploring the effect of pH, temperature and metal ions in natural waters (Spencer, Bolton and Baker, 2007; Baker, 2001, 2005; Sierra *et al.*, 2005; Reynolds, 2003). This research, determining the impact of quenching of OM fluorescence in natural waters, has demonstrated that amino acid-like fluorescence, such as tryptophan-like fluorescence, is more susceptible to quenching than humic-like substances. However, this does seem to be dependent on how accessible the tryptophan is; if the tryptophan is exposed, i.e. is free or bound to the surface of macromolecules, it is more likely to be quenched than if it is bound to the macromolecule interior (Coble *et al.*, 2014; Lakowicz, 2006).

1.2.1.1 Metal ions

Laboratory analysis to investigate the impact of metal ions has shown that collisional quenching frequently involves molecular oxygen and metal ions. (Reynolds and Ahmad, 1995). These quenchers cause the excitation state of the fluorophore to be deactivated, often by releasing energy as heat rather than photon emission (Coble *et al.*, 2014; Lakowicz, 2006). Contact with other molecules can also account for fluorescence quenching due to electronic coupling of interacting molecules (Coble *et al.*, 2014).

1.2.1.2 pH

Reynolds (2003) has shown that extremes in pH can alter the structure of OM molecules. The pH of the aquatic systems can also impact the structure and coiling of a molecule, although this is highly dependent on the specific fluorophore (Reynolds, 2003), demonstrated by Hudson *et al.*, (2007) who suggest that humic substances are impacted less by pH than proteins. Conversely, Coble *et al.*, (2014) state that proteinaceous fluorescent material is protected by other molecules and is, therefore, less susceptible to quenching by pH changes.

1.2.1.3 Temperature

Quenching in relation to temperature is important and greatly dependent upon the environmental conditions that the OM is exposed to (Spencer, Bolton and Baker, 2007). Increasing temperatures can lead to more molecule interactions and, therefore, increased

collisional quenching, causing radiationless return of the molecule to the ground state (Lakowicz, 2006; Baker, 2005). Baker (2005) has shown this within a range of samples at temperatures from 10°C to 45°C. Whilst Carstea *et al.*, (2014) agree that increases in temperature lead to increased collisional quenching, they conclude that the variable impact of temperature quenching on different fluorophores, determined by the large range of varying environmental factors between field sites and the exposure to heat sources, makes correction for temperature quenching extremely difficult to apply. This study does, however, state that corrections could be applied, with caution and awareness of inter-site variation, for temperatures below 20°C using the correction tools developed by Watras *et al.*, (2011). This correction method has also been verified by Khamis *et al.*, (2015) for *in situ* sensing across a range of freshwater systems, who suggested the use of internal correction algorithms within sensor development.

As well as temperature variations, freezing and thawing cycles have been shown to quench OM fluorescence due to the extensive modifications this causes to the molecular structure (Hudson *et al.*, 2009; Spencer, Bolton and Baker, 2007). Yet again, this research has shown that amino acid-like fluorescence is more likely to be quenched than humic-like fluorescence, but the extent of this depends on the exposure and binding of the amino acids (Coble *et al.*, 2014; Baker, 2005). Nevertheless, these temperature-induced changes are reversible as they do not impact the molecular structure (Hudson, Baker and Reynolds, 2007).

1.2.1.4 Photodegradation

Photodegradation is also a very important factor in determining the characteristics of OM fluorescence in natural waters. The extent to which photobleaching occurs is extremely variable and heavily dependent on the exposure time and intensity (Gonçalves-Araujo *et al.*, 2015; Coble *et al.*, 2014). The general impact of photodegradation is a decrease in fluorescence intensity and blue shifting (Coble, 1996), a shift in emission maxima towards shorter wavelengths (Shubina *et al.*, 2010). The quenching mechanisms discussed here have varying impacts on FOM and are extremely varied between waters, depending on multiple factors, including the OM composition and macromolecular structures.

1.2.1.5 Inner filter effects (IFE)

Fluorescence measurements are also susceptible to IFE. Although this is not a quenching mechanism, IFE occurs where there is absorbance of the excitation or emission wavelength by something other than the fluorophore, such as the cuvette, other fluorophores, or by additional absorbing components (Lakowicz, 2006). The main cause of this in natural environmental samples is turbidity, often caused by background substances that absorb light, such as suspended solids (Khamis, Bradley and Hannah, 2017; Saraceno *et al.*, 2009, 2017; Blaen *et al.*, 2016; Khamis *et al.*, 2015). In particular environments where the concentration of suspended sediments, such as silt, is extremely high, the detection of the emitted light can be prevented, even if the interfering particles do not absorb light, due to scattering (Downing *et al.*, 2012). Sensor fouling can also cause

optical interferences that impact the fluorescence signal (Blaen *et al.*, 2016). IFE can be corrected for, often done by empirically correcting the Raman scatter by subtracting a blank sample (Khamis *et al.*, 2015; Carstea, 2012; Henderson *et al.*, 2009; Hudson, Baker and Reynolds, 2007; Lakowicz, 2006). Whilst this is a simple and common practice when using benchtop fluorimeters, the impact, and possible correction for, of IFE on fluorescence intensity for *in situ* measurements is an important consideration.

1.2.1.6 Impact of quenching on fluorescence within aquatic systems

The impact of fluorescence quenching of OM in aquatic systems is extremely complicated and can have a profound impact on the fluorescence characteristics of a water body (Romera-Castillo *et al.*, 2014). However, all naturally occurring FOM observed within aquatic systems is essentially quenched, but it is noted, within the literature, that fluorescence intensity should not be altered notably if these variables are kept relatively constant and within natural ranges (Hudson, Baker and Reynolds, 2007; Spencer, Bolton and Baker, 2007; Reynolds, 2003; Baker, 2001). To fully understand the true impact of this, more research is required on natural samples rather than on extracted compounds or standards. This would provide a more comprehensive understanding of the interactions, complexity and heterogeneity of OM in natural environments (Baker, Elliott and Lead, 2007).

Fluorescence quenching potential is important when storing and analysing samples. Both Hudson *et al.*, (2009) and Spencer *et al.*, (2007) found that freezing or acidifying samples leads to a decrease in fluorescence intensity for all FOM, which further

decreases with each cycle of freezing and thawing. Further to this, quenching has implications regarding the design of fluorescence sensors and how different types of quenching may affect fluorescence detection (Sorensen *et al.*, 2018a; Blaen *et al.*, 2016). The benefits of correcting for some of the impacts of quenching and IFE must be considered with caution to ensure the sensors are still readily applicable to a broad range of freshwater environments, and seasonal and diurnal variations, that the sensor will be exposed to when deployed. However, pre-collection correction, built into the sensor, must only be included if it is definitively beneficial to data comparison and does not create the requirement for sensor calibration and validation for every water analysed (Singh, Inamdar and Scott, 2013).

1.3 Organic matter

Organic matter (OM), or natural organic matter (NOM), is the pool of carbon-based compounds within the environment (Coble *et al.*, 2014). OM is mainly comprised of organic compounds derived from plants and animals and their waste, meaning the composition of OM is highly variable and dependent upon origin, transformation and age. Organic matter (OM) is ubiquitous in natural waters, being a complex heterogeneous mixture that influences the transport of nutrients, and impacts the global biogeochemical and carbon cycles (Qian *et al.*, 2017; Bieroza and Heathwaite, 2016; Lambert *et al.*, 2016; Creed *et al.*, 2015; Wünsch, Murphy and Stedmon, 2015; Singh, Inamdar and Scott, 2013; Larsen *et al.*, 2010; Baker and Spencer, 2004). OM origin can be either allochthonous or autochthonous (Winter *et al.*, 2007; Stedmon and Markager, 2005; Alberts and Takács, 2004; Leenheer and Croué, 2003): allochthonous OM is derived from

the surrounding environment and so is influenced by the hydrology, geology and land-use of its source; whilst autochthonous OM is created *in situ* via microbial processes, either in recycling or formation processes (Carstea, 2012; Murphy *et al.*, 2008; Hudson, Baker and Reynolds, 2007). Aquatic OM varies both in composition and concentration, over different cyclic patterns (Blaen *et al.*, 2016; Spencer, Bolton and Baker, 2007); autochthonous OM increases in the summer with increased microbial and algal growth, while allochthonous OM often increases in wetter seasons as it enters rivers via the groundwater and marine waters via increased river discharge (Miller and McKnight, 2010). The composition of OM in aquatic systems is impacted by the biogeochemistry of the surrounding terrestrial environment, and the variety of allochthonous and autochthonous inputs into the system (Romera-Castillo *et al.*, 2014; Carstea, 2012; Larsen *et al.*, 2010; Saraceno *et al.*, 2009; Hudson, Baker and Reynolds, 2007; Stedmon and Markager, 2005). This, alongside the environment in which it exists, impacts the biochemical functions of OM across different environments (Hessen and Tranvik, 1998).

1.3.1 Aquatic organic matter and the "microbial carbon" pump

Carbon cycling has received attention in recent years due to its importance for past, present and future climatic understanding. The contribution of various carbon stores and sinks to carbon cycling has become an increasing focus within earth and environmental sciences, with the pressures on using climatic modelling to predict potential outcomes of anthropogenic activities on climate change (Anderson, Christian and Flynn, 2015). From this work various conceptual carbon "pumps" have been prescribed to represent the movement, uptake and storage of carbon within the

environment (Ridgwell and Arndt, 2015). Much of this work has focussed on long-term marine carbon cycling, as this is the largest reservoir and mechanism for movement of carbon globally (Ridgwell and Arndt, 2015). However, these mechanisms are also important within all aquatic environments throughout the hydrological continuum, particularly regarding transportation and fate of carbon sources (Coble *et al.*, 2014).

The "organic matter" (or "organic carbon") pump involves the removal of dissolved inorganic carbon (DIC) from solution, which is metabolically processed to produce particulate organic carbon (POC) and dissolved organic carbon (DOC) (Ridgwell and Arndt, 2015). The resulting POC is efficiently recycled at the surface, with some sinking and being processed at depth. The DOC is also processed and recycled within aquatic environments, often utilised in the "microbial carbon" pump. This is part of the biological pump which leads to DOC production from the microbial processing of OM (Ridgwell and Arndt, 2015). The knowledge of this "microbial pump" has increased over the past two decades (Jiao *et al.*, 2010). It is now understood that the most labile fractions of DOC are consumed rapidly, while the more recalcitrant fractions are more important for long-term carbon storage and cycling (Carlson and Hansell, 2015).

Understanding the "microbial carbon" pump is key for climatic modelling and predictions, as any substantial change in this DOC consumption, degradation and transformation could have a large impact of atmospheric CO_2 and, therefore, global climatic changes (Ridgwell and Arndt, 2015). However, due to the complexity of inputs, interactions and outputs, the "microbial carbon" pump is not well represented within current models. As to not over complicate climate models, or use parameters that are currently unknown in function or impact, many of the present day models use a "black

box" element to represent the "microbial carbon" pump (Anderson, Christian and Flynn, 2015). This adds a major element of uncertainty to any predictions derived from such models. Due to this, improving understanding of the mechanisms and function of microbial-OM interactions is vital.

1.3.2 Aquatic fluorescent organic matter

Naturally occurring aquatic fluorescent OM (AFOM) can be analysed to assess the water quality and relative OM composition, using fluorescence spectroscopy as an extremely sensitive and non-destructive technique for water analysis (Cooper *et al.*, 2016; Gabor *et al.*, 2015; Bieroza, Bridgeman and Baker, 2010; Baker, Elliott and Lead, 2007; Baker, 2005; Alberts and Takács, 2004; Cammack *et al.*, 2004; Reynolds, 2002). The capacity of a molecule to fluoresce is determined by the relaxation pathways from the excited state. As such, molecular structure is important in determining fluorescence ability, with more rigid molecules, such as aromatics, being more likely to fluoresce (Aiken, 2014; Chen *et al.*, 2003; Leenheer and Croué, 2003; Baker, 2002a). These more highly conjugated molecules are also more likely to fluoresce due to the smaller energy gap from the ground to excited state (Aiken, 2014; Carstea, 2012; Baker, 2002c, 2002a), allowing movement of delocalised electrons between energy levels. The excitation and emission maxima wavelengths of fluorophores are specific to the molecule (Carstea, 2012; Hudson, Baker and Reynolds, 2007; Lakowicz, 2006), allowing the use of excitation-emission spectra to analyse the relative composition of fluorophores in a sample (Murphy *et al.*, 2008; Sierra *et al.*, 2005; Boehme *et al.*, 2004; Chen *et al.*, 2003; Coble, 1996).

Although not a novel technique for investigating naturally occurring organic matter, increased use of excitation-emission matrix (EEM) fluorescence spectroscopy has led to a better understanding of AFOM, in particular fluorophores with short ultra-violet (UV) excitation wavelengths (Aiken, 2014; Baker, 2005). A range of excitation wavelengths is used in relation to the emission wavelengths, allowing an EEM to be plotted as a three-dimensional map of fluorescence intensity. EEMs provide a visual representation of fluorophores within a sample (Murphy *et al.*, 2014; Cory *et al.*, 2010; Hudson *et al.*, 2008; Liu, Lead and Baker, 2007; Baker *et al.*, 2004; Parlanti *et al.*, 2000; Coble, Schultz and Mopper, 1993); a freshwater EEM with AFOM peaks and spectral scatter identified is shown by Figure 1.2. These spectral scattering phenomenon are often corrected for via blank subtraction (Carstea, 2012; Henderson *et al.*, 2009; Hudson, Baker and Reynolds, 2007; Lakowicz, 2006). Raman scatter, seen in Figure 1.2, is caused by the vibration of the covalent bonds between the oxygen and hydrogen molecule of water when light energy is applied to the water (Park and Snyder, 2018; Carstea, 2012; Hudson, Baker and Reynolds, 2007). Rayleigh scatter, identified in Figure 1.2, is caused by the reflection of excitation energy and occurs in two locations: where the emission and excitation wavelength are equal to one another; and, where the emission wavelength is twice that of the excitation wavelength (Park and Snyder, 2018; Hudson, Baker and Reynolds, 2007).

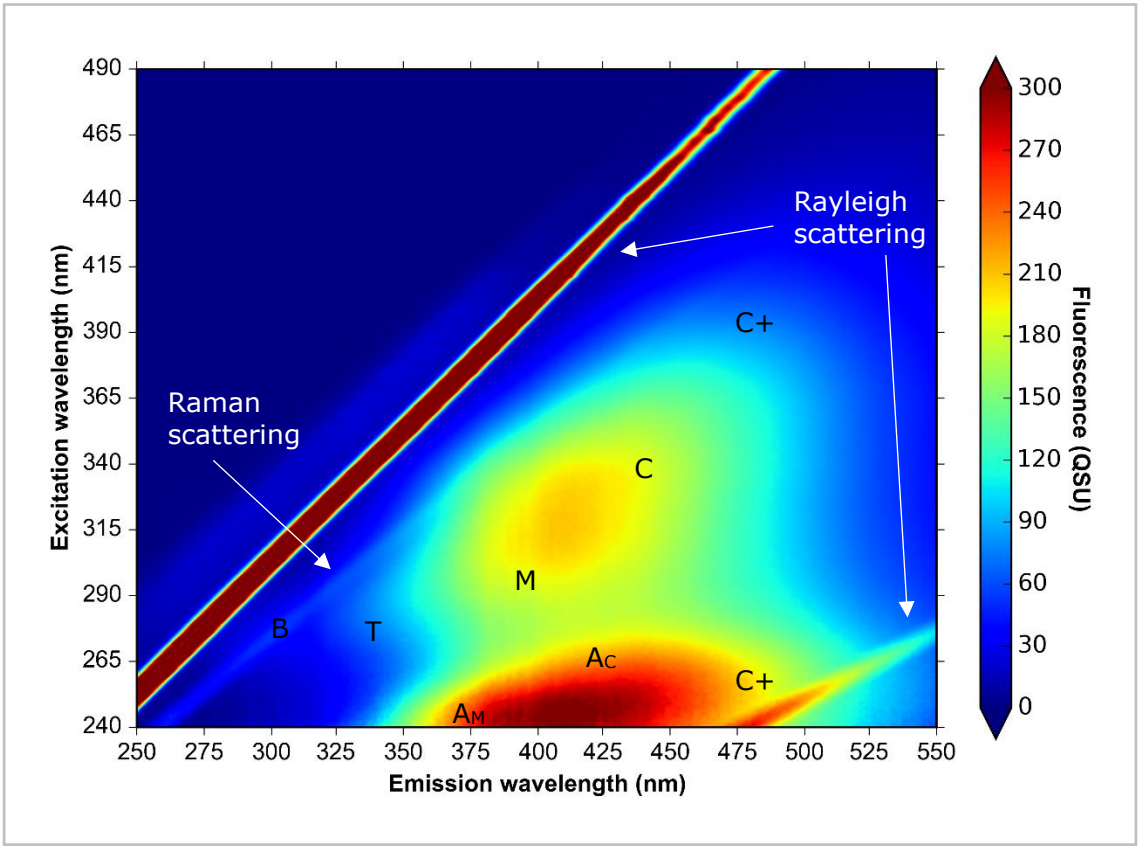

Figure 1.2: Excitation-emission matrix (EEM) with the position of previously characterised fluorescence peaks (described in Table 1.1, Coble *et al.*, 2014) and common EEM spectral features.

Fluorescence spectroscopy is an attractive method to study AFOM due to the relative ease of data collection and detail provided (Aiken, 2014). The development of this technology has met the demand for more rapid and sensitive analysis, <1 minute per sample in some cases (Henderson *et al.*, 2009; Baker and Spencer, 2004; Baker, 2002a), in comparison to other techniques, such as UV absorbance and high-performance liquid chromatography (HPLC) (Bieroza, Bridgeman and Baker, 2010; Henderson *et al.*, 2009; Chen *et al.*, 2003; Leenheer and Croué, 2003; Reynolds, 2003; Moran, Sheldon and Zepp, 2000). As well as speed of analysis, sensitivity and detail, EEM fluorescence spectroscopy is also a relatively non-intrusive tool for analysing the composition of AFOM (Carstea *et al.*, 2014, 2016; Baker *et al.*, 2015; Coble *et al.*, 2014; Yang, Shin and Hur, 2014). However,

a standard method for data processing is yet to be recognised. Due to this, there is some discussion within the field as to whether standards should be used for comparison, such as normalisation to quinine sulphate (Mostofa *et al.*, 2013; Shimotori, Watanabe and Hama, 2012; Shimotori, Omori and Hama, 2009; Kramer and Herndl, 2004), or machine calibration due to the variation in natural fluorescence caused by environmental factors (Hudson, Baker and Reynolds, 2007; Sierra *et al.*, 2005; Coble, Schultz and Mopper, 1993).

Although each fluorophore has a specific fluorescence emission peak wavelengths, it can be difficult to identify these from an EEM due to overlapping of fluorescent spectra (Wang, Cao and Meng, 2015; Murphy *et al.*, 2008). Much of the available literature frequently divides AFOM composition into humic-like and protein-like fluorescence, based on their properties being similar to that of the material standards (Xie *et al.*, 2017; Liu, Lead and Baker, 2007; Baker *et al.*, 2003; Leenheer and Croué, 2003; Coble, 1996): humic-like fluorescence includes allochthonous humic- and fulvic-acid material (Fellman, Hood and Spencer, 2010; Hudson, Baker and Reynolds, 2007); and protein-like fluorescence encapsulates the autochthonous AFOM, often termed 'microbially derived' (Hudson *et al.*, 2008; Baker, Elliott and Lead, 2007; Winter *et al.*, 2007; Elliott, Lead and Baker, 2006b, 2006a; Determann *et al.*, 1998). However, the complex composition and unknown origin of AFOM has led more recently to the use of peak nomenclature (Coble *et al.*, 2014), referring to the individual fluorescence peaks over using vague and overarching terminology (Table 1.1).

Table 1.1: Nomenclature of common fluorescence peaks for AFOM in natural waters, detailing peak name, spectral position, chemical characteristic, and environmental source.

Peak name	$\lambda_{ex}/\lambda_{em}$ (nm)	Fluorescence characteristic	Origin
A_B **B**	230/305 275/305	Tyrosine-like protein-like	Autochthonous, resembles tyrosine, may be free or bound amino acids
A_T **T**	230/340 275/340	Tryptophan-like protein-like	Autochthonous, resembles tryptophan, associated with microbial processes
A_M **M**	240/350-400 290-310/370-420	Humic-like	Autochthonous, originally identified with marine environments, associated with microbial biodegradation processes
A_C **C**	260/400-460 320-365/420-470	Humic-like	Allochthonous, resembles humic-acids, of terrestrial origin
C+	250/470-504 385-420/470-504	Humic-like	Allochthonous, resembles humic-acids, of terrestrial origin

Peak nomenclature and description derived from (Coble *et al.*, 2014, p. 78)

1.3.3 'Protein-like' fluorescence

Protein-like fluorescence ($\lambda_{ex}/\lambda_{em}$ 230-280/330-360 nm) is associated with biological activity and often closely resembles the fluorescence signature of three amino acids; tryptophan, tyrosine and phenylalanine (Zhu *et al.*, 2017; Hudson, Baker and Reynolds, 2007; Lakowicz, 2006; Cory and McKnight, 2005). These molecules are transient, labile and of low molecular weight, 204 Da, 181 Da and 165 Da respectively (Promega, 2010); the chemical structures for these amino acids are shown in Figure 1.3. This protein-like AFOM is attributed to and assumed to be of microbial origin (Hambly *et al.*, 2015; Coble *et al.*, 2014; Cammack *et al.*, 2004; Smith, Anderson and Webb, 2004), with much of the recent literature focussing on the use of tryptophan-like (Peak T) fluorescence as a surrogate for microbial activity (Baker *et al.*, 2015; Cumberland *et al.*, 2012), as originally highlighted by Hudson *et al.*, (2008).

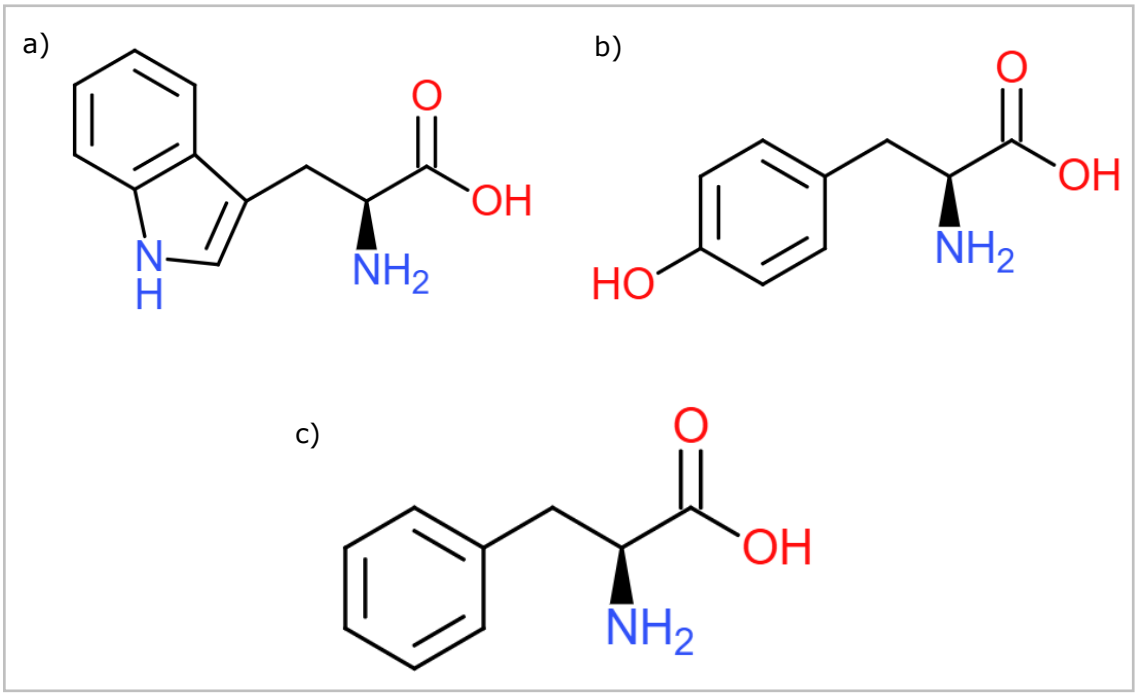

Figure 1.3: Structures of common 'protein-like' fluorophores: a) L-Tryptophan; b) L-tyrosine; and c) L-phenylalanine.

The composition of compounds that form protein-like fluorescence is still debated (Khamis *et al.*, 2015), particularly focussing on differences between bound and free amino acids. Some, for example Determann *et al.*, (1998) and Reynolds (2003), have argued that the amino acid-like fluorescent molecules are free, whilst others have stated that they are bound to humic substances (Elliott, Lead and Baker, 2006a; Baker, 2005; Zang *et al.*, 2000) or are a part of the microbial biomass (Jørgensen *et al.*, 2011; Liu, Lead and Baker, 2007; Smith, Anderson and Webb, 2004). These disputes further highlight the variation and complexity of AFOM within these natural systems. The increased use of parallel factor (PARAFAC) analysis has benefitted this discussion, see section 2.1.2.3. Whilst the positioning of these amino acid-like fluorescence peaks is less variable than humic-like fluorescence, PARAFAC analysis has demonstrated broad ranges of emission wavelengths associated with Peak T fluorescence, suggesting that the variation in signal arises from a combination of free and bound amino acid-like compounds (Yu *et al.*, 2015; Coble *et al.*, 2014).

1.3.4 Peak T fluorescence

Peak T, or 'tryptophan-like', fluorescence has received more attention within the literature, particularly in terms of 'microbially derived' AFOM, due to its association with proteins and areas of high primary productivity (Miller and McKnight, 2010; Hudson *et al.*, 2008; Elliott, Lead and Baker, 2006a; Baker and Spencer, 2004; Parlanti *et al.*, 2000; Coble, 1996). Peak T fluorescence is the most common, and often most intense, protein-like fluorescence peak seen within a range of natural freshwaters. It is also less impacted by instrument limitations and optical scatter interference than other amino

acids; particularly phenylalanine which is often obscured by the water Raman line and Rayleigh scatter in EEM analysis, and is, therefore, often excluded in the literature.

Although 'microbially derived' AFOM is mentioned throughout much of the literature, expansion of the exact nature, origin, transformation and fate of the associated fluorescence properties has not been as well explored as the humic-like fluorescence components. The current literature demonstrates that these fluorescence properties can be used as a proxy for microbial activity, as seen by statistically significant correlations between tryptophan-like fluorescence and the biological oxygen demand (BOD) (Baker *et al.*, 2015; Bridgeman *et al.*, 2013; Hudson *et al.*, 2008; Baker and Inverarity, 2004), a measure of the amount of oxygen required, by the microbial population present, to degrade the biodegradable organic matter (Bridgeman *et al.*, 2013; Cutrera *et al.*, 1999). Thus, Peak T fluorescence has also been correlated with algal populations and algal growth (Makarewicz *et al.*, 2018; Zhi *et al.*, 2015; Fukuzaki *et al.*, 2014; Ferrari and Mingazzini, 1995), with a particular focus on algal bloom identification (Fukuzaki *et al.*, 2014; Suksomjit *et al.*, 2009). Higher intensity Peak T fluorescence is also seen in waters with notable anthropogenic activity (Stedmon and Markager, 2005), particularly where there is a sewage or agricultural waste input, and, to a lesser degree, urban waters (Carstea, 2012; Baker, 2001, 2005; Baker and Spencer, 2004).

Nevertheless, the exact interactions between amino acid-like fluorescence, such as Peak T, and biological degradation of AFOM and metabolic activity have not been clearly defined (Coble *et al.*, 2014). Understanding of these relationships is further complicated by the evidence that microbial activity is both a source and a sink of amino acid-like fluorescence (Carstea *et al.*, 2016; Repeta, 2015; Stedmon and Markager, 2005; Cammack

et al., 2004; Moran, Sheldon and Zepp, 2000). While there is currently no clear explanation for these apparent complex interactions, several mechanisms have been proposed (Coble *et al.*, 2014). For example, Cammack *et al.*, (2004) suggested that amino acid-like AFOM is produced in bacterial growth. However, this hypothesis has been challenged due to the costly production of amino acids by bacteria and the lack of explanation as to why these molecules would be released from the bacterial cells (Coble *et al.*, 2014), whilst other literature has also associated this AFOM with bacterial population growth within bacterial culturing (Baker, Elliott and Lead, 2007; Moran, Sheldon and Zepp, 2000). Another theory for the microbial production of amino acid-like fluorescence is that it is a by-product formed after bacterial AFOM degradation that denatures the proteins, altering the structure and, therefore, the fluorescence signal (Coble *et al.*, 2014; Lakowicz, 2006; Determann *et al.*, 1998). However, there is still currently limited data that definitively demonstrates this or determines *in situ* production in freshwater systems, with detailed characterisation of AFOM properties.

More recently, surface freshwater research has endeavoured to determine enumeration of specific bacterial species using Peak T fluorescence. For example, a log correlation R = 0.74 across a 7-log range in *Escherichia coli* enumeration was identified for sewage impacted rivers (Baker *et al.*, 2015). This has been furthered within groundwater systems where there is little background fluorescence interference (Sorensen *et al.*, 2015a, 2016). Sorensen *et al.*, (2015a) explored the use of Peak T fluorescence to indicate low levels of microbial contamination in groundwater, utilised as drinking water supplies, reporting linear correlations, $R^2 = 0.57$ from < 2 to 700 cfu 100 ml^{-1}. The correlations identified vary between sampling locations, as Sorensen *et al.*, (2018b) present a strong significant

correlation ($R^2 = 0.71$) between Peak T and *E. coli* counts. This work indicates the potential use of Peak T fluorescence as an indicator of bacterial contamination, particularly as an alternative to the commonly used turbidity measurement; $R^2 = 0.48$ between turbidity and *E. coli* (Sorensen *et al.*, 2018b). The determination of correlation between Peak T fluorescence and total bacterial count is, however, highly dependent on the sampling location (Sorensen *et al.*, 2018b). To improve the application of Peak T fluorescence for identifying bacterial contamination, Sorensen *et al.*, (2018a) utilised a threshold system based on low, medium and high risk contamination. This demonstrated a current detection limit of medium risk contamination due to the high false negative rate within the low risk category. However, it was postulated that this could be limited by the detection limit of the laboratory bacteriological methodology, rather than the fluorescence signal (Sorensen *et al.*, 2018a). Although relationships between bacterial presence in freshwater environments and Peak T fluorescence have been demonstrated, the exact relationship between this fluorescence signal, biological degradation of AFOM and metabolic activity are nevertheless not clearly defined at present (Coble *et al.*, 2014).

1.3.5 'Humic-like' fluorescence

Humic-like AFOM is associated with stable complex larger aromatic compounds (Zhu *et al.*, 2017; Cooper *et al.*, 2016), such as fulvic and humic acids (Figure 1.4). These compounds range in molecular weight from 5-30 kDa (Perminova *et al.*, 2003). Associating this fluorescence with humic substances has, by definition, classified them as recalcitrant (Hessen and Tranvik, 1998). As set by Coble *et al.*, (1990), humic-like fluorescence has generally been referred to as peaks A and C, excitation-emission

wavelengths ($\lambda_{ex}/\lambda_{em}$) 230/400-500 nm and $\lambda_{ex}/\lambda_{em}$ 300-350/400-500 nm respectively. These fluorescence peaks have frequently been discussed as not being involved in microbial processing, due to their recalcitrant properties, but being of terrestrial origin, namely fulvic and humic acids: fulvic acids are soluble in water; humic acids are soluble in aqueous solutions with a pH >2 (Hudson, Baker and Reynolds, 2007). However, with the complex nature of AFOM and the unknown microbial interactions with these materials, it seems unlikely that these peaks are simply of a singular origin. Demonstrating this is made more difficult by the poorly defined chemistry of the fluorescence molecules, typified by the use of the term '-like fluorescence' (Coble *et al.*, 2014; Stubbins *et al.*, 2014).

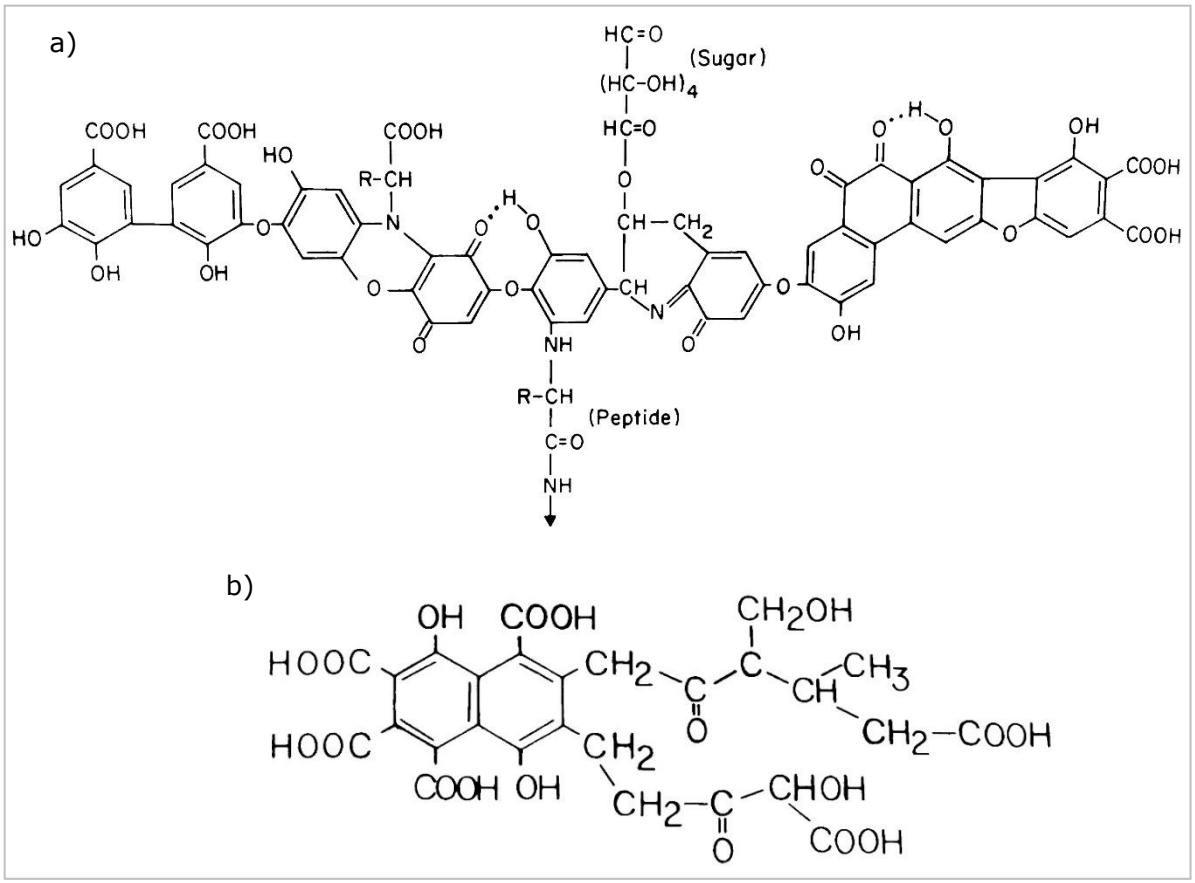

Figure 1.4: Proposed structures of common 'humic-like' fluorophores: a) humic acid and b) fulvic acid. Theoretical structures cited in Aiken *et al.*, (1985) *Humic substances in soil, sediment and water: geochemistry, isolation, and characterization* [Figure 4 and 6]. p. 24-25. Reproduced with permission of the Licensor through PLSclear. In memory of George R. Aiken, died 7th December 2016.

Recent work has suggested that these fluorescent materials are microbially degraded and, therefore, involved in microbial processing (Singh, Inamdar and Scott, 2013). Although the majority of these 'humic-like fluorescence' regions are referred to as being of allochthonous origin, humic-like fluorescence Peak M is thought to be biologically transformed and degraded allochthonous humic-like substances, demonstrating an autochthonous origin (Harun *et al.*, 2015, 2016; Coble *et al.*, 2014). Although this work has highlighted the complexity of AFOM and interactions with the microbiology, it is still 'protein-like fluorescence' that is almost unanimously referred to as 'microbially derived' throughout the literature (Coble *et al.*, 2014; Barker *et al.*, 2013). However, this recent development has demonstrated how microbial communities interact differently with different AFOM, both in terms of activity and through time.

Frequently less documented, particularly in freshwater AFOM research, is this ability of aquatic microbial communities to be a major contributor to the AFOM pool (Hansell and Carlson, 2015; Lee *et al.*, 2015; Kramer and Herndl, 2004). As such, these microbial interactions may have a global biogeochemical impact (Martínez-Pérez *et al.*, 2017; Guillemette and del Giorgio, 2012; Omori *et al.*, 2011). Humic-like AFOM is often not considered to be bioavailable (Cooper *et al.*, 2016), but has been shown to be utilised and produced during bacterial metabolism within marine environments (Asmala *et al.*, 2014; Guillemette and del Giorgio, 2012; Shimotori, Watanabe and Hama, 2012; Romera-Castillo *et al.*, 2011; Kramer and Herndl, 2004; Moran, Sheldon and Zepp, 2000). Recent findings by Kallenbach *et al.*, (2016) have also highlighted the ability of bacteria to produce extracellular humic material, contributing to soil organic matter. The discovery of this dual functionality, as a carbon source and sink, has highlighted the importance of

the role of bacterial communities in aquatic systems and the further research that is required to decipher the regulation and metabolic pathways responsible for these interactions (Guillemette and del Giorgio, 2012), with specific focus now required for freshwater systems.

Research has been conducted regarding marine AFOM and microbiological interactions, due to the importance of ocean OM as a carbon reservoir and the impact of deep ocean circulation in relation to carbon cycling and climate change (Nelson and Gauglitz, 2016; Ziervogel *et al.*, 2016; Hansell and Carlson, 2015; Timko *et al.*, 2015; Fukuzaki *et al.*, 2014; Jørgensen *et al.*, 2011, 2014; Omori *et al.*, 2011). This research has led to an improved understanding of autochthonous OM production and consumption by a range of microorganisms, specifically relating to the production of recalcitrant humic-like AFOM. Whilst there has been a focus on phytoplankton and bacterioplankton (Guillemette and del Giorgio, 2012; Romera-Castillo *et al.*, 2011; Suksomjit *et al.*, 2009; Kramer and Herndl, 2004), due to the importance of these organisms in the ocean microbial carbon pump (Mopper, Kieber and Stubbins, 2015; Ridgwell and Arndt, 2015; Tanaka *et al.*, 2014; Suksomjit *et al.*, 2009; Kramer and Herndl, 2004), there has also been research into the impact of marine bacteria on the AFOM composition (Nelson and Gauglitz, 2016; Jørgensen *et al.*, 2014; Shimotori, Omori and Hama, 2009; Ogawa *et al.*, 2001). It is evident from these studies that bacterial populations have a direct impact on the AFOM properties and amount of labile AFOM in marine systems (Jørgensen *et al.*, 2014; Ogawa *et al.*, 2001). This has greatly enhanced our knowledge of bacterial-OM interactions in marine environments. However, freshwater research is still lacking much of the fundamental understanding of these types of reactions, while it is clear that the bacterial

processes from which the AFOM originates in both systems are likely to overlap. As such, it is important for all aquatic research to aim to understand these interactions, particularly regarding the transport of organic carbon, via OM, along the hydrological continuum.

1.4 Characteristics of fluorescent organic matter in aquatic systems

Fluorescence spectroscopy has been increasingly used for the analysis of AFOM in a range of aquatic systems, with much of the literature focussing on fluorescence as a technique for determining the AFOM 'fingerprint' of an aquatic system (Xiao *et al.*, 2017; Aiken, 2014; Koch *et al.*, 2014). This has led to an improved understanding regarding how AFOM interacts within the aquatic system (Stedmon and Bro, 2008; Hudson, Baker and Reynolds, 2007), with numerous studies relating to characteristics, reactivity, age and source (Spencer, Bolton and Baker, 2007; Cory and McKnight, 2005; Baker *et al.*, 2004; Stedmon, Markager and Bro, 2003; Coble, Schultz and Mopper, 1993). This has exposed the different AFOM characteristics between water systems, whilst simultaneously identifying similarities and commonalities.

The sensitivity of fluorescence analysis, and technological improvements, has led to the analysis of AFOM in aquatic environments across multiple disciplines and within many applications (Carstea, Baker and Savastru, 2014; Cory *et al.*, 2010; Hudson, Baker and Reynolds, 2007; Liu, Lead and Baker, 2007). These technological developments have also provided portable equipment, allowing for *in situ* real-time monitoring at high temporal

resolutions (Blaen *et al.*, 2016; Khamis *et al.*, 2015; Tedetti, Joffre and Goutx, 2013; Carstea, 2012; Spencer, Bolton and Baker, 2007).

1.4.1 Marine AFOM

Much of the earlier research conducted focussed on the analysis of marine AFOM, particularly regarding tracing water bodies (Gonçalves-Araujo *et al.*, 2015; Miller and McKnight, 2010; Murphy *et al.*, 2008; Boehme *et al.*, 2004) and characterising AFOM and determining its origins (e.g. Coble, 1996). Marine AFOM research has been dominated by the properties and distribution of coloured dissolved organic matter (CDOM), alongside degradation processes and how this impacts lability of this OM (Martínez-Pérez *et al.*, 2017; Gonçalves-Araujo *et al.*, 2015; Coble *et al.*, 2014). Terrestrial OM is an important carbon source in marine waters and is important for deep ocean cycling (Makarewicz *et al.*, 2018; Nelson and Gauglitz, 2016; Ridgwell and Arndt, 2015; Timko *et al.*, 2015). An increased interest in this within recent literature has been driven by rapid climate change and the potential global and local impacts of this on ocean cycling and ecosystems (Coble *et al.*, 2014). The use of fluorescence techniques has become popular due to the sensitivity required for monitoring low levels of AFOM in marine systems, caused by the dilution of these inputs (Coble *et al.*, 2014). Further to the monitoring of terrestrial AFOM, there has been interest in identifying protein-like fluorescence and the related biological activity within marine environments (Parlanti *et al.*, 2000; Determann *et al.*, 1998). More recently within marine OM research, microbial interactions with different components of AFOM has identified the bioavailability of humic-like material

(Asmala *et al.*, 2014; Guillemette and del Giorgio, 2012), as discussed in section 1.3.5. This has emphasised the significance of microbial-OM interactions.

1.4.2 Freshwater AFOM

Freshwater AFOM is extensively investigated, with a focus on the optical properties of AFOM, composition, source and reactivity (Coble *et al.*, 2014). This has provided insight into the biogeochemical importance of OM in freshwater systems. The focus of AFOM research in freshwater science has been dominated by the biological, such as microbial mineralisation, and hydrological controls, residence time and storm events for instance, on ecosystems (Peleato, Legge and Andrews, 2017; Lambert *et al.*, 2016; Coble *et al.*, 2014; Kothawala *et al.*, 2014; Miller and McKnight, 2010). Much of this work has focussed on temporal analysis of both humic-like and protein-like AFOM changes and dynamics, attributed to allochthonous and autochthonous sources respectively, from diurnal to seasonal scales (Lambert *et al.*, 2016; Coble *et al.*, 2014). Fluorescence characterisation within freshwaters has also been used to analyse point and diffuse anthropogenic pollution, including industrial wastewater pollution (Baker, 2002a), agricultural runoff (Cohen, Levy and Borisover, 2014; Naden *et al.*, 2010), and wastewater within urban catchments (Baker and Inverarity, 2004). The reactivity of OM within these natural systems has been researched throughout this body of literature with protein-like fluorescence identified as bioavailable AFOM and attributed to bacterial production and processes (Coble *et al.*, 2014; Fellman, Hood and Spencer, 2010; Cammack *et al.*, 2004). The biodegradation of humic-like AFOM has also been researched, with much of this classification of AFOM being considered as recalcitrant, as discussed in section 1.3.5.

Whilst this is assumption of humic-like AFOM being solely terrestrial and allochthonous in origin is being challenged, further work is required to understand and determine bacterial-OM interactions.

1.4.3 Groundwater AFOM

Groundwater OM fluorescence has long been investigated, particularly regarding those used for drinking waters. EEM fluorescence spectroscopy has allowed for the often low AFOM signals in groundwater systems to be monitored (Sorensen *et al.*, 2015a, 2016). This has facilitated monitoring groundwater connectivity using AFOM signals as tracers from surface and river water exchanges. Alongside this, AFOM monitoring has become essential for determining potential leachate and pollutant problems that could make the use of groundwaters unsafe (Sorensen *et al.*, 2015c, 2015a, 2018a; Graham *et al.*, 2015). This has arisen from the understanding gained in both marine and freshwater OM studies, where fluorescence has been used to better understand AFOM characteristics, source and biological processing (Coble *et al.*, 2014). Tracing hydrological connections and contamination monitoring in groundwaters has increased with the development of portable *in situ* fluorescence sensing. This work has highlighted the ability of fluorescence sensing to monitor microbial presence (Sorensen *et al.*, 2015a, 2016, 2018b, 2018a; Baker *et al.*, 2015). However, further work must be undertaken to truly understand the relationship between AFOM and its relationship with microbial processes.

1.4.4 Wastewater AFOM: contamination of aquatic systems

In addition to OM characteristics, there has been a recent surge in the use of AFOM analysis in natural waters to monitor pollution and trace wastewater contamination (Peleato, Legge and Andrews, 2017; Graham *et al.*, 2015; Tedetti, Joffre and Goutx, 2013; Carstea, 2012; Stedmon *et al.*, 2011; Murphy *et al.*, 2008; Baker, Elliott and Lead, 2007). Research into wastewater contamination (e.g. Baker, 2002c), sewage contamination (e.g. Reynolds, 2002), and relatively extensive work regarding the impact of treated sewage water in freshwater and marine systems has been conducted (e.g. Baker, 2001; Baker and Spencer, 2004). This has allowed for comprehensive research into the impact of anthropogenic OM, from sewage, agriculture and industry, in aquatic environments (Henderson *et al.*, 2009; Baker *et al.*, 2004; Baker, 2002b; Reynolds, 2002; Reynolds and Ahmad, 1997). This work has also found that tryptophan-like, specifically Peak T, fluorescence is high in wastewater and so can be used to trace anthropogenic substances in natural waters, monitor water quality and to indicate BOD (Hudson *et al.*, 2008; Baker and Inverarity, 2004; Baker *et al.*, 2003; Reynolds, 2002; Reynolds and Ahmad, 1997). However, comparatively, wastewater fluorescence is not as well investigated as natural waters. This is in part due to the optical challenges which often arise within these waters, alongside the required applications, often driven by policy.

1.4.5 Drinking water AFOM: contamination detection and treatment

In comparison to other aquatic research, monitoring AFOM in drinking water sources, treatment systems and distribution networks is a recent application of fluorescence

spectroscopy. OM is ubiquitous to all waters used to supply drinking water, enabling the use of fluorescence monitoring through treatment and distribution systems (Lidén, Keucken and Persson, 2017; Lavonen *et al.*, 2015; Coble *et al.*, 2014; Matilainen *et al.*, 2011; Westerhoff, Chao and Mash, 2004), and to determine potential contamination events (Henderson *et al.*, 2009). OM monitoring in drinking waters is also important for understanding the disinfection by-product (DBP) formation potential during chlorination processes, as OM is known to be a pre-cursor to these carcinogenic compounds (Golea *et al.*, 2017; Zhu *et al.*, 2017; Yang *et al.*, 2015; Bridgeman, Bieroza and Baker, 2011; Hua *et al.*, 2010; Beggs, Summers and McKnight, 2009; Roccaro, Vagliasindi and Korshin, 2009). Although current literature and understanding of AFOM creates an exciting potential new development in the application of fluorescence spectroscopy, further work is required to recognise the full potential in drinking water applications.

1.5 Summary: key research gaps

Regardless of the large body of research conducted and literature available on AFOM characteristics, there are still gaps in the knowledge and understanding of the processes involved. The key areas for further research are:

- Fundamental understanding of AFOM-microbial interactions and how this can inform OM fluxes within aquatic systems. Then, to build upon this understanding to provide a more detailed understanding of these interactions and the complexity of AFOM exchanges within environmental systems.
- The impact of AFOM: as a local nutrient source; on the transportation of OM throughout the hydrological continuum; on the local and wider ecology and

ecological status of aquatic systems; and, the influence of AFOM on global biogeochemical cycling.

- Using knowledge and research to exploit the phenomenon of naturally occurring AFOM, using fluorescence peaks, such as Peak T, as novel water quality parameters to inform water resource management.
- To further develop, and test, current technology for monitoring AFOM *in situ* utilising the most current scientific research to underpin these developments. This should inform the range of applications, environments suitable for sensor deployment, and the benefits of these sensors for monitoring water quality, ensuring the full potential of this technology is realised.

Chapter 2 Experimental parameters and method development

2.1 Fluorescence measurements

Throughout this research fluorescence measurements were collected using two spectrofluorometers; an Aqualog® (Horiba Ltd., Japan) and a FluoroSENS (Gilden Photonics Ltd., UK). *In situ* fluorescence sensors (UviLux, Chelsea Technologies Group Ltd., UK) were also deployed in a long-term monitoring program to measure fluorescence peaks T and C within a freshwater system. Details of the UviLux sensor are provided in chapter 4. This section provides the technical details for the Aqualog® and FluoroSENS spectrofluorometers and the parameters used throughout this research.

2.1.1 Fluorescence spectroscopy

2.1.1.1 Aqualog® spectrofluorometer

The Aqualog® (Horiba Ltd., Japan) is a spectrofluorometer which employs a 150-W xenon arc-lamp. The excitation wavelength ranges from 240-800 nm and the emission wavelengths that can be detected are 250-800 nm. The instrument has an excitation monochromator, blazed at 250 nm and an emission CCD detector at a right angle to the excitation beam to collect the fluorescence spectra (Figure 2.1) (HORIBA Ltd., 2013). Instrument correction is provided by the reference detector. Simultaneous measurement of the sample's spectral transmittance and absorbance properties is collected by a single-

channel detector, colinear with the beam (Figure 2.1), for IFE correction (detailed in section 2.1.2.1) (HORIBA Ltd., 2013).

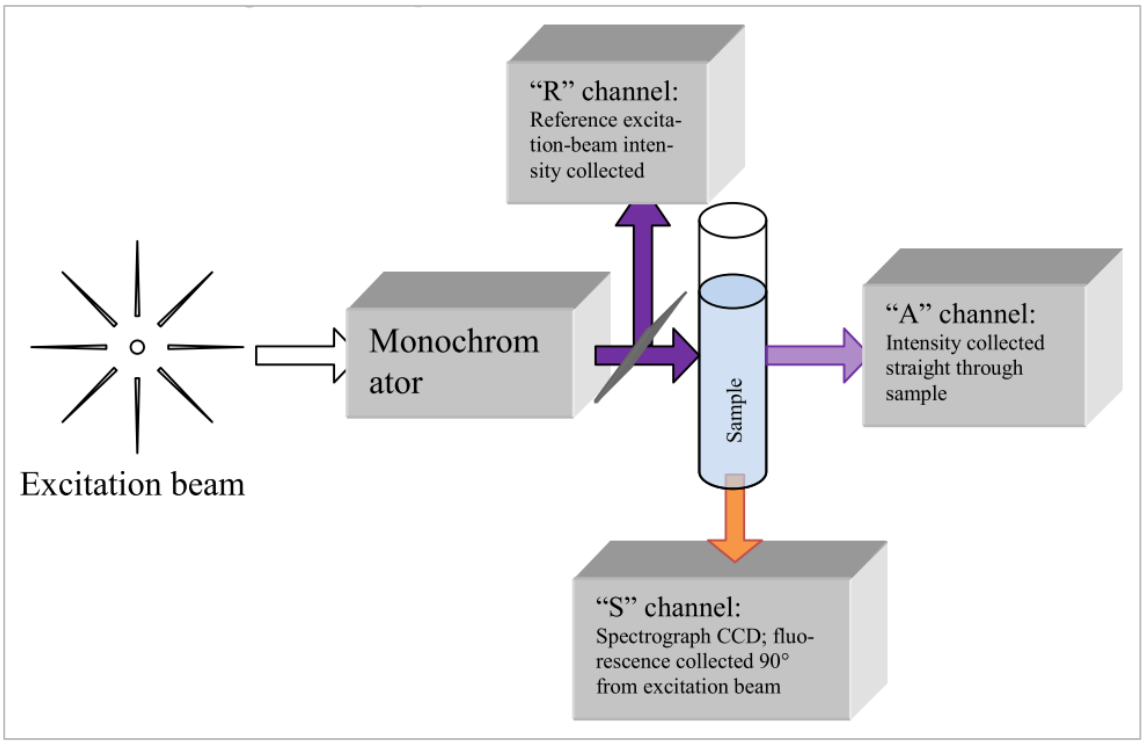

Figure 2.1: Schematic of the excitation light source, emission and reference detectors of the Aqualog®, Horiba Ltd., Japan (HORIBA Ltd., 2013). Image used with the permission of HORIBA Ltd.

Instrument function and data output is controlled via the Aqualog® spectroscopy software. The scan parameters employed were; excitation wavelengths from 200 to 500 nm via 1 nm steps, and emission wavelengths of 247.88 to 829.85 nm in 1.16 nm steps. The integration time used varied depending upon sample type; 0.5 s for bacterial cultures and 0.6 s for environmental samples. Sample transmittance and absorbance measurements were collected for IFE correction, detailed in section 2.1.1.1.1. A standard 3.5 mL quartz cuvette with a 10 mm path-length was used for environmental sample analysis and initial culturing. A 1400 µL quartz cuvette with a 10 mm path-length was

used for bacterial cultures. Some samples were also diluted where required, to prevent CCD saturation, using the blank medium specific to the sample type.

2.1.1.1.1 Aqualog® Absorbance measurements and IFE correction

The transmittance detector signal is used to calculate the absorbance (Abs) and transmittance (T) values within the Aqualog®. I_0 is taken from the sample blank and I from the sample being evaluated (HORIBA Ltd., 2013). The transmission (T_λ), percent transmission ($\%T_\lambda$) and absorbance values (Abs) at a given wavelength are calculated as follows:

$$T_\lambda = \frac{I}{I_0} \qquad \text{Equation 2.1}$$

$$\%T_\lambda = 100\ x\ \frac{I}{I_0} \qquad \text{Equation 2.2}$$

$$Abs = -\log_{10}(T) \qquad \text{Equation 2.3}$$

Common practice for IFE correction is to use the absorbance measurements from the sample and blank, as discussed above. For accurate IFE correction, the sample concentration must fall within the linear Beer-Lambert region for the absorbance spectra associated with the EEM (HORIBA Ltd., 2013). The algorithm employed by the Aqualog® requires measuring the absorbance spectra of the sample for the overlapping range of both the excitation and emission spectra. The use of this algorithm requires the use of a standard cuvette with 10 mm pathlength (HORIBA Ltd., 2013). The following equation is applied to each excitation-emission wavelength coordinate within the EEM:

$$F_{ideal} = F_{obs} \times 10^{\frac{Abs_{Ex} + Abs_{Em}}{2}}$$ Equation 2.4

Where F_{ideal} is the ideal fluorescence signal spectrum in the absence of IFE, F_{obs} is the observed fluorescence signal, and Abs_{Ex} and Abs_{Em} are the measured absorbance values at the respective excitation and emission wavelengths (HORIBA Ltd., 2013).

2.1.1.2 FluoroSENS

The fluoroSENS (Gilden Photonics Ltd., UK) fluorimeter is a high performance, fully integrated benchtop fluorimeter that utilises a 150-W xenon arc-lamp. The instrument utilises the Czerny-Turner design with flexible excitation and emission monochromators, with a 300 mm focal length. Both the excitation and emission monochromators have triple gratings, 300 nm and 500 nm blaze respectively, and variable a bandpass (0.1 nm to 10 mm) (Gilden Photonics, 2009). The emission is detected using a single-photon counting photomultiplier. Instrument correction, provided by the reference photodiode detector, is applicable but fluorescence spectra cannot be corrected for IFE using simultaneous absorbance detection (Gilden Photonics, 2009).

A fluoroSENS (Gilden Photonics Ltd., UK) fluorimeter was used to collect initial fluorescence spectroscopy data, using a 3.5 mL quartz cuvette with a 10 mm path-length. The following scan parameters were employed: excitation wavelengths from 200 to 450 nm at 5 nm steps; emission wavelengths of 250 to 550 nm with 5 nm bandpass; integration time of 200 ms.

2.1.2 Fluorescence spectra post-processing, interpolation and data analysis

2.1.2.1 Post-processing of fluorescence spectra

Spectra measured on the Aqualog® were blank subtracted, corrected for IFE (for both excitation and emission wavelengths) and first and second order Rayleigh Scattering masked (±10 nm at $\lambda_{ex}=\lambda_{em}$ and $2\lambda_{ex}=\lambda_{em}$) (Coble *et al.*, 2014; McKnight *et al.*, 2001). Instrument validation was undertaken daily with a quinine sulphate standard (Starna Cells, USA), with CV being < 3% (n = 5) in all events. This fluorescence data is reported in quinine sulphate units (QSU), determined from normalising data to the fluorescence from 1 μg L^{-1} quinine sulphate in 0.105 M perchloric acid at λ_{ex} = 347.5 nm and λ_{em} = 450 nm (Mostofa *et al.*, 2013; Shimotori, Watanabe and Hama, 2012; Shimotori, Omori and Hama, 2009; Kramer and Herndl, 2004). This allows for quantitative analysis.

Raw relative fluorescence data, measured on the fluoroSENS, were normalised to the water Raman line at $\lambda_{ex}280/\lambda_{em}310$(300-315) nm and output in arbitrary units (A.U.) (Baker, 2002c; Determann *et al.*, 1998). Peak-picking analysis was undertaken using an R (The R Foundation) script customised from Lapworth and Kinniburgh, (2009).

2.1.2.2 Fluorescence interpolation: EEM generation

Graphical EEM generation was carried out using a custom script written in Python™ (Python Software Foundation). Where samples were diluted the EEM matrix was multiplied by the dilution factor. The script crops the data window to λ_{ex} 240-490 nm, λ_{em} 250-550 nm to allow for the analysis of the UV spectra, the area of interest within

aquatic fluorescent organic matter (AFOM) work. Data λ_{ex} <240 nm was discounted due to the data quality produced by the Aqualog® caused by the signal to noise ratio.

2.1.2.3 Analysis of fluorescence spectral data

The increased implementation of fluorescence spectroscopy has led to the development of multiple methods for analysing the resultant data (Bridgeman *et al.*, 2015). This is particularly important within complex sample matrices as, although EEMs enable the visual comparison of samples, dominant fluorophores can often mask other fluorescent compounds with similar optical properties (Stedmon and Bro, 2008). Some of these analytical techniques include 'peak-picking', self-organising maps (SOMs) and the commonly utilised parallel factor (PARAFAC) analysis. PARAFAC analysis, although the norm within the field, is not without its limitations, whilst 'peak-picking' permits for a more focussed and detailed understanding of certain peaks of interest, allowing for the comparison of fluorescence peaks between samples.

PARAFAC analysis is a multivariate statistical analysis that decomposes EEM data (Murphy *et al.*, 2014). This trilinear component analysis decomposes common polygons within the dataset and allows for the comparison of components of different water samples, highlighting variations in OM fluorescence (Qian *et al.*, 2017; Harun *et al.*, 2015; Stedmon, Markager and Bro, 2003). Furthermore, PARAFAC analysis can be employed to identify overlapping components within the EEM data that may not be visible as independent peaks (Cory *et al.*, 2010; Larsen *et al.*, 2010). However, it can be limited in this regard, often incorporating similar, yet different, fluorescence components as one

(Yu *et al.*, 2015; Shutova *et al.*, 2014). This occurs most commonly when samples from multiple sources are combined into a single PARAFAC model, and can be avoided by creating datasets of samples from similar environments (Yu *et al.*, 2015; Fellman, Hood and Spencer, 2010).

The custom Python™ (Python Software Foundation) script used for EEM generation (section 2.1.2.2) also incorporated peak picking for specific fluorescence peaks. PARAFAC analysis was used to decompose the EEM data (Stedmon and Bro, 2008) using Solo (Eigenvector Research Inc., WA, USA) software, which employs the PLS-Toolbox with MATLAB®. The PARAFAC model was validated by CORCONDIA and investigation of the models' residuals. For specific fluorescence peaks of interest peak-picking analysis was undertaken using Python™.

2.2 Dissolved oxygen measurements

Initially the dissolved oxygen (DO) of the samples was determined using both a DO meter and standard Winkler titrations, as described below (APHA AWWA WEF, 1999). Slight differences were identified between the absolute values reported by the two methods but the trend in the data was similar ($R^2 = 0.97$, $p < 0.05$). It is likely that variations in the measurements obtained using the different methods are caused by method specific limitations, such as the subjective nature of colour change identification for the titration method. As such, the DO meter was used for all further DO measurements.

2.2.1 Winkler titration

Winkler titrations were conducted as per the standard method [ES EN 1889-2:1998] (APHA AWWA WEF, 1999), which involves fixing the DO content of the bottle by adding 2 mL of 48% manganese sulphate followed by 2 mL of alkali-iodide-azide solution to form a precipitate. 2 mL of concentrated sulphuric acid is then added to dissolve the precipitate. Once this process has taken place the samples need to be titrated within 8 hours.

0.0125 M sodium thiosulphate was used as the titrant, made daily from a stable stock 0.1 M solution. This was added to 100 mL of the fixed sample until the colour turned to 'pale straw'. Once the desired colour was reached, 2 mL of starch solution was added to the conical flask as a colour indicator. Titrant was added further until the solution turned from dark blue to colourless. When using 0.0125 M sodium thiosulphate as a titrant with 100 mL of sample, 1 mL of titrant used is equal to 1 mg/L DO.

2.2.2 Dissolved oxygen meter

An optical DO meter (HQ10, Hach, CO, USA) was also used to record dissolved oxygen measurements. Each sample was read in triplicate and data averaged. Calibration of the DO meter was carried out daily.

2.3 Measuring biochemical oxygen demand

Biochemical oxygen demand (BOD) is a standard measure for determining the bioavailable organic content of water. BOD analysis measures the amount of oxygen required, by the microbial population present, to degrade the biodegradable fraction of organic matter (Cutrera *et al.*, 1999). The 5-day BOD test (BOD_5) is a common analysis used within industry to determine the amount of biodegradable organic material within a sample, providing a proxy that infers biological activity. This involves an initial dissolved oxygen (DO) measurement on day 0, incubating water samples at 20°C in the dark for 5 days, and then taking a second reading on day 5. The BOD of the sample is represented by the difference between the initial and final DO.

The BOD_5 tests were carried out in accordance with the standard methods (APHA AWWA WEF 1999). Samples were added to stoppered bottles which were filled until overflowing to allow for the creation of a water seal. A bottle was prepared for each sampling time point, as not to introduce oxygen into the sample.

The standard method describes the possibility that samples where oxygen may be a limiting factor, such as wastewaters, require dilution to ensure there is an excess supply of oxygen. The dilution water was made using distilled water with nutrient additives. The additives were a phosphate buffer, 0.25 M calcium chloride solution, 1 M magnesium sulphate solution and 2 mM ferric chloride. 1 mL of each nutrient solution was added for every litre of dilution water. To saturate the dilution water with oxygen, it was aerated for 24 hours before being used. Further to dilution, some samples, such as treated wastewaters and chemical standards, require a bacterial seed. A

glucose/glutamic acid (150 mg/L) solution was also prepared to provide a carbon source for diluted samples.

2.4 Bacterial enumeration

2.4.1 Flow cytometry

Flow cytometry is used to analyse chemical and physical characteristics of particles in a fluid and is frequently employed in biotechnology for cell enumeration, utilising fluorescent labelling protocols. Flow cytometry has become increasingly used due to the rapid data acquisition over traditional enumeration techniques, which require a minimum 18 hour incubation time. Flow cytometry, depending upon the stain utilised, also allows for the identification of a range of cell types and determination of viability. This has made it very popular for bacterial enumeration due to the known issues with culturing bacteria, particularly from complex environmental samples.

Bacterial enumeration was performed by flow cytometry using a Accuri® C6 (BD Biosciences, USA). The flow cytometer was validated daily to ensure <2.5% instrument error. Samples were run at a flow rate of 11 μL/min using a core size of 5 μm for one minute. Manually drawn gates were created to discriminate between bacterial cells and background particulates.

2.4.1.1 BacLight™ Green

Initial experiments focussed on absolute bacterial enumeration with samples fixed using 4% paraformaldehyde (PFA), with a final concentration of 2% (v/v). BacLight™ Green (Molecular Probes™, Invitrogen, USA) was used to stain bacterial samples. A 1x working concentration was used, from a 2x concentrated stock solution, and samples were incubated at room temperature for 15 minutes in the dark.

2.4.1.2 BacLight™ LIVE/DEAD®

To differentiate between viable and non-viable cells, samples were stained using BacLight™ LIVE/DEAD® (Molecular Probes™, Invitrogen, USA) bacterial viability staining kit. Samples were not fixed to allow the analysis of viability and were analysed within one hour of collection. A 2x concentrated stock was made using filter sterilised water (Molecular Probes™ 2004). Samples (50 μL) were stained, at 1x working concentration, for 15 minutes, in the dark, prior to analysis. All bacterial enumeration data is reported in cells mL^{-1}. Two manually drawn gates were used to distinguish live and dead cells (Molecular Probes™ 2004)

2.4.2 Optical density

Optical density (OD) is attenuation determined by absorbance and scattering, routinely used to represent the relative increase in cell numbers within a sample when monitoring bacterial growth (Hall *et al.*, 2014). A 1 mL aliquot of the sample was put into a disposable

cuvette (Sarstedt AG & Co., Germany) and OD measured at 600 nm (WPA Spectrawave S1200, Biochrom, UK).

2.5 Collection and storage of water samples

2.5.1 Sampling location

The freshwater samples were collected from a water body at the University of the West of England (N 51° 29′ 56″, W 2° 32′ 39″), shown in Figure 2.2. This water body receives OM inputs from both allochthonous and autochthonous sources, such as surface runoff and biological matter respectively, and is artificially aerated, providing an oxygen rich environment. The use of this sampling location allows sample integrity to be preserved due to the proximity to the laboratory. The long-term installation of a telemetry system, with historical water quality data, also makes this a preferable location.

Figure 2.2: Sample site for environmental freshwater sample collection (N 51° 29′ 56″, W 2° 32′ 39″). Samples were collected from the location of the buoys, which is where the sensor suite is installed at a depth of ~30 cm.

2.5.2 Collection technique

Water samples were collected from the location of the buoys (Figure 2.2), approximately 30 cm from the surface. Collection was carried out using a five litre HDPE container that was cleaned with a 1% Virkon™ (Virkon Disinfectant Technologies, UK) solution, and then rinsed thoroughly to ensure there would be no bacterial or chemical contamination of the sample. Prior to collection, the aspirator was also rinsed three times with water from the water body.

2.5.3 Storage and handling of water samples

Water samples were analysed or prepared for experimental setups within 2 hours of collection to limit changes in the composition and characteristics. Samples were not stored prior to use or analysis, and as such did not need to be chilled or fixed, allowing sample integrity to be maintained.

2.6 Culturing bacterial inoculum

2.6.1 Standardised mixed bacterial culture

A standardised bacterial inoculum, containing a non-pathogenic bacterial mixture (Cole Parmer Instrument Company, USA), was used to provide a source of bacteria for the mixed culture model system (section 2.7.2). The inoculum was activated by rehydrating the capsule contents in 500 mL of sterile de-ionised water and aerating the mixture for

an hour for acclimatisation. The inoculum was then added to individual sample bottles, 0.5% (v/v).

2.6.2 Laboratory bacterial cultures

Bacterial cultures were obtained from a culture collection at the University of the West of England, Bristol. Cultures were streaked onto nutrient agar (Oxoid Ltd., UK) plates from frozen stocks and incubated for 24 hours at 37°C. Species, strain and the justification for species analysis is detailed in Table 2.1. Overnight liquid cultures were obtained by inoculating media (section 2.7.1.1) with pure bacterial colonies, obtained from the overnight streak plates, and incubating at 37°C, shaking at 150 rpm.

Table 2.1: Bacterial species and strains obtained from the University of the West of England culture collection.

Bacterial species	Strain	Justification
Escherichia coli	ATCC 10536	Presence in freshwaters can indicate sewage contamination (Sigee, 2004)
Bacillus subtilis	ATCC 6633	Ubiquitous soil bacterium (Graumann, 2007)
Pseudomonas aeruginosa	NCIMB 8295	Ubiquitous in freshwater systems (Elliott, Lead and Baker, 2006a; Sigee, 2004)

2.6.3 Culturing bacterial strains from environmental water samples

To identify AFOM production by environmental bacteria, strains were isolated and cultured from the freshwater body samples (section 2.5). The water was vacuum filtered through 0.2 μm filters (Whatman® 0.2 μm nitrocellulose membrane filters, GE Healthcare, UK). Filters were then placed on three different types of agar plates to select for different bacteria: R2A agar (Oxoid Ltd., UK) was used for total environmental counts; Brilliance™ *E. coli*/Coliform medium (Oxoid Ltd., UK) to allow for the identification of *E. coli*, coliforms and *P. aeruginosa*; and Difco™ *Pseudomonas* Isolation Agar (Difco Laboratories, USA) differential media as another way of selecting for *P. aeruginosa*. Agar plates were incubated for 24 hours at 37°C. Twelve single colonies were then sub-cultured on nutrient agar plates for 24 hours at 37°C.

These unknown environmental bacterial isolates were run through an identification process using a BiOLOG MicroStation™ (BioTek Instruments, USA). Prior to the inoculum preparation, a Gram stain (Black, 2005) was conducted to ensure the correct inoculating fluid and well-plates were used for identification. Cultures were prepared using the inoculating fluid (BioTek Instruments, USA) to the required cell density using a BiOLOG Turbidimeter (BioTek Instruments, USA); 52% and 19% transmittance for Gram negative and positive bacteria respectively. The inoculum was then transferred to the corresponding pre-prepared 96-well plates; SF-N2 MicroPlate™ for Gram negative bacteria and SF-P2 MicroPlate™ for Gram positive bacteria (BioTek Instruments, USA). A catalase test (MacFaddin, 2000) was also undertaken for the 12 species to narrow the species library search further. Six of the environmental bacteria species isolated, which

were identified with probability >90 % to at least the Genus level (Table 2.2), were investigated further.

Table 2.2: Identification (BiOLOG MicroStation™, BioTek Instruments, USA) and characteristics of bacterial species isolated from an environmental freshwater.

	BiOLOG Identification	Gram (+/-)	Catalase (+/-)
1	*Escherichia coli*	-	+
2	*Enterobacter nimipressuralis*	-	+
3	*Bacillus subtilis*	+	+
4	*Pseudomonas sp.*	-	+
5	*Aeromonas sp.*	-	-
6	*Staphylococcus aureus*	+	+

2.6.4 Obtaining a microbial community inoculum from an environmental freshwater sample

An environmental freshwater sample (section 2.5) was used to obtain the community inoculum; one sub-sample was used without filtration whilst one was filtered at 11 μm to remove particulate matter but retain cells, where not attached to particles or within a biofilm. 1 mL of this each inoculum (both unfiltered and filtered) was added to 9 mL of the minimal media (section 2.7.1.1). Inoculated media were then incubated overnight at a range of temperatures; 25°C, 30°C and 37°C. Once grown up overnight, cultures were centrifuged for 10 minutes at x 4000 g and washed three times in osmotically stable ¼ strength Ringer solution (Oxoid Ltd., UK), to remove media/supernatant and organic matter. The cell pellets were then resuspended in 10 mL of the minimal media and used as a mixed culture inoculum.

2.7 Development of laboratory model systems for investigating microbial processing of aquatic fluorescent organic matter in freshwater systems

Laboratory model systems were developed to allow for a more in-depth understanding of bacterial-AFOM dynamics and interactions, in particular how such interactions are impacted by microbial communities within a system as well as certain physicochemical parameters, such as temperature. Two model systems were developed: Model system 1 for determining fast-acting bacterial production of AFOM at a species level; and, Model system 2 to represent a low nutrient environment and assess microbial processing and production of AFOM with increased residence time.

2.7.1 Model System 1: Monoculture model system – determining fast-acting bacteria-AFOM interactions at a species level

A laboratory model system was developed to allow optimum growth of bacterial monocultures, further investigating the microbial production of AFOM. The base media used was the minimal media developed (section 2.7.1.1). This media was inoculated with liquid inoculum of each bacterial species (section 2.6.2), using a 1 in 100 dilution.

2.7.1.1 Development of a low-fluorescent minimal medium: DM+

A low-fluorescent medium was required for the growth of bacterial monocultures. Growth media usually contains proteinaceous material which gives rise to background fluorescence. Therefore, exploratory work was undertaken to develop a minimal

medium for optimum growth of a range of bacterial species. Two known minimal media, M9 minimal salt medium (Geerlof, 2010) and Davis and Mingioli liquid medium, without the addition of amino acids (Davis and Mingioli, 1950), were used within this exploratory work. Additionally, $CaCl_2$ and trace element solution (Kragelund and Nybroe, 1994) were further added to the Davis and Mingioli minimal medium. Each media type was inoculated with bacterial monocultures and Costar® 3596 96-well plates (Corning® Inc., USA) were used to monitor growth over a 24-hour period. An Infinite® 200 PRO (Tecan Trading AG, Switzerland) plate reader was used to obtain OD data every 15 minutes for the well-plates. Experiments were run in triplicate and data averaged to determine the best growth medium; examples of this with *Bacillus subtilis* and *Pseudomonas aeruginosa* are shown in Figure 2.3. The final basal medium developed, hereby referred to as DM+ minimal media, contained a 0.2% v/v glucose solution, as the sole carbon source, and with sources of phosphate, nitrogen, sodium and magnesium (Davis and Mingioli, 1950), $CaCl_2$ (final concentration 0.035% v/v) and trace elements (concentration 0.1% v/v), obtained from Kragelund and Nybroe (1994).

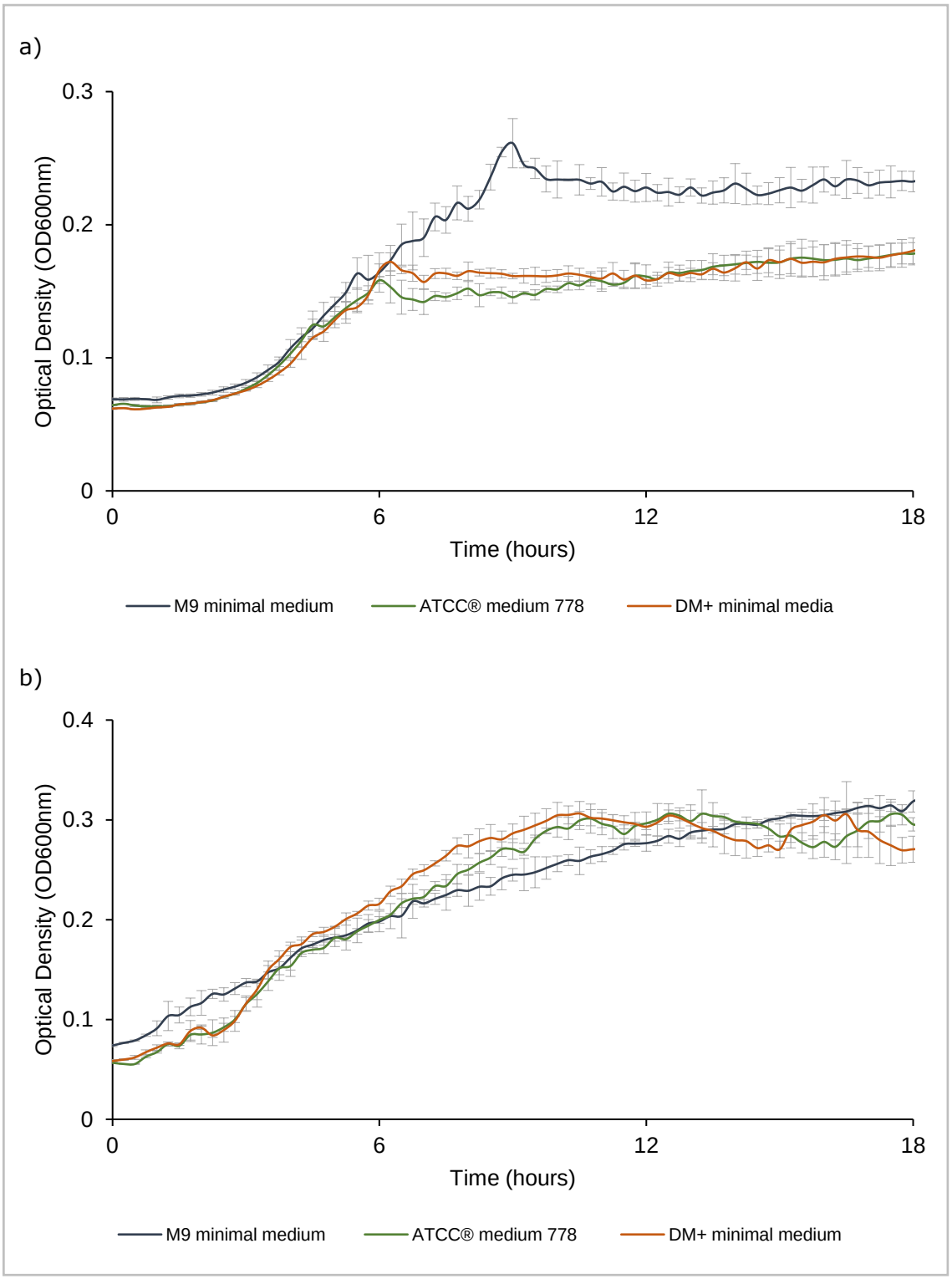

Figure 2.3: Optical density (OD_{600nm}) data for a) *Bacillus subtilis* and b) *Pseudomonas aeruginosa* growth curves (n = 3, ± 1 standard deviation), obtained from using an Infinite® 200 PRO (Tecan Trading AG, Switzerland) plate reader. Data shown compares the bacterial growth within the minimal medium developed here (DM+) and two commonly used minimal media, M9 minimal medium (Geerlof, 2010) and ATCC® medium 778 (Davis and Mingioli, 1950).

Further exploratory work was undertaken to quantify the contribution, if any, of the developed minimal media (DM+) to the background fluorescence. The basal media (ATCC® medium 778) was initially sterilised via autoclaving at 121°C for 15 minutes (Davis and Mingioli, 1950), but this produced a complex fluorescence signal (Figure 2.4a). To prevent this, the media was sterile filtered using Sartobran® 300 0.2 µm cellulose filter (Sartorius Stedim Biotech, Germany), resulting in the fluorescence signal shown in Figure 2.4b. Glucose solution was also sterile filtered (Minisart® 0.2 µm cellulose filter, Sartorius Stedim Biotech, Germany), whilst the $CaCl_2$ and trace element solutions were autoclaved at 121°C for 15 minutes, before being added to the basal medium, prior to inoculation.

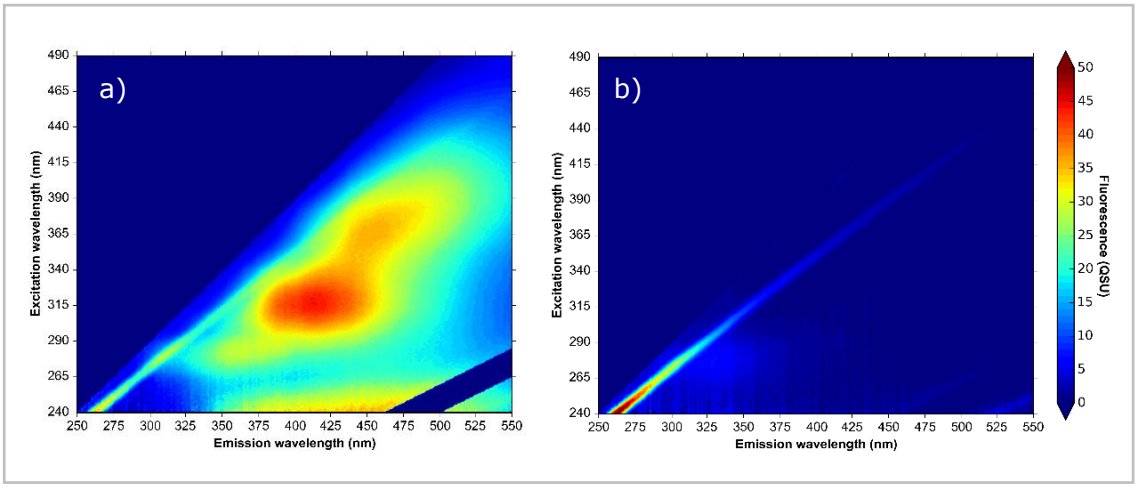

Figure 2.4: Fluorescence excitation-emission matrices of the DM+ minimal medium developed, subjected to two different sterilisation protocols: a) sterilised via autoclaving at 121°C for 15 minutes; b) sterile filtered (Sartobran® 300 0.2 µm cellulose filter; Sartorius Stedim Biotech, Germany). Fluorescence is reported in quinine sulphate units (QSU); 1 QSU is equivalent to the fluorescence intensity, of 1 µg/L quinine sulphate at $\lambda_{ex}/\lambda_{em}$ 347.5/450 nm.

2.7.1.2 Bacterial growth curves

Growth curves (n = 9 i.e. nine independent replicates) of each laboratory bacterial strain (Table 2.1) were undertaken by inoculating 150 mL of the sterile minimal medium (section 2.7.1.1) from a fresh overnight plate culture (section 2.6.2) and incubating the samples at 37°C, shaking at 150 rpm. 2 mL aliquots were collected every 30 minutes for fluorescence measurements (section 2.1.1.1) and optical density (OD) measurements (section 2.4.2).

2.7.1.3 Bacterial culture analysis

Media was inoculated from a fresh overnight plate culture (section 2.6.2) with each of the bacterial species and incubated overnight at 37°C, shaking at 150 rpm throughout. Overnight cultures were centrifuged at 5000 x g for 5 minutes (Allegra X-30R, Beckman Coulter™, USA) to form a bacterial pellet. Samples were segregated to provide information about intra- and extracellular AFOM and to address some of the current understanding surrounding the contribution of cell lysis to the AFOM signal (Elliott, Lead and Baker, 2006a). The supernatant was pipetted off and filtered using a Minisart® 0.2 μm cellulose filter (Sartorius Stedim Biotech, Germany) to guarantee all cells were removed. The pellet was resuspended and washed 3 times in 5 mL of osmotically stable ¼ strength Ringer solution (Oxoid Ltd., UK) to ensure that any supernatant or media was no longer present. To physically lyse the cells, a 1 mL aliquot of the resuspended cells was sonicated (Ultrasonic Processor XL 2020, Misonix Inc., US) in three 10 second pulses at a fixed frequency of 20 KHz, not exceeding 40% amplitude, and kept over ice

throughout (Doron, 2009). Physical lysis was undertaken, rather than chemical lysis techniques, to ensure the fluorescence properties of the sample was not altered (nine independent replicates). An endospore suspension for *B. subtilis* was prepared as described by Lawrence and Palombo (2009). To check for the presence of endospores and the removal of vegetative cells, an endospore stain was conducted using the Schaeffer-Fulton method (Schaeffer and Fulton, 1933). All samples (raw, supernatant, resuspended cells and lysed cells) were subject to fluorescence-EEM spectroscopic analysis. Flow cytometry bacterial enumeration was not used as the BacLight® LIVE/DEAD viable staining kit was ineffective with *P. aeruginosa*, due to excretory mechanisms within the cells. This was verified by lack of significant correlation between flow cytometry enumeration and traditional colony counts in cfu/mL (Gilchrist *et al.*, 1973), obtained using 50µL of liquid culture dispensed via a Whitley Automated Spiral Plater (Don Whitley Scientific Ltd., UK).

2.7.1.4 Model System 1: Culturing bacteria isolates from an environmental freshwater

The monoculture laboratory model system (section 2.7.1) was further adapted to analyse the ability of bacterial species isolated from an environmental freshwater (section 2.6.3) and an isolated mixed environmental culture (section 2.6.4) to produce and process AFOM.

The six bacteria isolates (Table 2.2) were cultured overnight in the minimal media (section 2.7.1.1) at three different temperatures, 25°C, 30°C and 37°C. A range of

temperatures were employed to assess the impact of selective conditions on growth, species preference and the AFOM signal. Isolated environmental mixed cultures were also used to assess the impact of microbial interactions on AFOM produced within a model system. Overnight mixed cultures were incubated at a range of temperatures, 25°C, 30°C and 37°C, in line with the temperature at which initial culturing had occurred. The potential impact of residence time on AFOM production was also explored by culturing for 24, 48 and 72 hours. All cultures were then subject to analysis, as described in section 2.7.1.3. Each sub-sample type was analysed for fluorescence-EEM spectroscopy and experiments conducted in triplicate.

2.7.2 Model System 2: Mixed culture model system – bacterial-AFOM interactions over a 10-day incubation period

The BOD method (section 2.3) was altered as described below to develop this laboratory model system to investigate the microbial processing of AFOM. Samples were either collected (environmental, section 2.5) or prepared (synthetic). These were incubated, with triplicate sample bottles, at 20°C in the dark over a 10-day period in individual airtight 300 mL bottles, sealed with PARAFILM (APHA AWWA WEF, 1999).

The dilution water from the BOD Standard Method (section 2.3) was used as the base media for the synthetic samples in the mixed culture model system, to limit AFOM production and better simulate environmental AFOM fluorescence intensity. Glucose and glutamic acid were both added as carbon sources (APHA AWWA WEF, 1999). The use of this media composition prevents a strong background fluorescence signal

(Shimotori, Watanabe & Hama, 2012), whilst providing sufficient nutrients for bacterial growth. This is beneficial over a nutrient rich media, such as nutrient broth (Oxoid Ltd., UK), even in dilute form (Figure 2.5), or the addition of a protein source, such as peptone water (Oxoid Ltd., UK), as these have a particularly intense fluorescence signal in the protein-like region, inhibiting the identification of production and utilisation within the AFOM region. Although this can be corrected for, using blank subtraction and inner-filter correction, using a non-fluorescent media reduces the likelihood of negative values and minimises attenuation of the base sample. The standardised mixed bacterial culture (section 2.6.1) was used as the bacterial inoculum for the synthetic samples. Additionally, some synthetic samples were supplemented with 2% (v/v) environmental water to act as an OM source, hereafter referred to as supplemented synthetic samples. To account for any fluorescence development via abiotic pathways two negative controls were used;

i. media with heat treated inoculum
ii. media without bacterial inoculum

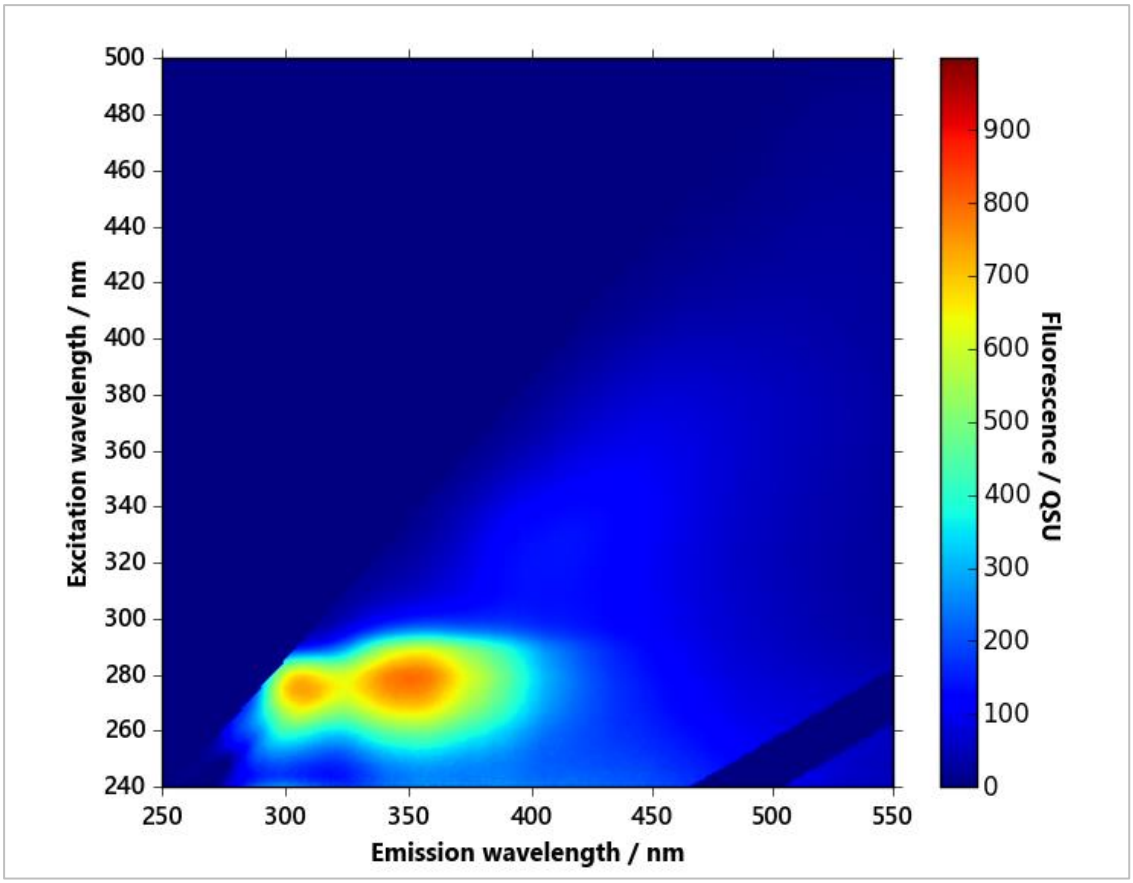

Figure 2.5: Fluorescence excitation-emission matrix of nutrient broth at 5% concentration. Fluorescence is reported in quinine sulphate units (QSU); 1 QSU is equivalent to the fluorescence intensity, of 1 μg/L quinine sulphate at $\lambda_{ex}/\lambda_{em}$ 347.5/450 nm.

2.7.2.1 Bacterial AFOM: production hour by hour

To further develop the mixed culture model system, synthetic samples were then used in time-resolved experiments whereby aliquots of 5 mL were taken hourly from one litre Duran® bottles (Duran Group, Germany) and incubated in static conditions at the following temperatures; 20°C, 25°C, 30°C and 37°C. Aliquots were subject to fluorescence-EEM spectroscopic analysis (section 2.1.1.1) and flow cytometry (section 2.4.1) with BacLight® LIVE/DEAD viability stain (section 2.4.1.2).

2.8 *In situ* monitoring of physicochemical, biological and fluorescence characteristics

2.8.1 Discrete sampling of a freshwater system

Discrete samples of the environmental surface freshwater body were collected over a six month period, as described in section 2.5. Aliquots of each sample were analysed using fluorescence-EEM spectroscopy (section 2.1.1). Filtration was undertaken for some samples: no filtration for AFOM analysis; 11 μm (Whatman™ Type 1, GE Healthcare UK Ltd., UK) vacuum filtration removes large particles, reducing light scattering; 0.45 μm syringe filtration (Millex®-HA cellulose filter, Merck-Millipore, Ireland) allows analysis of the dissolved fluorescent fraction (DOM); and 0.2 μm syringe filtration (Minisart® 0.2 μm cellulose filter, Sartorius Stedim Biotech, Germany removes bacterial and algal cells from the sample, providing supernatant extracellular AFOM. Sub-samples were sent to Wessex Water Scientific Services, a UK accredited laboratory, ISO 17025 (2005) for standardised chemistry and microbiology analysis, detailed in Table 2.3.

Table 2.3: Chemical and microbiological tests conducted on raw environmental samples, undertaken by Wessex Water Scientific Services, an accredited laboratory, ISO 17025 (2005).

	Parameter	**Description**	**Units**
Chemistry	Chloride	Chloride on Aquakem	mg/L
	Nitrate		mg/L N
	Nitrite	Nitrite on Aquakem	mg/L N
	Phosphate	Orthophosphate on Aquakem	mg/L P
	Sulphate	Sulphate on Aquakem	mg/L
	Total Organic Nitrogen (TON)	TON on Aquakem	mg/L N
	Electrical Conductivity (EC)	EC at 25°C	µS/cm
	pH		
	Turbidity		NTU
Microbiology	2 day total count	Total plate count, incubated for 2 days at 37°C	cfu/mL
	3 day total count	Total plate count, incubated for 3 days at 22°C	cfu/mL
	Clostridium	Confirmed *Clostridium perfringens* for raw waters	cfu/100 mL
	Coliforms	Raw water coliform microbiology: *Escherichia coli* and Total coliforms	cfu/100 mL
	Enterococci	Confirmed *Enterococci* for raw waters	cfu/100 mL
	Pseudomonas aeruginosa	Confirmed *Pseudomonas aeruginosa* for raw waters	cfu/100 mL

2.8.2 Online *in situ* sensors: real-time water measurements

Table 2.4 details the suite of sensors that are installed *in situ* in a freshwater water body (N 51° 29′ 56″, W 2° 32′ 39″). The sensors provide a good overview of the

physicochemical parameters of the water body. These sensors are calibrated annually and cleaned on a regular basis (every two to four weeks). This water body is an artificial freshwater system that serves the purpose of an urbanised drainage basin, as well as supporting a variety of wildlife. As such, it provides a good testing ground for a range of contaminants.

Table 2.4: Description of sensors installed *in situ* for long-term monitoring of a freshwater body.

Sensor	Parameters measured	Units
Eureka Manta 2	Water temperature	°C
	pH	NA
	Dissolved oxygen	mg/L
	Electrical Conductivity (EC)	µS/cm
CTG UviLux CDOM	Peak C Fluorescence $\lambda_{ex}/\lambda_{em}$ 280/360	QSU
CTG UviLux Tryptophan	Peak T Fluorescence $\lambda_{ex}/\lambda_{em}$ 280/450	QSU
CTG UniLux Turbidity		FNU

2.8.2.1 Sensor data collection

The sensor suite is digitised and installed in a remotely accessed telemetry system, which utilises Adcon Addit4 radio telemetry units (RTU's) (Adcon Telemetry Group, Austria). Data are collected via addVANTAGE Pro 6.6 (Adcon Telemetry Group, Austria), where it can be viewed in real-time and historical data downloaded for data analysis. The sensors report data in 15 minute time intervals for high temporal resolution continuous monitoring.

Chapter 3 Bacterial engineers: the direct production of bacterial aquatic fluorescent organic matter

3.1 Introduction

The notion of allochthonous and autochthonous organic matter (OM) within freshwater systems is well documented throughout the literature system (Coble *et al.*, 2014; Carstea, 2012; Larsen *et al.*, 2010; Hudson, Baker and Reynolds, 2007). Within this, autochthonous aquatic fluorescent organic matter (AFOM) is discussed as the 'protein-like' fluorescence region, with the only other biological processing of AFOM proposed being biodegradation of some of the smaller humic acids (Coble *et al.*, 2014). In addition to the protein-like region of fluorescence ($\lambda_{ex}/\lambda_{em}$ 230-280/330-360 nm), the remainder of the freshwater AFOM spectra is largely considered to be humic or fulvic acid-like compounds. These are discussed as being stable, non-labile higher molecular weight molecules (Cooper *et al.*, 2016), derived from terrestrial sources and, therefore, considered to be an allochthonous input into the system (Coble *et al.*, 2014). However, it has been suggested, within marine AFOM research, that bacterial metabolic processes could also be responsible for some of the humic-like FOM in these environments (Guillemette and del Giorgio, 2012; Shimotori, Watanabe and Hama, 2012; Romera-Castillo *et al.*, 2011; Kramer and Herndl, 2004). Whilst microbially-mediated processes are suggested for the formation of the humic-like AFOM in the marine environment, this has yet to be demonstrated within freshwater ecosystems. This is due to the lack of direct evidence of autochthonous production of higher molecular weight AFOM.

Due to the association of protein-like fluorescence with microbial production, particularly in the Peak T region, it has been suggested that Peak T fluorescence could be used as a proxy for bacterial activity. Recent literature has attempted to correlate Peak T fluorescence with bacterial presence, specifically aimed at species enumeration (Sorensen *et al.*, 2015a, 2016; Baker *et al.*, 2015). This has led to studies focussed on the correlation between *E. coli*/coliform counts and Peak T fluorescence, a demand driven by current water quality policy. However, correlating these parameters with Peak T has had limited success and seems to be dependent upon the system being assessed.

It is clear from the current available literature that a more detailed understanding of the fundamental microbial-OM interactions in freshwater systems is needed. This chapter addresses the use of a laboratory model system to analyse the relationship between Peak T fluorescence and bacterial growth. By using a minimal media and bacterial monocultures, the dynamics of bacterial-AFOM derivation can be assessed. The data within this chapter has been published in a peer reviewed journal (Fox *et al.*, 2017), presented in Appendix 1.

3.2 Results – Model System 1: Monoculture model system

Monocultures of laboratory strain bacteria (Table 2.1) were used within laboratory Model System 1. Each individual bacterial species was analysed for fluorescence, exhibiting unique fluorescence signatures. Peak T fluorescence was the dominant peak seen in all samples, exhibiting high fluorescence intensities. This limited the application of PARAFAC analysis, whereby no robust model, CORCONDIA >90% (Bro and Kiers,

2003), that adequately explained the dataset could be identified. Subsequently, peak picking (Asmala *et al.*, 2016), an established method for spectral analysis, was applied to peaks identified within the EEMs.

Table 3.1: Identification of the fluorescence peaks, generated via bacterial processing, during bacterial growth curves and culturing experiments.

Named Fluorescence Peak	$\lambda_{ex}/\lambda_{em}$ (nm)	Peak Association
T	280/300-380	Attributed to amino acid (tryptophan) presence.
C	350/400-480	Common aquatic AFOM associated with humic substances.
A_C	250/400-460	Observed alongside Peak C but considered to be separate due to varying ratios between the two peaks. Excites in the UVC region.
C+	410/450-500	Typically associated with soils and freshwaters and attributed to terrestrially sourced CDOM.
M	240/370-430	Originally observed in marine environments but now associated with recent microbial activity in aquatic systems.
A_M	300/370-430	Associated with Peak M due to simultaneous occurrence, excites in the UVC region
X	440/510-550	Previously uncharacterised – likely to be a high molecular weight fluorophore

Nomenclature and association derived from Coble *et al.*, (2014).

3.2.1 Monitoring bacterial growth and fluorescence development

3.2.1.1 Escherichia coli

Figure 3.1 shows the *E. coli* growth curve, with Peak T as the dominant fluorescence peak present at time zero, upon initial inoculation with *E. coli* cells (Dartnell *et al.*, 2013; Sohn *et al.*, 2009). The intensity of Peak T increases alongside the optical density (OD) of the sample throughout the growth curve. There is a log increase in the intensity of Peak T fluorescence during the exponential stage of the growth curve (growth phase after acclimatisation; Hogg, 2005). This leads to a strong significant correlation between the increase in Peak T and OD, $R^2 = 0.9821$ ($p < 0.001$).

Peak C fluorescence develops during the exponential phase of the growth curve, whilst exhibiting a lag in relation to the OD (Figure 3.1). The Peak C fluorescence intensity continues to increase during the stationary phase, in which cell deaths are equal to newly formed cells (Elliott, Lead and Baker, 2006a; Hogg, 2005). A positive correlation between Peak C intensity and OD is identified, $R^2 = 0.8624$ ($p < 0.001$). The observed maximum fluorescence intensity of Peak C is a factor of 10 lower than Peak T (Figure 3.1a). Peak X (Table 3.1) is only present within the stationary phase, albeit at comparatively low fluorescence intensities (~ 30 QSU).

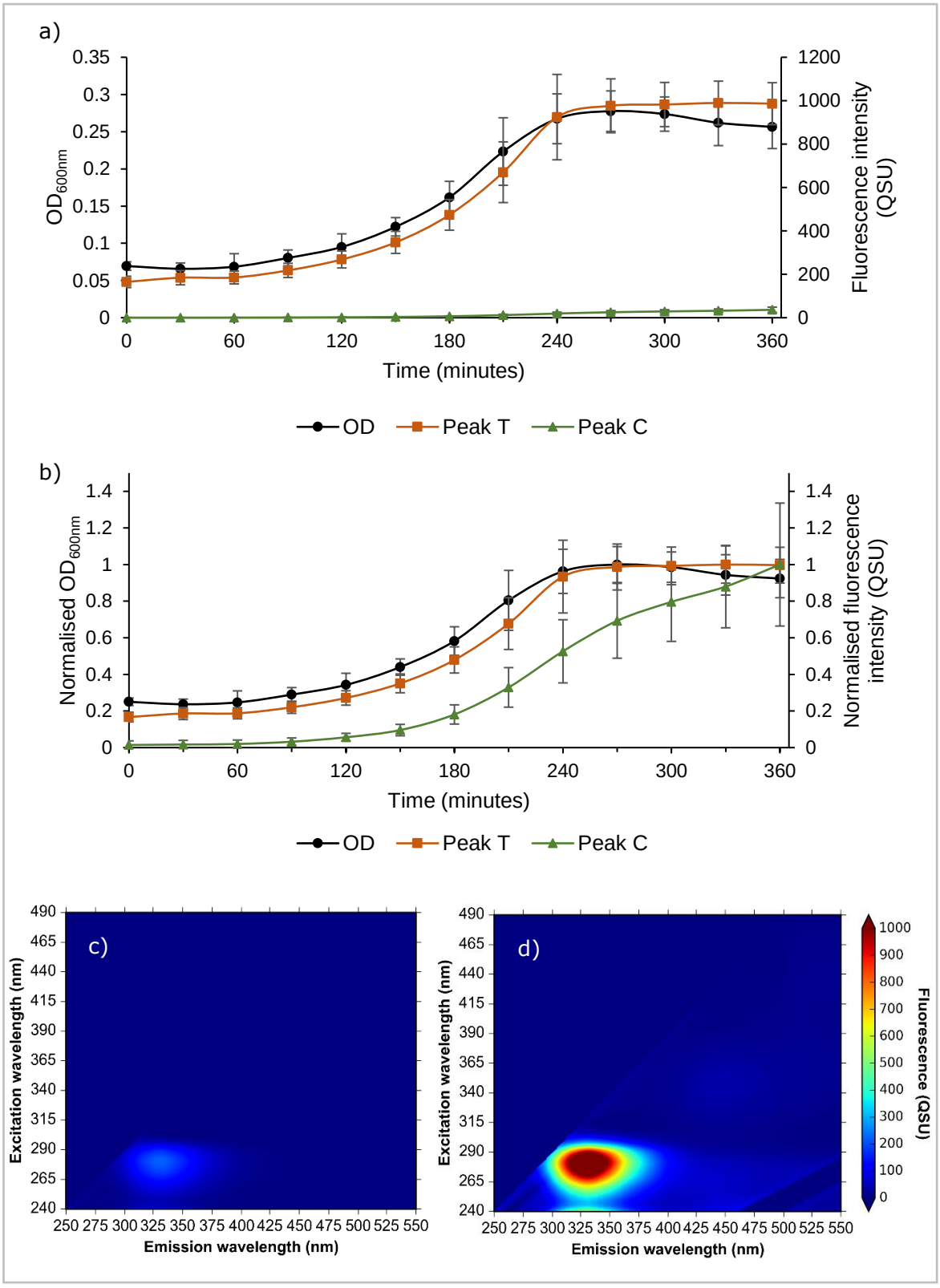

Figure 3.1: Fluorescence and optical density (OD_{600nm}) data for *Escherichia coli* growth curve, showing: a) optical density and fluorescence, QSU (1 QSU = 1 µg L^{-1} quinine sulphate) ± 1 standard deviation (n = 9); b) optical density and fluorescence data normalised to the maximum value ± 1 standard deviation (n = 9); c) excitation-emission matrix at time zero; and, d) excitation-emission matrix at 360 minutes.

3.2.1.2 Bacillus subtilis

Figure 3.2 highlights Peak T as the dominant fluorescence peak within the *B. subtilis* growth curve. Peak T intensity increases by an order of magnitude throughout the growth curve, in line with the increased OD, demonstrating a strong significant correlation, $R^2 = 0.9879$ ($p < 0.005$). Figure 3.3 demonstrates the EEM of a *B. subtilis* endospore suspension obtained from within this study. This shows the presence of Peak T fluorescence, and other protein-like fluorescence peaks.

Peak C demonstrates a sudden rise, at 360 minutes, within the *B. subtilis* growth curve. This occurs prior to the increases in both OD and Peak T development (Figure 3.2), with a strong positive correlation between Peak C fluorescence intensity and the OD being identified, $R^2 = 0.9465$ ($p < 0.005$). Florescence Peaks M and A_M are produced and observed at very low intensities within the early stationary phase of the growth curve.

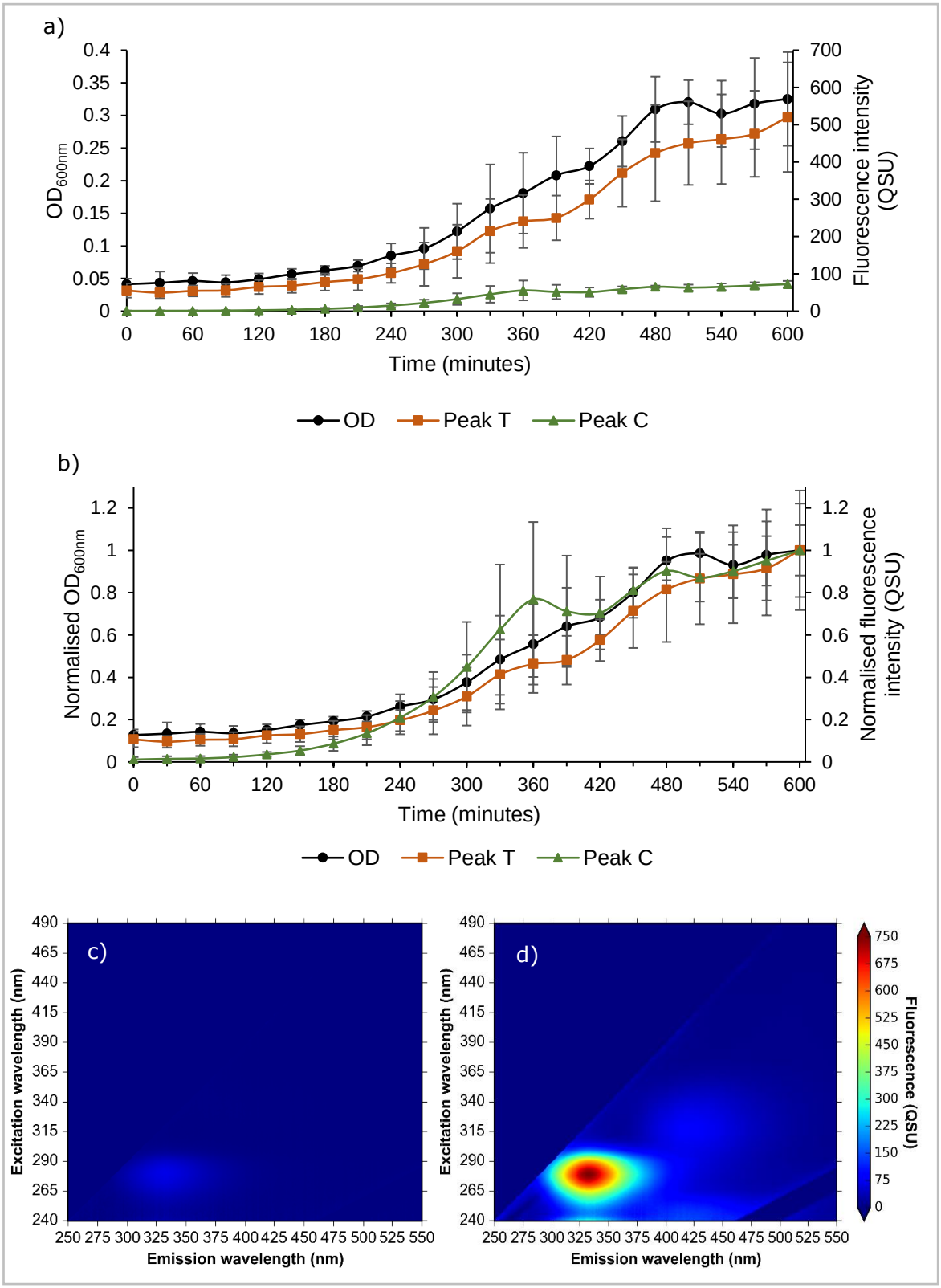

Figure 3.2: Fluorescence and optical density (OD_{600nm}) data for *Bacillus subtilis* growth curve, showing: a) optical density and fluorescence, QSU (1 QSU = 1 µg L^{-1} quinine sulphate) ± 1 standard deviation (n = 9); b) optical density and fluorescence data normalised to the maximum value ± 1 standard deviation (n = 9); c) excitation-emission matrix at time zero; and, d) excitation-emission matrix at 360 minutes.

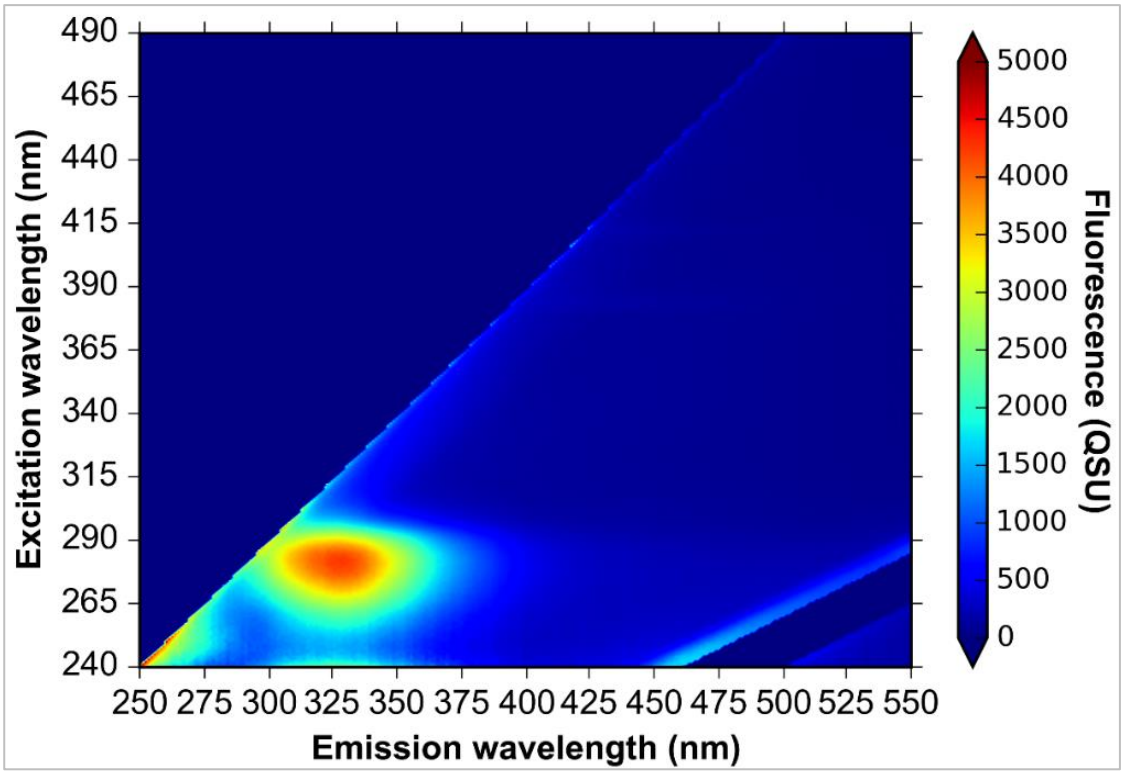

Figure 3.3: Fluorescence excitation-emission matrix of *Bacillus subtilis* endospores, QSU (1 QSU = 1 μg L^{-1} quinine sulphate).

3.2.1.3 Pseudomonas aeruginosa

Peak T is seen throughout the *P. aeruginosa* growth curve (Figure 3.4), as with the other monocultures analysed here, increasing by an order of magnitude within the exponential phase. A relatively weaker correlation, $R^2 = 0.7601$ ($p < 0.005$), is identified between Peak T and the OD across the entire length of the growth curve. This is caused by the upregulation of Peak T, independent of cell number seen at 330 minutes, in the late exponential, early stationary phase (Figure 3.4). Prior to this (within the lag and exponential phases of the growth curve), the Peak T fluorescence development tracks the OD ($R^2 = 0.9674$, $p < 0.05$).

A possible explanation for the increase in Peak T intensity is the production of exotoxin A; an iron-scavenging enzyme that is produced by *P. aeruginosa* upon entry into stationary phase (Somerville *et al.*, 1999; Lory, 1986). The binding of NAD+ to the enzyme active site of Exotoxin A quenches Peak T fluorescence; this can be used to determine protein activity (Beattie and Merrill, 1996, 1999; Beattie, Prentice and Merrill, 1996). This quenching phenomena may also explain the subsequent sudden decline in Peak T fluorescence intensity at 450 minutes (Figure 3.4).

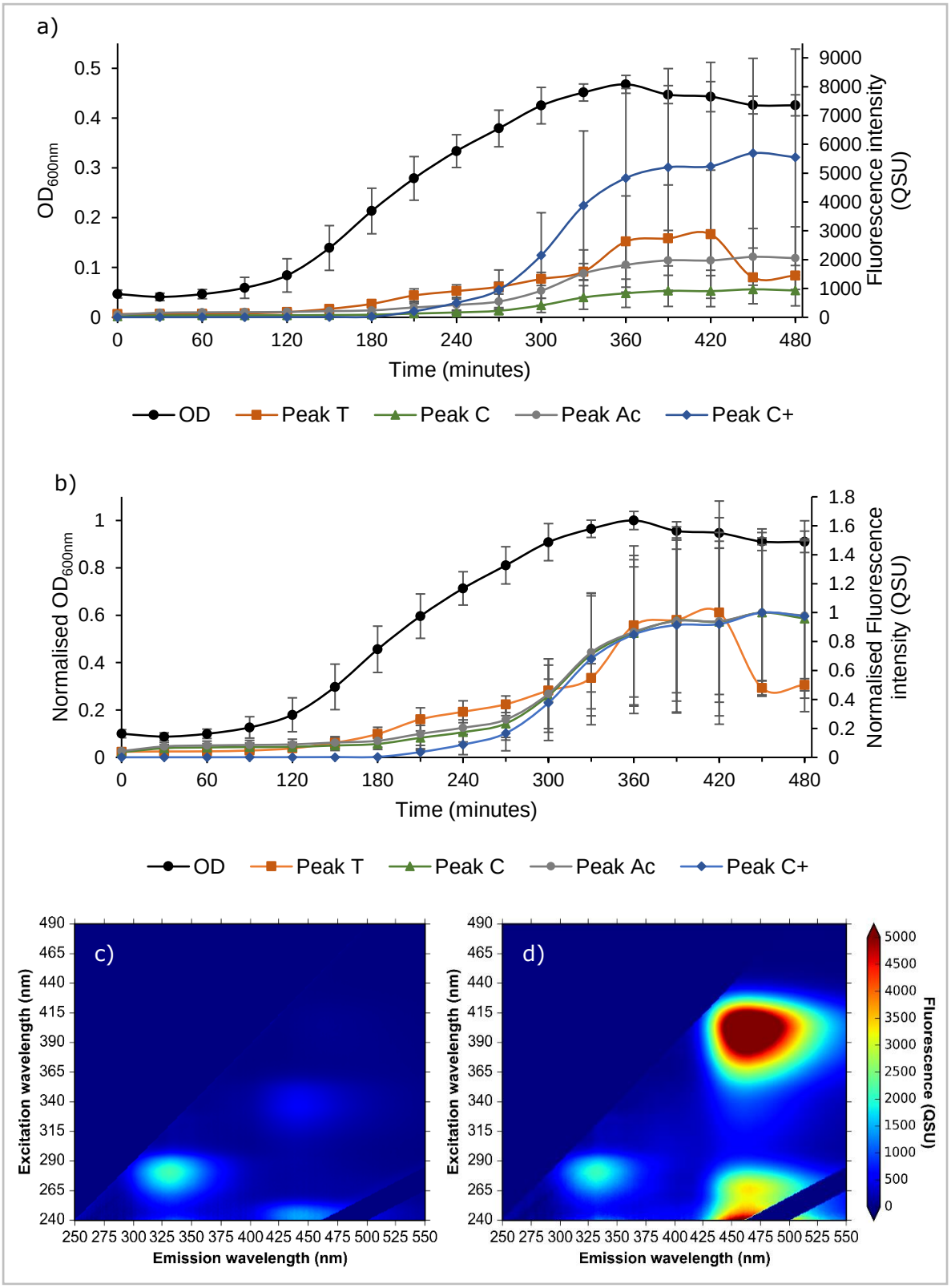

Figure 3.4: Fluorescence and optical density (OD_{600nm}) data for *Pseudomonas aeruginosa* growth curve, showing: a) optical density and fluorescence, QSU (1 QSU = 1 µg L^{-1} quinine sulphate) ± 1 standard deviation (n = 9); b) optical density and fluorescence data normalised to the maximum value ± 1 standard deviation (n = 9); c) excitation-emission matrix at time zero; and, d) excitation-emission matrix at 360 minutes.

P. aeruginosa has the most complex EEM spectra of the species analysed within this study, as described elsewhere (Dartnell *et al.*, 2013; Elliott, Lead and Baker, 2006a; Smith, Anderson and Webb, 2004). Peaks C and A_C are immediately identified upon inoculation and during the lag phase (a period of acclimatisation; Hogg, 2005), alongside Peak T. Both these peaks increase log-fold throughout the growth curve, with both Peaks C and A_C being correlated with the OD, despite a lag in fluorescence intensity at the beginning of the exponential phase; $R^2 = 0.7024$ ($p < 0.005$) and $R^2 = 0.7146$ ($p < 0.005$) respectively.

Peak C+ is also seen within the *P. aeruginosa* growth curve, developing rapidly and to a high intensity during the stationary phase (Figure 3.4). This peak is associated at present with complex high molecular weight terrestrial OM. However, fluorescence in this region of the spectra is associated with the siderophore pyoverdine (Dartnell *et al.*, 2013; Wasserman, 1965); an extracellular iron-scavenging metabolite produced by *P. aeruginosa,* associated with microbial virulence (da Silva and de Almeida, 2006). The data suggests that this Peak C+ fluorescence could be derived from the building and exporting of pyoverdine.

3.2.2 Bacterial fluorescence: overnight culturing

Overnight cultures of each species were analysed to determine the presence of AFOM in the supernatant, AFOM within resuspended cells and lysed cells (section 2.7.1.3). This provides a preliminary understanding of where the observed fluorescence is located post AFOM production.

Peak T fluorescence was the only ubiquitous fluorescence peak common to all bacterial species cultured overnight (Table 3.2). The highest intensity for Peak T fluorescence is seen within the resuspended and lysed cells, although it is present in the supernatant with the amount of extracellular Peak T varying between species (5-25%). Peak C fluorescence was observed in both the supernatant and cell lysis fractions for *E. coli* and *B. subtilis* (shown in Table 3.2), as well as all elements of the *P. aeruginosa* culture.

Peak A_C is also seen in all fractions of the *P. aeruginosa* culture and in the *E. coli* supernatant, while Peak M is observed within all fractions of the *P. aeruginosa* culture, but is only present in the *B. subtilis* supernatant. Peak C+ was also observed in the *E. coli* supernatant, but at far lower levels compared to all fractions of the *P. aeruginosa* culture. Peak X (Table 3.2) is not characterised within current aquatic AFOM research, although it is noted in life science research (Smith, Anderson and Webb, 2004). However, it is identified at low fluorescence intensities in the supernatant for the three laboratory species cultured and analysed (Table 3.2).

Table 3.2: Identified peaks generated through bacterial processing in the different fractions of the overnight cultures.

Named fluorescence Peak	*Escherichia coli*			*Bacillus subtilis*			*Pseudomonas aeruginosa*		
	Supernatant	Resuspended cells	Lysed cells	Supernatant	Resuspended cells	Lysed cells	Supernatant	Resuspended cells	Lysed cells
T	*	*	*	*	*	*	*	*	*
C	*		*	*		*	*	*	*
A_C	*						*	*	*
C+	*						*	*	*
M				*			*	*	*
A_M							*		
X	*			*			*		

* Indicates presence of fluorescence peak in sample fraction

3.3 Discussion

At present, microbially derived AFOM is often discussed in terms of protein-like fluorescence within the literature (Coble *et al.*, 2014; Hudson *et al.*, 2008; Reynolds, 2002; Determann *et al.*, 1998). Certain regions of humic-like fluorescence, such as Peak M, are also discussed as being biodegraded and, therefore, involved in microbial processes (Harun *et al.*, 2015, 2016; Coble *et al.*, 2014). However, although there is a large body of literature surrounding characterisation and origin of AFOM, the limitations and true microbial-OM interactions are not overly well understood at a fundamental level.

Utilising Model System 1 with monocultures, the work here determines the direct relationship between the underpinning microbiological processes and the origin of AFOM. This research has demonstrated a range of microbially engineered AFOM, providing evidence of the dynamic relationship between bacterial growth and the fluorescence signal, discussed below. This provides insights into the phenmenon of fluorescence variation at a highly resolved temporal scale.

3.3.1 Fluorescent organic matter production and bacterial growth

3.3.1.1 Peak T fluorescence

The work here (Figures 3.1, 3.2 and 3.4) demonstrates a clear correlation between bacterial growth and Peak T within monocultures, particularly within the exponential growth phase ($R^2 > 0.95$). These strong and significant correlations identified between Peak T and bacterial population growth, inferred by using the OD, are in agreement with some previous studies (Deepa and Ganesh, 2017; Baker *et al.*, 2015; Dartnell *et al.*, 2013;

Cumberland *et al.*, 2012; Sohn *et al.*, 2009). Much of this previous work has attempted to correlate Peak T fluorescence with *E. coli* and/or coliform counts with varying degrees of success. However, variations in Peak T intensity during the stationary phase has also highlighted species specific sources of Peak T that can be attributed to metabolically active cells; tryptophan is an essential amino acid, necessary for protein formation during growth and other metabolic pathways, and so will be produced as a result of cell multiplication and metabolic processing (Coble *et al.*, 2014; Hogg, 2005). This emphasises the use of Peak T fluorescence as an indicator of microbial activity. From this, it can be stated that Peak T fluorescence is an indicator of bacterial activity, and presence to some extent. However, it cannot provide a proxy for enumeration, despite the correlations identified, due to multiple contributing factors.

For the *B. subtilis* growth curve, the fluorescence intensity of Peak T continues to increase in the stationary phase (Figure 3.2). It is likely that this is related to endospore production from this species, as demonstrated by the EEM of the endospore suspension (Figure 3.3). From this figure, it can additionally be suggested that Peak T fluorescence is also attributed to structural proteins, rather than solely pure amino acids, as endospores are not metabolically active.

The *P. aeruginosa* growth curve (Figure 3.4) also demonstrates a correlation with Peak T and the OD during the exponential phase, $R^2 = 0.97$. However, Peak T is again highlighted as not solely related to bacteria enumeration as a sudden increase followed by a decrease in Peak T fluorescence intensity is seen within the stationary phase. This is likely to be another species specific response, caused by the production of Exotoxin A

and subsequent binding of NAD+ to the enzyme active site, causing quenching of the Peak T fluorescence, as discussed in section 3.2.1.3.

3.3.1.2 Peak C fluorescence

Peak C fluorescence has been suggested as an alternative proxy for bacterial presence to Peak T (Sorensen *et al.*, 2018b). The correlations here definitely support this association. However, the lag observed within the *E. coli* growth curve (Figure 3.1), in conjunction with continued increase in Peak C intensity during the stationary phase of the growth curve, supports the notion that bacterial metabolic activity, rather than enumeration, may be the driver for Peak C fluorophore production. Within the *B. subtilis* growth curve (Figure 3.2), an increase in Peak C fluorescence intensity precedes the Peak T, with a strong correlation identified. It has previously been suggested that Peak C, in the presence of *Bacillus sp.*, may be related to endospore production (Smith, Anderson and Webb, 2004). However, Figure 3.3 clearly demonstrates endospores produce a protein-like fluorescence spectra, suggesting *Bacillus sp.* undergo metabolic processes which produce compounds which fluoresce in the Peak C region of the EEM.

Furthermore, the observed maximum fluorescence intensity of Peak C is seen in lower intensities than Peak T, with it being a factor of 10 lower than Peak T within the *E. coli* growth curve (Figure 3.1). This suggests that in the environment, where Peak C fluorescence is commonly of greater intensity than that of Peak T, the majority Peak C mainly originates from allochthonous terrestrial sources. The lower intensity fluorescence seen in the growth curve data allows the determination that microbially-

derived Peak C may be a metabolic by-product or a secondary metabolite produced mainly during the stationary phase.

3.3.1.3 Bacterially engineered 'humic-like' fluorescence

As well as the most common and dominant fluorescence peaks, other humic-like peaks are seen to be produced *in situ* during the monoculture growth curves (Figures 3.1, 3.2 and 3.4). Peaks M and A_M are shown to be produced directly, as suggested by marine-based literature (Shimotori, Omori and Hama, 2009; Coble, 1996), rather than simply a result of photo- and biodegradation of Peak C (Coble *et al.*, 2014). Peak C+ fluorescence is seen at very high intensities within the *P. aeruginosa* growth curve. The positioning of this peak within the EEM is associated with the siderophore pyoverdine (Dartnell *et al.*, 2013; Wasserman, 1965), suggesting Peak C+ may be as a result of pyoverdine production by *P. aeruginosa*, as discussed in section 3.2.1.3. Peak C+ has been seen in freshwater environments and is currently attributed to terrestrial allochthonous OM (Coble *et al.*, 2014). However, this work proves that microbial compounds produced *in situ* may provide an autochthonous source of Peak C+ fluorescence. As such, Peak C+ may act as a biomarker for an active *P. aeruginosa* community, although further investigation within natural environmental systems is required.

3.3.2 Bacterial fluorescent aquatic organic matter; intracellular or extracellular?

Further to the identification of the growth phase in which different AFOM is produced, monocultures were incubated overnight and the samples segregated into different components (supernatant, resuspended cells and lysed cells) to identify the intraceullar and extracellular (exported from cells) nature of the AFOM. This provides an insight into the metabolic role of the compounds produced by different bacterial species. From this the potential available microbially-engineered AFOM can be postulated, i.e. extracellular material, within natural systems, providing insight into the potential fate of AFOM.

3.3.2.1 Intracellular Peak T fluorescence

The ubiquitous presence of Peak T fluorescence within all sample fractions for the overnight monocultures (Table 3.2) highlights the inability of Peak T to act as an enumeration proxy, particularly within complex microbial communities. Whilst seen in the supernatant fraction, suggesting some Peak T accounts for extracellular FOM, the highest intensities are seen in the resuspended and lysed cells. From this it can be deduced that the majority of Peak T fluorescence is intracellular material, either functional or structural molecules, explaining the presence of Peak T upon inoculation and its increase in intensity with cell multiplication (as per the growth curves). The intracellular nature of the FOM further suggests that Peak T can be used as an indicator of microbial presence. However, its omnipresence in all the bacterial species analysed,

clearly demonstrates the inability of Peak T fluorescence to act as an indicator of specific species presence in complex aquatic microbial communities.

3.3.2.2 Extracellular Peak C fluorescence

Peak C fluorescence is seen within the supernatant and lysed cell fractions from the overnight *E. coli* and *B. subtilis* fractions (Table 3.2). Its presence in the supernatant can be attributed to either (1) material exported out of the cell (either metabolic by-products or functional proteins) or (2) cellular debris resulting from cell lysis during growth (prior to sampling). The extracellular nature of this fluorescence peak for these species also suggests the possibility that Peak C may be derived from compounds that fluoresce when not within a cell, where the fluorescence is quenched or inhibited. The presence of Peak C in all elements of the *P. aeruginosa* culture, indicates that these molecules, for this species, are likely to be functional proteins exported to become extracellular OM. The data here indicates that the fluorophores that give rise to Peak C fluorescence are likely to be derived from multiple sources, and can be attributed to either cell lysis (Elliott, Lead and Baker, 2006a) or microbial metabolic by-products or extracellular proteins (Guillemette and del Giorgio, 2012; Shimotori, Omori and Hama, 2009).

3.3.2.3 Bacterially engineered humic-like fluorescence

Whilst Peak M is identified in relation to both *B. subtilis* and *P. aeruginosa*, Peak A_M is only observed in the supernatant of *P. aeruginosa* (Table 3.2). These peaks are thought to occur simultaneously in the environment (Coble *et al.*, 2014). However, the independent

development of these peaks suggests Peak A_M could be attributed to either species specific proteins or bacterial metabolic by-products. As such, Peaks M and A_M must be considered separately due to the likelihood that they are derived from different fluorophores. The ubiquitous presence, and high intensity, of Peak C+ fluorescence in the *P. aeruginosa* sample fractions suggests the intracellular production and extracellular output of pyoverdine, as discussed previously.

Although Peak X (Table 3.2) is previously uncharacterised within aquatic AFOM studies, current understanding of fluorophore structures leads to the proposal that Peak X is likely derived from high molecular weight compounds, characterised as humic and fulvic acids (Lakowicz, 2006). Within the current body of environmental AFOM literature, this OM is usually attributed to terrestrial allochthonous material. However, it is only present within the supernatant for the overnight monocultures of the bacterial species cultured (Table 3.2). This suggests it is likely to be secreted from the cells as a metabolic byproduct, further demonstrating the ability of bacteria to rapidly produce high molecular weight OM *in situ*.

The data here shows 'humic-like' fluorescence peaks to be both intracellular and extracellular, depending upon species specific metabolic processes. This suggests that the microbially-derived element of these fluorescence peaks may be related to functional or structural biological molecules. Another possible origin for some of this AFOM is degradation of OM *in situ* (Coble *et al.*, 2014; Coble, 1996). Although the work here does not provide information regarding the exact microbial metabolic pathways for the range of autochthonously produced microbially-derived AFOM, the ability of these molecules to be exported from cells and exist within suggests that they are unlikely to represent

cellular structural material. The ability of bacteria to produce such a range of AFOM changes the current understanding and view within aquatic OM research regarding the complexity of OM origin.

3.3.3 Chapter 3: key findings

- Peak T fluorescence does not provide a proxy for enumeration but is an indicator of bacterial activity and presence, to some extent. This is highlighted by the intracellular nature of Peak T AFOM and its ubiquitous presence in all bacterial species cultured.
- Bacteria can rapidly produce high molecular weight OM *in situ*. The extracellular identification of the majority of this AFOM attributes this to bacterial metabolic by-products or extracellular proteins.
- *In situ* production of Peak C+ fluorescence may provide a biomarker for an active *P. aeruginosa* community.

Chapter 4 Microbial processing and production of aquatic fluorescent organic matter

4.1 Introduction

Current literature has explored the characteristics of aquatic fluorescent organic matter (AFOM) across a range of aquatic systems (Khamis, Bradley and Hannah, 2017; Carstea *et al.*, 2016; Coble *et al.*, 2014; Henderson *et al.*, 2009; Hudson, Baker and Reynolds, 2007). This has demonstrated the microbial origin of a range of AFOM, with research focussing on the use of Peak T fluorescence as a proxy for microbial presence and/or activity. This has been driven by statistically significant correlations between tryptophan-like fluorescence and the biological oxygen demand (BOD) (Baker *et al.*, 2015; Bridgeman *et al.*, 2013; Hudson *et al.*, 2008; Baker and Inverarity, 2004). BOD is a well-used water quality parameter, assessing microbial activity through the degradation of labile OM (Bridgeman *et al.*, 2013; Cutrera *et al.*, 1999). These correlations have led to the use of Peak T as an *in situ* indicator of this parameter (Yang, Shin and Hur, 2014; Henderson *et al.*, 2009; Hudson *et al.*, 2008; Reynolds, 2002; Reynolds and Ahmad, 1997). Nonetheless, the underpinning microbial-AFOM interactions within environmental systems are still not well understood.

The data in chapter 3 has highlighted the ability of bacteria to engineer a range of AFOM *in situ*. To determine the application of this in natural systems, bacterial isolates from an environmental freshwater (section 2.5.1) were cultured using Model System 1. As well as using monocultures, a mixed microbial community, isolated from the same

environmental freshwater sample, was cultured using Model System 1 to assess the impact of using a mixed culture.

Model System 2 was developed to analyse the relationships between Peak T fluorescence and dissolved oxygen, along with bacterial enumeration. Longer incubation times were used within this model system to assess the potential impact of residence time and a low nutrient medium was employed to better replicate environmental fluorescence intensities. By simplifying the sample matrix and analysing the samples on a higher temporal scale, the true dynamics of microbial-FDOM interactions can be assessed. From this, the applicability of Peak T fluorescence as a proxy for other water quality parameters can be determined, alongside the potential use of Peak T as a standalone new water quality parameter.

4.2 Results

4.2.1 Model System 1: Processing and production of AFOM by bacterial isolates from an environmental freshwater

Peak picking was applied to the EEMs obtained from the environmental monocultures and mixed cultures. Due to the dominance of certain fluorescence peaks, particularly Peaks T and C+, PARAFAC analysis did not provide a robust model of the monoculture and mixed culture data sets; n = 268 and n = 234, respectively. The fluorescence peaks identified are detailed in Table 4.1.

Table 4.1: Fluorescence peaks identified from the environmental isolate overnight bacterial monocultures and mixed community cultures.

Named Fluorescence Peak	$\lambda_{ex}/\lambda_{em}$ (nm)
T	280/320-360
C	350/420-460
A_C	250/420-460
C+	400/440-490
A_M	240/380-420
M	300/380-420
B	250/290-320
X	440/510-550

4.2.1.1 Overnight bacterial monocultures

Six bacterial species (Table 2.2), isolated from an environmental freshwater (section 2.6.3), were cultured overnight to ensure that the phenomenon of AFOM production seen with the laboratory bacterial strains (chapter 3), is replicated by environmental bacterial strains. Cultures were incubated at 25°C, to attempt to replicate environmental conditions; 30°C, to ensure growth but not limit the bacteria; and, 37°C, to provide optimum growth conditions for any pathogenic species. However, the data presented was obtained from the 30°C 24 hour cultures as this was identified as the optimum temperature for growth across the species cultured.

Table 4.1 shows the range of fluorescence peaks identified within the environmental isolate monocultures, except for Peak B which was not identified in any of the overnight monocultures. This is likely to be due to the incubation time and the labile nature of this

AFOM. As seen previously, Peak X was identified only in the supernatant fraction for all six cultures, in relatively low fluorescence intensities, as was fluorescence Peak AC. The presence of Peak M was also only identified in the supernatant of *P. aeruginosa*, in agreement with the AFOM identified from the laboratory strain of *P. aeruginosa* (section 3.2), and *S. aureus.* The presence of the other fluorescence peaks identified for the environmental *E. coli* and *B. subtilis* are comparable to that of the laboratory strains (Table 3.2). The fluorescence spectra of the environmental *P. aeruginosa* demonstrates a comparable range of AFOM within the supernatant fraction, whilst Peaks T and C+ are the only significant fluorescence peaks identified within the cell sample fractions.

Figure 4.1 shows the fluorescence intensity of four of the identified fluorescence peaks within the different sample fractions for all six cultured environmental bacteria. Figure 4.1a demonstrates that Peak T is the sole ubiquitous and dominant fluorescence peak, as it is seen in all sample fractions for all species analysed. Furthermore, the presence of Peak T mainly within the cell fractions is highlighted, although some extracellular Peak T is seen within the supernatant for all species. This is in agreement with the previous data (section 3.3.2.1).

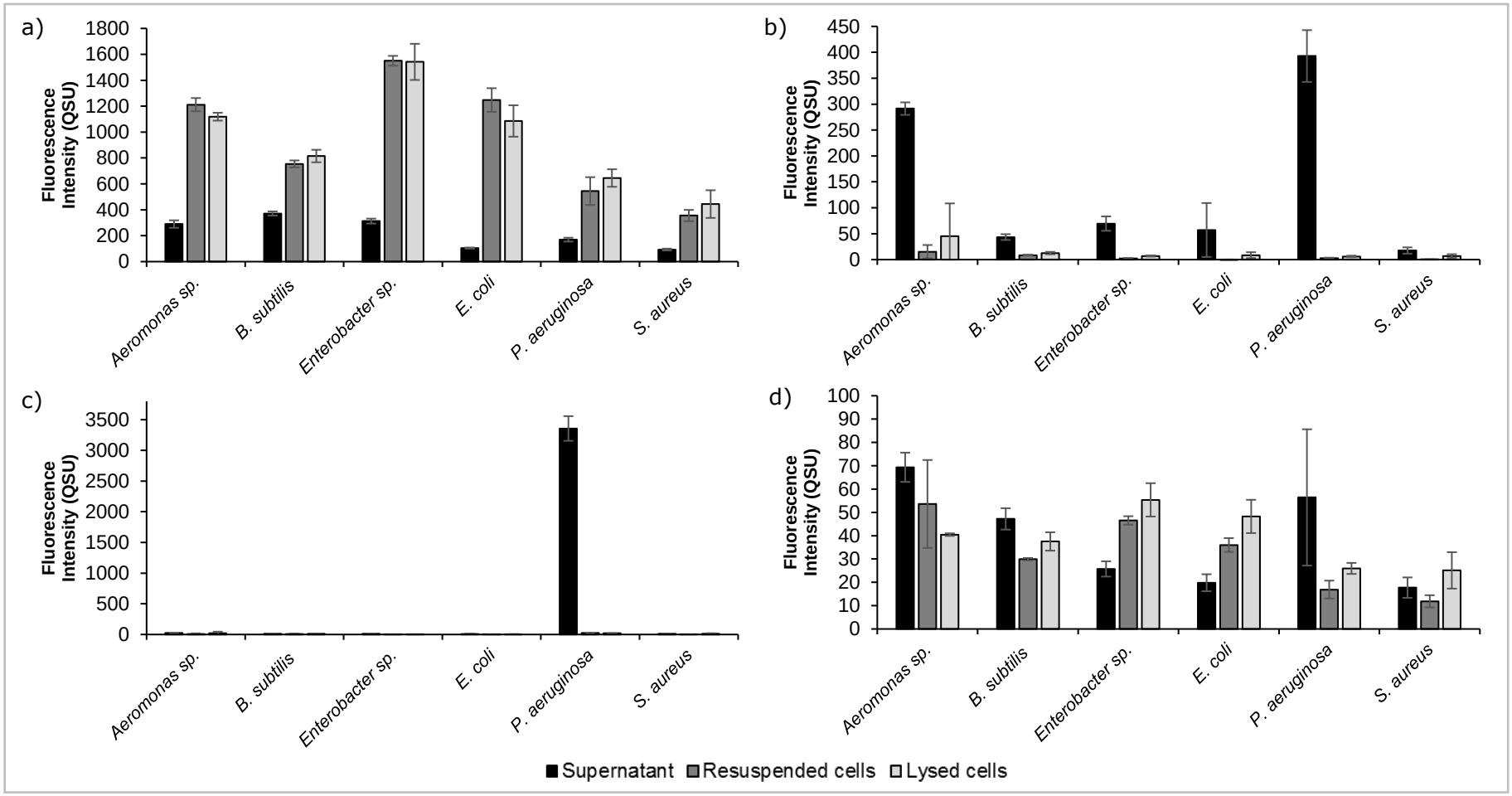

Figure 4.1: Fluorescence intensity (QSU, 1 QSU = 1 μg L^{-1} quinine sulphate), ± 1 standard deviation (n = 3), of fluorescence peaks of interest in each of the sample fractions for the six bacterial species (isolated from an environmental freshwater sample), cultured at 30°C, n = 3 with +/- 1SD: a) Peak T, $\lambda_{ex}/\lambda_{em}$ 280/330-360nm; b) Peak C, $\lambda_{ex}/\lambda_{em}$ 350/420-460nm; c) Peak C+, $\lambda_{ex}/\lambda_{em}$ 400/440-480nm; d) Peak M, $\lambda_{ex}/\lambda_{em}$ 300/380-420nm.

Peak C fluorescence is mainly identified in the supernatant sample fraction for all six species cultured (Figure 4.1b). It is seen in much lower intensities in the resuspended and lysed cell fractions, suggesting the majority of this AFOM is exported outside of the cell, existing as extracellular material. Figure 4.1c highlights the extracellular presence Peak C+ for the environmental strain of *P. aeruginosa*, as seen with the laboratory cultures. Peak M, shown in Figure 4.1d, is seen in all species and all sample fractions, albeit at low fluorescence intensities in comparison to some of the other fluorescence peaks shown in Figure 4.1.

4.2.1.2 Overnight culturing of an isolated mixed microbial community

Mixed cultures were incubated at 25°C, 30°C and 37°C to provide a range of growth conditions, including the selection of pathogenic bacteria. This also allows for the assessment of the impact of temperature, and the potential selective growth this may cause, on the AFOM produced. Samples were also analysed at three time-points – 24, 48 and 72 hours – to assess the impact of residence time on AFOM. However, the data shown here is all from the 24 hour time-point. The fluorescence signal at the other time-points indicated variable fluorescence peak intensity but no additional peaks were identified with increased residence time in the minimal media used within the model system.

All the fluorescence peaks identified in Table 4.1 were seen within the mixed microbial community cultures, except Peak X. Peak X is seen in the supernatant of all the bacterial monocultures but has not previously been discussed within aquatic AFOM research.

From the community data, it can be suggested that competition for resources prevents Peak X from being present in the mixed cultures and environmental samples alike. The microbial production of the range of AFOM seen is in line with the previous data but provides direct evidence that environmental bacterial strains are capable of producing such high molecular weight fluorescent compounds.

Filtering the freshwater to be cultured for use as inoculum culture ensures that only planktonic bacteria are present within the initial culture. It also removes particulate matter, reducing potential contamination, background fluorescence, scatter and biofilm structures. The use of unfiltered samples was also undertaken to understand the potential role of biofilms, in relation to freshwater fluorescence, and to encourage a more complete and reflective community to develop within the model system.

Table 4.2 demonstrates the relative increase in peak fluorescence intensity from the initial inoculum at time zero to the 24 hour time-point for each sample fraction. The most notable difference between the filtered and unfiltered samples is the wider variety of fluorescence peaks present within all fractions of the sample, at all incubation temperatures, for the cultures obtained from the unfiltered environmental inoculation. At time zero, the samples inoculated within the unfiltered culture contained fluorescence peaks T and C, whilst the filtered inoculum produced Peak T fluorescence only. The impact of temperature on the AFOM produced is also seen, as the samples at 25°C have the highest variety of AFOM across the sample fractions, while the samples incubated at 37°C demonstrate the least variety.

Table 4.2: Relative increase in fluorescence intensity, from time zero (initial inoculum), of AFOM peaks within sample fractions after 24 hour incubation period. Three incubation temperatures were employed; 25°C, 30°C and 37°C.

Named Fluorescence Peak	Filtered									Unfiltered								
	Supernatant			Resuspended cells			Lysed cells			Supernatant			Resuspended cells			Lysed cells		
	25	30	37	25	30	37	25	30	37	25	30	37	25	30	37	25	30	37
T				**	**	**	**	**	*				**	**	**	*	*	*
C	***	***	**	*	*		*	*		***	***	***	*	*	*	*	*	*
C+	***	***	*	*			*			***	***	***	**	*	*	**	*	*
M	**	**	*	*	*	*	*	*	*	*	*	*	*	*	*	*	*	*
B	*			*	*	*	*	*	*	*	*	*	*	*	*	*	*	*

Increase in intensity identified, but less than an order of magnitude

* Increase by an order of magnitude

** Increase by two orders of magnitude

*** Increase by three orders of magnitude

Peak T fluorescence is not seen within the sample supernatant at the 24 hour time point. However, the 48 and 72 hour data demonstrate low intensity Peak T fluorescence, suggesting this AFOM is present as extracellular material with increased residence time and metabolic activity. However, Peak T is seen within the cell sample fractions at the 24 hour time-point, with the intensity increasing most within the resuspended cells (Table 4.1). Increased Peak B fluorescence is seen within all sample fractions of the mixed cultures. This is, again, reflective of what is often seen within environmental samples, although it was not seen in the monocultures. Peak M, a common surface freshwater AFOM peak, is also seen in higher fluorescence intensities within the mixed cultures than the monocultures.

Peak C is seen in the highest intensities within the supernatant sample fractions, in line with the other data. The presence of this in the cell samples highlights some intracellular Peak C. Peak C+ is present in the highest intensities within the supernatant fraction. This is in line with the *P. aeruginosa* data, shown previously, and the presence of *P. aeruginosa* in the original environmental samples used to culture. This was identified using Difco™ *Pseudomonas* Isolation Agar (Difco Laboratories, USA) and also within a UKAS laboratory water quality assessment (Wessex Water Scientific Services, UK; ISO 17025 (2005)).

4.2.2 Model System 2: Mixed culture model system – microbial processing and production of AFOM over time

Initially, Model System 2 (section 2.7.2) was used to incubate an environmental freshwater (section 2.5), to investigate microbial processing, over a 10-day incubation period in order to understand the impact of residence time and explore microbial-OM interactions and AFOM variations over a longer period of time. Variation in the fluorescence signal, both decreasing and increasing in intensity, was identified within all repeats (Figure 4.2a).

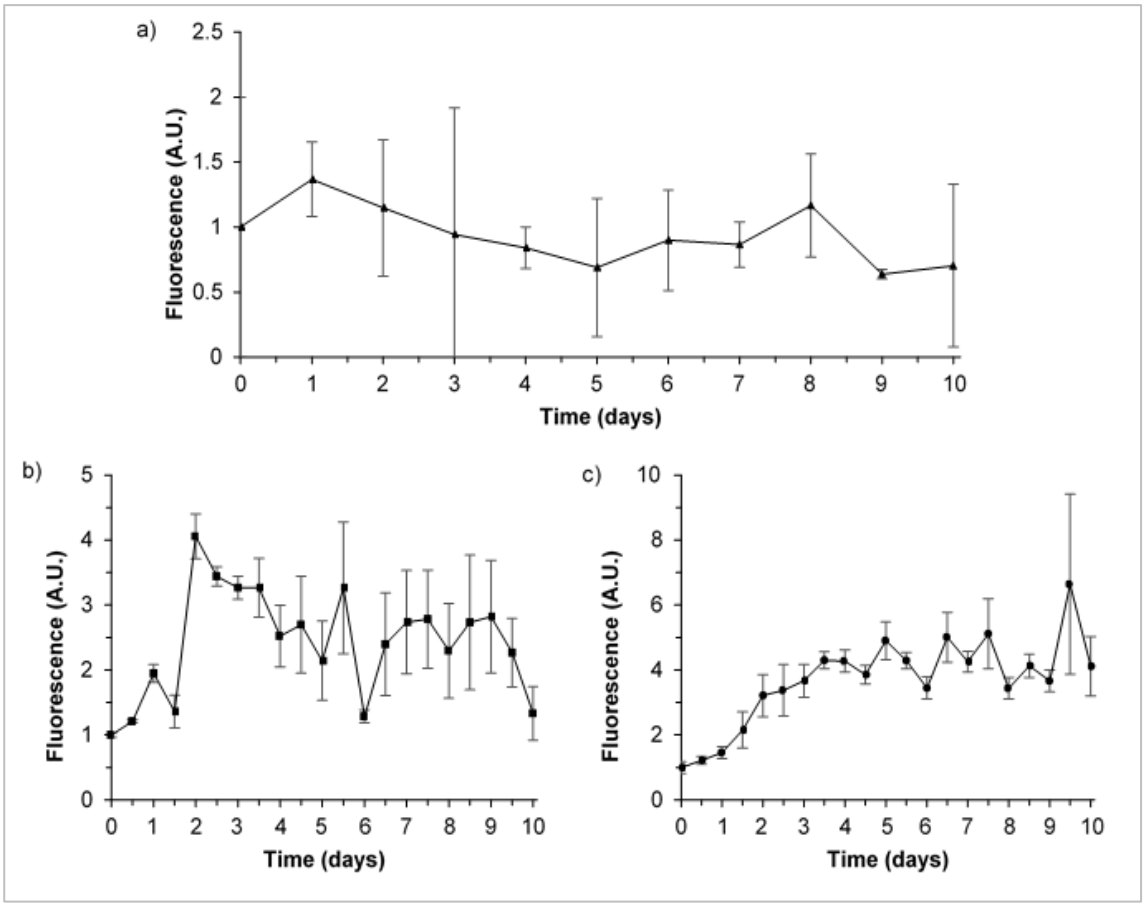

Figure 4.2: Variation of Peak T fluorescence ($\lambda_{ex}280/\lambda_{em}340$-360 nm) data throughout the 10-day experimental period. a) averaged environmental samples ± 1 standard deviation (n = 3); b) averaged supplemented synthetic samples ± 1 standard deviation (n = 3) and c) averaged synthetic samples (n = 5). See section 2.7.1 for sample definitions. All fluorescence data reported as arbitrary units (A.U.) normalised to time zero and corrected to the water Raman line at $\lambda_{ex}280/\lambda_{em}310$(300-315) nm.

To enable better understanding of microbial processing within a defined system, more simplistic sample matrices were employed; supplemented synthetic and synthetic samples (section 2.7.2). Using a minimal base media for the synthetic samples removes background FOM, allowing detailed investigation into the microbial production and consumption of FOM. This low nutrient media was also used to better replicate environmental systems, limiting the AFOM production and ensuring the fluorescence intensity is within the range of that seen in the environment. The variation of Peak T fluorescence throughout the 10-day period was observed in these samples (Figure 4.2). Fluctuations in Peak T fluorescence highlight the variable nature of microbial production and consumption of FOM, even within a controlled closed model system.

To allow for quantitative analysis, the 10-day experiments for all sample types were repeated and the measured fluorescence intensities standardised using quinine sulphate units, QSU (section 2.1.2) (Mostofa *et al.*, 2013; Shimotori, Watanabe and Hama, 2012; Shimotori, Omori and Hama, 2009; Kramer and Herndl, 2004). The fluorescence spectra data set, containing 217 EEMs in total from synthetic, supplemented and environmental samples, was then subjected to PARAFAC analysis. This analysis of the EEM data (n=217) (excluding EEMs with scattering anomalies) identified the common presence of five fluorescence components (Table 4.3). The five-component PARAFAC model accounted for 97.64% of the total variation in fluorescence, adequately describing the AFOM spectral variability. These fluorescence components have been previously described and are commonly attributed to freshwater AFOM, namely humic-like (components 2 and 4) and protein-like (components 1, 3 and 5) fluorescence peaks; components and fluorescence peaks are detailed in Table 4.3.

Table 4.3: Identified PARAFAC analysis components and fluorescence peaks generated through microbial processing of environmental and synthetic samples over a 10-day experimental period.

PARAFAC Component	Named Fluorescence Peak*	$\lambda_{ex}/\lambda_{em}$ (nm)	Description
1	T Tryptophan-like	275/340	Autochthonous peak, described unanimously in the literature as microbially-derived and associated with protein presence.
2	M A_M Humic-like (Marine-like)	300/410 240/410	Biologically or photochemically degraded terrestrial humic-like, sometimes referred to as 'marine-like' OM (Coble, 1996).
3	B Tyrosine-like	265/290	Autochthonous peak, described as microbially-derived and associated with amino-acid and protein presence.
4	C+ C Humic-like	260/490 390/490 260/430 360/430	Double maxima components of terrestrial allochthonous higher molecular weight aromatic compounds, noted as humic-like fluorescence.
5	B	250/300	Region similar to Peak B, associated with autochthonous production or possible photodegraded OM.

*Nomenclature consistent with peak ranges from Coble *et al.*, (2014).

4.2.2.1 Microbial AFOM processing over time: freshwater environmental samples

Environmental freshwater samples that were analysed over a 10-day period show that both components 1 and 3, Peak T and B respectively, decline from day zero to day five (Figure 4.3). By day ten, Peak T has further declined, whilst the intensity of Peak B increased beyond the original intensity observed at day zero (Figure 4.3). This phenomenon of variations in the fluorescence intensities was observed on all occasions (Figures 4.2 and 4.3). Components 2 and 4 were omnipresent within the environmental samples. Some variation in the fluorescence intensity of these components was seen throughout the 10-day experimental period, although the measured intensity was consistently higher than components 1 and 3 (Figure 4.3).

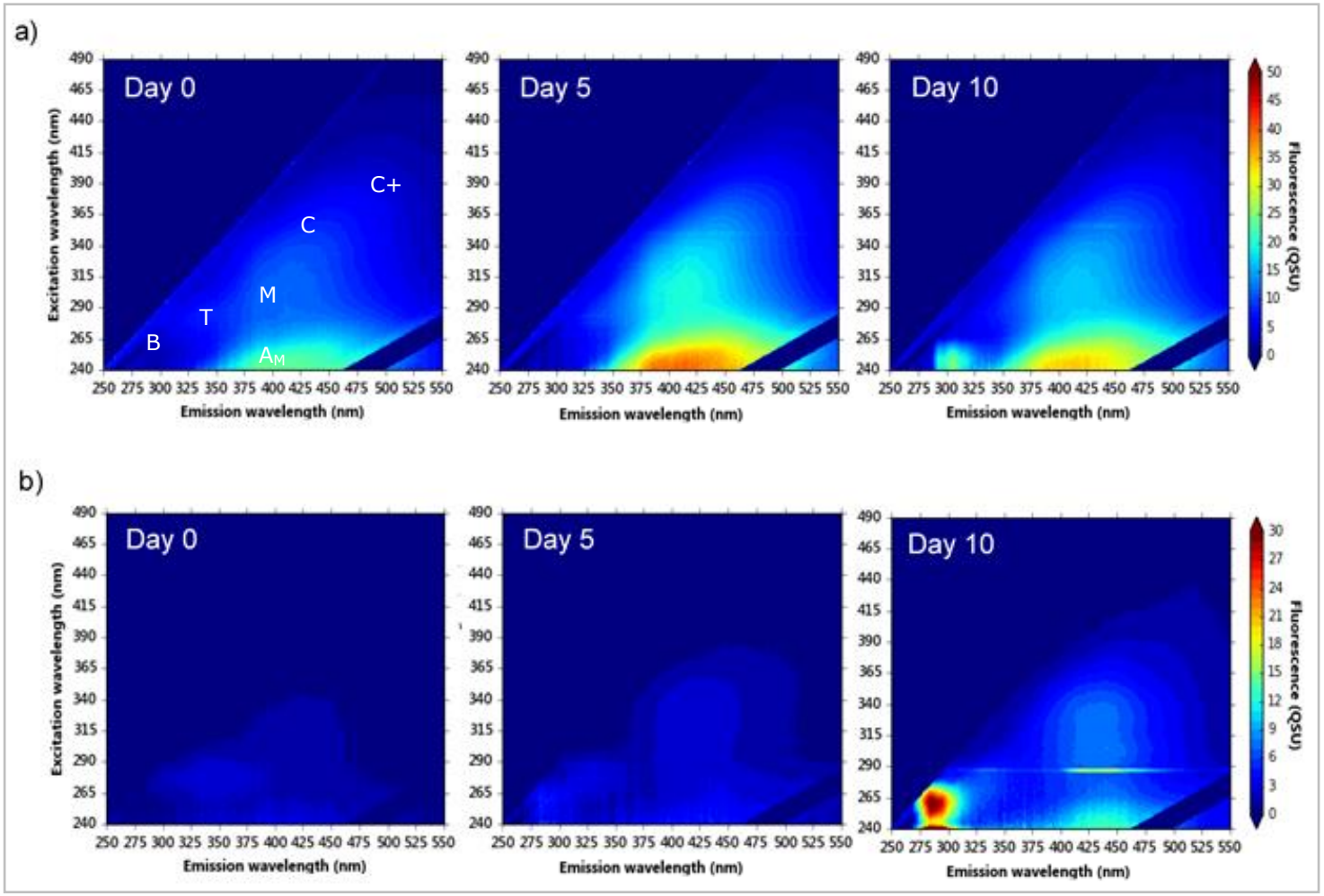

Figure 4.3: Excitation-emission matrices of a) environmental samples and b) supplemented synthetic samples incubated at 20°C over a 10-day experimental period. Coloured bars are in quinine sulphate units, QSU (1 QSU = 1 μg L^{-1} quinine sulphate).

4.2.2.2 Bacterial AFOM processing over time: supplemented synthetic samples

The incubation of environmental cultures highlighted the issues of sample matrix complexity and background fluorescence. To further explore microbial-AFOM interactions at this resolution, supplemented synthetic samples were used within Model System 2. These samples provide an insight into fluorescence variation within the model system over the 10-day experimental period, with some sample matrix similarity to the environmental samples. The supplemented synthetic samples exhibited an initial background fluorescence consistent with the fluorescence components observed in the environmental samples, albeit at lower intensities (Figure 4.3). By day two of the experiment, Peak T fluorescence (component 1) was shown to develop from a low baseline of 3 QSU to a maxima of 25.2 QSU. By day five the fluorescence intensity of Peak T decreased to 2 QSU and remained low (between 0.5-5.5 QSU) throughout the remaining experimental period (Figure 4.3). This variation in fluorescence intensity highlights the necessity of high-frequency monitoring to understand dynamic changes in Peak T that identify the utilisation of this AFOM by the microbial community, alongside production (Coble *et al.*, 2014). Components 2 and 4 (Table 4.3) were also present in the supplemented synthetic samples, with the phenomenon of variation in component intensity also seen. The maximum intensity for these components, a factor of six higher than the starting intensity, was reached by day two. The fluorescence then decreased, remaining stable until a second maxima was reached on day nine, half the intensity of that seen on day two. The observed variation associated with the fluorescence intensities of components 2 and 4 throughout the experimental period, allows us to propose bioavailability of this AFOM.

4.2.2.3 Bacterial AFOM processing over time: synthetic samples

The characterisation of AFOM formed within synthetic samples during microbial processing reveals the presence of PARAFAC components 2, 3 and 4 in all samples (Table 4.3). Once developed, the fluorescent peaks that give rise to components 2 and 4 persisted throughout the 10-day experiment, a phenomenon seen in all experimental repeats (Figure 4.2) and in agreement with the other samples studied. Again, the variation in fluorescence intensity of these humic-like components throughout the 10-day experimental period was identified, exhibiting a Coefficient of Variance (n = 5) between 54% and 104%. Interestingly, component 3 (Peak B) varied greatly throughout the 10-day experimental period (exhibiting a Coefficient of Variance (n = 5) between 73% and 232%) suggesting that both production and consumption of Peak B takes place *in situ*.

The work here provides further evidence that Peak T is derived from an active bacterial population. The development of Peak T fluorescence (component 1) can be accelerated via incubation at 30°C when compared to data derived from samples incubated at 20°C as shown in Figure 4.4. Both incubation temperatures produced a variable Peak T fluorescence intensity throughout the 10-day experimental period. The 30°C Peak T data also showed a second increase in fluorescence intensity at day 7, whilst the live bacterial cell numbers and DO remained steady.

Changes in dissolved oxygen and Peak T fluorescence were monitored daily for environmental samples. This data indicated that Peak T fluorescence intensity was variable over time while DO declined and then plateaued, as expected. While variation in Peak T was seen, use of synthetic samples removed masking or interference from

other background fluorescence, such as Peak C. This data clearly demonstrates that Peak T fluorescence is extremely variable (Figure 4.4), whilst the DO declines rapidly over the first two days and then plateaus, but is not depleted meaning it does not become a limiting factor. This means no significant correlations are identified between the intensity of Peak T and the enumeration of bacterial cells, either living or total; likely to be due to the differences in dynamics observed at this sampling frequency.

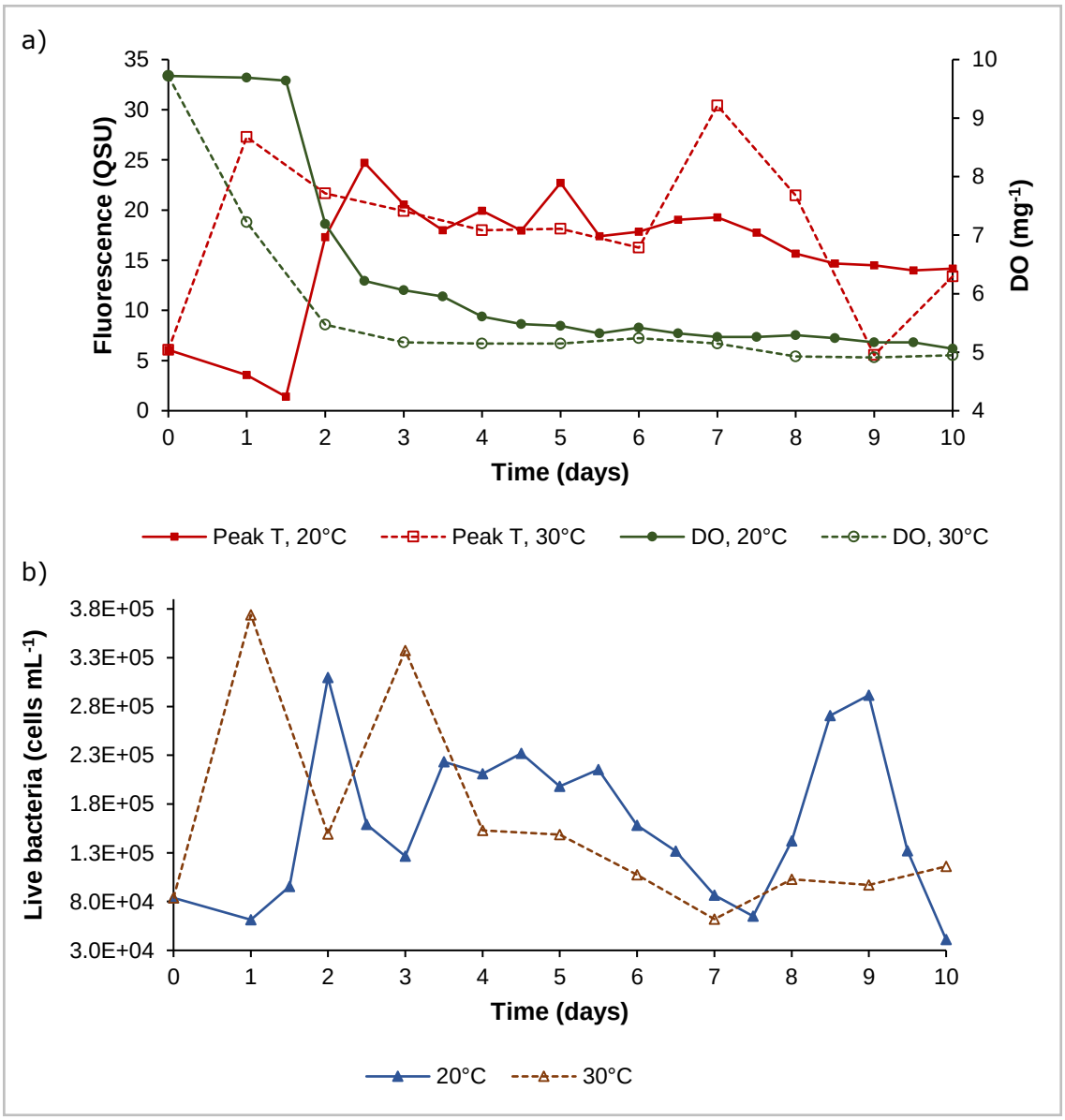

Figure 4.4: Data for synthetic samples incubated at 20°C and 30°C over a 10-day microbial processing period: showing a) Peak T fluorescence and dissolved oxygen and; b) the number of living bacteria (cells mL^{-1}).

4.2.2.3.1 Hourly monitoring of synthetic samples: bacterial growth and fluorescence development

To further understand the development of bacterial-OM fluorescence within Model System 2, synthetic samples were cultured and incubated at a series of temperatures. Samples were analysed at hourly intervals over a 48-hour period and then again after 120 hours.

The EEMs from this dataset were included in a five-component PARAFAC model (Table 4.3). Component 2 was identified within some of the synthetic samples. Low intensity fluorescence for component 4 was also seen in some of the samples; a "shoulder" of this fluorescence can be seen in Figure 4.4b. Peaks T and B were present in all samples (see Figure 4.5). Interestingly, Peak B seen in the synthetic samples, identified as component 5, differed slightly in wavelength position to Peak B observed in the environmental samples (component 3), see Table 4.3. Throughout the 48-hour period the OM that gives rise to Peak B fluorescence was shown to be produced and assimilated, resulting in large variations in the fluorescence intensities (see Figure 4.5).

Peak T fluorescence was observed in all samples at all temperatures (component 1, Table 4.3). For the first 24 hours, the development of Peak T fluorescence observed in all samples was minimal (~ 3 QSU_{min}). However, Peak T fluorescence was seen to develop five-fold (16.8 QSU_{max}) by the 120 hour time point at 20°C incubation (Figures 4.5 and 4.6), in agreement with data gained from the 10-day experiments. The data shown in Figure 4.6a shows that higher incubation temperatures relate to the production and development of Peak T, likely to be as a function of increased bacterial metabolic activity.

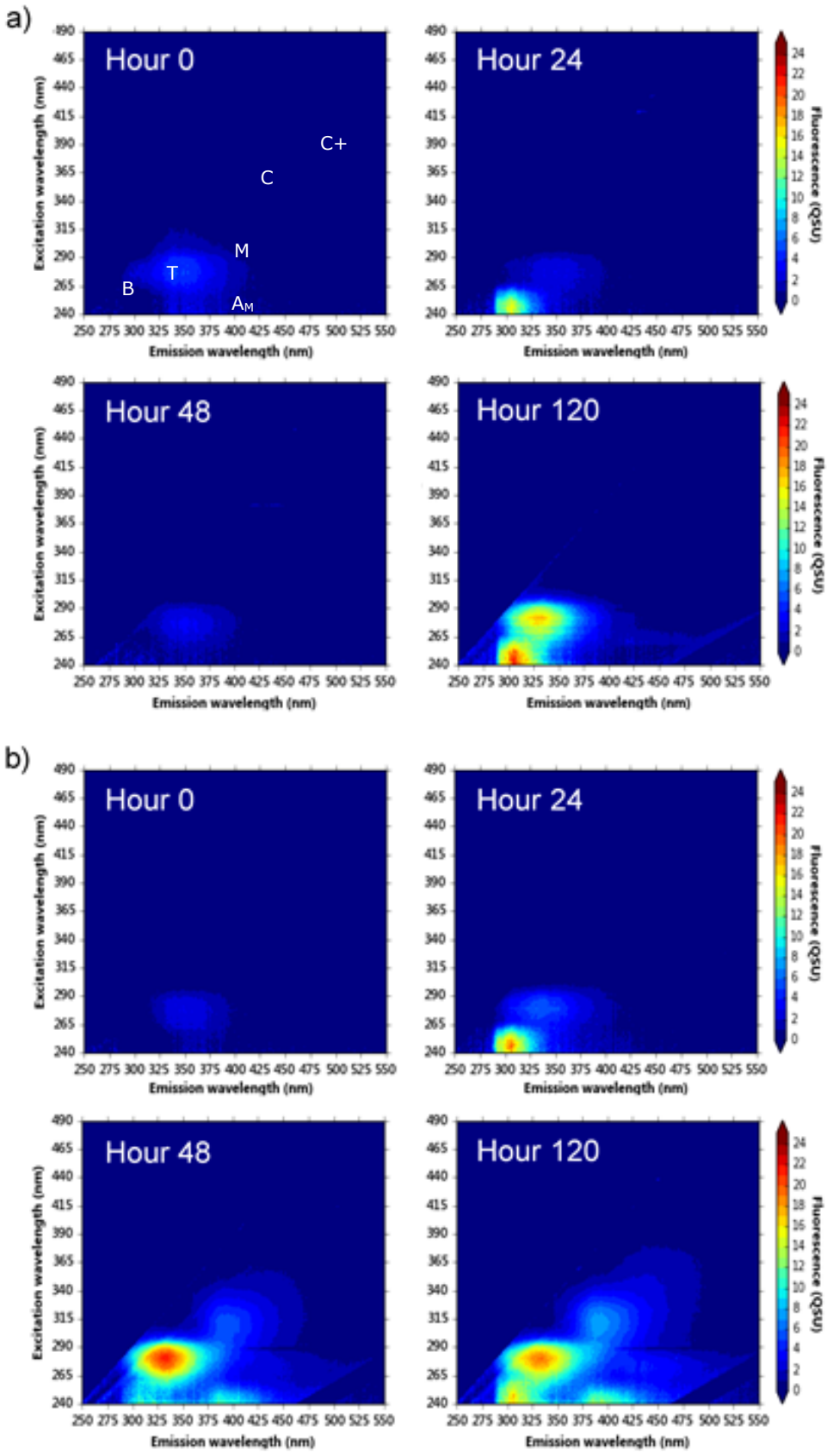

Figure 4.5: Excitation-emission matrices of synthetic samples incubated at a) 20°C and b) 37°C over a 5-day microbial processing period (analysis performed hourly during the first 48-hours). Coloured bars are in quinine sulphate units, QSU (1 QSU = 1 μg L^{-1} quinine sulphate).

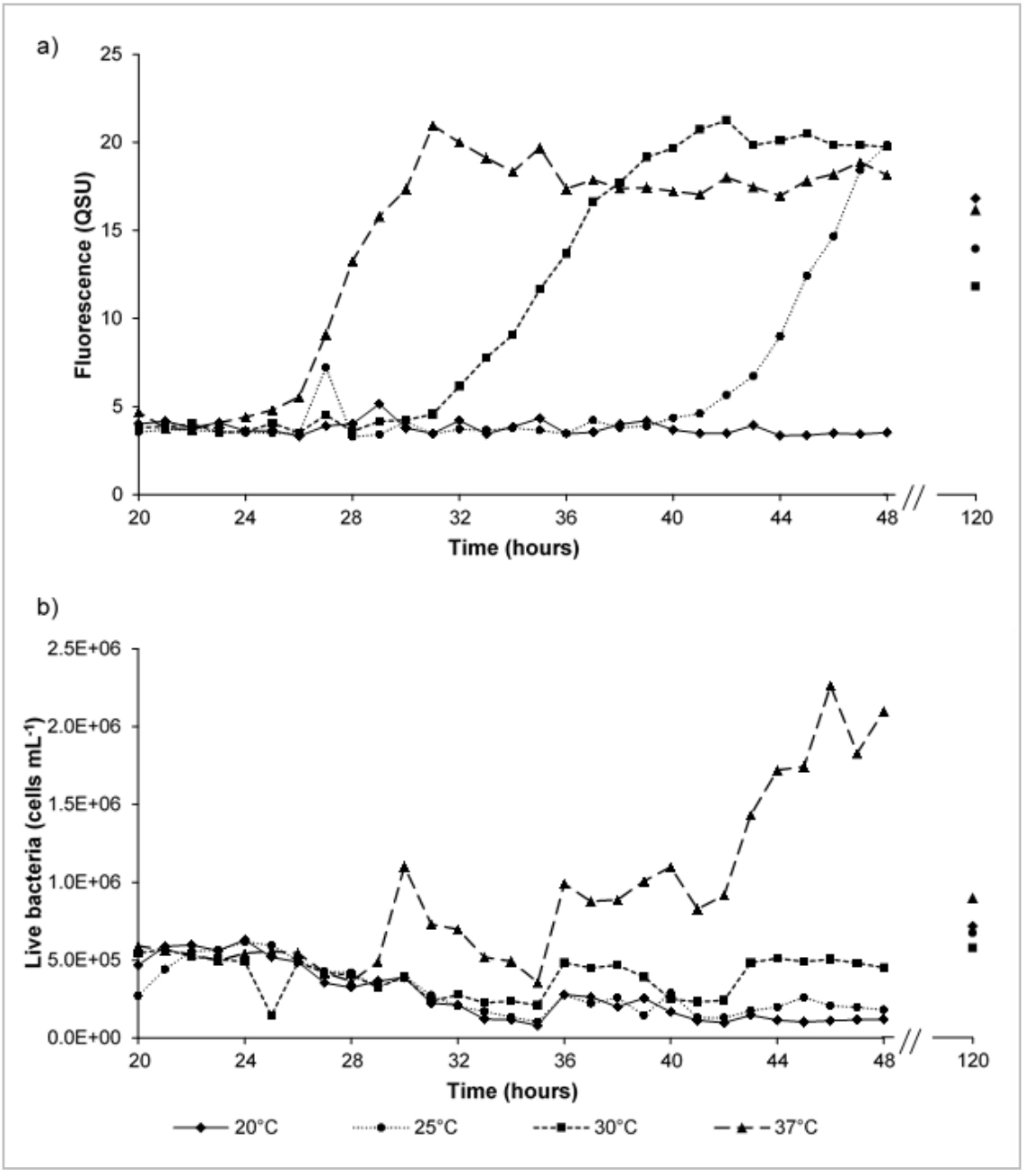

Figure 4.6: Fluorescence and bacterial enumeration data for synthetic samples incubated at a range of temperatures over a 5-day experimental period, showing; a) Peak T fluorescence, QSU (1 QSU = 1 μg L-1 quinine sulphate); and b) the number of living bacteria (cells mL-1). Data shown is from 20 to 48-hrs plus a single time point at day five (120 hours).

Analysis undertaken at hourly intervals from samples incubated at 37°C show that an observed log-fold increase in living bacterial numbers (5.0×10^5 live cells mL^{-1} to 2.4×10^6 live cells mL^{-1}) was preceded by a four-fold increase (from 5 QSU to 20 QSU) in Peak T fluorescence intensity. Although the initial induction of Peak T fluorescence can be identified, by monitoring the fluorescence phenomenon dynamics at hourly intervals, no significant correlations between the Peak T fluorescence intensity and the bacteria cell enumeration are observed for either live, dead or total cell counts.

4.3 Discussion

4.3.1 Model System 1: AFOM processing and production by bacterial isolates from an environmental freshwater

4.3.1.1 Bacterial isolate monocultures

The monocultures here, using the bacterial species from an environmental sample, were employed to determine the potential bacterial AFOM range in natural waters. These display similar fluorescent signatures to the corresponding laboratory strains (chapter 3), suggesting fluorescence spectroscopy may be applicable as a tool for monitoring the presence of particular species with specific fluorescence signatures.

Peak T fluorescence is shown to be intracellular, with the highest intensities seen in the resuspended and lysed cells, shown clearly in Figure 4.1a; this is in agreement with the data in chapter 3. However, its omnipresence in all the bacterial species analysed (Figure 4.1a), as well as other microorganisms such as algae (Makarewicz *et al.*, 2018; Zhi *et al.*, 2015; Suksomjit *et al.*, 2009), clearly demonstrates the inability of Peak T fluorescence to

act as an indicator of specific species presence in complex aquatic microbial communities; this may explain the variation in correlations between Peak T and bacterial enumeration identified within the current body of literature (Bridgeman *et al.*, 2015; Sorensen *et al.*, 2015a). However, Peak T fluorescence can provide information regarding microbial activity, caused by an influx of nutrients into the system, via pollution events, as well as the potential to act as an indicator for microbial contamination events, such as sewage pollution.

Peak C fluorescence was ubiquitous and seen to be variable in intensity and presence within the sample fractions for the environmental isolate monocultures (Figure 4.1b). The majority of this AFOM is shown to be extracellular, demonstrated by its omnipresence and highest intensity within the supernatant for all environmental species. This fluorescence peak is universal to surface freshwaters and considered allochthonous in origin (Coble *et al.*, 2014). The *Aeromonas sp.* culture also demonstrated a high Peak C fluorescence intensity within the supernatant, suggesting that this AFOM is likely to be a functional protein that has a specific purpose for this species or genus group. Peak C fluorescence intensity was also seen to be high for the *Pseudomonas aeruginosa* isolate, as it had the highest intensity Peak C fluorescence of all the species cultured within this work. This data highlights the likelihood of a microbial contribution to this environmental Peak C fluorescence. While it is clear that bacteria can produce Peak C fluorescence, at present the mechanisms for this production are unknown. However, it can be suggested that microbial Peak C fluorescence is related to metabolic products that are produced within the cell and exported, likely to be functional proteins or metabolic by-products.

Although Peak C+ was present within the other species signals (Figure 4.1c), the intensity of this fluorescence peak within the *P. aeruginosa* isolate again demonstrates the potential of this fluorescence peak to be used as a biomarker for *P. aeruginosa*. The application of this may be limited for environmental monitoring, although identifying the presence of *P. aeruginosa* is common within drinking water analysis, but could have a far-reaching impact within health and clinical sciences, where *P. aeruginosa* is an important pathogenic bacterium.

Peak M is identified as both intracellular and extracellular material, due to the ubiquitous presence of Peak M within the sample fractions for the environmental isolates (Figure 4.1). This demonstrates the ability of bacteria to engineer this AFOM *in situ* and suggests that this fluorescence is related to proteins or metabolic by-products that are common across the six species cultured here.

When looking at the range of fluorescent peaks that each environmental bacterial isolate can produce, we begin to see, for the first time, the true complexity of microbial FOM potential. The data from the environmental bacterial monocultures clearly demonstrates the ability of environmental bacteria to produce a range of AFOM. This is in agreement with the data in chapter 3 and highlights the ability of bacteria to produce higher molecular weight and more complex compounds than suggested previously in freshwater AFOM research.

4.3.1.2 AFOM production by a microbial community isolated from an environmental freshwater

The monoculture data highlights that bacterial AFOM production is species specific. This production also varies with the incubation temperatures used, suggesting that the environmental conditions and residence time of the microbes has an impact on the ability and intensity of microbial AFOM. Also, whilst the monocultures indicate the ability of bacteria to produce AFOM without competition, no information is provided as to how mixed cultures and competition for resources between species may impact the range and intensity of AFOM produced. To understand how these interactions may impact the microbial production of AFOM, mixed communities were cultured overnight and subjected to the same analysis as the overnight monocultures; microbial community obtained from an environmental water sample (section 2.6.4).

Culturing a complex microbial community, albeit in controlled and limited conditions, highlights the complexity of the potential microbially-engineered AFOM in natural systems, as shown by Tables 4.1 and 4.2. All the fluorescence peaks detailed in Table 4.1 were identified in the mixed microbial community cultures, apart from Peak X. This is not in agreement with the monoculture data, but is in line with the lack of presence of this peak within environmental samples and, therefore, discussion of this AFOM in the literature. The presence of this high molecular AFOM in the monocultures, where it is not seen within a microbial community, suggests that Peak X production is limited by competition with other species or that it is a metabolic by-product that is utilised by the community. Another possible explanation is that Peak X is 'lost' in the background

AFOM as it is only seen in relatively low fluorescence intensities, <50 QSU, within the monocultures.

Peak T is seen with low fluorescence intensities in the supernatant fractions of the samples and high intensity within the resuspended cells, and seems to vary little when incubated at the different temperatures (Table 4.2). This is in agreement with the data obtained from the bacterial monocultures. The high intensity within the resuspended cells suggests that Peak T may be used for microbial enumeration; we know from the monoculture data that this is not possible within complex microbial communities. The increase in Peak T fluorescence seen for the 24 hour supernatant samples is less than an order of magnitude change, although a low fluorescence intensity increase, comparative to the resuspended cells, is seen with extended culturing time, i.e. at the 48 and 72 hour time points. This indicates that surplus Peak T is produced within cells, which is then exported, within stationary growth phase but, whilst the microbial community is adapting to the new environment, Peak T is valuable for growth and activity. This highlights the potential importance of residence time for extracellular Peak T fluorescence, although more research into this phenomena is required. It also demonstrates how the environmental conditions and requirements for optimum growth can impact the microbial community and, in turn, microbial AFOM production. This further enhances the use of Peak T in determining changes in the microbial activity and, therefore, infer a change in environmental conditions, such as nutrient input from pollution events, or a surge in microorganisms, i.e. from sewage contamination.

Peak C+ contrasts with Peak T in that the majority of the fluorescence intensity is associated with the supernatant sample fraction (Table 4.2). This demonstrates the

extracellular nature of this AFOM, in agreement with the monoculture model system data discussed previously, which determined the likely origin of Peak C+ as an exotoxin. Surprisingly, the samples incubated at 37°C have lowest Peak C+ intensity. The association of this fluorescence with *P. aeruginosa*, a pathogenic bacterium, would suggest that it should be the most intense at that temperature. Although *P. aeruginosa* was identified in all the samples, the environmental source of the microbial community utilised means it is likely that 37°C inhibits these metabolic processes and/or growth of the corresponding species.

The cultures obtained from unfiltered water samples are likely to contain a more complex microbial community, as well as particulate and dissolved OM. By monitoring the relative increase in intensity of the AFOM present, it is possible to identify microbially engineered AFOM from any residual OM provided by the inoculum. The data in Table 4.2 indicates that using a more complex community (from unfiltered water samples) as the inoculum leads to a more varied AFOM signal after incubation. This seems to be of particular importance for the resuspended cell sample fraction, indicating variation between the species' AFOM production capabilities. It is also possible that filtering the sample prior to culturing the inoculum removes the majority of microbes besides bacteria and viruses, and may result in the culturing of only planktonic microbes. This can impact biofilm production, with visible biofilm production observed within the overnight cultures for the unfiltered water sample inoculum. However, within the work presented here, this can only be speculated but provides an interesting avenue for further research and a potentially essential developmental understanding for the issue of biofouling within *in situ* sensing. It also highlights the importance of sample integrity

and requires us to question collection and storage practices for samples to be analysed for fluorescence.

4.3.2 Model System 2: Microbial production and processing of AFOM over time

4.3.2.1 Microbially engineered protein-like fluorescence

The data obtained from Model System 2 demonstrated the increase and decrease in the Peak T fluorescence signal (Component 1, Table 4.3) over time, for all sample types; environmental, supplemented synthetic and synthetic. This is clearly demonstrated by the peak picking data in Figure 3.1 and the EEMs presented in Figure 3.2. The variation in fluorescence intensity over the 10-day experimental period indicates both production and processing of AFOM *in situ*. This provides evidence that Peak T fluorescence can be of autochthonous origin and is labile (Coble *et al.*, 2014). However, whilst the variation in the fluorescence signal fluctuation over time is reproducible, the importance of the sample matrix and community composition is highlighted by the variation between experiments, as demonstrated by Figure 4.2.

The use of the mixed culture model system with synthetic samples highlights the autochthonous origins of the proteinaceous AFOM, namely peaks T and B; identified within the PARAFAC analysis as components 1 and 3 respectively (Table 4.3). Peak B is seen to vary greatly throughout the 10-day experimental period, suggesting both production and consumption of the OM *in situ*. This further supports previous studies that reported Peak B as a labile and microbially-derived compound (Cammack *et al.*,

2004; Parlanti *et al.*, 2000). The work here also provides further evidence that Peak T is derived from an active bacterial population, via bacterial metabolic processes as has been previously suggested in recent literature (Cooper *et al.*, 2016; Ziervogel *et al.*, 2016). This is highlighted by the accelerated development of Peak T fluorescence when increasing the incubation temperature, from 20°C to 30°C (Figure 4.4). This further supports the hypothesis that Peak T fluorescence is a microbial metabolic product, agreeing with the suggestion by Ogawa *et al.*, (2001) that the rate of OM formation is dependent on the rate of microbial activity, and therefore metabolism. The increase in Peak T intensity for the 30°C with steady bacterial numbers and DO also indicates that Peak T can provide extra information about microbial activity and metabolic processing. This is further supported by the lack of significant correlation identified between Peak T and bacterial numbers within this work. By using different temporal scales to other Peak T/DO research, the work here contradicts some of the correlations identified in recent research. This is not unexpected within a microbial community where complex microbial interactions occur. However, this does allow for the suggestion that Peak T fluorescence is not a suitable proxy for bacterial enumeration, but rather is indicative of microbial activity. Furthermore, variable Peak T fluorescence intensity is seen for both incubation temperatures, again suggesting that this AFOM is both processed and produced *in situ* by the bacterial community.

4.3.2.1.1 Fluorescence, microbes and dissolved oxygen

Previous research supports a relationship between Peak T fluorescence and the BOD (Hudson *et al.*, 2009; Baker and Inverarity, 2004; Reynolds, 2002), leading Peak T

fluorescence to be used as a surrogate for the BOD_5 test, often required by water management policy. BOD_5 is a widely utilised method for approximating bioavailable organic matter, by determining the change in oxygen over a 5 day period as an indication of biological activity (Jouanneau *et al.*, 2014). However, the fast-acting dynamics of Peak T fluorescence at the 5 day resolution of the BOD test make it difficult to apply Peak T as a BOD_5 proxy. By measuring fluorescence and dissolved oxygen at a higher temporal resolution, the true relationship between these parameters can be idenitifed.

The data shown in Figure 4.4, from Model System 2, shows variation in Peak T fluorescence intensity, with a steady decline in DO. This is demonstrated by the environmental samples suggesting that the correlations identified within the literature, between Peak T and BOD_5, may be artificial and not causal but created from the temporal resolution of the analysis. However, interference from the background fluorescence within the environmental samples prevented the true variation and dynamics of Peak T fluorescence to be determined.

By using synthetic samples, shown in Figure 4.4, Peak T could be identified without interference from Peak C. Monitoring the induction of Peak T fluorescence highlights the variability of Peak T fluorescence. This, alongside the steady decline in DO meant no significant correlations were identified. However, it is likely that significant correlations would have been present for the day zero and day five data points, as per the BOD_5 test and the observation from previous studies that have led to the suggestion of using Peak T fluorescence as a proxy for BOD_5 (Khamis *et al.*, 2015; Bridgeman *et al.*, 2013; Baker and Inverarity, 2004). The time-resolved data shows correlations identified in previous literature to be superficial, as previously suggested (Reynolds and Ahmad, 1995).

By investigating the dynamic relationship between DO mass transfer and Peak T fluorescence, using higher temporal resolution analysis, clear variation between the time points can be seen. This provides evidence that the BOD_5 test is non-representative of such an active system (Carstea *et al.*, 2016), rendering it unsuitable for comparison with fluorescence of a dynamic system and explaining the lack of significant correlations in the data presented here. From this study it can be concluded that the BOD_5 and Peak T fluorescence cannot be correlated due to the disparities between the analysis techniques (Carstea *et al.*, 2016). Regarding the dynamics of the system, the BOD_5 test is inherently flawed due to the assumptions made about the system and its representation of a demand without providing any information concerning the rate or kinetics of the demand. The study data discussed also highlights the importance of metabolic activity within the microbial community and how this impacts the fluorescence signal development, supporting the notion that Peak T fluorescence should be used as an indicator for labile material, independent from BOD_5 analyses, proposed by Hudson *et al.* (2008). This makes the prospect of real-time monitoring of microbial activity in freshwater aquatic systems a reality.

4.3.2.2 Microbially engineered humic-like fluorescence

The detailed dynamics of the mixed culture model system reveal *in situ* production and consumption from the net balance of AFOM involved during microbial processes, within all sample types. The use of environmental samples within this model system allows us to try to understand what may happen in real-world systems. The omnipresence of fluorescence peaks C and M (Figure 4.3), traditionally considered terrestrial/humic-like,

within these environmental samples supports the notion that the majority of this environmental AFOM, components 2 and 4 (Table 4.3), is recalcitrant in nature (Tanaka *et al.*, 2014; Hudson *et al.*, 2009; Spencer *et al.*, 2008). This is in line with the general understanding that component 4 represents high molecular weight non-bioavailable AFOM, currently considered to be of allochthonous origin (Cooper *et al.*, 2016), and component 2, Peak M, is biodegraded material derived from component 4, terrestrial AFOM Peak C (Coble *et al.*, 2014). However, some variation in fluorescence intensity for these components was seen over time, suggesting the possibility of these AFOM components being produced and processed *in situ*. Fully understanding the potential of the microbial community to influence these humic-like components is hampered by the background fluorescence from the environmental samples.

The use of supplemented synthetic samples (Figure 4.3), within the mixed culture model system, removed much of the background fluorescence seen in the environmental samples whilst providing a natural OM source. The increase, and phenomenon of variable fluorescence intensity, seen within the supplemented synthetic samples further supports the notion suggested from the environmental samples; humic-like fluorescence can be produced and utilised *in situ* by the microbial community. This proposed bioavailability changes the thinking within much of the freshwater AFOM research as it demonstrates that these fluorescence peaks are not solely attributed to terrestrial allochthonous sources. This is in line with marine-based AFOM studies (Fukuzaki *et al.*, 2014; Romera-Castillo *et al.*, 2011; Kramer and Herndl, 2004) and has been proposed in freshwater systems (Guillemette and del Giorgio, 2012). However, the use of closed model systems and high-frequency monitoring allows for the determination, beyond

speculation, of both production and consumption of a range of AFOM compounds and highlights the dynamic changes to AFOM composition that can occur via microbial processes.

The use of synthetic samples within the mixed culture model system clearly demonstrates the ability of the microbial community to produce AFOM *in situ*, albeit under controlled closed conditions. These samples provide clear evidence, in line with the environmental and supplemented synthetic samples, that 'microbially-derived' AFOM is not restricted to proteinaceous material or degradation of humic-like compounds. This is in agreement with recent FOM research for marine environments (Timko *et al.*, 2015; Shimotori, Watanabe and Hama, 2012), soils (Kallenbach, Frey and Grandy, 2016) and some freshwater literature (Guillemette and del Giorgio, 2012). Once developed these fluorescence peaks are again seen to be persistent yet varying throughout the 10-day experimental period. This is in line with the phenomenon seen throughout the use of Model System 2 and demonstrates fast-acting microbial dynamics are involved in the consumption and production of Peaks M, A_M, C and C+ (Lee *et al.*, 2015). The microbial building of higher molecular weight recalcitrant OM, as shown here, could have important implications for longer-term carbon storage and transportation throughout the aquatic continuum (Asmala *et al.*, 2014; Jørgensen *et al.*, 2014; Tanaka *et al.*, 2014; Ogawa *et al.*, 2001). Biodegradation is associated with component 2 (Table 4.3) and Peak C has previously been observed to be microbially derived (Guillemette and del Giorgio, 2012; Shimotori, Watanabe and Hama, 2012; Kramer and Herndl, 2004; McKnight *et al.*, 2001), as well as the *in situ* production and consumption of Peak C+, not previously reported.

4.3.2.3 Microbially engineered AFOM: hourly fluorescence and bacterial enumeration measurements

Increasing the temporal resolution of the fluorescence monitoring to hourly provides details regarding the fast-acting dynamics of bacterial-OM interactions not discussed elsewhere in the literature. These time resolved experiments further demonstrate the lability of Peak B (Figure 4.6) and the fast-acting dynamics associated with it mean that no significant correlation between Peak B fluorescence and bacterial numbers can be obtained. However, its omnipresence, alongside Peak T, asserts these fluorescence peaks as 'microbially-derived' and associates low intensities with cell presence alone. The five-fold increase in Peak T fluorescence intensity, seen in both Figure 4.5 and 4.6, further highlights the dynamics of microbial metabolism and the impact this has on the origin of such AFOM. For the hourly monitored samples (Figure 4.6), there is an observed lag in Peak T fluorescence development suggesting that residence time may be important for the production of autochthonous AFOM, particularly with competition within a microbial community sustained in nutrient limited environments (as shown here). The impact of incubation at a range of temperatures clearly demonstrates the relationship between microbial metabolic activity and fluorescence intensity, suggested from synthetic sample data obtained during the 10-day experiment. This directly supports the hypothesis that heterotrophic microbial metabolism, and its rate, are key drivers in the production of microbially-derived AFOM (Cammack *et al.*, 2004; Ogawa *et al.*, 2001; Parlanti *et al.*, 2000).

The fluorescence intensity increase preceding that of the cell multiplication suggests upregulation of bacterial metabolic processes, in the nutrient limited system, prior to cell

multiplication. This provides potential evidence that microbially-derived fluorescence is the result of metabolic activity. It is likely that this lag is the reason that significant correlations cannot be identified between the Peak T fluorescence and microbial enumeration. This is in agreement with the daily samples from the 10-day experimental period previously discussed (section 4.3.2.1). From this it can be recommended that Peak T fluorescence cannot be used to determine species specific enumeration in surface freshwater systems where there is high AFOM background (Sorensen *et al.*, 2018b; Baker *et al.*, 2015) and groundwater with little fluorescence (Sorensen *et al.*, 2015a, 2016, 2018a). From the work here, it can be suggested that the correlations identified in other work may be due to the temporal resolution used in monitoring samples and not truly reflective of the complex microbial-OM interactions that occur within these dynamic systems. By utilising this resolution, the bacterial origin of Peak T fluorescence can be clearly identified. Therefore, it can be proposed that the microbially-derived fluorescence observed in aquatic systems is a function of heterotrophic microbial metabolism and is not representative of bacterial cell enumeration.

In addition to the importance of microbial metabolism, the data also highlights the need to study further the role of low nutrient environments in production and assimilation of AFOM. In the model synthetic aquatic systems that were used to investigate the production and assimilation of AFOM, the Peak T fluorescence QSU_{max} was approximately 25 (see Figures 4.4, 4.5 and 4.6). It is likely that this maximum is limited by nutrient availability, further supporting the theory that aquatic fluorescence organic matter is intrinsically related to the microbial metabolism at a community level which is, in turn, limited within the environmental constraints of the system.

The time resolved analysis of synthetic samples (Figure 4.5) also provides further clear direct evidence that AFOM, attributed to Peak M and Peak A_M (Table 4.3), can be manufactured without the presence of terrestrial OM material, namely Peak C (Guillemette and del Giorgio, 2012; Shimotori, Omori and Hama, 2009), as reported in marine OM research (Jørgensen *et al.*, 2014; Shimotori, Watanabe and Hama, 2012; Kramer and Herndl, 2004; Ogawa *et al.*, 2001). However, this experiment provides a detailed insight into dynamic production and assimilation of microbially-derived FOM in freshwater systems, both temporally and over a range of temperatures. From this, further evidence is provided regarding the possibility that Peak M can be attributed to microbially-derived extracellular AFOM production. The shoulder of Peak C+ seen at the 120 hour time points (Figure 4.5) is in agreement with Peak C+ production in the 10-day experiments. This highlights the importance of different metabolic processes, community composition and residence time on the AFOM signal of a waterbody. However, this does further support the hypothesis that allochthonous production of OM extends beyond proteinaceous material into higher molecular weight compounds.

4.3.3 Chapter 4: key findings

- The temporal scales used within the different laboratory model systems expose, for the first time, the evolution of bacterial AFOM over time. This reveals the details of the fast-acting dynamics of bacterial-OM interactions and AFOM production, not discussed elsewhere in the literature.
- Peak T fluorescence is not an appropriate proxy for bacterial enumeration, particularly in surface freshwater systems with high AFOM background.

- BOD_5 and Peak T fluorescence should be used as independent water quality parameters, with *in situ* Peak T fluorescence providing a real-time indicator of microbial activity in freshwater aquatic systems.
- Bacteria can produce a range of complex high molecular weight AFOM, *in situ*, likely to be metabolic by-products or the production of functional proteins, created within the bacterial cell and exported.
- Peak C+ can act as a biomarker for *P. aeruginosa*, which could have cross-disciplinary applications, such as within clinical and health science.

Chapter 5 Monitoring quality of a freshwater system

5.1 Introduction

Monitoring quality of surface freshwater bodies is of global interest, particularly with increasing pressures from population growth, urbanisation and increased agricultural and industrial pollution (Patil, Sawant and Deshmukh, 2012). At present, policy and regulation drives the monitoring of freshwater systems. This has led the water industry and environmental agencies to collect discrete samples and conduct routine testing at off-site laboratories (Dunn *et al.*, 2014; Cook *et al.*, 2013). These discrete samples are collected at varying temporal and spatial scales, often weekly or monthly and at points of interest. However, this often does not capture events, such as sewage contamination, within freshwater systems due to their dynamic nature. The variety of external sources and internal processes make it very difficult to obtain useful long-term data from this method of monitoring.

There are well established *in situ* sensors for the online monitoring of many physicochemical parameters, such as pH and electrical conductivity (EC). Discrete sampling is, however, still required to monitor other parameters of interest, such as microbiological contamination (Cook *et al.*, 2013), due to a shortage of suitable online detection techniques (Besmer and Hammes, 2016). Such parameters are intrinsically transient and so discrete sampling does not adequately report variations within a dynamic system and cannot provide real-time information on events. Current practice employs other physicochemical sensors as proxies for microbiological monitoring, such

as turbidity meters. However, turbidity is not considered a reliable indicator of microbiological contamination. Recent literature (Sorensen *et al.*, 2015a, 2016; Coble *et al.*, 2014; Hudson *et al.*, 2008) has suggested the use of monitoring aquatic fluorescent organic matter (AFOM) as an alternative indicator.

To date, much research exploring the use of Peak T fluorescence to monitor these dynamic aquatic systems has relied upon discrete sampling, with *in situ* sensors often being used for short term monitoring. This chapter addresses the use of online *in situ* sensing for a long term monitoring study, for both traditional water quality physicochemical parameters and fluorescent organic matter. The impact of biofouling on *in situ* sensors is also explored, particularly in relation to the fluorescence data. The continuous online *in situ* data is compared to regular discrete sampling, with samples analysed at an ISO accredited off-site laboratory for a range of parameters, replicating common water quality monitoring practice, alongside laboratory fluorescence measurements. The influence of sample storage and treatment is also considered in relation to the intensity of AFOM identified by discrete sampling.

5.2 Continuous monitoring: online *in situ* sensing

Continuous online *in situ* monitoring of the surface freshwater body (section 2.8) was undertaken from May to December 2017. Data were collected via a telemetry system (section 2.8.2.1) and the mean calculated for each physicochemical parameter for each calendar month (Table 5.1). From this data it is clear that the pH of the water body is within natural limits, 7.5-8.5, and, therefore, not considered to have much impact on the

quenching of the fluorescence signal. The EC is variable throughout the monitoring period, with no discernible changes easily identified between the different months. Dissolved oxygen (DO) is shown to be higher and more stable, as demonstrated by the standard deviation, for the winter months, when the water temperature is lower. The water temperature peaks in July, with a gradual decline through the autumn and into the winter months, as expected. This is reflected within the fluorescence data from the *in situ* Peak T and C UviLux sensors (Figure 5.1, Chelsea Technologies Group Ltd., UK), whereby the fluorescence intensity for both peaks demonstrates a decline with a decrease in temperature.

Table 5.1: Mean values from the online *in situ* sensor data for physicochemical and fluorescence parameters. Values averaged per calendar month (n = 2879/2975, ± 1 standard deviation).

	Physicochemical Parameter					
Month (2017)	**pH**	**Temperature (°C)**	**EC (µS/cm)**	**Dissolved Oxygen (mg/L)**	**Peak T Fluorescence (QSU)**	**Peak C Fluorescence (QSU)**
May	7.54 ± 0.26	17.66 ± 2.01	587.04 ± 79.81	6.10 ± 2.29	24.87 ± 6.66	28.86 ± 6.56
June	7.86 ± 0.60	19.57 ± 2.60	636.34 ± 75.08	6.86 ± 4.77	27.82 ± 6.24	24.86 ± 11.61
July	7.76 ± 0.78	20.00 ± 1.83	534.55 ± 79.34	7.93 ± 4.02	22.87 ± 7.40	17.19 ± 6.10
Aug	7.51 ± 0.53	18.75 ± 1.06	579.55 ± 37.81	7.11 ± 2.73	23.43 ± 11.14	27.05 ± 3.30
Sept	7.62 ± 0.23	16.14 ± 1.20	514.56 ± 75.52	7.00 ± 1.43	16.61 ± 12.40	25.07 ± 4.11
Oct	7.81 ± 0.11	13.87 ± 1.17	551.61 ± 46.76	6.96 ± 0.73	19.37 ± 8.96	21.50 ± 1.97
Nov	8.02 ± 0.17	9.29 ± 1.43	565.94 ± 48.84	8.02 ± 0.66	14.55 ± 1.08	18.57 ± 1.15
Dec	8.53 ± 0.07	6.34 ± 1.50	654.03 ± 90.89	9.51 ± 0.71	12.26 ± 0.83	16.91 ± 2.36

5.2.1 Online *in situ* fluorescence monitoring: UviLux fluorometer

The UviLux fluorometer (Figure 5.1) from Chelsea Technologies Group Ltd. (UK) is an innovative, sensitive, low cost, *in situ* digital UV fluorometer. The sensors are easily portable with a diameter of 70 mm and length of 185 mm. The sensor is available in a range of variants that enable real-time monitoring of the following parameters: Single ring aromatics (BTEX), Polycyclic Aromatic Hydrocarbons (PAH); optical brighteners, used for detecting household wastewater misconnections; Coloured Dissolved Organic Matter (CDOM), Peak C; and, Tryptophan-like fluorescence, Peak T, associated with bacterial contamination in waste, recycled and natural water supplies. UviLux employs a UV LED light source and a compact photomultiplier tube (PMT) to provide extremely sensitive measurements, at the parts per trillion level. The light cowl enables the use of UviLux sensors in high ambient light, which can be of great importance for use in surface waters. The sensors have long-term calibration stability and optical filtration for both excitation and emission paths provides turbidity rejection, although this is not internally corrected for. Lack of inherent turbidity correction affects the ability of the UviLux to be utilised for a range of applications, including environmental surface waters and wastewaters. The robust and chemically inert housing facilitates broad application and the low power consumption makes the sensor attractive for off-grid deployment, as well as permanent or long-term monitoring installations.

Figure 5.1: Image of the UviLux sensor (Chelsea Technologies Group Ltd., UK), complete with light cowl. Used with permission of the creator, Chelsea Technologies Group Ltd.

5.2.1.1 Long-term in situ monitoring: fluorescence Peaks T and C

Figure 5.2 displays the data obtained from the online *in situ* fluorescence sensors from July 2017-December 2017. The data for each sensor is relatively noisy and it is possible that overlapping spectra cause the data to trend together. To remove this, and display true Peak T events within the system, a T/C ratio (Figure 5.2b) was also considered. This may be particularly important if the sensors were to be deployed within a monitoring system with a threshold-based alarm mechanism. However, some events occur at similar magnitudes within both sensor datasets (Figure 5.2a), suggesting that intense Peak C events may impact the fluorescence region of the Peak T signal. Peak T events are seen after cleaning and redeployment of sensors, identified within both the Peak T signal and ratio data. These events occur for across a time period of two-three days

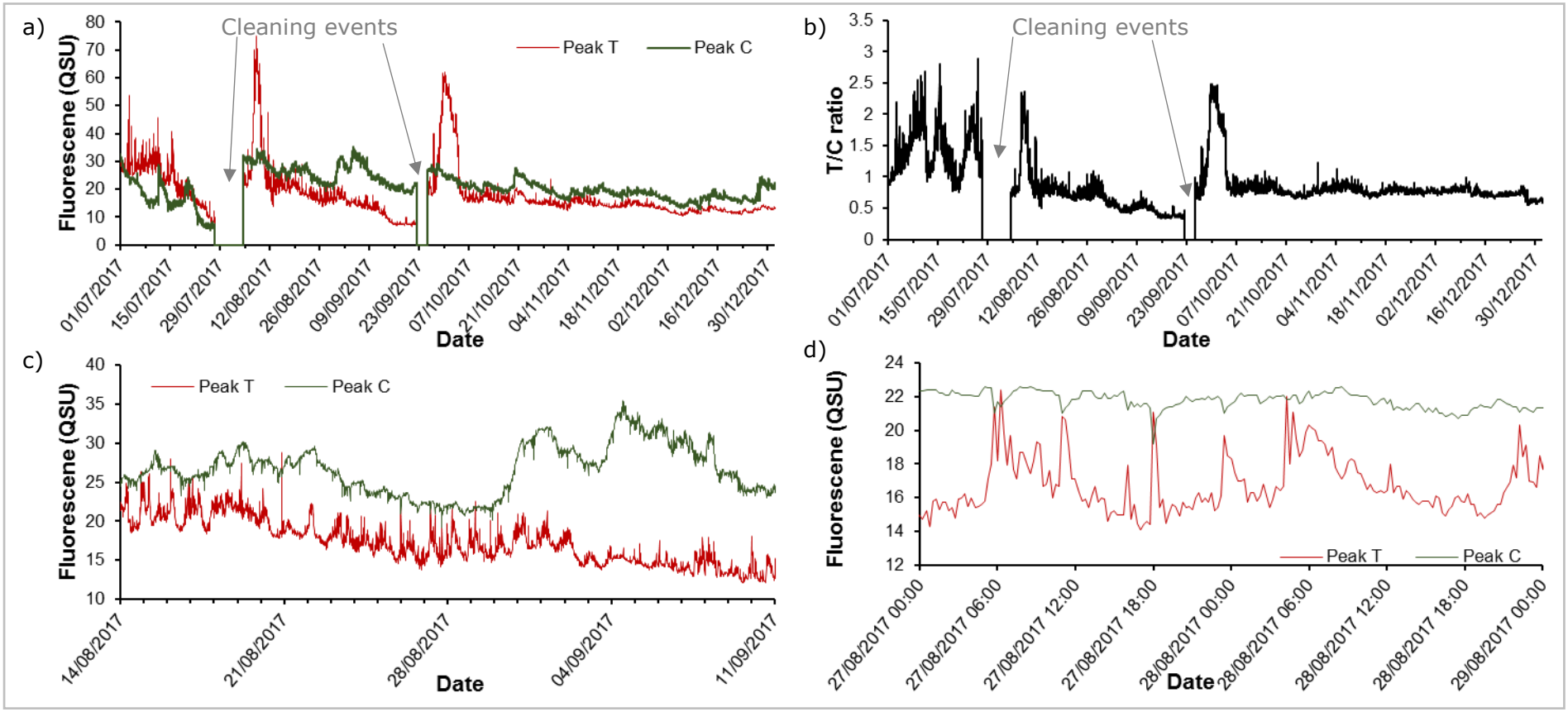

Figure 5.2: Continuous online *in situ* monitoring of Peak T and C fluorescence within the surface freshwater, measured using UviLux Tryptophan and CDOM sensors (Chelsea Technologies Group Ltd., UK) respectively. Online data collection is undertaken at 15 minute intervals: a) Peak T and C data from sensor deployment July 2017-December 2017; b) Ratio of Peak T and Peak C *in situ* fluorescence from July 2017-December 2017; c) Peak T and C data from 4 week period, commencing 14th August 2017, demonstrating diurnal variation in fluorescence intensity; d) Peak T and C data from a 48-hour period, highlighting diurnal variation in Peak T fluorescence intensity. Blank data periods seen within a) and b) are caused by removal of the sensors for cleaning.

It is clear from Figure 5.2 that the *in situ* fluorescence measurements are impacted by fouling of the sensor windows, as with all *in situ* aquatic monitoring. This is seen by a drop off in fluorescence over time after cleaning and re-deployment. During this gradual decline, the diurnal variation in Peak T is still identifiable within the data, with fluorescence intensity peaking during daylight hours. To assess the impact of fouling, sensors here were deployed with longer periods of time between deep cleaning, which involves an ethanol soak and manual cleaning of the windows and sensor housing. Additionally, windows were routinely wiped and sediment build-up removed at the collection time-point for each discrete sample.

5.3 Discrete sampling

Discrete samples (section 2.8.1) were collected weekly from the water body at the location of the *in situ* sensors (section 2.5.1). Samples were subsampled within an hour of collection for chemical and microbiological analysis off-site at a UK accredited laboratory (ISO 17025 (2005). Table 5.3 contains the mean data for each month collected from this analysis. This freshwater system is very eutrophic, i.e. it has a high nutrient load, and is physicochemically relatively stable throughout the sampling period (Table 5.3). The steady pH and variable EC data trends are in agreement with the continuous online *in situ* data (Table 5.1). The chemical composition of the water body is also similar across the months sampled; with chloride, sulphate and orthophosphate data displaying little variability between the mean values for each calendar month (Table 5.3). The nitrite levels within this system are low, apart from in June, and decline throughout the sampling period, with lower and stable nitrite concentrations seen in the colder months.

The calculated nitrate values highlight the increased presence of bioavailable nitrogen within the system in the latter months, which may be related to decreased microbial activity and/or lower assimilation of nitrate due to reduced plant growth at this time.

The microbiological data provided (Table 5.2) by the off-site laboratory demonstrates the presence of pathogenic and commonly tested bacteria in water quality analysis in all discrete samples from the freshwater body; the presence of coliforms, *Escherichia coli*, *Clostridium perfringens*, *Enterococci sp.* and *Pseudomonas aeruginosa,* specifically, were also identified within all samples. This data is presence focussed and measured using thresholds, rather than enumeration. However, the presence of any of the species cultured is a fail by Drinking Water Inspectorate (DWI) standards.

Table 5.2: Presence and absence data for the microbiological cultures obtained from the analysis of discrete samples from the surface freshwater body, undertaken at an off-site laboratory (UK accredited laboratory, ISO 17025 (2005)); n = 3-4. Data is reported via a threshold system, and presented here as universal presence, greater than (>) or less than (<) the threshold value.

Bacterial culturing analysis	**Units**	**Threshold**	**Presence in samples (2017)**					
			June	July	Aug	Sept	Oct	Nov
2 day plate count (37°C)	cfu / ml	3000	>	>	>	>	<	<
3 day plate count (22°C)	cfu / ml	3000	>	>	>	>	>	>
Total coliforms	cfu /100 ml	1000	>	>	<	>	>	>
Escherichia coli	cfu /100 ml	100	>	>	>	>	>	>
Clostridium perfringens	cfu /100 ml	100	>	>	<	>	>	>
Enterococci sp.	cfu /100 ml	100	>	>	<	>	>	>
Pseudomonas aeruginosa	cfu /100 ml	50	>	>	<	>	>	>

Table 5.3: Mean monthly data for the physicochemical parameters obtained from the analysis undertaken at an off-site laboratory (UK accredited laboratory, ISO 17025 (2005)); n = 3-4, ± 1 standard deviation. Mean peak picked fluorescence intensity data, QSU (1 QSU = 1 μg L^{-1} quinine sulphate) for Peak T ($\lambda_{ex}/\lambda_{em}$ 280/330-360 nm) and Peak C ($\lambda_{ex}/\lambda_{em}$ 350/420-460 nm) per calendar month. Data obtained from excitation-emission matrices (n = 3-4, ± 1 standard deviation) from the surface freshwater body discrete samples.

Month (2017)	Physicochemical Parameter								Fluorescence	
	pH	Turbidity (NTU)	EC (μS/cm at 20°C)	Chloride (mg/L)	Sulphate (mg/L)	Orthophosphate (mg/L P)	Nitrite (mg/L NO_2)	Nitrate (mg/L NO_3)	Peak T (QSU)	Peak C (QSU)
June	7.63 ± 0.22	52.75 ± 18.98	567.75 ± 61.49	48.00 ± 7.70	103.50 ± 14.39	0.74 ± 0.17	0.20 ± 0.07	4.90 ± 1.27	47.57 ± 6.02	27.10 ± 7.78
July	7.98 ± 0.19	59.50 ± 4.80	491.50 ± 66.23	44.00 ± 6.68	91.75 ± 24.05	0.48 ± 0.13	0.09 ± 0.05	4.43 ± 1.63	57.93 ± 16.35	26.99 ± 2.54
Aug	7.50 ± 0.10	50.00 ± 16.09	580.34 ± 40.61	49.00 ± 3.61	113.67 ± 5.13	0.45 ± 0.03	0.06 ± 0.01	5.23 ± 0.85	39.51 ± 1.77	20.80 ± 2.47
Sept	7.55 ± 0.06	27.50 ± 6.81	497.75 ± 94.49	41.50 ± 8.19	94.75 ± 24.14	0.44 ± 0.07	0.05 ± 0.03	7.00 ± 2.04	27.67 ± 1.91	17.68 ± 3.24
Oct	7.65 ± 0.07	33.50 ± 24.75	525.50 ± 34.65	40.50 ± 3.54	111.50 ± 7.78	0.61 ± 0.01	0.05 ± 0.01	8.15 ± 0.07	24.58 ± 3.11	15.06 ± 0.68
Nov	7.60 ± 0.08	11.53 ± 5.20	540.75 ± 75.07	41.25 ± 6.02	113.25 ± 20.85	0.67 ± 0.10	0.04 ± 0.01	8.80 ± 1.85	17.72 ± 3.70	13.26 ± 1.50

Samples were also analysed using fluorescence spectroscopy on site. PARAFAC analysis was conducted on the fluorescence spectra data set obtained from the laboratory analysis of the freshwater discrete samples. This analysis of the EEM data (n=96) (excluding EEMs with scattering anomalies) could only identify the common presence of two fluorescence components (Table 5.4). Although the two-component PARAFAC model is statistically valid (CORCONDIA = 100), the model only accounted for 90.61% of the total variation in fluorescence. However, increasing the number of components within the PARAFAC model resulted in a model that is not considered to be statistically robust (CORCONDIA < 50) (Bro and Kiers, 2003). It is clear from Figure 5.3 and Table 5.4 that this model does not adequately describe the spectral variability in the AFOM of the samples. The fluorescence components identified encompass multiple fluorescence peaks common to freshwater AFOM (Table 5.4). It is likely this is caused by all the samples being from the same water source, albeit at different time points. As such, it is the intensity of the fluorescence peaks that varies between samples, rather than the AFOM composition (Figure 5.3). The occurrence of peaks simultaneously throughout the data set limits the ability of the PARAFAC to decompose the fluorescence spectra.

Table 5.4: Identified PARAFAC analysis (section 2.1.2.3) components from the excitation-emission matrices obtained from the environmental discrete-samples data set (n = 96). Polygon position and associated fluorescence peaks (Coble *et al.,* 2014) are detailed.

PARAFAC Component	**Spectral position of component polygon** $\lambda_{ex}/\lambda_{em}$ (nm)	**Fluorescence peaks within polygon**	**Peak position** $\lambda_{ex}/\lambda_{em}$ (nm) (Coble *et al.*, 2014)
1	240-380/380-480	M	290-310/370-420
		A_M	240/350-400
		C	320-365/420-470
		A_C	260/400-460
2	240-300/290-360	T	275/340
		A_T	230/340
		BTEX	255/310

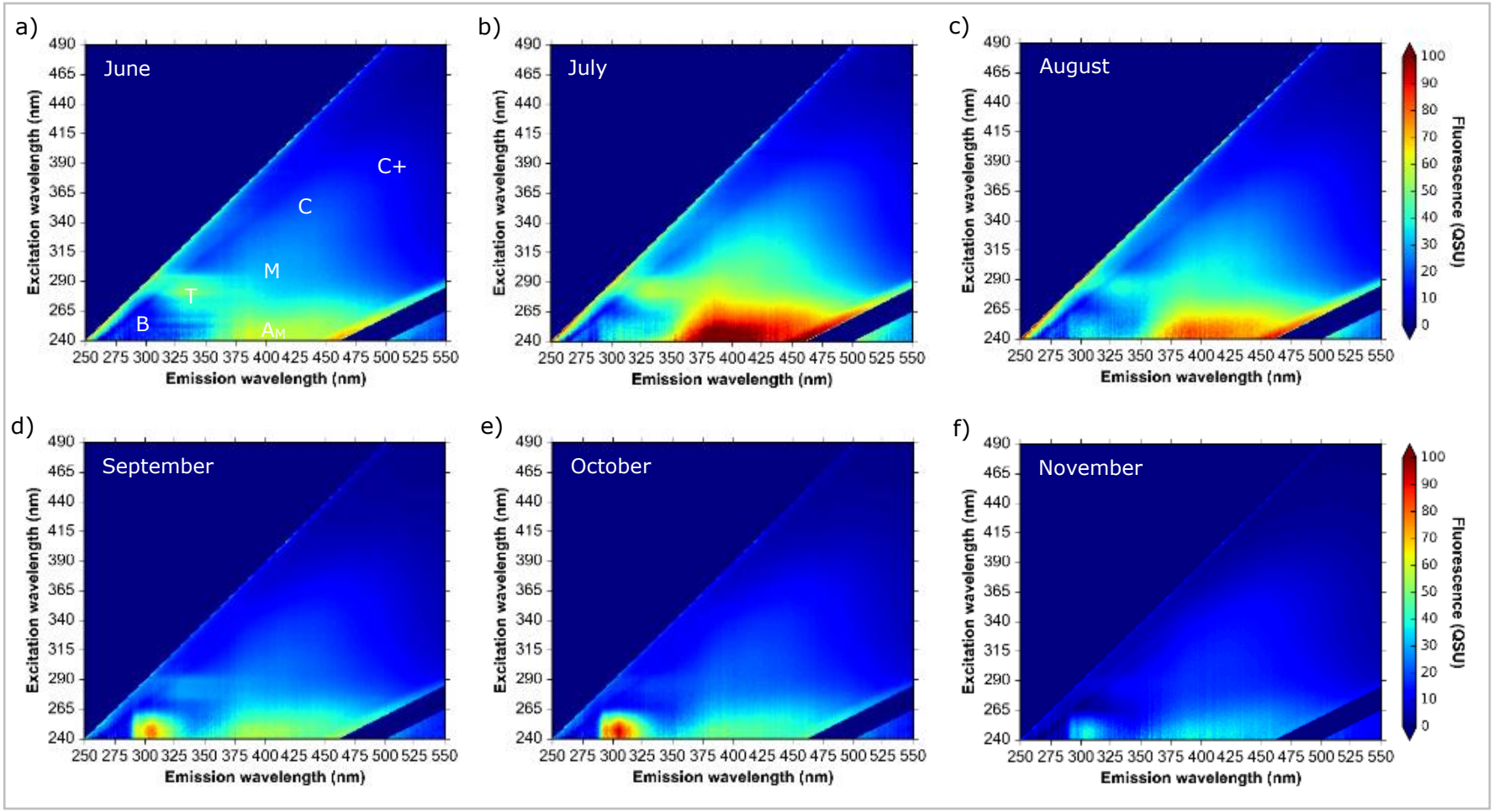

Figure 5.3: Excitation-emission matrices of discrete samples from the surface freshwater body at the end of each calendar month sampled in 2017: a) June; b) July; c) August; d) September; e) October; and f) November. Coloured bars are in quinine sulphate units, QSU (1 QSU = 1 μg L^{-1} quinine sulphate).

The EEMs, shown in Figure 5.3, highlight variation in the AFOM signal intensity throughout the sampling period. The highest fluorescence intensity of the overall AFOM fluorescence spectra is seen in the months with the higher water temperatures (Table 5.1). This is in agreement with the *in situ* fluorescence data (Table 5.1) and is evident in the peak picking data for fluorescence peaks T and C, obtained from the discrete samples (Table 5.4). The increase in intensity of the other fluorescence peak regions, with warmer water temperature, demonstrates the potential for *in situ* AFOM production to contribute to the environmental fluorescence spectra. Within environmental systems, AFOM origin is highly complex. However, the impact of temperature on microbial metabolic activity and AFOM production, demonstrated by the data in chapters 3 and 4, leads to the proposition that microbial production of AFOM is likely to be responsible for some of the increases in Peak A_M fluorescence intensity.

A peak is seen within these EEMs at $\lambda_{ex}/\lambda_{em}$ 255/310 nm. This peak is not discussed within the freshwater naturally occurring AFOM literature as it is associated with BTEX (benzene, toluene, ethylbenzene, and xylene) contamination (Persichetti, Testa and Bernini, 2013). The variable presence and fluorescence intensity of this peak is potentially related to increased runoff during rainfall events, as the waterbody receives runoff from the University campus carparks.

5.3.1 Fluorescence intensity and water temperature

The peak picking data from the EEM of each sample (Table 5.3) demonstrates a general decline in fluorescence intensity, in line with decreasing temperature. This is in agreement with the *in situ* fluorescence data (Table 5.1) and is also clearly seen by the EEMs in Figure 5.3. Significant correlations between the water temperature at the time of sampling and the fluorescence intensity for Peaks T and C were identified (Figure 5.4); $R^2 = 0.61$, $p < 0.001$, and $R^2 = 0.50$, $p < 0.01$, respectively. No significant relationships were identified between water temperature and the fluorescence for the discrete sampling time points, although a similar trend, increasing fluorescence with increased temperature, is exhibited by the monthly mean data (Table 5.1).

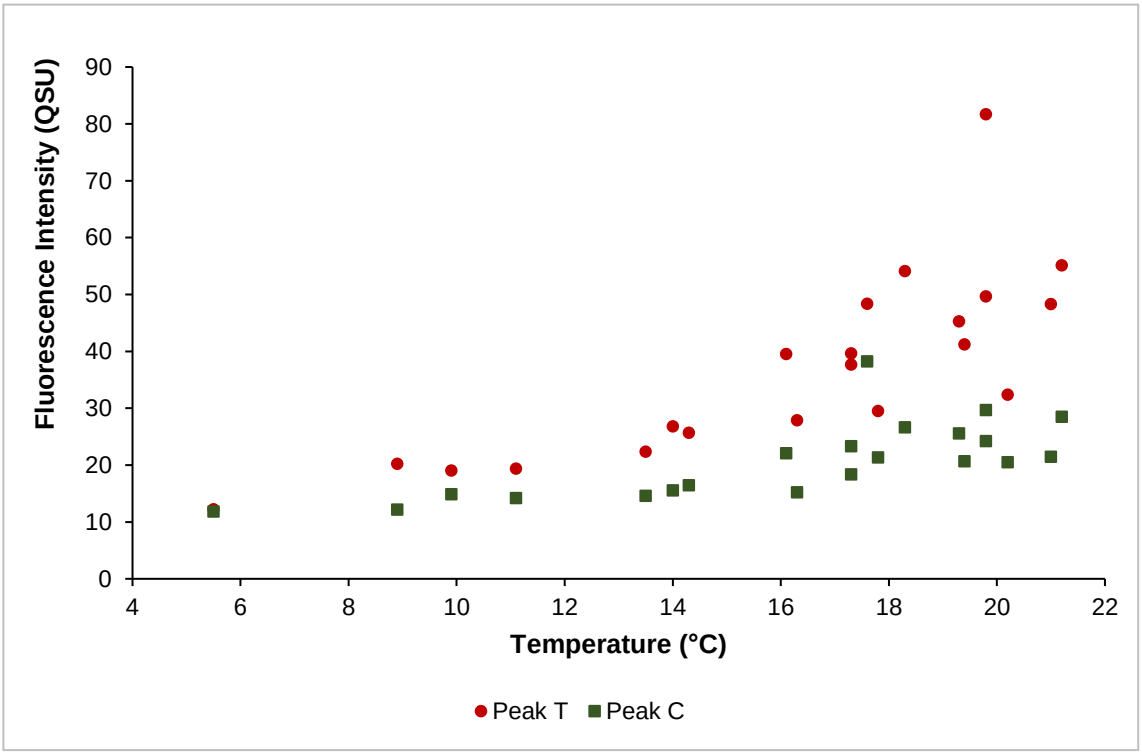

Figure 5.4: Water temperature (°C) at the time of the discrete sample collection against the benchtop fluorescence intensity for peaks T and C. Fluorescence data is presented in quinine sulphate units, QSU (1 QSU = 1 μg L^{-1} quinine sulphate).

5.4 Comparison of *in situ* and laboratory fluorescence measurements

Similar to the online *in situ* fluorescence intensity data, shown in Figure 5.2 and Table 5.1, the EEM fluorescence data (Table 5.3) further highlights the stability of Peak C fluorescence relative to the variability in Peak T. This is in line with other surface freshwater monitoring, whereby Peak C is seen to vary less and, therefore, considered to be less labile and terrestrially sourced (Coble *et al.*, 2014).

Table 5.3 and Figure 5.3 highlight that Peak T fluorescence is seen in higher intensities than Peak C; this is not reflected within the *in situ* fluorescence data (Table 5.1). It is likely that interference and scatter within the environment, which is not corrected for in the *in situ* data, is responsible for these discrepancies. The *in situ* sensors are also impacted by bio-fouling of the windows, which impacts the fluorescence intensity reported (Figure 5.2). Furthermore, this highlights the issue when comparing *in situ* continuous monitoring of a dynamic system with discrete samples, which reflect not only a snapshot in time, but also alter from collection to analysis. To minimise the impact of this, samples were analysed within one hour of collection.

5.5 Filtration of environmental freshwater samples: impact on fluorescence intensity

Unfiltered discrete samples from the environmental monitoring were analysed for fluorescence spectroscopy within 1 hour of sample collection (Section 5.3). Samples were also sub-sampled into sterile bottles containing 20 mg/L sodium thiosulphate for the off-site laboratory microbiological analysis. The use of sodium thiosulphate is common

within drinking water analysis sample collection to prevent any further disinfection from the presence of chlorine (The Public Health Laboratory Service Water Sub-Committee, 1953). As such, it is important to understand the potential impact on the AFOM signature that this may have if fluorescence is to be used to monitor potable water sources. Figure 5.5 shows that the addition of sodium thiosulphate to the sample has no significant impact on the fluorescence intensity of Peaks T and C.

The samples were also subjected to filtration using a range of pore sizes (section 2.8.1), to assess the impact of this on sample integrity. Although sample filtration is common practice (Zhu *et al.*, 2017; Asmala *et al.*, 2016; Miller and McKnight, 2010; Cammack *et al.*, 2004), there is currently no standard method for this. It is important to understand the impact of a range of filtration practices on AFOM fluorescence intensity when assessing discrete sampling for monitoring the water quality of natural systems. 11 μm filters were employed as these are frequently used within environmental sample collection to remove large particulate matter. It is clear from Figure 5.5 that, although particulate matter and some microorganisms are removed from the sample, this filtration has no significant impact on the fluorescence intensity of Peaks T and C. Some samples demonstrate an increase in fluorescence intensity for Peaks T and C post-11 μm filtration. This is likely to occur due to the variation between each subsample of the main sample, highlighting the issue of using discrete samples and subsampling within such dynamic systems.

0.45 μm filtration was undertaken (on samples in August-November) as this is often considered to be the dissolved fraction of OM, in line with the filtration techniques for dissolved organic carbon (Thurman, 1985). Filtration at this pore size removes

particulate OM, alongside many microorganisms, including algae and some bacteria. It is clear from Figure 5.5 that this results in FOM removal, with Peak T fluorescence intensity being impacted more heavily. This is evidenced by the mean reduction of 60% fluorescence intensity for Peak T and 19% reduction for Peak C, between the unfiltered and filtered samples. A paired t-test was conducted to determine if filtration at 0.45 μm filtration significantly reduced the fluorescence intensity of Peaks T and C. The mean reduction for Peak T ($M = 16.06$ QSU, $SD = 2.05$, $n = 13$) and Peak C ($M = 3.10$ QSU, $SD = 0.33$, $n = 13$) were both significantly greater than 0; $t(12) = 7.84$, two-tail $p < 0.001$ and , $t(12) = 9.49$, two-tail $p < 0.001$, respectively.

Samples were also filtered at 0.2 μm, which is considered to provide sterile-filtered samples. No significant difference was seen between the fluorescence intensity for the samples filtered with a 0.45 μm filter and a 0.2 μm filter (Figure 5.5). The mean reduction in fluorescence intensity after filtration at 0.2 μm for these samples was 40% for Peak T and 16% for Peak C. Filtration has a greater impact on Peak T fluorescence intensity, likely due to the removal of microorganisms that contain intracellular Peak T AFOM (chapters 3 and 4). A paired t-test was performed to determine the significance of filtration at 0.2 μm upon the fluorescence intensity of Peaks T and C. The mean reduction for Peak T ($M = 14.60$ QSU, $SD = 5.36$, $n = 22$) and Peak C ($M = 3.20$ QSU, $SD = 0.53$, $n = 22$) were both significantly greater than 0; $t(21) = 2.72$, two-tail $p < 0.05$ and , $t(21) = 6.00$, two-tail $p < 0.001$, respectively. This provides evidence that filtering samples at 0.2 μm also significantly reduces the fluorescence intensity of peaks T and C.

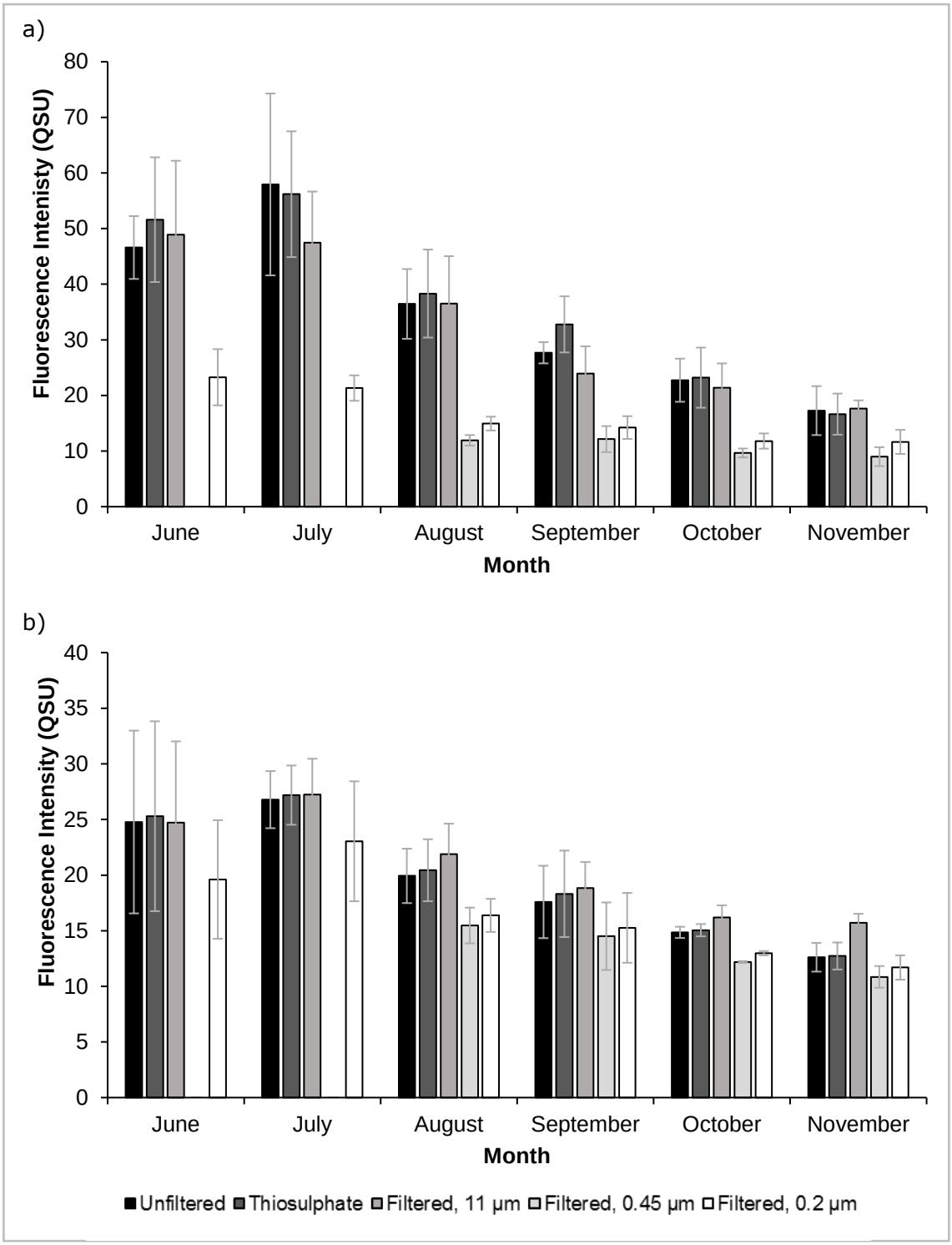

Figure 5.5: Monthly mean fluorescence intensity (n = 3-4, per month), reported in quinine sulphate units, QSU (1 QSU = 1 µg L^{-1} quinine sulphate), of Peaks T (a) and C (b) from the discrete samples (± 1 standard deviation). Data sets derived from a range of storage conditions and filtration applied prior to fluorescence spectroscopic analysis. There is no data for 0.45µm filtration for June and July.

5.6 Discussion

In this study, AFOM measurements have been undertaken using laboratory spectrofluorometers to analyse discrete samples, alongside acquisition of data for traditional microbiological and physicochemical water quality parameters. Whilst this has provided a wealth of information regarding OM characterisation and composition, technological developments have made *in situ* fluorescence monitoring a possibility (Ruhala and Zarnetske, 2017). Although the application of *in situ* monitoring has received more attention recently (Sorensen *et al.*, 2015a, 2016, 2018b, 2018a; Khamis, Bradley and Hannah, 2017; Saraceno *et al.*, 2017; Bridgeman *et al.*, 2015; Khamis *et al.*, 2015; Carstea, 2012), there is little available data exploring longer term monitoring of freshwater systems. The work here addresses this by utilising single fluorescence peak sensors, in conjunction with traditional water quality parameters, revealing the potential for this technology as well as exposing further developments to improve the application.

5.6.1 Water quality monitoring: physicochemical parameters and fluorescence intensity

Many of the physicochemical parameters measured are relatively stable throughout the monitoring period, for both the data collected from the *in situ* sensing (Table 5.1) and from the laboratory testing (Table 5.3). No relationship between the fluorescence signals and the water quality parameters, i.e. DO, temperature and EC, were identified within the continuous data. This highlights the notion that fluorescence data provides different information about the water quality and is not a proxy for current parameters but should be considered as a novel water quality parameter. The water temperature (Table 5.1)

varies monthly, reflecting seasonal variations. The impact of temperature variations on fluorescence quenching has long been recognised in relation to higher temperatures leading to increased collisional quenching (Carstea, Baker and Savastru, 2014; Coble *et al.*, 2014; Lakowicz, 2006). Whilst seasonal changes in temperature of environmental water bodies is gradual, the impact of diurnal temperature changes has been noted by Watras *et al.*, (2011). However, temperature variation is not seen to have a significant impact on fluorescence quenching within these samples, since although increased temperatures are paired with increased Peak T fluorescence intensity (Tables 5.1 and 5.2), Peak C remains relatively stable throughout. This is also reflected in the EEMs presented in Figure 5.3, and the fluorescence intensity data for peaks T and C obtained from these (Table 5.3). Higher water temperatures would increase the metabolic rate of microbial activity (Ogawa *et al.*, 2001), as demonstrated by the laboratory cultures in chapter 3. The increase in fluorescence intensity correlated with higher water temperatures, therefore, further indicates that the AFOM, particularly Peak T (Figure 5.4), can be indicative of microbial activity in freshwaters (Ziervogel *et al.*, 2016; Coble *et al.*, 2014). The highly eutrophic nature of this system means that the algal contribution to Peak T may be higher than the bacterial contribution. However, due to the unknown composition of the complex microbial community and the ubiquitous presence of Peak T with all bacterial types (chapters 3 and 4), Peak T fluorescence cannot be used to enumerate bacteria within this aquatic system.

The stability of Peak C fluorescence intensity, in comparison with Peak T, demonstrates the ability of the T/C ratio to be used to identify events driven by changes in Peak T fluorescence. Peak T is seen to be more variable, making it the more suitable fluorescence

peak for monitoring microbial activity in complex aquatic ecosystems. It can be suggested that the majority of the Peak C fluorescence present within this system is of allochthonous terrestrial origin (Coble *et al.*, 2014; Hudson, Baker and Reynolds, 2007), with microbially engineered Peak C being a much smaller contributor to the overall fluorescence intensity (Shimotori, Watanabe and Hama, 2012), as identified in chapters 3 and 4. Whilst the ratio can remove noise from the data, the data here highlights the importance of understanding the background fluorescence of the locations to be monitored. From this, it is clear that reporting the individual data outputs, alongside the T/C ratio, is important for data analysis and event identification (Zhou *et al.*, 2017). It also demonstrates the need for further research into the relationship between peaks T and C, to determine a more robust way of combining the data.

The use of Peak T fluorescence to monitor microbial activity is further evidenced here by the diurnal variation in fluorescence intensity (Figure 5.2). Further to the impact of temperature in the summer months, it is also likely that the hours of sunlight impact the microbial activity, particularly algal activity, leading to increased Peak T. The diurnal variation is clearly identified within the T/C ratio (Figure 5.1b), demonstrating that Peak T is the driver for this variation and highlighting the necessity of using both fluorescence peaks T and C to understand AFOM dynamics within freshwaters (Zhou *et al.*, 2017; Bridgeman, Bieroza and Baker, 2011). The diurnal variation is likely to be related to microbial activity within the system, related to both temperature and sunlight; interference from sunlight does not impact the fluorescence signal due to the built-in light cowl (Figure 5.1). Thus, algal Peak T fluorescence is likely to be the major contributing factor to this diurnal effect, as increased sunlight will cause an increase in

algal metabolic activity (Zhi *et al.*, 2015; Fukuzaki *et al.*, 2014; Herlemann *et al.*, 2014; Carstea, 2012; Spencer *et al.*, 2008). Although bacterial metabolic activity will impact Peak T, the data here does not allow for the algal and bacterial Peak T fluorescence to be separately distinguished. To determine this, it is important to monitor other water quality parameters, such as chlorophyll-a, which could then be used to distinguish algal blooms from increases in bacterial load (Makarewicz *et al.*, 2018). This further supports the application of *in situ* Peak T fluorescence monitoring for overall microbial community activity, not bacterial enumeration, due to the multiple factors which contribute to variations in Peak T fluorescence.

In addition to the variation in fluorescence intensity with water temperature, DO is shown to be higher at lower temperatures, with the data for May-August demonstrating more variable DO with higher water temperatures. The reason for this is potentially two-fold, with DO solubility being higher at lower temperatures and reduced microbial activity leading to lower oxygen consumption (Jørgensen *et al.*, 2011). However, Peak T fluorescence demonstrates higher intensities with lower, albeit more variable, DO values. From this, it can be postulated that increased microbial activity may also contribute to the lower DO in the summer months.

Moreover, the nitrite and nitrate data, obtained from the laboratory analysis of the discrete samples (Table 5.3), suggests decreased activity within this highly eutrophic system in the winter months. As available nitrogen is often a limiting factor for microbial activity, lower nitrate values would indicate increased microbial activity (Bieroza and Heathwaite, 2016). This can be suggested from the higher Peak T fluorescence intensity in conjunction with lower nitrate levels (Table 5.3). The turbidity data obtained from the

discrete samples also implies lower bacterial presence in the winter months; turbidity is commonly used as a proxy for bacterial contamination (Sorensen *et al.*, 2018a). However, in a complex system, such as the one monitored here, turbidity is affected by multiple factors, including the effects of rainfall events, such as dilution, and the addition of POM and DOM. Although the fluorescence and turbidity data show similar trends, the data here suggests *in situ* fluorescence is a water quality parameter independent of turbidity and providing higher sensitivity to changes in microbial community activity.

Although the data here highlights the potential advantages of using *in situ* fluorescence sensing, there are developments required to improve the application of this technology. As *in situ* fluorescence sensing usage has increased, research has identified a number of corrections that improve the data output (Khamis *et al.*, 2015; Watras *et al.*, 2011, 2014). These corrections include algorithms for spectral interferences from turbidity and absorbance, which prevent 'real' fluorescence being reported. As such, within complex matrices, it is difficult to compare *in situ* and EEM data. Regardless, the usefulness of this comparison must be questioned as the *in situ* data reflects a dynamic and ever changing sample within a system, particularly in flowing waters, whereas discrete sampling represents a static point in time. This highlights the limitations of discrete sampling and the inability to compare real-time *in situ* data with discrete sample data.

5.6.2 Impact of sensor fouling on the fluorescence signal

Another current limitation to the *in situ* sensors is fouling, in particular biofouling where biofilm structures build upon the sensor windows interfering with the fluorescence

signal (Khamis, Bradley and Hannah, 2017; Ruhala and Zarnetske, 2017; Blaen *et al.*, 2016). This is a problem common to all *in situ* sensing and is currently mitigated by frequent maintenance, with some sensors now employing physical biofouling removal, using wipers built into the sensor. The data in Figure 5.1 highlights the impact of biofouling, with a drop-off in fluorescence over time, between cleaning of the probes, with fouling seemingly having less of an impact in the winter months, when reduced microbial activity decreases the potential for biofilm production. This accumulation of biofilm prevents the identification of events within the sample beyond a certain level of biofilm development (Fischer, Friedrichs and Lachnit, 2014). Biofilm accumulation also seems to affect the sensor signal, with two large Peak T events, lasting two to three days, identified post deep cleaning of the sensors (Figure 5.2). It is difficult to determine whether these are AFOM events within the water or related to biofouling, of the sensor window, or lack of this phenomenon. As these events occur shortly after cleaning, it is possible that this is a result of the attachment phase of a biofilm on the window which leads to a spike in Peak T (Lemus Pérez and Rodríguez Susa, 2017; Fischer, Friedrichs and Lachnit, 2014). Determining the cause of these events requires further exploration to ensure that it is not also related to the sensor cleaning protocol. The influence of biofilms on the sensor windows requires further work to determine the true impact this can have on the fluorescence signal detected, with the development of biofouling prevention and/or removal techniques required to make sensors more autonomous and fit for the purpose of long-term monitoring.

5.6.3 Impact of sample filtration on fluorescence intensity

Further to the physicochemical, biological and fluorescence analysis of the discrete samples, the impact of filtration was also measured. Sample filtration is common practice within environmental water sample collection, particularly if discrete samples require transportation, meaning measurements cannot be undertaken shortly after collection (Zhu *et al.*, 2017; Asmala *et al.*, 2016; Miller and McKnight, 2010; Cammack *et al.*, 2004). Many filter at ≤ 0.7 μm to obtain the dissolved fraction of OM (Repeta, 2015; Aiken, 2014), with others using 0.45 μm filtration in line with dissolved organic carbon methods (Thurman, 1985). Figure 5.5 demonstrates the impact of filtration, predominantly on Peak T fluorescence intensity, providing evidence that filtering samples at ≤ 0.45 μm significantly reduces the intensity of the AFOM signal. This filtration removes microbial cells and, therefore, AFOM. This is particularly evident in the summer samples, further indicating the relationship between microbial cells and Peak T fluorescence. However, it is possible to use filtration of samples to discern between extracellular and intracellular Peak T fluorescence within environmental samples (Herlemann *et al.*, 2014), as highlighted within chapters 3 and 4. This data demonstrates the importance of on-site analysis and the necessity for careful consideration of sample storage and transportation. By exploring the impact of filtration on sample integrity, the work here exposes the potential for much of the previous literature to have underestimated Peak T fluorescence, inhibiting the understanding of its origin and potential as a water quality parameter.

5.6.4 Chapter 5: key findings

- *In situ* Peak T fluorescence can monitor overall microbial community activity, not bacterial enumeration; the contribution of algal AFOM is likely to be a major driver of variations in Peak T fluorescence intensity.
- Microbially engineered humic-like AFOM is likely to be a smaller contributor to the overall AFOM fluorescence intensity than allochthonous terrestrial AFOM in natural freshwater systems.
- Biofouling of *in situ* sensors currently limits the application of fluorimeters for long-term autonomous monitoring of freshwater systems.
- Preserving sample integrity when using fluorescence spectroscopy is essential. Collection, storage and transportation of samples must be carefully considered.

Chapter 6 Validation of an effective and reliable sensor to measure the phenomenon of aquatic fluorescent organic matter *in situ*

6.1 Introduction

Water quality sensors are widely commercially available for the monitoring of basic physicochemical parameters, but these sensors do not provide information regarding biotic parameters or processes within aquatic systems. Real-time technologies provide advantages in terms of streamlining the data collection process, potentially minimising human error and time delay, cost reduction in data collection, and, critically, produce a higher quantity and quality of data on temporal and spatial scales.

Extensive research is ongoing into the application of fluorescence based sensor technology for water quality management, but few commercially available devices are in existence on the market. This is occurring by adapting available technologies, such as *in situ* real-time portable fluorimeters for the identification of anthropogenic pollutants, such as polycyclic aromatic hydrocarbons (PAH) and optical brighteners. Recently portable fluorimeters have been developed for sensing biological contamination, using microbially derived fluorescence signals. There is a focus on the application of Peak T fluorescence sensing, as this has been shown, within the literature, as an indirect indicator of bacterial metabolism (Coble *et al.*, 2014; Hudson *et al.*, 2008; Cammack *et al.*, 2004), as well as a tracer for sewage contamination within aquatic systems (Sorensen *et*

al., 2015a, 2016; Hudson *et al.*, 2008; Elliott, Lead and Baker, 2006a; Baker *et al.*, 2003; Reynolds, 2002, 2003).

This chapter will detail the current limitations of the UviLux (Chelsea Technologies Group Ltd., UK), discussed in chapter 5, for certain applications. From this information, the design for the prototype of the new generation sensor (V-Lux) and the correction factors built into the new sensor will be detailed. The work reported here was undertaken at Chelsea Technologies Group Ltd. (CTG) and is commercial in confidence. Figures are provided by CTG. Units within this chapter are reported in ppt, ppb and ppm, as per the industry standard: 1 ppt is equivalent to 1 ng/L; 1 ppb is equivalent to 1 μg/L; and, 1 ppm is equivalent to 1 mg/L.

6.2 Application of *in situ* fluorometers: UviLux

The freshwater sensors are aimed at environmental monitoring and have been used for a range of applications within surface freshwaters (Bieroza and Heathwaite, 2016). Further to surface freshwaters, the UviLux sensors have been employed to assess the impact of various leachate in groundwater globally, and have demonstrated good correlations with bacterial enumeration within these systems (Sorensen *et al.*, 2015a, 2016). Alongside research and environmental water quality assessment, another key market is the water industry, mainly water utility companies, who are focussed on improving the efficiency and reducing the cost of water treatment, regarding both drinking water supply and waste water treatment. Whilst the application of fluorescence techniques for contamination events and wastewaters is well documented, monitoring

OM in source waters of drinking water treatment and monitoring the efficacy of the treatment process could provide an essential tool to trace contamination. Fluorescence may also be applicable to monitor disinfection by-products (DBPs) in distributed drinking water (Roccaro, Vagliasindi and Korshin, 2009). However, as UV and chlorination are common practice within drinking water treatment, the quenching effects on the fluorescence signal must be assessed. A case study is presented to determine the potential impact of chlorination on aquatic fluorescent organic matter (AFOM).

6.2.1 Case study: Quenching of AFOM signal with the addition of chlorine

There is currently a gap in the market for provision of a real time Peak T fluorosensor as an early warning system for identifying contamination or pollution events in drinking water distribution. However, the impact of residual chlorine within distribution networks must be considered when determining the use of fluorescence for monitoring AFOM.

All waters used to provide drinking water are known to contain both dissolved and natural organic matter, DOM and NOM respectively, that produces a fluorescence signature (Coble *et al.*, 2014; Matilainen *et al.*, 2011). These fluorescent aromatic compounds could potentially be used to monitor their presence in distribution and treatment systems (Westerhoff, Chao and Mash, 2004), and although this idea has not yet been applied in a commercial capacity, there is significant scope for applying

fluorescence based techniques in this sector. This could be of particular importance regarding the increasing awareness and concern for public health surrounding Disinfection By-Products (DBP), with specific focus on carcinogenic trihalomethanes, as these can be produced during chlorination processes (Hua *et al.*, 2010; Roccaro, Vagliasindi and Korshin, 2009; Westerhoff, Chao and Mash, 2004).

The key to DBP management is source water control, specifically regarding OM control and management (Bridgeman, Bieroza and Baker, 2011). Although high molecular weight aromatics are easily removed within treatment, low molecular weight autochthonous material is a major precursor for these DBPs, but is difficult to monitor at present due to spatial and temporal variations in source water OM and the use of multiple source waters (Bridgeman, Bieroza and Baker, 2011; Bieroza, Bridgeman and Baker, 2010). Fluorescence techniques offer a sensitive detection methodology for monitoring the removal of NOM and to determine the OM characteristics within source waters and throughout treatment processes (Bridgeman, Bieroza and Baker, 2011; Bieroza, Bridgeman and Baker, 2010; Beggs, Summers and McKnight, 2009). Alongside DBP precursor monitoring, fluorescence can also be used to determine contamination events in distribution networks or recycled water systems by monitoring Peak T (Henderson *et al.*, 2009), and this has been shown experimentally (Hambly *et al.*, 2010).

6.2.1.1 Methodology

A chlorine stock (10 ppm) was added to an L-tryptophan (Sigma-Aldrich Co., USA) solution (300 ppb) and environmental samples from two different surface freshwaters:

Dead River, N 51° 23′ 40″, W 0° 22′ 33″, and a lake within Molesey Heath park, N 51° 23′ 31″, W 0° 22′ 36″. Chlorine was added to produce final concentrations of 0.1-4.0 ppm, which was verified using SenSafe® test strips (Industrial Test Systems, Inc., USA). The maximum concentration, 4.0 ppm, is below the guideline of 5.0 ppm set by the World Health Organisation for residual chlorine within distribution systems (Drinking Water Inspectorate, 2010). Chlorine was dosed into the samples which were analysed 10 minutes after the dosing, using fluorescence spectroscopy (HORIBA Aqualog®, HORIBA Ltd., Japan), with the parameters detailed in section 2.1.1.1. 5 mg of sodium thiosulphate was then added to the 4.0 ppm chlorine sample, removing any free chlorine and preventing further chlorination effects. An EEM of this sample was then conducted to determine if quenching of the AFOM was reversible. Analysis of all samples was rerun two hours after the dosing. Data was peak picked to determine the quenching impact of chlorine on peaks T and C fluorescence (section 2.1.2.3).

6.2.1.2 Results and Discussion

The data for the L-tryptophan samples, Figure 6.1, highlights how vulnerable free tryptophan is to chlorine quenching. The fluorescence intensity was reduced by 30% for the weakest chlorine concentration, after only 10 minutes contact time. The Peak T fluorescence is completely quenched within the sample with a final chlorine concentration of 0.4 ppm. The data demonstrates that the majority of the quenching occurs with short contact times. For low concentration chlorine solutions, some of the fluorescence appears to recover with time. This data suggests that chemical quenching of Peak T may prevent the application of fluorescence technologies for monitoring water

treatment works, post chlorination. However, elevated Peak T fluorescence within distribution networks could identify misconnections or contamination within the system.

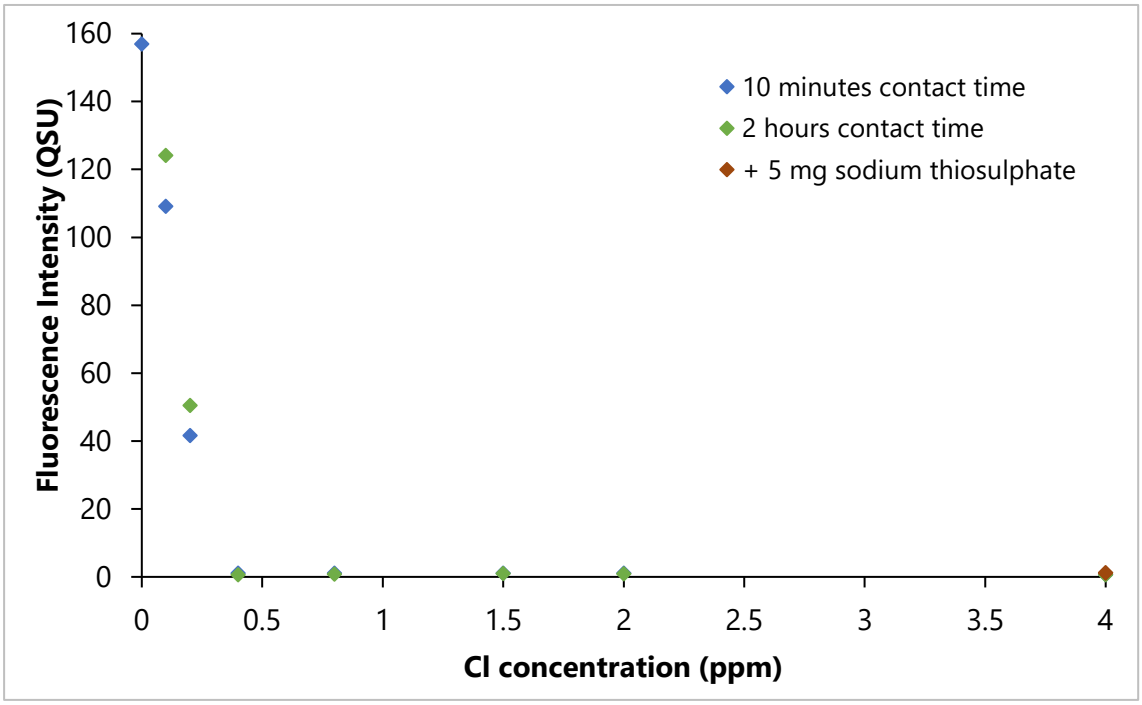

Figure 6.1: Impact of chlorine addition on Peak T fluorescence of an L-Tryptophan solution (300 ppb). Data is peak picked from excitation-emission matrices at $\lambda_{ex}/\lambda_{em}$ 280/350 nm. Chlorine dosing 1 refers to the fluorescence intensity after 10 minutes contact time with the chlorine dosing; chlorine dosing 2 is the intensity measured after 2 hours contact time. Fluorescence intensity is reported in quinine sulphate units (QSU); 1 QSU is equivalent to the fluorescence intensity, of 1 ppb quinine sulphate at $\lambda_{ex}/\lambda_{em}$ 347.5/450 nm.

The EEMs in Figure 6.2 clearly demonstrate the quenching seen by the addition of chlorine to environmental surface freshwaters. This highlights the quenching of all regions of AFOM, not solely Peak T. This quenching was seen in both environmental samples tested (Figures 6.2 and 6.3), with Figure 6.3a demonstrating the impact of chlorine dosing on fluorescence quenching for both peaks T and C. This data further demonstrates the impact of chlorine dosing on AFOM intensity. However, the Peak T

within the environmental samples is not fully quenched, as seen with the chemical tryptophan solution (Figure 6.1). Figure 6.3 also shows that increasing the contact time, although having little impact, does not allow the fluorescence intensity to recover. This suggests that the environmental Peak T fluorescence is less vulnerable to quenching, perhaps as it is not free tryptophan (Coble *et al.*, 2014) and, as Peak T in environmental samples is attributed to a range of fluorophores, not solely pure tryptophan (Bridgeman, Bieroza and Baker, 2011).

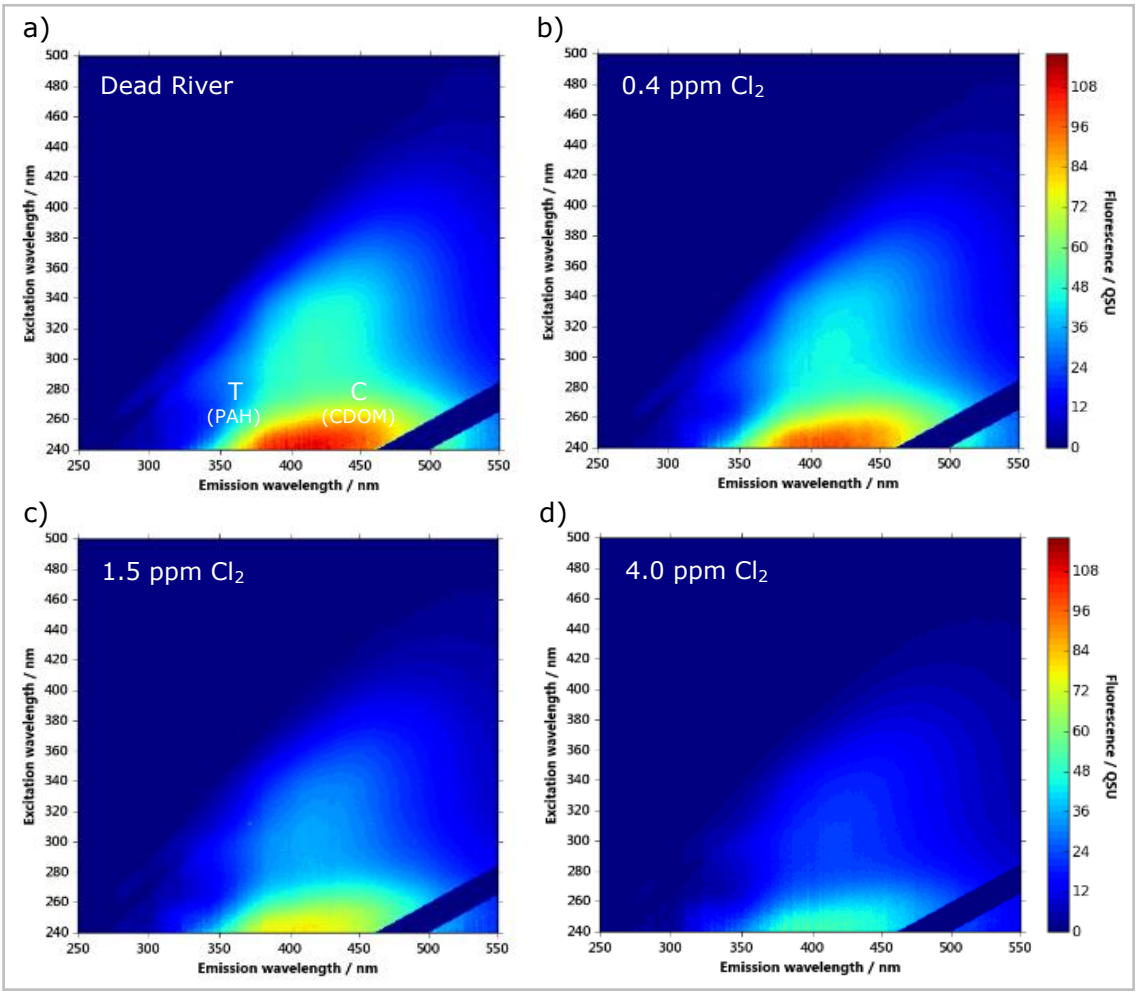

Figure 6.2: Fluorescence excitation-emission matrices of: a) an environmental surface freshwater (Dead River, N 51° 23′ 40″, W 0° 22′ 33″); and b), c) and d) for the environmental sample dosed with chlorine, resulting in 0.4 ppm, 1.5 ppm and 4.0 ppm chlorine solutions respectively. Fluorescence is reported in quinine sulphate units (QSU); 1 QSU is equivalent to the fluorescence intensity, of 1 ppb quinine sulphate at $\lambda_{ex}/\lambda_{em}$ 347.5/450 nm.

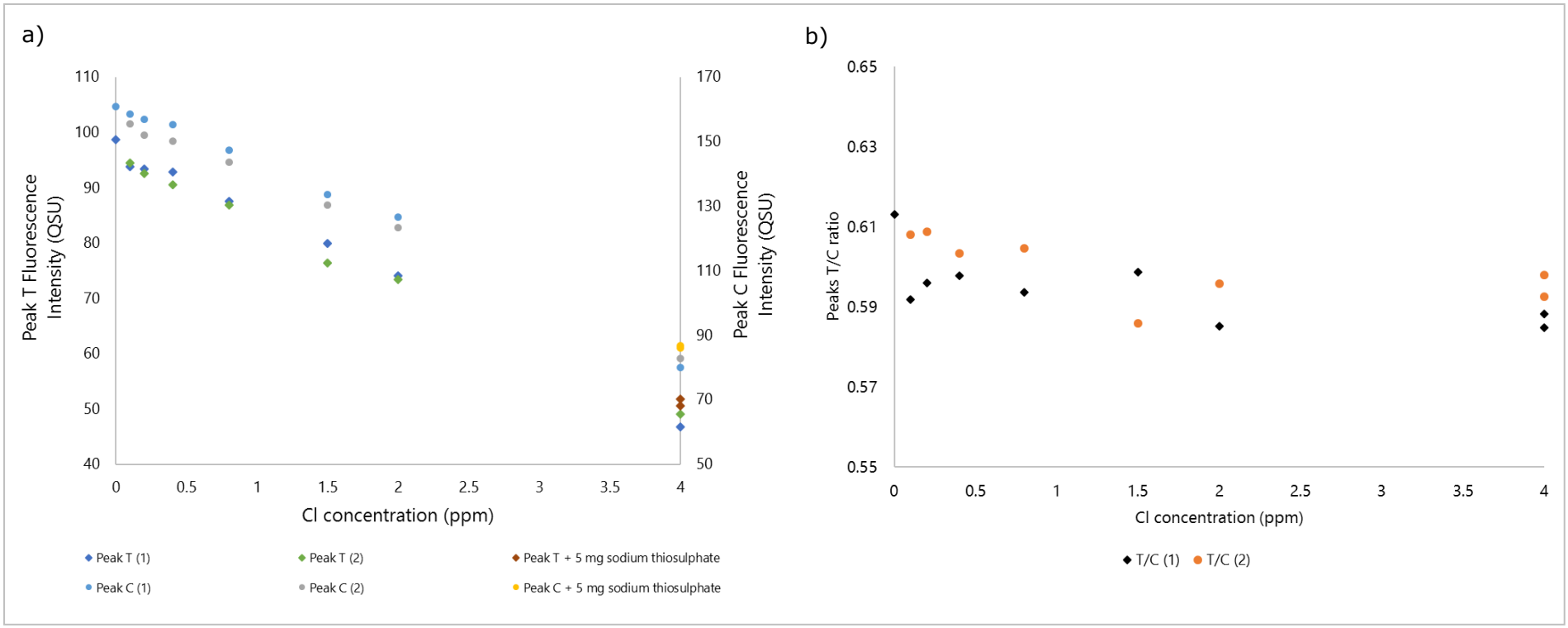

Figure 6.3: Impact of chlorine addition on the fluorescence intensity of an environmental surface freshwater sample (Molesey Heath park lake, N 51° 23′ 31″, W 0° 22′ 36″). Data is peak picked from excitation-emission matrices at $\lambda_{ex}/\lambda_{em}$ 280/350 nm for Peak T, and $\lambda_{ex}/\lambda_{em}$ 280/450 nm for Peak C. Fluorescence intensity is reported in quinine sulphate units (QSU); 1 QSU is equivalent to the fluorescence intensity, of 1 ppb quinine sulphate at $\lambda_{ex}/\lambda_{em}$ 347.5/450 nm. (1) refers to the fluorescence intensity after 10 minutes contact time with the chlorine dosing; (2) is the intensity measured after 2 hours contact time. a) shows the fluorescence intensity for peaks T and C with the chlorine addition; b) demonstrates the T/C ratio of the samples with chlorine dosing.

Although complete fluorescence quenching is not seen within the environmental samples, it is clear that quenching would affect the ability to use fluorescence technologies for in-line monitoring within water treatment, which employs chlorination. However, as the response to chlorine quenching between peaks T and C is linear, it may be possible to use the T/C ratio to enable a threshold based monitoring system to identify unusual Peak T events (Baker *et al.*, 2015; Bridgeman, Bieroza and Baker, 2011). Figure 6.3b highlights the robustness of this ratio to chlorine quenching, within both environmental samples analysed.

6.2.1.3 Conclusions

The data presented within this case study shows that whilst fluorescence can be used as an indicator of contamination in distribution systems and to assess microbial loading prior to chlorination, it is not a suitable technique to assess AFOM throughout a water treatment works post-chlorination. Chlorine quenching is not reversed by the addition of sodium thiosulphate, impacting the potential use of fluorescence techniques for by-products (DBPs) monitoring. By monitoring the Peak C prior to treatment, to ensure the reduction of OM loading in the pre-chlorination stages, DBP precursors can be monitored. However, quenching of all AFOM peaks means that it cannot be used for in-line DBP detection. To realise the full potential of fluorescence sensors for in-line treatment monitoring, further work must be undertaken onsite to determine the impact of actual treatment on fluorescence quenching.

6.2.2 UviLux limitations

Increasing demand for *in situ*, portable and low cost fluorometers, has presented the necessity for the UviLux sensor to evolve and develop into a more sophisticated sensor, addressing current end user issues with the UviLux range. This is in line with current research and market demands. From this, it has become apparent that new generation fluorescence sensors must include in-built correction for absorbance and turbidity, to improve the validity of the data and the function of the sensor (Khamis *et al.*, 2015). Furthermore, the use of multiple wavelengths to identify sources provides the user with a more complete dataset, allowing more sophisticated data interpretation and monitoring.

The UviLux sensors output data in μg/L or ppt equivalents of the calibration solution. This does not always correlate to the true concentration present in a test water sample and calibration curves will vary according to the complexity of the water sample under test. This also leads to variable sensitivity between sensors, making it difficult to compare sensors and ratio output data. Units should be standardised to a common fluorescence unit that can also be replicated with laboratory measurements. This will allow for intra-site comparison and inter-sensor measurements. This is particularly important for complex aquatic matrices and field-based studies, such as the data presented in section 5.2.1.

Alongside unit standardisation, another key limitation of the UviLux sensors is fouling, particularly bio-fouling, of the sensor windows. This is particularly important for long-term continuous deployment and for particular surface freshwaters, as shown in section

5.2.1. The full impact of bio-fouling needs to be assessed, and appropriate measures put in place to reduce its effects where necessary.

6.3 Unit standardisation

One of the issues with the previous generation of sensors was the comparison of data between locations and between sensor variants, e.g. Tryptophan and CDOM. This was due to the units that the sensors reported in, fluorescence equivalent to 1 ppb of the calibration compound, i.e. Tryptophan for the Tryptophan sensor, PTSA for the CDOM sensor etc. To facilitate data interpretation and benchtop comparison, sensor data is now reported in commonly used fluorescence units, quinine sulphate units (QSU); 1 QSU is equivalent to the recorded fluorescence intensity, on a spectrofluorometer (HORIBA Aqualog®, Japan), of 1 ppb quinine sulphate standard in 0.1 M perchloric acid (Starna Cells, USA) at $\lambda_{ex}/\lambda_{em}$ 347.5/450 nm. This also provides the ability to quantitatively compare inter and intra sample site, and sensor, fluorescence intensity variation.

QSU, as a measure, provides standardisation of units across instrumentation and applications. By standardising the data, a more sophisticated approach to data interpretation can be undertaken. The use of QSU for the shorter wavelength fluorescence peaks, such as Peak T, is not as representative as for Peak C for example. This is due to the excitation and emission wavelengths of the quinine sulphate reference (Figure 6.4). However, a single unit must be employed to allow for sensor and data comparison. Whilst the use of QSU may not be ideal, standardisation does provide

comparable sensor sensitivity for different fluorescence parameters; something that is required across the market and to facilitate research and industry data comparison.

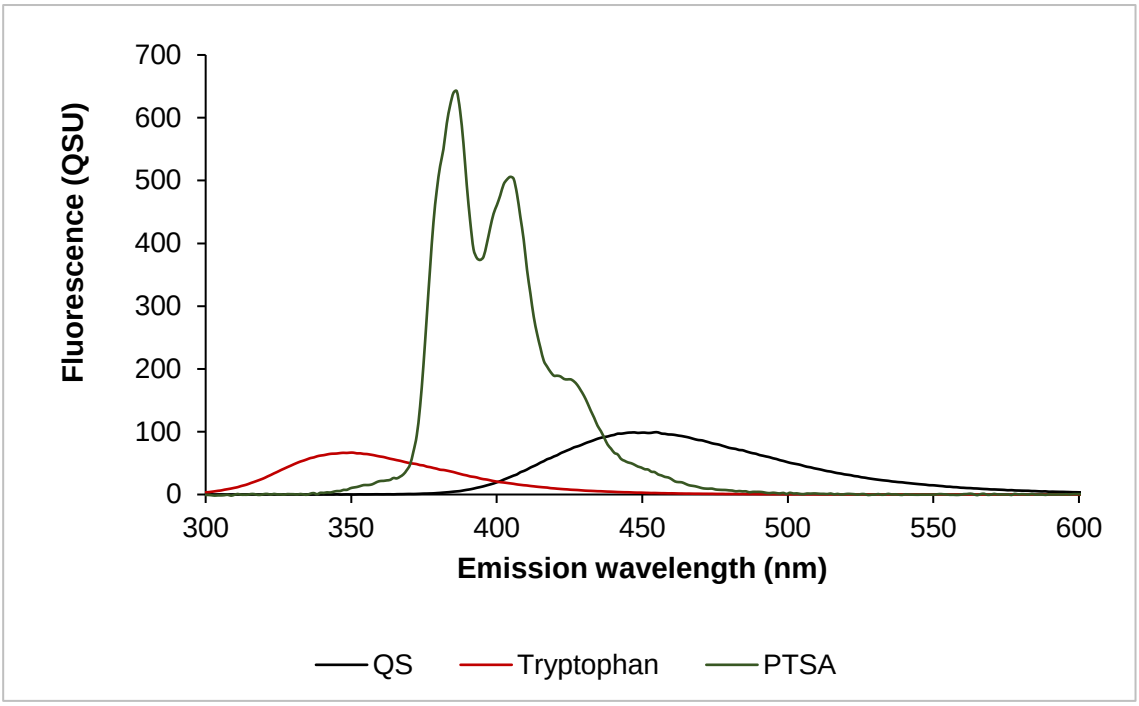

Figure 6.4: Emission spectra of quinine sulphate and the calibration standards for the Tryptophan and CDOM sensors, L-Tryptophan and p-Toluenesulphonic acid (PTSA) solutions respectively. Fluorescence intensity is provided in quinine sulphate units (QSU); where 1 QSU is the equivalent to 1 ppb of quinine sulphate at $\lambda_{ex}/\lambda_{em}$ 347.5/450 nm. Used with permission of the creator, Chelsea Technologies Group Ltd.

6.3.1 Sensor QSU conversion factor generation

The QSU factor is used to convert the channel data, thus all the fluorescence data is reported in QSU for the various target wavelengths. The QSU factor is generated by undertaking laboratory fluorescence spectroscopic analysis on the calibrations standards at a range of concentrations, reflective of the expected range of the parameter across the different applications. The data used is the average of the emission spectra for the

emission wavelengths prescribed by the optical filter used within the sensor. The excitation wavelength used reflects that of the sensor UV LED.

To ensure using the mean of the spectra across the filter bandpass was reflective of the sensor view, a weighted average model was constructed. This was undertaken by utilising emission spectra from EEM data for different environmental samples. The weighted model accounted for the emission filter transmittance at the different wavelengths, the PMT response and the fluorescence data. This demonstrated no significant difference between the data for a weighted average model and using the mean value. As such, the mean value across the emission bandpass is used within the sensors. However, the use of absorbance corrected data significantly improved the agreement between sensor and benchtop output, highlighting the requirement for in-built absorbance correction.

6.4 V-Lux – New generation portable fluorometer

The aim of the V-Lux sensor (Figure 6.5) is to meet the market demand for a single sensor with multiple parameters. This is a generic fluorometer design (Figures 6.5 and 6.6), both across measurement parameters and applications, which will ultimately replace CTG's UniLux, TriLux, UviLux and AquaTracka range of fluorometers. The creation of a multi-parameter sensor will provide a detailed optical assessment of the location and allow for corrections to be undertaken on the real-time data output, improving sensor functionality. The combination of multiple parameters, highlighted by the schematics in Figure 6.6, also aims to reduce the cost, making fluorescence monitoring a more cost-

effective technique. This is to be achieved in part by using silicon photomultiplier (SiPMs) detectors as an alternative to the expensive Photomultiplier Tubes (PMTs) currently used in UviLux. Sensors will also be miniaturised to reduce cost of materials and improve portability.

Figure 6.5: Image of the V-Lux sensor (Chelsea Technologies Group Ltd., UK). Used with permission of the creator, Chelsea Technologies Group Ltd.

Due to the multiple operating environments that the sensor variants will be required to operate in the sensors have a depth rating of 6000 m and operational temperature range of -4°C to 55°C. The housing is made from titanium, with the sensor windows being made of sapphire with copper surrounding bezels, as shown by the image in Figure 6.5, and in the schematics in Figure 6.6. The sensor size is also reduced from the UviLux, at a diameter of 45 mm and length of 130 mm. The internal UV illumination and copper

bezels will protect against window fouling to some extent and a wiper accessory will be available for deployments where deemed necessary.

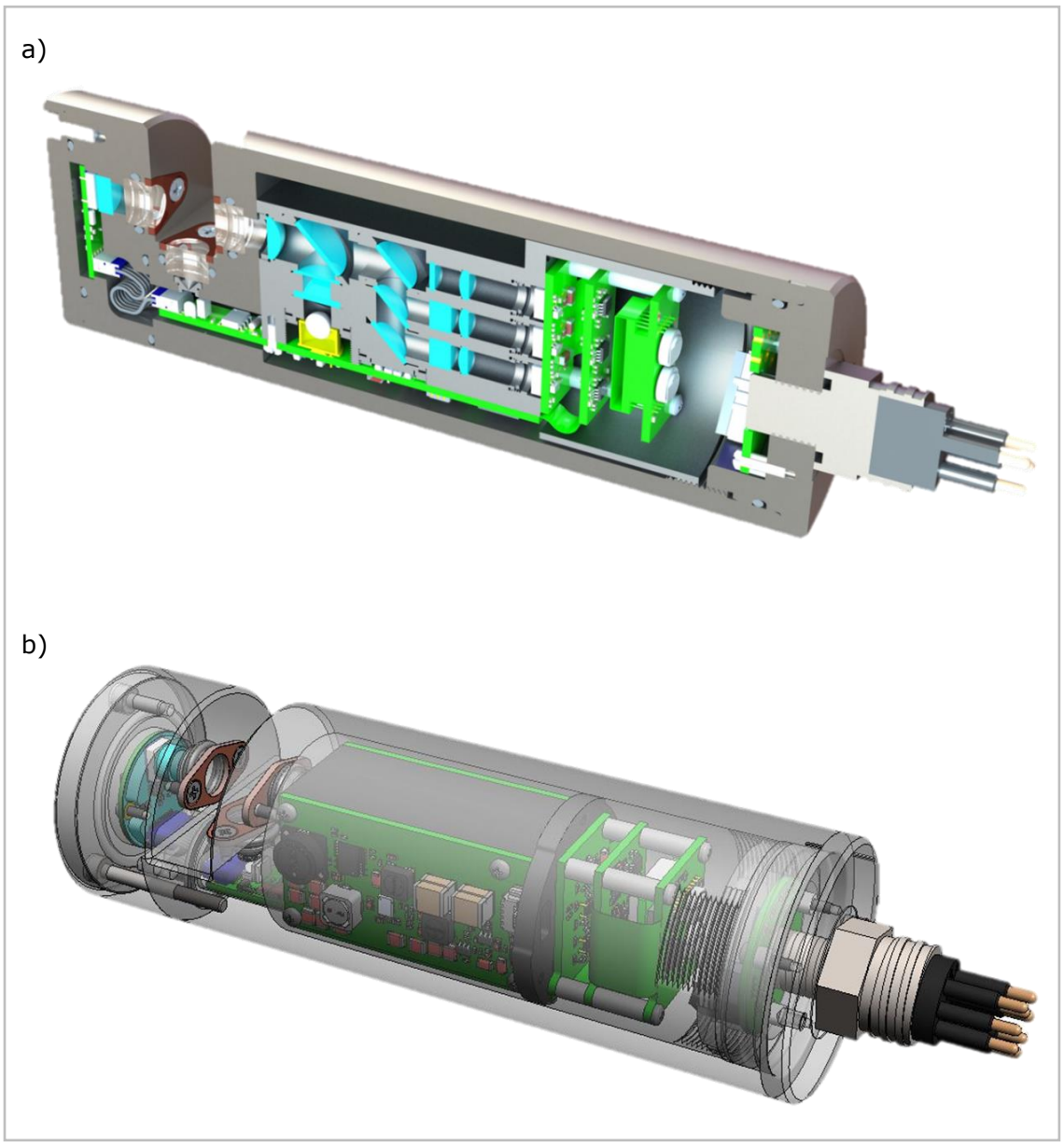

Figure 6.6: Computer-aided design schematics of the V-Lux sensor: a) cross-sectional schematic; b) schematic of the internal build. Used with permission of the creator, Chelsea Technologies Group Ltd.

The details provided below briefly outline the measurement parameters (Table 6.1) and optical specifications of the Tryptophan V-Lux variant of the new multiwavelength fluorometer; the target market for this sensor is environmental pollution monitoring. Fluorescence data will be output in QSU, as discussed previously. A chlorophyll channel has also been incorporated as algae has been shown to produce a significant Peak T signal – thus enabling the identification of bacterial or algal Peak T events. By exciting at the same wavelength, using a 280 nm UV LED in this case, and reporting the data in the same units, a ratio can be used to identify true spikes in the monitored system. The co-monitoring of two optical regions allows the T/C ratio to be reported alongside the individual signals.

Table 6.1: Parameters to be monitored by the V-Lux Tryptophan sensor variant.

Parameter	Excitation λ (nm)	Emission filter λ (nm)	Dynamic Range	Sensitivity
Chlorophyll fluorescence	280	682 ±15	0-700 µg/L (chlorophyll-a)	0.01 µg/L (chlorophyll-a)
Tryptophan fluorescence	280	365 ± 25	0-600 QSU 0-1200 µg/L (Tryptophan)	0.02 QSU 0.04 µg/L (Tryptophan)
CDOM fluorescence	280	450 ± 25	0-600 QSU 0-800 µg/L (PTSA)	0.02 QSU 0.04 µg/L (PTSA)
Absorbance	280		0-3.5 OD	0.002 OD
Turbidity	860	860	0-1000 FNU	0.01 FNU

All channels within the V-Lux sensor require calibration, undertaken at time of purchase and annually as part of the technical support. This ensures that the sensor error is kept to a minimum and allows for correction of the sensor signal, if necessary, that may be caused by drift in the LED output for example. Within the calibration procedure, as for the UviLux sensors, the V-Lux channels will be subject to a range of concentrations of the calibration compound to determine the dynamic range of each channel parameter (Table 6.1). To pass the calibration the sensors must demonstrate both precision and accuracy: precision of the sensor signals is determined by a CV of <1% (n = 50); accuracy is assessed by the linearity of the relationship between the concentration of the calibration compound and the signal output (> R^2 = 0.9995).

6.4.1: Optical design

This section describes the optical design principles to be employed in the new V-Lux multiwavelength fluorometers.

The V-Lux Tryptophan sensor has two main optical variants: one for UV fluorescence detection, the second for visible algal pigment excitation. Figure 6.7 provides a schematic of the layout for the UV Multiwavelength Fluorometer.

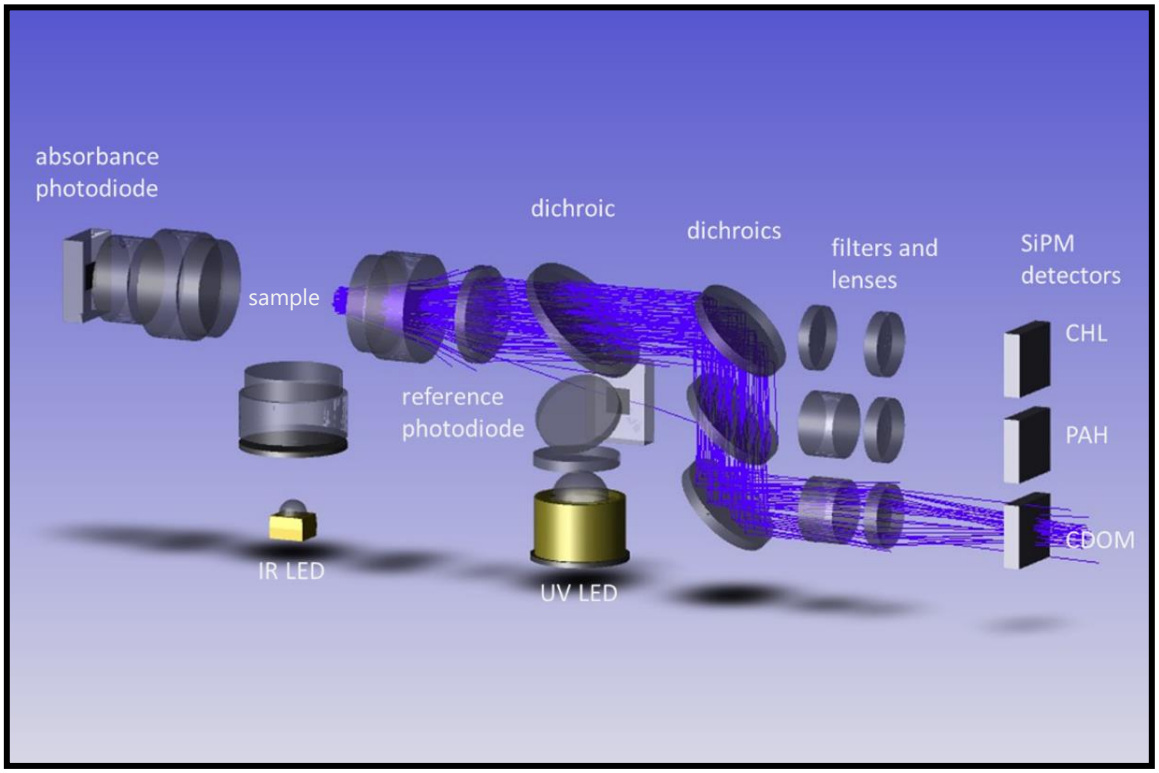

Figure 6.7: Layout of the multiwavelength UV fluorometer illustrating the CDOM detection path. Used with permission of the creator, Chelsea Technologies Group Ltd.

For fluorescence measurements the output from the UV LED source is reflected off the first dichroic filter and is focussed into the sample through a C-Cut Sapphire window using a fused-silica lens. Chlorophyll, Tryptophan (here referred to as PAH) and CDOM fluorescence generated in the sample is collected and collimated by the same fused-silica lens and passes back through the first dichroic filter. A second dichroic filter allows longer wavelength chlorophyll fluorescence to pass through where it is filtered and then focussed onto a Multi-Pixel Photon Counter (MPPC) detector, which will subsequently

be referred to as a Silicon Photomultiplier (SiPM). The shorter fluorescence wavelengths associated with PAH and CDOM fluorescence reflect off the second dichroic filter. A third dichroic filter is then used to split the PAH (reflected) from CDOM (transmitted) wavelengths. CDOM emission is then reflected off a mirror and directed to a discrete SiPM.

Optical transmission is measured using a UV-enhanced photodiode positioned opposite the excitation window. A notch filter (not shown) blocks ambient light interference across the visible wavelengths and allows both UV (absorbance) and infrared (turbidity) wavelengths to pass through. A reference photodiode monitors the output of the UV LED and this signal is used to track both output drift (with time and temperature) in LED intensity and provides the reference for the transmission measurement.

Turbidity measurements are achieved using an infrared LED (860 nm) as the source. Output from this LED passes through an aperture, which limits the angular spread of the light. Scattered light generated in the sample from IR light interacting with suspended particulates is then detected using the UV-enhanced photodiode. The turbidity measurement has been designed to be compliant with the ISO 7027:1999(E) standard requirements.

6.4.2 Turbidity and absorbance correction

There are a number of factors that interfere with the measured fluorescence response. It is important to mitigate for these factors to improve sensor data output. Elevated measured signal, arising from scattered excitation light breaking through to the detector, can be mitigated by the use of good quality filters in both the excitation and emission paths of the fluorometer. Raman scattering can lead to elevated background signals. This can be minimised by careful selection of the fluorescence excitation and emission wavelengths and the bandpass characteristics of the filters used. Attenuation of the measured signal arising from absorbance in the sample, either from the compound being detected, i.e. the inner filter effect, or from other non-fluorescent dissolved compounds, and turbidity scattering also interferes with the fluorescence measurements. Independent measurement of both absorbance and turbidity enables the data to be corrected for these effects.

The algorithms developed to correct for both types of interference are detailed below. These algorithms are based on independent turbidity and absorbance measurements, either within the same instrument or independently. The approach described is then validated using experimental data acquired from a UviLux Tryptophan fluorometer.

6.4.2.1 Correction methodology

The effects of turbidity and absorbance on measured fluorescence are illustrated in Figure 6.8.

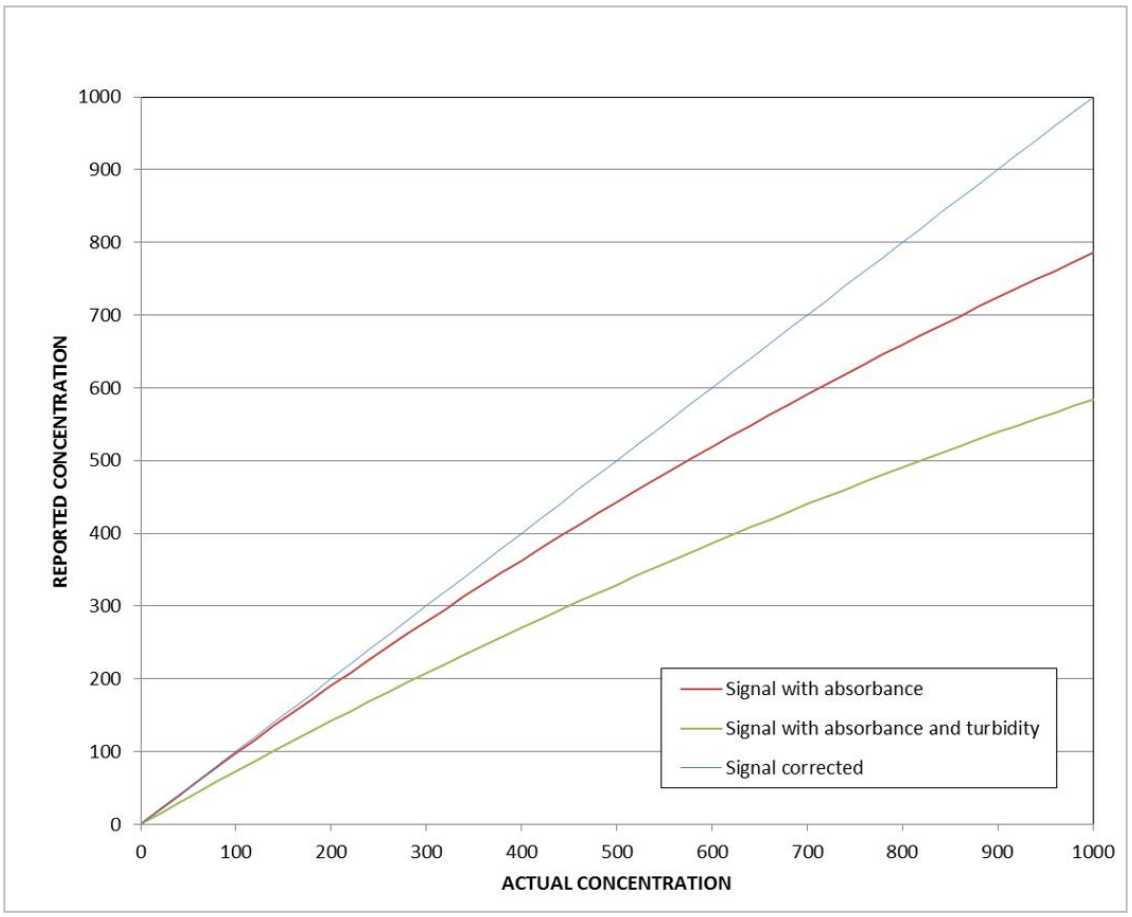

Figure 6.8: Plot based on experimental data illustrating the suppression of signal arising from sample absorbance and turbidity.

Both absorbance and turbidity introduce non-linearity to the measured response. Experiments have shown that these interferences are additive and that the fluorescence signal can be corrected using a standard attenuation correction derived from an equation of the following form:

EQUATION REDACTED (Equation 6.1)

Experiments have demonstrated that the fluorescence pathlength factor *C_AbsFPL* is approximately 6 times larger than *T_AbsFPL*, so a single correction based on the measured absorbance is not adequate to fully correct for both turbidity and 'colour'.

6.4.2.2 Turbidity factors

To implement the correction in Equation 6.1, it is necessary to determine the contribution to the total measured absorbance arising from turbidity, *T_Abs*, at the excitation wavelength. This is then used along with the calibrated fluorescence pathlength factor *T_AbsFPL* to adjust the signal for turbidity interference.

To calculate *T_Abs*, a calibration must be performed relating the measured absorbance, at the fluorescence excitation wavelength, as a function of turbidity. An example is presented in Figure 6.9, using formazin as the turbidity standard.

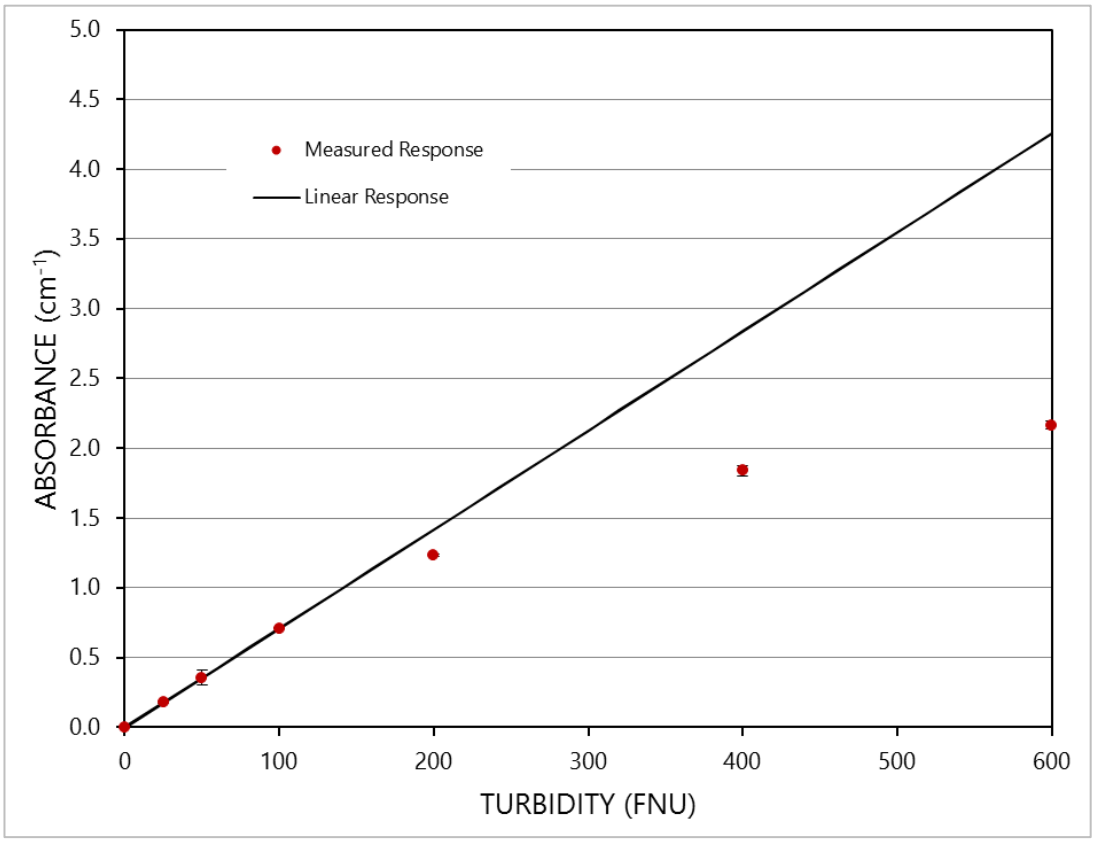

Figure 6.9: Measured benchtop absorbance (at 280 nm excitation) as a function of turbidity, using formazin as the turbidity standard.

As can be seen in Figure 6.9, the effect of turbidity on the absorbance is non-linear. This response suggests that at low turbidity light is scattered out of the sample volume and is not seen by the detector. However, as turbidity increases secondary scattering leads to an increase in the light detected, which has the result of limiting the increase in absorbance at higher turbidity and introduces non-linearity to the absorbance response.

The typical particle size of the formazin standard is comparable to the wavelength of light, so Raleigh Scattering formulae cannot be used to fit the response, as these only work with particle sizes less than 10% of the wavelength. A Mie Scattering model would have to be used which is too complicated for this application. The measured response

observed in Figure 6.9 can, however, be fitted using a logistic equation of the following form:

EQUATION REDACTED (Equation 6.2)

In practice, the calibration constants needed for the logistic fit can be determined by running a dose response curve to a turbidity level that introduces non-linearity in the measured absorbance and then using Equation 2 to fit the response, as illustrated in Figure 6.10.

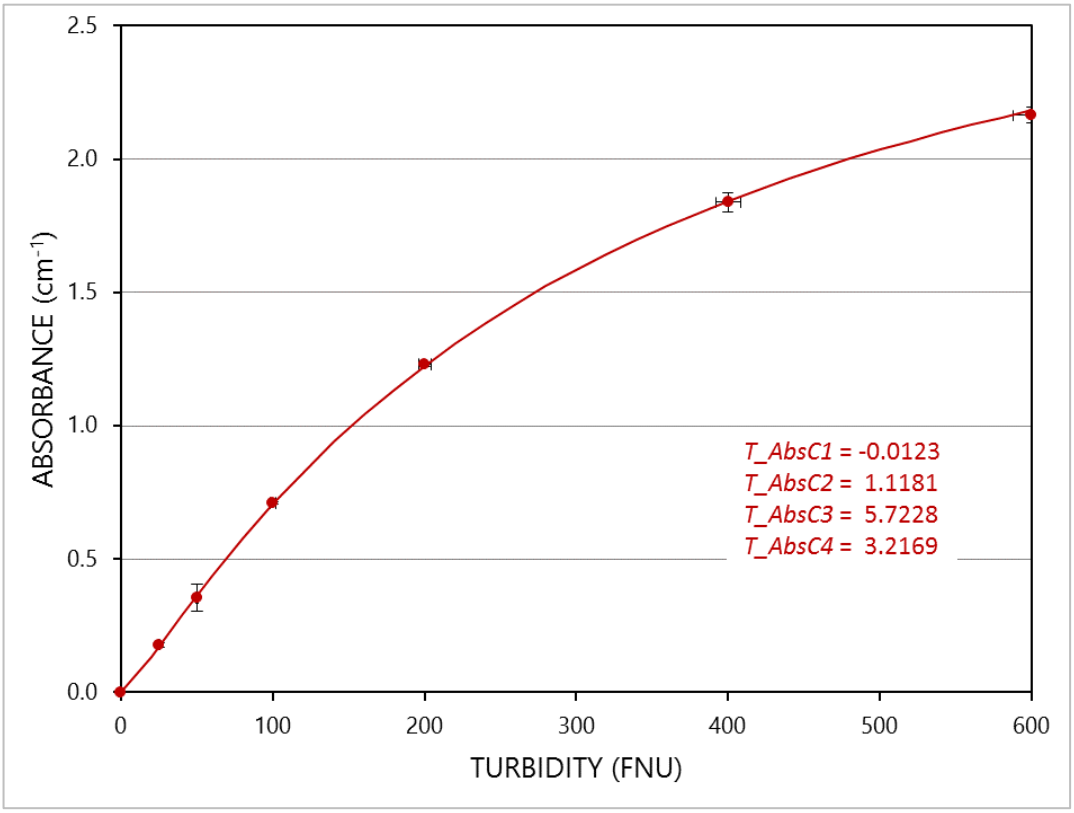

Figure 6.10: Measured absorbance as a function of turbidity fitted using a logistic equation.

The results for the uncorrected fluorescence are shown in the blue markers in Figure 6.8. The fluorescence is significantly attenuated as the turbidity increases. Given the relationship between turbidity and absorbance that has been established (Figure 6.10), T_AbsFPL was optimised to provide the turbidity-corrected data points shown in the orange markers in Figure 6.11.

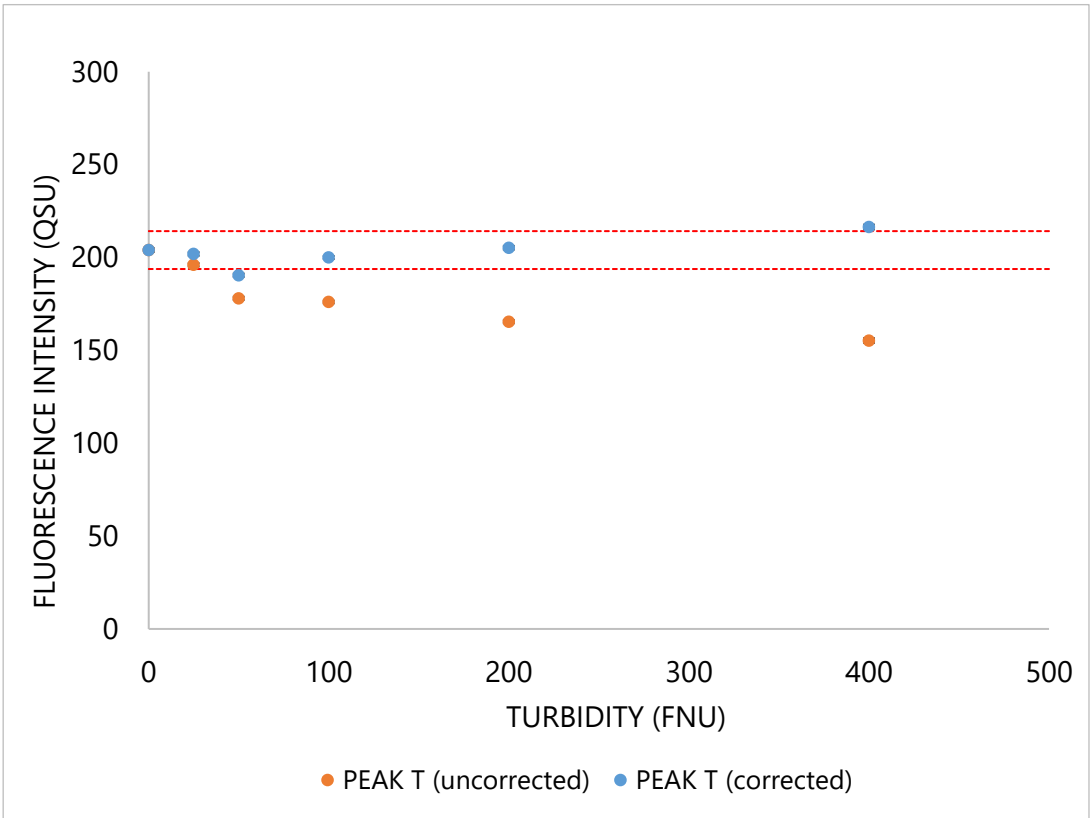

Figure 6.11: Plot of the uncorrected Tryptophan fluorescence and turbidity-corrected Tryptophan fluorescence, obtained from sensor data. The red dotted lines indicate 5% deviation limits. Three standard deviation error bars are shown on the uncorrected Tryptophan fluorescence, determined from 1 Hz data acquisition with n = 50. Three standard deviation error bars are also shown on the turbidity-corrected Tryptophan fluorescence, where the uncertainty in the turbidity-corrected Tryptophan fluorescence has been calculated.

The relationship between absorbance and turbidity depends on sensor geometry, excitation wavelength and the size of the particles generating the turbidity, which implies that a specific calibration might be needed for different sample types. If turbidity is measured at 860 nm, as required by the ISO 7027:1999(E) standard for turbidity measurements, colour is unlikely to be an interfering factor. The effect of particle absorbance at the excitation wavelength should be accounted for through the absorbance measurement.

A simpler approach can be used to calculate *T_AbsFPL*, the second calibration variable required for the turbidity correction. A fixed level of background turbidity will lower the slope of a fluorescence dose response, as illustrated in Figure 6.12.

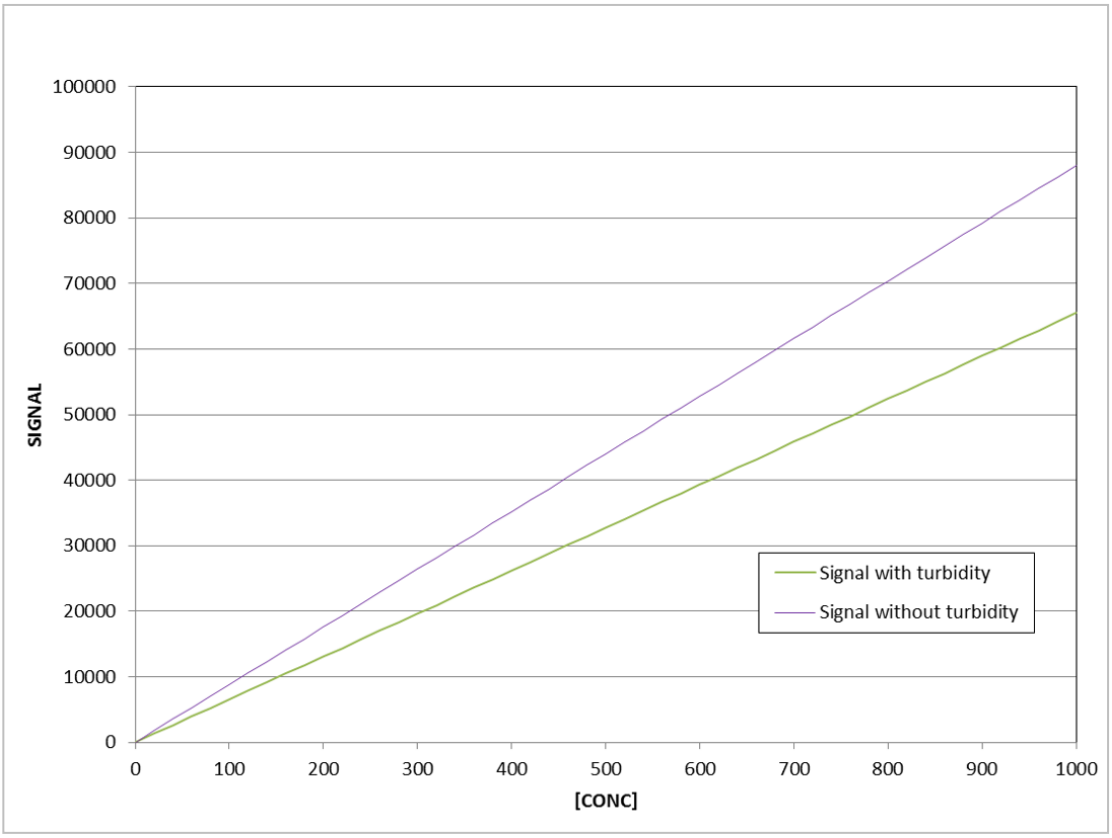

Figure 6.12: Theoretical plot based on actual data illustrating the suppression of the fluorescence signal arising from a fixed level of turbidity.

T_AbsFPL can be calculated by running a two-point fluorescence calibration both with and without a known level of background turbidity, using a fluorophore concentration low enough to avoid the inner filter effect, i.e. *C_Abs* = 0, and simultaneously recording the measured absorbance. The following equation can then be used to correct the turbidity affected signal by adjusting the value of *T_AbsFPL*:

$$F\_SigCorr = F\_Sig \times 10^{(T\_Abs \times T\_AbsFPL)} \quad \text{(Equation 6.3)}$$

Where: *F_SigCorr* is the true fluorescence signal without background turbidity; *F_Sig* is the reduced fluorescence signal with background turbidity; *T_Abs* is the measured absorbance at the excitation wavelength (assuming there is no 'colour' absorbance); and, *T_AbsFPL* is the fitted fluorescence pathlength parameter.

6.4.2.3 Absorbance factors

Having determined the contribution to the total absorbance arising from turbidity, the contribution from 'colour' absorbance is then simply:

$$C\_Abs = Abs - T\_Abs \quad \text{(Equation 6.4)}$$

Where: *Abs* is the total absorbance measured at the excitation wavelength, and *C_Abs* is the contribution to the total absorbance arising from dissolved 'colour'.

Finally, the remaining pathlength variables *C_AbsFPL* and *T_AbsFPL*, needed in Equation 6.1, are determined by independently measuring the effect that both dissolved 'colour' and turbidity has on the fluorescence response. *C_AbsFPL* can be determined by running a calibration without turbidity up to concentrations that generate non-linearity in the fluorescence response, Figure 6.13, while simultaneously recording the measured absorbance.

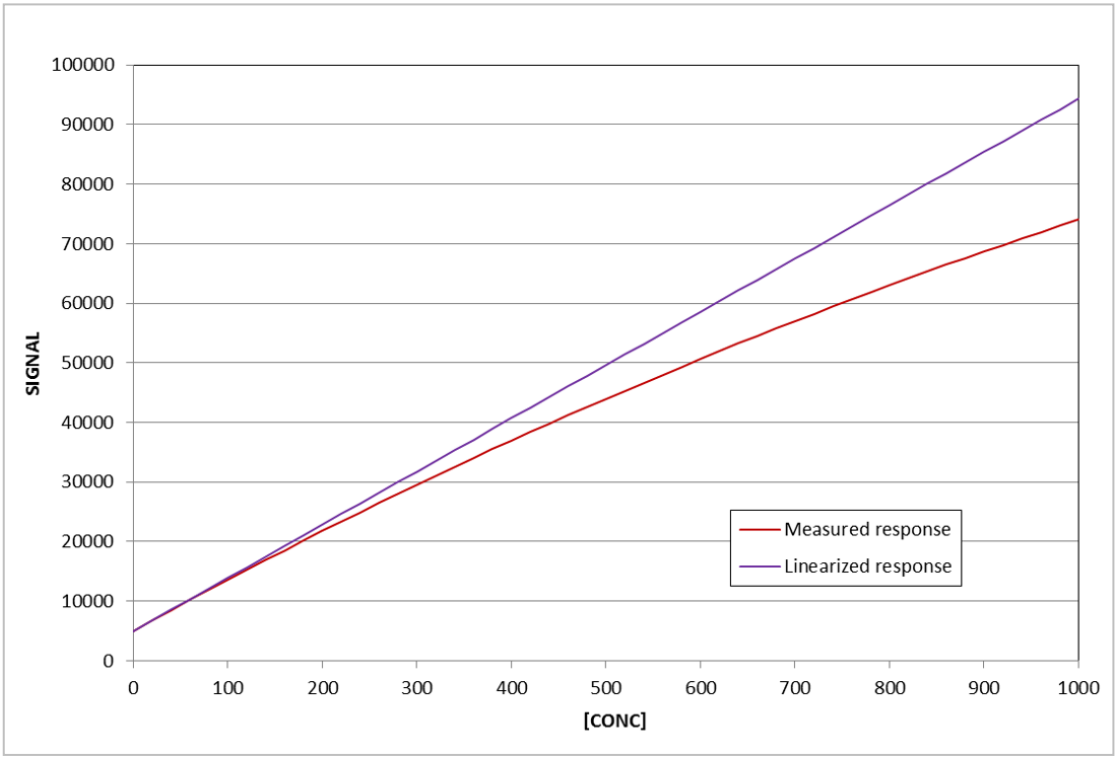

Figure 6.13: Theoretical plot based on actual data illustrating the suppression of the fluorescence signal arising from the inner filter effect.

The response can be linearised using the following equation:

$$F\_SigCorr = F\_Sig \times 10^{(C\_Abs \times C\_AbsFPL)} \qquad \text{(Equation 6.5)}$$

Where: *F_SigCorr* is the linearised signal response; *F_Sig* is the measured non-linear fluorescence signal; *C_Abs* is the measured absorbance at the excitation wavelength (assuming there is no turbidity); *C_AbsFPL* is the fitted pathlength parameter.

6.5 Discussion

Fluorescence techniques have increasingly been used to improve understanding of aquatic systems and monitor water quality and contamination events (Sorensen *et al.*, 2015c, 2015b, 2016, 2018b; Khamis, Bradley and Hannah, 2017; Blaen *et al.*, 2016; Baker *et al.*, 2015; Bridgeman *et al.*, 2015; Khamis *et al.*, 2015). *In situ* AFOM monitoring has recently become of interest within the field, due to the sensitivity and non-destructive nature of this technique (Ruhala and Zarnetske, 2017). High-frequency measurements greatly improve the temporal resolution of fluorescence data, proving the ability to detect short-term events. This is particularly attractive when compared to traditional discrete sampling methods, which are expensive and add to through life costs, making these fluorometers a cost-effective alternative (Sorensen *et al.*, 2018a; Ruhala and Zarnetske, 2017; Blaen *et al.*, 2016; Khamis *et al.*, 2015).

Although the application of *in situ* fluorometers is increasing, this research has highlighted the current shortcomings of the technologies available, limiting their use within water quality monitoring. These mainly surround measurement correction requirements that arise from spectral phenomena, such as correcting for absorbance and turbidity (Khamis, Bradley and Hannah, 2017; Khamis *et al.*, 2015). The development of the V-Lux correction algorithms addresses this, by concurrently monitoring turbidity and absorbance, as well as temperature. This provides real-time in-built corrections for the detected absorbance and turbidity. This enhances the agreement between *in situ* sensor data and benchtop laboratory readings, producing data that is more reflective of the 'true' AFOM signals (Khamis *et al.*, 2015).

The standardisation of the sensor units allows for quantitative measurements, which can easily be compared to benchtop work. Unit standardisation, critically, enables the output from different sensors to be compared directly with reference to a traceable standard. Standardisation also allows for the equivalent sensitivity between fluorescence channels, permitting the use of channel ratios. With increasing market demand, there are more AFOM sensors being developed. By applying a standard unit, the V-Lux is well placed for field trials that compare available sensors, monitoring locations and studies that ground-truth sensor data with discrete sampling methods. As discussed, this comparison to benchtop data is further improved by the addition of the correction factors (Ruhala and Zarnetske, 2017; Khamis *et al.*, 2015).

Further to the in-built signal corrections and unit standardisation, the multi-channel nature of the V-Lux sensor greatly improves applicability of the sensor within a range of aquatic systems, providing a more detailed optical assessment of the aquatic environment in a way that could not be achieved cost effectively using existing discrete sensors. The measurement of multiple fluorescence peaks allows for a more detailed understanding of the AFOM for water quality monitoring and contamination identification, particularly when categorising risk (Sorensen *et al.*, 2018a; Bridgeman *et al.*, 2015). The ability of V-Lux to monitor multiple fluorescence peaks and report both as individual signals and as a ratio provides a detailed understanding of the real-time AFOM dynamics. However, Sorensen et al. (2018b) has demonstrated the potential requirement for only Peak C fluorescence as an indicator of bacterial contamination, particularly in groundwater systems. Whilst this suggests that the V-Lux sensor may be overly complex for particular applications, the focus for the development of V-Lux has

been regarding monitoring surface waters, where multiparameter monitoring is essential for more robust measurements. On the other hand, the extra information gained from the multiple channel sensor provides the user with a more comprehensive understanding. The addition of a chlorophyll channel is an important development that allows for the differentiation between algal Peak T fluorescence, indicative of eutrophication events, and bacterial Peak T (Makarewicz *et al.*, 2018). The identification of the likely Peak T source is beneficial for managing water quality and determining the possible source, be it sewage, agricultural runoff, or eutrophication, for example.

The V-Lux sensor is a more-cost effective technology for comprehensively monitoring AFOM in aquatic systems. The size and weight of the sensor improves its portability, but there is still a question over whether the copper bezels and the UV LED output is enough to keep the windows free from fouling and reduce the maintenance requirements. It is, therefore, necessary to conduct further research into biofouling (Khamis, Bradley and Hannah, 2017; Blaen *et al.*, 2016), as highlighted by the data presented in section 5.2.1, and potential solutions for this to further enhance sensor autonomy, particularly for long-term monitoring applications. Future work must also be conducted to fully understand the T/C ratio and improve the meaningfulness of this data; a simple ratio is may not reflect the relationship between peaks T and C, requiring the development of a more complex algorithm. Field deployment of the sensor within a range of environments and applications is essential to determine further necessary adaptations. This is also essential for understanding the efficacy of the changes made and the suitability of the sensor for different scenarios.

6.5.1 Chapter 6: key findings

- The limitations, and potential applications, of the UviLux fluorimeters have been assessed, highlighting the developments necessary for improving the suitability of *in situ* fluorimeters across a range of environmental applications.
- The benefits of standardising the units used to report fluorescence measurements are identified. From this, it is clear that standardisation protocols must be created to provide clarification across fluorescence data and allow for inter-instrument comparison.
- A new *in situ* fluorimeter, V-Lux, has been developed, and validated, in light of the limitations highlighted within the literature and by applying the understanding gained from the research undertaken within this thesis. The addition of in-built corrections broadens the scope of application for the sensors, although extensive field testing is now required.

Chapter 7 Final Discussion and Conclusions

7.1 Synopsis

The main aim of this research was to understand the bacterial origin of aquatic fluorescent organic matter (AFOM) by exploring bacterial-OM interactions and AFOM evolution at a range of temporal scales. This work was centred around the fundamental understanding of the origin of Peak T fluorescence, to enhance the knowledge surrounding the association of its presence and variation with microbial activity (Hambly *et al.*, 2015; Coble *et al.*, 2014; Baker *et al.*, 2008; Hudson, Baker and Reynolds, 2007; Reynolds, 2003). Alongside this, microbial-AFOM interactions, both production and processing, of a range of AFOM was identified; this led the research to further explore the variety of microbially engineered AFOM and consider the potential impact of this for global biogeochemical cycling. The other focus of this research was to determine the potential applications of Peak T fluorescence within water quality monitoring and resource management. To facilitate this, another objective within this research was to develop a way to reliably measure the phenomenon of microbially engineered AFOM *in situ* and determine the application of this as a novel parameter for monitoring water quality in freshwater systems.

To identify the relationship between Peak T AFOM and bacterial communities, simplified laboratory model systems were used, as detailed in chapters 3 and 4. Understanding the potential microbial production of a range of AFOM within aquatic systems is important for global biogeochemical cycling, carbon storage and

transportation of labile OM through the hydrological continuum (Qian *et al.*, 2017; Bieroza and Heathwaite, 2016; Coble *et al.*, 2014; Baker and Spencer, 2004). This work has highlighted the ubiquitous bacterial production of Peak T, establishing its use as a proxy for bacterial activity within aquatic systems, rather than bacterial enumeration. The laboratory data obtained has also demonstrated the ability of bacteria to produce a range of AFOM compounds, indicating the potential for other fluorescence peaks to be utilised as biomarkers.

By employing EEM fluorescence spectroscopy alongside bacterial monocultures, within Model System 1 (chapter 3), it was possible to ascertain the variety of microbially engineered AFOM. Strong significant correlations between Peak T fluorescence and optical density (OD) were identified from the monoculture growth curves (R^2 = 0.97-0.99). However, the continued bacterial production of Peak T within the stationary phase suggested that Peak T should be used as a reporter of metabolically active bacteria, rather than a proxy for bacterial enumeration. This conclusion was further supported by the ubiquitous presence of Peak T production by the nine bacterial strains cultured within Model System 1. The ubiquity and continuous production of Peak T within a metabolically active community demonstrated here also explains the variety of correlations identified within the literature, when applied to real-world environments. This provides strong evidence for the application of Peak T fluorescence to infer variation in microbial activity within a system. As part of a monitoring network, including commonplace physicochemical parameter monitoring, the use of Peak T fluorescence as a water quality parameter could greatly enhance the knowledge of

aquatic systems and allow the source of activity and, therefore, contamination to be identified.

Additionally, this work identified the microbial production of AFOM, currently understood to be of terrestrial allochthonous origin (Coble *et al.*, 2014), altering the understanding of the contribution to AFOM by microbial communities. Although Peak T was seen to be ubiquitous within all the bacterial strains, the ability of bacteria to produce other AFOM molecules seems to vary between species. This has highlighted the importance of metabolic processes in AFOM production, and suggests that AFOM other than Peak T may act as biomarkers for specific species, or groups of bacteria with particular functions, such as the production of pyoverdine, identified as Peak C+, by *Pseudomonas aeruginosa*. This also suggests the potential importance of variation in environmental conditions, such as nutrient availability and temperature, on the microbial production of AFOM, which could have wide ranging impacts on global biogeochemical cycling, although further work is required to truly assess this.

To enhance the understanding of bacterial-OM interactions, both monocultures and a mixed community, isolated from a freshwater sample, were employed and samples fractioned to determine extracellular and intracellular AFOM (chapter 4). This work identified Peak T fluorescence as mainly intracellular material, with the highest intensities seen within resuspended cells. This highlighted the likely origin of Peak T AFOM as being functional proteins, involved in metabolic activity, although further proteomic and molecular work may be able to fully identify the processes responsible for driving this AFOM production. This verified Peak T fluorescence as an indicator of microbial metabolic activity, as well as an indication of presence, providing a novel

water quality parameter for understanding *in situ* microbial activity, and therefore enhancing understanding of ecosystem interactions. Other AFOM peaks, characterised as humic-like fluorescence, were also identified as intracellular, albeit at much lower intensities than Peak T. The majority of these AFOM fluorescence peaks were seen in the supernatant sample fraction, indicating exportation from the cells. This suggests that the molecules responsible for this AFOM signal are likely to be derived from bacterial metabolic by-products, structural proteins or specific functional molecules, such as pyoverdine. The extracellular nature of these compounds could prove essential for global cycling, with this OM being available for utilisation and degradation via a range of processes. Further understanding the processes of the production of this AFOM and identification of the compounds responsible could greatly enhance aquatic biogeochemical research and fill in the knowledge gaps pertaining to the 'black box' of processes within biogeochemical modelling. In turn, this could have wide-reaching effects on understanding present, past and future potential changes in the environment due to changes in biogeochemical cycling from a variety of pressures, including climate change and anthropogenic pollution, such as industrial and agricultural contamination.

A second laboratory model system (Model System 2, chapter 4) was developed to assess microbial-OM interactions in natural freshwater samples and synthetic samples, employing a standardised mixed bacterial culture. Monitoring AFOM evolution hourly in Model System 2 exposed the Peak T production with microbial population growth, providing further evidence that metabolically active microbial communities produce Peak T *in situ*. Model System 2 was then further developed to assess the impact of residence time on bacterial AFOM evolution and determine the relationship between

Peak T and dissolved oxygen (DO) at a daily temporal scale. Monitoring DO in tandem with fluorescence, at this resolution, identified the variable and fast-acting dynamics of these aquatic systems. From this data, the lack of a reflective relationship between DO and Peak T can be established, with Peak T fluorescence being a dynamic parameter that assesses microbial activity through time, providing more detailed understanding of microbial activity than 5-day oxygen demand. As such, the work here suggests that the correlation between BOD_5 and Peak T identified within the literature is dependent upon the temporal resolution. It can, therefore, be suggested that comparison of BOD_5 and Peak T is unsuitable, with each parameter being beneficial for water quality management independent of each other (Hudson *et al.*, 2008).

The water quality monitoring study presented here (chapter 5), demonstrates the use of Peak T fluorescence as an independent water quality parameter, with *in situ* sensing being used to identify periods of enhanced microbial activity. This is demonstrated by diurnal variations in fluorescence intensity, and increased intensity with water temperature and, therefore, metabolic processing. However, by monitoring a single fluorescence peak it is not possible to determine the microbial origin, i.e. algal or bacterial, of this Peak T (Makarewicz *et al.*, 2018; Fukuzaki *et al.*, 2014; Ferrari and Mingazzini, 1995). If the microbial origin of AFOM is to be understood, and the application of *in situ* fluorescence to be fully recognised, then similar exploratory work must be undertaken, assessing the contribution of a range of microorganisms, such as algae and viruses. Also, without correcting for absorbance or turbidity effects, the data output by the fluorescence sensors does not reflect the 'true' fluorescence signal (Khamis, Bradley and Hannah, 2017; Khamis *et al.*, 2015). The discrete sampling within

this study highlights the limitations of this methodology, such as sample collection and storage, demonstrating the benefits of *in situ* sensing over traditional spot samples with lengthy and expensive laboratory analysis (Ruhala and Zarnetske, 2017). Nevertheless, this study reveals the limitations of current *in situ* sensing technologies, particularly biofouling.

To improve the application of *in situ* fluorescence sensing, the development of a new generation sensor, V-Lux, is detailed here (chapter 6). This sensor provides corrected (for turbidity and absorbance) and standardised fluorescence data, in QSU. By developing the corrections the sensor reports the 'true' fluorescence signal (Khamis *et al.*, 2015), expanding the application of the sensor and enhancing its suitability to a range of complex environments. Further to this, the integration of multiple fluorescence channels enhances the ability of the V-Lux sensor to identify contamination via thresholds and the addition of chlorophyll monitoring allows for the microbial source of Peak T fluorescence, algal or bacterial, to be deciphered (Makarewicz *et al.*, 2018). Although extensive field trials for the V-Lux are now required, this sensor provides a more cost-effective and portable alternative to traditional water quality monitoring programs, reliant upon discrete sampling, with the potential for improved temporal and spatial monitoring resolution.

7.2 Conclusions

The key objectives of this research were three-fold:

- to assess the application of Peak T fluorescence as a novel biotic water quality parameter;
- to determine bacterial production and processing of AFOM over time;
- to develop, and validate, a new generation sensor to measure this phenomenon *in situ*.

7.2.1 Peak T fluorescence: a novel water quality parameter

This research provides the first direct evidence that Peak T fluorescence can be engineered by bacteria *in situ* over short time periods. Monitoring bacterial growth and fluorescence, as well as identifying the intracellular nature of Peak T AFOM, has highlighted the application of Peak T fluorescence for determining the dynamics of microbial activity within aquatic systems. The ubiquitous presence of Peak T within the bacterial cultures presented within this study leads to the conclusion that Peak T fluorescence can indicate microbial presence and provide a proxy for activity, but cannot be utilised for species or community enumeration.

7.2.2 Bacterial engineers: AFOM production

Secondly, this research introduces the ability of bacteria to produce complex, high molecular weight AFOM molecules, previously associated with terrestrial recalcitrant

material, within short periods of time. The work here identifies this AFOM as extracellular, revealing its importance for transportation of OM throughout the hydrological continuum. From the extensive evidence provided here, it can be concluded that bacterially-engineered AFOM is important for carbon storage and within global biogeochemical cycles. In addition, the monocultures researched here suggest the potential for other AFOM peaks to be utilised as biomarkers to identify the presence of particular species.

7.2.3 Sensing *in situ* microbial AFOM: a new generation sensor

Finally, the work presented demonstrates the application of *in situ* fluorescence sensing for the measuring of variations in Peak T fluorescence as an independent water quality parameter for determining microbial activity. The development of a new generation sensor facilitates the application of this novel parameter within water quality monitoring. The derivation of in-built sensor corrections, using known and novel algorithms, provide a sensor that can report the real-time 'true' fluorescence signal of an aquatic system *in situ*. This technology platform, alongside the underpinning understanding provided by the laboratory model systems developed here, presents a novel water quality parameter for determining microbial activity in aquatic systems.

7.3 Recommendations for Future Work

This study has contributed to the knowledge of bacterial production of AFOM, providing direct evidence that it is related to metabolic activity. However, this study has not identified the specific processes that lead to AFOM production. Further work must be undertaken to characterise, in detail, the composition of microbial communities. This could be undertaken utilising common molecular techniques, such as 16S rRNA and 18S rRNA. Once community composition is better detailed, future work should also explore, in depth, the metabolic pathways responsible for the microbial production and transformation of AFOM. Introducing molecular techniques to the field of AFOM, to assess potential contributing metabolic pathways, would greatly enhance understanding of the true origins of microbially derived AFOM. The field of AFOM would benefit greatly from the determination of the interactions of metabolic pathways and the function of the range of proteins produced, identified within proteomic studies that contribute to AFOM. This would allow for a detailed understanding of the origin and transformation of organic matter within aquatic environments. This knowledge would inform the real contribution of the microbial community to global biogeochemical cycling. From this understanding, it may be possible to further our knowledge of biogeochemical cycling, with a specific focus on the current 'black box', which is often used to describe the ecological processes involved. This could have far reaching implications on our understanding of local and global systems, as well as to improve our modelling outputs for current, future and past climatic predictions.

From the work undertaken here it is clear that the bacterial community contributes to the AFOM, particularly Peak T, within environmental systems. However, the bacterial

production of other AFOM, albeit at low fluorescence intensities, has highlighted the potential autochthonous source of all AFOM. Further work should be undertaken to look at the relative contribution of bacterial and algal AFOM, to fully understand 'microbial' AFOM origin. To truly use fluorescence to determine 'microbial' activity, extensive research into different microorganisms must be undertaken, to identify the relative contribution to the AFOM signal. This is particularly important when assessing the source of an AFOM event; i.e. if an event is to be attributed to a particular source such as a eutrophication event or sewage input. Whilst monitoring chlorophyll, as seen within the V-Lux design (chapter 6), attempts to assess this, this does not provide quantification of the contribution. The use of chlorophyll monitoring may also be misleading, as it may indicate the presence of cyanobacteria and/or certain algae. At present, the use of chlorophyll indicates only algal presence, and not activity. As such, associating Peak T variation with chlorophyll is potentially flawed and incompatible. It is, therefore, essential that the algal contribution to AFOM, and the relationship between this and chlorophyll, amongst other common algal pigments, is explored in detail. To develop this understanding, model systems must be developed to explore the basic algal-AFOM interactions, with a focus on time-scales. This must then be expanded into more complex systems, and full scale microbial communities. By unpicking and modelling different sections of the natural system, the fundamental underpinning knowledge required to inform ecosystem-level understanding can be gained. Only then, can the full potential of the fluorescence technology be realised and successfully applied within complex real-world systems.

The work here raises questions regarding the extent to which bacterially produced AFOM occurs in freshwater systems and the role that any production plays in the biogeochemical cycling throughout the hydrological continuum. It is, therefore, also important to fully understand how the underpinning knowledge gained in this study is applied within the environment. Future work should develop more complex model systems to simulate a range of conditions. The importance of residence time, and temporal scales, have been discussed here and within the literature. However, the impact of varying environmental conditions, and not within stable systems, is less well understood. Within the more complex model systems designed, the impact of flow rates, hydrological events and pollution events should be addressed, as this could have important implications on the suitability of *in situ* sensing in different environments and hydrological systems. It is also essential to understand how nutrient limitations and loading impacts the AFOM signal. This is important for understanding the contribution of metabolically active communities, particularly regarding potential biological and chemical constraints which may limit the fluorescence intensity. It is also important to understand that such events may not always result in increased activity, but may alter the aquatic conditions such that this has a detrimental impact on the microbial community. Thus, the potential impact on AFOM of preferential growth, competition and the development of anoxic environments, must also be assessed.

Within this work, the potential for fluorescence peaks to act as biomarkers for specific bacterial species has also been highlighted. Future research could look at the potential use of this technique for monitoring bacterial species of interest. Whilst this could be undertaken within aquatic environments, the research here has shown that many of the

species of interest for drinking water safety are not discernible using fluorescence spectra. However, the application of AFOM measurements may be extended outside of the water sector, with possible importance within health care and food production. With the increased sensitivity and speed of EEM-fluorescence analysis, it may be possible to create a database of species spectra, from which pathogenic species may be identifiable. Such application has already been considered within healthcare science, to assess the cleanliness of surfaces within hospital environments (Dartnell *et al.*, 2013).

Within this study, the impact of biofouling of *in situ* sensors has been discussed. Although this is a problem throughout *in situ* environmental monitoring, further work must be undertaken to understand the true impact of biofouling on the fluorescence signal and determine effective methods for prevention and/or removal. To do this, it may be possible to develop biofilm model systems which include *in situ* sensors within a flow chamber system. This could then provide understanding of the time scales of biofilm production, as well as the impact this has on sensor signal, in turn, informing the potential mitigation and/or corrective measures to be introduced as part of the sensor design. Additionally, the application of fluorescence measurements for detection of biofilm presence and characterising communities may provide an alternative technology within biofilm studies.

Finally, the newly developed sensor, V-Lux, requires extensive field trials to be undertaken across a range of environments and applications. This is essential to test the effectiveness of the developments made to both the sensor hardware and software. This information will provide the ability to further optimise the sensor for the application within a range of different environments, as well as assessing its application within a

range of environments. From the field work, the full potential of the sensor can be determined, providing further information regarding the use of fluorescence as an independent water quality parameter, with the potential of enhancing global water management.

Chapter 8 References

Ahmad, S.R. and Reynolds, D.M. (1999) Monitoring of water quality using fluorescence technique: Prospect of on-line process control. *Water Research*. 33 (9), pp. 2069–2074.

Aiken, G.R. (2014) Fluorescence and Dissolved Organic Matter. In: Andy Baker, Darren M. Reynolds, Jamie R. Lead, Paula G. Coble, and Robert G. M. Spencer (eds.). *Aquatic Organic Matter Fluorescence* Cambridge Environmental Chemistry Series. Cambridge University Press. pp. 35–74.

Aiken, G.R., McKnight, D.M., Wershaw, R.L. and MacCarthy, P. (1985) *Humic substances in soil, sediment and water: geochemistry, isolation, and characterization*Wiley-Interscience publication. George R. Aiken (ed.). Wiley.

Alberts, J.J. and Takács, M. (2004) Total luminescence spectra of IHSS standard and reference fulvic acids, humic acids and natural organic matter: Comparison of aquatic and terrestrial source terms. *Organic Geochemistry*. 35 pp. 243–256.

Anderson, T.R., Christian, J.R. and Flynn, K.J. (2015) *Chapter 15 - Modeling DOM Biogeochemistry A2 - Hansell, Dennis A.* In: Craig A B T - Biogeochemistry of Marine Dissolved Organic Matter (Second Edition) Carlson (ed.). Academic Press. pp. 635–667.

APHA AWWA WEF (1999) BOD method.*Standard Methods for the Examination of Water and Wastewater 20th edition*.

Asmala, E., Autio, R., Kaartokallio, H., Stedmon, C.A. and Thomas, D.N. (2014) Processing of humic-rich riverine dissolved organic matter by estuarine bacteria: Effects of predegradation and inorganic nutrients. *Aquatic Sciences*. 76 (3), pp. 451–463.

Asmala, E., Kaartokallio, H., Carstensen, J. and Thomas, D.N. (2016) Variation in Riverine Inputs Affect Dissolved Organic Matter Characteristics throughout the

Estuarine Gradient. *Frontiers in Marine Science*. 2 (January), pp. 1–15.

Baker, A. (2002a) Fluorescence excitation-emission matrix characterization of river waters impacted by a tissue mill effluent. *Environmental Science and Technology*. 36 pp. 1377–1382.

Baker, A. (2001) Fluorescence excitation – emission matrix characterization of some sewage impacted rivers. *Environ. Sci. Technol*. 35 (5), pp. 948–953.

Baker, A. (2002b) Fluorescence properties of some farm wastes: Implications for water quality monitoring. *Water Research*. 36 pp. 189–195.

Baker, A. (2002c) Spectrophotometric discrimination of river dissolved organic matter. *Hydrological Processes*. 16 (October 2001), pp. 3203–3213.

Baker, A. (2005) Thermal fluorescence quenching properties of dissolved organic matter. *Water Research*. 39 pp. 4405–4412.

Baker, A., Cumberland, S.A., Bradley, C., Buckley, C. and Bridgeman, J. (2015) To what extent can portable fluorescence spectroscopy be used in the real-time assessment of microbial water quality? *Science of the Total Environment*. 532 pp. 14–19.

Baker, A., Elliott, S. and Lead, J.R. (2007) Effects of filtration and pH perturbation on freshwater organic matter fluorescence. *Chemosphere*. 67 pp. 2035–2043.

Baker, A. and Inverarity, R. (2004) Protein-like fluorescence intensity as a possible tool for determining river water quality. *Hydrological Processes*. 18 pp. 2927–2945.

Baker, A., Inverarity, R., Charlton, M. and Richmond, S. (2003) Detecting river pollution using fluorescence spectrophotometry: Case studies from the Ouseburn, NE England. *Environmental Pollution*. 124 pp. 57–70.

Baker, A. and Spencer, R.G.M. (2004) Characterization of dissolved organic matter from source to sea using fluorescence and absorbance spectroscopy. *Science of the Total*

Environment. 333 (1–3), pp. 217–232.

Baker, A., Tipping, E., Thacker, S.A. and Gondar, D. (2008) Relating dissolved organic matter fluorescence and functional properties. *Chemosphere*. 73 (11), pp. 1765–1772.

Baker, A., Ward, D., Lieten, S.H., Periera, R., Simpson, E.C. and Slater, M. (2004) Measurement of protein-like fluorescence in river and waste water using a handheld spectrophotometer. *Water Research*. 38 pp. 2934–2938.

Barker, J.D., Dubnick, A., Lyons, W.B. and Chin, Y.-P. (2013) Changes in Dissolved Organic Matter (DOM) Fluorescence in Proglacial Antarctic Streams. *Arctic, Antarctic, and Alpine Research*. 43 (3), pp. 305–317.

Beattie, B.K. and Merrill, A.R. (1999) A Fluorescence Investigation of the Active Site of *Pseudomonas aeruginosa* Exotoxin A. *Journal of Biological Chemistry*. 274 (22), pp. 15646–15654.

Beattie, B.K. and Merrill, A.R. (1996) *In vitro* Enzyme Activation and Folded Stability of *Pseudomonas aeruginosa* Exotoxin A and Its C-Terminal Peptide. *Biochemistry*. 35 (28), pp. 9042–9051.

Beattie, B.K., Prentice, G.A. and Merrill, A.R. (1996) Investigation into the Catalytic role for the Tryptophan Residues within Domain III of *Pseudomonas aeruginosa* Exotoxin A. *Biochemistry*. 35 (48), pp. 15134–15142.

Beggs, K.M.H., Summers, R.S. and McKnight, D.M. (2009) Characterizing chlorine oxidation of dissolved organic matter and disinfection by-product formation with fluorescence spectroscopy and parallel factor analysis. *Journal of Geophysical Research: Biogeosciences*. 114 (4), pp. 1–10.

Besmer, M.D. and Hammes, F. (2016) Short-term microbial dynamics in a drinking water plant treating groundwater with occasional high microbial loads. *Water Research*. 107 pp. 11–18.

Bieroza, M.Z., Bridgeman, J. and Baker, A. (2010) Fluorescence spectroscopy as a tool for determination of organic matter removal efficiency at water treatment works. *Drinking Water Engineering and Science*. 3 pp. 63–70.

Bieroza, M.Z. and Heathwaite, A.L. (2016) Unravelling organic matter and nutrient biogeochemistry in groundwater-fed rivers under baseflow conditions: Uncertainty in *in situ* high-frequency analysis. *Science of The Total Environment*. 572 pp. 1520–1533.

Black, J.G. (2005) *Microbiology: Principles and Explorations*. 6th edition. Wiley.

Blaen, P.J., Khamis, K., Lloyd, C.E.M., Bradley, C., Hannah, D. and Krause, S. (2016) Real-time monitoring of nutrients and dissolved organic matter in rivers: Capturing event dynamics, technological opportunities and future directions. *Science of the Total Environment*. 569–570 pp. 647–660.

Boehme, J., Coble, P., Conmy, R. and Stovall-Leonard, A. (2004) Examining CDOM fluorescence variability using principal component analysis: Seasonal and regional modeling of three-dimensional fluorescence in the Gulf of Mexico. *Marine Chemistry*. 89 pp. 3–14.

Bridgeman, J., Baker, A., Brown, D. and Boxall, J.B. (2015) Portable LED fluorescence instrumentation for the rapid assessment of potable water quality. *Science of the Total Environment*. 524–525 pp. 338–346.

Bridgeman, J., Baker, A., Carliell-Marquet, C. and Carstea, E. (2013) Determination of changes in wastewater quality through a treatment works using fluorescence spectroscopy. *Environmental Technology*. 34 (June), pp. 3069–3077.

Bridgeman, J., Bieroza, M. and Baker, A. (2011) The application of fluorescence spectroscopy to organic matter characterisation in drinking water treatment. *Reviews in Environmental Science and Biotechnology*. 10 (3), pp. 277–290.

Bro, R. and Kiers, H.A.L. (2003) A new efficient method for determining the number of components in PARAFAC models. *Journal of Chemometrics*. 17 pp. 274–286.

Butturini, A. and Ejarque, E. (2013) Technical Note: Dissolved organic matter fluorescence - A finite mixture approach to deconvolve excitation-emission matrices. *Biogeosciences*. 10 pp. 5875–5887.

Cammack, W.K.L., Kalff, J., Prairie, Y.T. and Smith, E.M. (2004) Fluorescent dissolved organic matter in lakes: Relationships with heterotrophic metabolism. *Limnology and Oceanography*. 49 (6), pp. 2034–2045.

Carlson, C.A. and Hansell, D.A. (2015) DOM Sources, Sinks, Reactivity, and Budgets. In: Dennis A. Hansell and Craig A. Carlson (eds.). *Biogeochemistry of Marine Dissolved Organic Matter* 2nd Ed. Academic Press. pp. 65–126.

Carstea, E.M. (2012) Fluorescence Spectroscopy as a Potential Tool for *In-situ* Monitoring of Dissolved Organic Matter in Surface Water Systems. *Water Pollution*.

Carstea, E.M., Baker, A., Bieroza, M. and Reynolds, D.M. (2010) Continuous fluorescence excitation-emission matrix monitoring of river organic matter. *Water Research*. 44 (18), pp. 5356–5366.

Carstea, E.M., Baker, A., Bieroza, M., Reynolds, D.M. and Bridgeman, J. (2014) Characterisation of dissolved organic matter fluorescence properties by PARAFAC analysis and thermal quenching. *Water Research*. 61 (0), pp. 152–161.

Carstea, E.M., Baker, A. and Savastru, R. (2014) Comparison of river and canal water dissolved organic matter fluorescence within an urbanised catchment. *Water and Environment Journal*. 28 (1), pp. 11–22.

Carstea, E.M., Bridgeman, J., Baker, A. and Reynolds, D.M. (2016) Fluorescence spectroscopy for wastewater monitoring: A review. *Water Research*. 95 pp. 205–219.

Chen, J., LeBoeuf, E.J., Dai, S. and Gu, B. (2003) Fluorescence spectroscopic studies of natural organic matter fractions. *Chemosphere*. 50 (2003), pp. 639–647.

Coble, P.G. (1996) Characterization of marine and terrestrial DOM in seawater using excitation-emission matrix spectroscopy. *Marine Chemistry*. 51 pp. 325–346.

Coble, P.G., Lead, J., Baker, A., Reynolds, D.M. and Spencer, R.G.M. (2014) *Aquatic Organic Matter Fluorescence*. Cambridge University Press.

Coble, P.G., Schultz, C.A. and Mopper, K. (1993) Fluorescence contouring analysis of DOC intercalibration experiment samples: a comparison of techniques. *Marine Chemistry*. 41 pp. 173–178.

Cohen, E., Levy, G.J. and Borisover, M. (2014) Fluorescent components of organic matter in wastewater: Efficacy and selectivity of the water treatment. *Water Research*. 55 pp. 323–334.

Cook, C., Prystajecky, N., Ngueng Feze, I., Joly, Y., Dunn, G., Kirby, E., Özdemir, V. and Isaac-Renton, J. (2013) A comparison of the regulatory frameworks governing microbial testing of drinking water in three Canadian provinces. *Canadian Water Resources Journal / Revue canadienne des ressources hydriques*. 38 (3), pp. 185–195.

Cooper, K.J., Whitaker, F.F., Anesio, A.M., Naish, M., Reynolds, D.M. and Evans, E.L. (2016) Dissolved organic carbon transformations and microbial community response to variations in recharge waters in a shallow carbonate aquifer. *Biogeochemistry*. 129 pp. 215–234.

Cory, R.M. and McKnight, D.M. (2005) Fluorescence spectroscopy reveals ubiquitous presence of oxidized and reduced quinones in dissolved organic matter. *Environmental Science and Technology*. 39 (21), pp. 8142–8149.

Cory, R.M., Miller, M.P., McKnight, D.M., Guerard, J.J. and Miller, P.L. (2010) Effect of instrument-specific response on the analysis of fulvic acid fluorescence spectra.

Limnology and Oceanography: Methods. 8 pp. 67–78.

Creed, I.F., McKnight, D.M., Pellerin, B.A., Green, M.B., Bergamaschi, B.A., Aiken, G.R., Burns, D.A., Findlay, S.E.G., Shanley, J.B., Striegl, R.G., Aulencbach, B.T., Clow, D.W., Laudon, H., McGlynn, B.L., et al. (2015) The river as a chemostat: fresh perspectives on dissolved organic matter flowing down the river continuum. *Canadian Journal of Fisheries and Aquatic Sciences*. 1 pp. 1–37.

Cumberland, S., Bridgeman, J., Baker, A., Sterling, M. and Ward, D. (2012) Fluorescence spectroscopy as a tool for determining microbial quality in potable water applications. *Environmental Technology*. 33 (6), pp. 687–693.

Cutrera, G., Manfredi, L., Valle, C.E. and González, J.F. (1999) On the determination of the kinetic parameters for the BOD test. *Water SA*. 25 (3), pp. 377–380.

Dartnell, L.R., Roberts, T.A., Moore, G., Ward, J.M. and Muller, J.P. (2013) Fluorescence Characterization of Clinically-Important Bacteria. *PLoS ONE*. 8 (9), pp. 1–13.

Davis, B.D. and Mingioli, E.S. (1950) Mutants of Escherichia coli requiring methionine or vitamin B12. *Journal of Bacteriology*. 60 pp. 17–28.

Deepa, N. and Ganesh, A.B. (2017) Minimally invasive fluorescence sensing system for real-time monitoring of bacterial cell cultivation. *Instrumentation Science & Technology*. 45 (1), pp. 85–100.

Determann, S., Lobbes, J.M., Reuter, R. and Rullkötter, J. (1998) Ultraviolet fluorescence excitation and emission spectroscopy of marine algae and bacteria. *Marine Chemistry*. 62 pp. 137–156.

Doron, N. (2009) *Sonication of bacterial samples*.

Downing, B.D., Pellerin, B.A., Bergamaschi, B.A., Saraceno, J.F. and Kraus, T.E.C. (2012) Seeing the light: The effects of particles, dissolved materials, and temperature on *in*

situ measurements of DOM fluorescence in rivers and streams. *Limnology and Oceanography: Methods*. 10 pp. 767–775.

Drinking Water Inspectorate (2010) *Chlorine*.

Dunn, G., Harris, L., Cook, C. and Prystajecky, N. (2014) A comparative analysis of current microbial water quality risk assessment and management practices in British Columbia and Ontario, Canada. *Science of the Total Environment*. 468–469 pp. 544–552.

Elliott, S., Lead, J.R. and Baker, A. (2006a) Characterisation of the fluorescence from freshwater, planktonic bacteria. *Water Research*. 40 pp. 2075–2083.

Elliott, S., Lead, J.R. and Baker, A. (2006b) Thermal quenching of fluorescence of freshwater, planktonic bacteria. *Analytica Chimica Acta*. 564 (October 2005), pp. 219–225.

Fellman, J.B., Hood, E. and Spencer, R.G.M. (2010) Fluorescence spectroscopy opens new windows into dissolved organic matter dynamics in freshwater ecosystems: A review. *Limnology and Oceanography*. 55 (6), pp. 2452–2462.

Ferrari, G.M. and Mingazzini, M. (1995) Synchronous fluorescence-spectra of dissolved organic-matter (DOM) of algal origin in marine coastal waters. *Marine Ecology-Progress Series*. 125 pp. 305–315.

Firth, P. (1999) The Importance of Water Resources Education for the Next Century. *Journal of the American Water Resources Association*. 35 (3), pp. 487–492.

Fischer, M., Friedrichs, G. and Lachnit, T. (2014) Fluorescence-based quasicontinuous and *in situ* monitoring of biofilm formation dynamics in natural marine environments. *Applied and Environmental Microbiology*. 80 (12), pp. 3721–3728.

Fox, B.G., Thorn, R.M.S., Anesio, A.M. and Reynolds, D.M. (2017) The *in situ* bacterial

production of fluorescent organic matter; an investigation at a species level. *Water Research*. 125 pp. 350–359.

Fukuzaki, K., Imai, I., Fukushima, K., Ishii, K.I., Sawayama, S. and Yoshioka, T. (2014) Fluorescent characteristics of dissolved organic matter produced by bloom-forming coastal phytoplankton. *Journal of Plankton Research*. 36 (3), pp. 685–694.

Gabor, R.S., Burns, M.A., Lee, R.H., Elg, J.B., Kemper, C.J., Barnard, H.R. and McKnight, D.M. (2015) Influence of leaching solution and catchment location on the fluorescence of water-soluble organic matter. *Environmental Science and Technology*. 49 (7), pp. 4425–4432.

Geerlof, A. (2010) M9 mineral medium. *Helmholtz Center Munich*. pp. 14–15.

Gilchrist, J.E., Campbell, J.E., Donnelly, C.B., Peeler, J.T. and Delaney, J.M. (1973) Spiral plate method for bacterial determination. *Applied microbiology*. 25 (2), pp. 244–252.

Gilden Photonics (2009) *FluoroSENS(R)*.

Golea, D.M., Upton, A., Jarvis, P., Moore, G., Sutherland, S., Parsons, S.A. and Judd, S.J. (2017) THM and HAA formation from NOM in raw and treated surface waters. *Water Research*. 112 pp. 226–235.

Gonçalves-Araujo, R., Stedmon, C.A., Heim, B., Dubinenkov, I., Kraberg, A., Moiseev, D. and Bracher, A. (2015) From Fresh to Marine Waters: Characterization and Fate of Dissolved Organic Matter in the Lena River Delta Region, Siberia. *Frontiers in Marine Science*. 2 (December), pp. 1–13.

Graham, P.W., Baker, A., Andersen, M.S. and Acworth, I. (2015) Field Measurement of Fluorescent Dissolved Organic Material as a Means of Early Detection of Leachate Plumes. *Water, Air, and Soil Pollution*. 226 (7), .

Graumann, P. (2007) *Bacillus: Cellular and Molecular Biology*. Peter Graumann (ed.). 1st

edition. Caister Academic Press.

Guillemette, F. and del Giorgio, P.A. (2012) Simultaneous consumption and production of fluorescent dissolved organic matter by lake bacterioplankton. *Environmental Microbiology*. 14 (6), pp. 1432–1443.

Hall, B.G., Acar, H., Nandipati, A. and Barlow, M. (2014) Growth Rates Made Easy. *Molecular Biology and Evolution*. 31 (1), pp. 232–238.

Hambly, A.C., Arvin, E., Pedersen, L.F., Pedersen, P.B., Seredyńska-Sobecka, B. and Stedmon, C.A. (2015) Characterising organic matter in recirculating aquaculture systems with fluorescence EEM spectroscopy. *Water Research*. 83 pp. 112–120.

Hambly, A.C., Henderson, R.K., Storey, M. V., Baker, A., Stuetz, R.M. and Khan, S.J. (2010) Fluorescence monitoring at a recycled water treatment plant and associated dual distribution system - Implications for cross-connection detection. *Water Research*. 44 (18), pp. 5323–5333.

Hansell, D.A. and Carlson, C.A. (2015) Preface. In: Dennis A. Hansell and A. Carlson, Craig (eds.). *Biogeochemistry of Marine Dissolved Organic Matter* 2nd Ed. Academic Press.

Harun, S., Baker, A., Bradley, C. and Pinay, G. (2016) Spatial and seasonal variations in the composition of dissolved organic matter in a tropical catchment: the Lower Kinabatangan River, Sabah, Malaysia. *Environ. Sci.: Processes Impacts*. 18 (1), pp. 137–150.

Harun, S., Baker, A., Bradley, C., Pinay, G., Boomer, I. and Hamilton, R.L. (2015) Characterisation of dissolved organic matter in the Lower Kinabatangan River, Sabah, Malaysia. *Hydrology Research*. 46 (3), pp. 411–428.

Henderson, R.K., Baker, A., Murphy, K.R., Hambly, A., Stuetz, R.M. and Khan, S.J. (2009) Fluorescence as a potential monitoring tool for recycled water systems: A review.

Water Research. 43 (4), pp. 863–881.

Herlemann, D.P.R., Manecki, M., Meeske, C., Pollehne, F., Labrenz, M., Schulz-Bull, D., Dittmar, T. and J??rgens, K. (2014) Uncoupling of bacterial and terrigenous dissolved organic matter dynamics in decomposition experiments. *PLoS ONE*. 9 (4), pp. 1–12.

Hessen, D. and Tranvik, L.J. (1998) *Aquatic Humic Substances: Ecology and Biogeochemistry*. Ecological. Springer.

Hogg, S. (2005) *Essential Microbiology*. 1st edition. Wiley.

HORIBA Ltd. (2013) *Aqualog(R): Operation Manual (Revision E)*.

Hua, B., Veum, K., Yang, J., Jones, J. and Deng, B. (2010) Parallel factor analysis of fluorescence EEM spectra to identify THM precursors in lake waters. *Environmental Monitoring and Assessment*. 161 (1–4), pp. 71–81.

Hudson, N., Baker, A. and Reynolds, D.M. (2007) Fluorescence Analysis of Dissolved Organic Matter in Natural, Waste and Polluted Water - A Review. *River Research and Applications*. 23 pp. 631–649.

Hudson, N., Baker, A., Reynolds, D.M., Carliell-Marquet, C. and Ward, D. (2009) Changes in freshwater organic matter fluorescence intensity with freezing/thawing and dehydration/rehydration. *Journal of Geophysical Research: Biogeosciences*. 114 (June), pp. 1–11.

Hudson, N., Baker, A., Ward, D., Reynolds, D.M., Brunsdon, C., Carliell-Marquet, C. and Browning, S. (2008) Can fluorescence spectrometry be used as a surrogate for the Biochemical Oxygen Demand (BOD) test in water quality assessment? An example from South West England. *Science of the Total Environment*. 391 pp. 149–158.

Jiao, N., Herndl, G.J., Hansell, D.A., Benner, R., Kattner, G., Wilhelm, S.W., Kirchman,

D.L., Weinbauer, M.G., Luo, T., Chen, F. and Azam, F. (2010) Microbial production of recalcitrant dissolved organic matter: long-term carbon storage in the global ocean. *Nature Reviews Microbiology*. 8 pp. 593.

Jørgensen, L., Stedmon, C.A., Granskog, M.A. and Middelboe, M. (2014) Tracing the long-term microbial production of recalcitrant fluorescent dissolved organic matter in seawater. *Geophysical Research Letters*. 41 (7), pp. 2481–2488.

Jørgensen, L., Stedmon, C.A., Kragh, T., Markager, S., Middelboe, M. and Søndergaard, M. (2011) Global trends in the fluorescence characteristics and distribution of marine dissolved organic matter. *Marine Chemistry*. 126 (1–4), pp. 139–148.

Jouanneau, S., Recoules, L., Durand, M.J., Boukabache, A., Picot, V., Primault, Y., Lakel, A., Sengelin, M., Barillon, B. and Thouand, G. (2014) Methods for assessing biochemical oxygen demand (BOD): A review. *Water Research*. 49 (1), pp. 62–82.

Kallenbach, C.M., Frey, S.D. and Grandy, A.S. (2016) Direct evidence for microbial-derived soil organic matter formation and its ecophysiological controls. *Nature Communications*. 7 pp. 1–10.

Kellerman, A.M., Kothawala, D.N., Dittmar, T. and Tranvik, L.J. (2015) Persistence of dissolved organic matter in lakes related to its molecular characteristics. *Nature Geoscience*. 8 (6), pp. 454–457.

Khamis, K., Bradley, C. and Hannah, D.M. (2017) Understanding dissolved organic matter dynamics in urban catchments: insights from *in situ* fluorescence sensor technology. *Wiley Interdisciplinary Reviews: Water*. 5 (February), pp. e1259.

Khamis, K., Sorensen, J.P.R., Bradley, C., Hannah, D.M., Lapworth, D.J. and Stevens, R. (2015) *In situ* tryptophan-like fluorometers: assessing turbidity and temperature effects for freshwater applications. *Environmental Science: Processes & Impacts*. 17 pp. 740–752.

Koch, B.P., Kattner, G., Witt, M. and Passow, U. (2014) Molecular insights into the microbial formation of marine dissolved organic matter: Recalcitrant or labile? *Biogeosciences*. 11 (15), pp. 4173–4190.

Kothawala, D.N., Stedmon, C.A., Müller, R.A., Weyhenmeyer, G.A., Köhler, S.J. and Tranvik, L.J. (2014) Controls of dissolved organic matter quality: Evidence from a large-scale boreal lake survey. *Global Change Biology*. 20 (4), pp. 1101–1114.

Kragelund, L. and Nybroe, O. (1994) Culturability and Expression of Outer Membrane Proteins during Carbon, Nitrogen, or Phosphorus Starvation of *Pseudomonas fluorescens* DF57 and *Pseudomonas putida* DF14. *Applied and Environmental Microbiology*. 60 (8), pp. 2944–2948.

Kramer, G.D. and Herndl, G.J. (2004) Photo- and bioreactivity of chromophoric dissolved organic matter produced by marine bacterioplankton. *Aquatic Microbial Ecology*. 36 pp. 239–246.

Lakowicz, J.R. (2006) *Principles of Fluorescence Spectroscopy*. 3rd edition. Springer.

Lambert, T., Teodoru, C.R., Nyoni, F.C., Bouillon, S., Darchambeau, F., Massicotte, P. and Borges, A. V. (2016) Along-stream transport and transformation of dissolved organic matter in a large tropical river. *Biogeosciences*. 13 (9), pp. 2727–2741.

Lapworth, D.J. and Kinniburgh, D.G. (2009) An R script for visualising and analysing fluorescence excitation-emission matrices (EEMs). *Computers and Geosciences*. 35 (10), pp. 2160–2163.

Larsen, L.G., Aiken, G.R., Harvey, J.W., Noe, G.B. and Crimaldi, J.P. (2010) Using fluorescence spectroscopy to trace seasonal DOM dynamics, disturbance effects, and hydrologic transport in the Florida Everglades. *Journal of Geophysical Research: Biogeosciences*. 115 pp. 1–14.

Lavonen, E.E., Kothawala, D.N., Tranvik, L.J., Gonsior, M., Schmitt-Kopplin, P. and

Köhler, S.J. (2015) Tracking changes in the optical properties and molecular composition of dissolved organic matter during drinking water production. *Water Research*. 85 pp. 286–294.

Lawaetz, A.J. and Stedmon, C.A. (2009) Fluorescence intensity calibration using the Raman scatter peak of water. *Applied Spectroscopy*. 63 (8), pp. 936–940.

Lawrence, H.A. and Palombo, E.A. (2009) Activity of Essential Oils Against *Bacillus subtilis* spores. *Journal of Microbiology and Biotechnology*. 19 (12), pp. 1590–1595.

Lee, C., Sultana, C.M., Collins, D.B., Santander, M. V., Axson, J.L., Malfatti, F., Cornwell, G.C., Grandquist, J.R., Deane, G.B., Stokes, M.D., Azam, F., Grassian, V.H. and Prather, K. a. (2015) Advancing Model Systems for Fundamental Laboratory Studies of Sea Spray Aerosol Using the Microbial Loop. *The Journal of Physical Chemistry A*. pp. 150805131932006.

Leenheer, J.A. and Croué, J.-P. (2003) Characterizing Dissolved Aquatic Organic Matter. *Environmental Science & Technology*. 37 pp. 18A–26A.

Lemus Pérez, M.F. and Rodríguez Susa, M. (2017) Exopolymeric substances from drinking water biofilms: Dynamics of production and relation with disinfection by products. *Water Research*. 116 pp. 304–315.

Lidén, A., Keucken, A. and Persson, K.M. (2017) Uses of fluorescence excitation-emissions indices in predicting water treatment efficiency. *Journal of Water Process Engineering*. 16 pp. 249–257.

Liu, R., Lead, J.R. and Baker, A. (2007) Fluorescence characterization of cross flow ultrafiltration derived freshwater colloidal and dissolved organic matter. *Chemosphere*. 68 pp. 1304–1311.

Lory, S. (1986) Effect of Iron on Accumulation of Exotoxin A-Specific mRNA in *Pseudomonas aeruginosa*. *Journal of Bacteriology*. 168 (3), pp. 1451–1456.

MacFaddin, J.F. (2000) *Biochemical Tests for Identification of Medical Bacteria*. 3rd edition. Lippincott Williams & Wilkins.

Makarewicz, A., Kowalczuk, P., Sagan, S., Granskog, M.A., Pavlov, A.K., Zdun, A., Borzycka, K. and Zabłocka, M. (2018) Characteristics of Chromophoric and Fluorescent Dissolved Organic Matter in the Nordic Seas. *Ocean Science Discussions*. (January), pp. 1–41.

Martínez-Pérez, A.M., Nieto-Cid, M., Osterholz, H., Catalá, T.S., Reche, I., Dittmar, T. and Álvarez-Salgado, X.A. (2017) Linking optical and molecular signatures of dissolved organic matter in the Mediterranean Sea. *Scientific Reports*. 7 (1), pp. 1–11.

Matilainen, A., Gjessing, E.T., Lahtinen, T., Hed, L., Bhatnagar, A. and Sillanpää, M. (2011) An overview of the methods used in the characterisation of natural organic matter (NOM) in relation to drinking water treatment. *Chemosphere*. 83 (11), pp. 1431–1442.

McKnight, D.M., E. W. Boyer, P. K. Westerhoff, P. T. Doran, T. Kulbe and Anderson, D.T. (2001) Spectroflourometric characterization of dissolved organic matter for indication of precursor organic material and aromaticity. *Limnology and Oceanography*. 46 (1), pp. 38–48.

Miller, M.P. and McKnight, D.M. (2010) Comparison of seasonal changes in fluorescent dissolved organic matter among aquatic lake and stream sites in the Green Lakes Valley. *Journal of Geophysical Research*. 115 pp. 1–14.

Mladenov, N., Bigelow, A., Pietruschka, B., Palomo, M. and Buckley, C. (2017) Using submersible fluorescence sensors to track the removal of organic matter in decentralized wastewater treatment systems (DEWATS) in real time. *Water Science and Technology*. pp. wst2017573.

Molecular Probes Inc. (2004) *LIVE/DEAD ® BacLight ™ Bacterial Viability Kits*.

Mopper, K., Kieber, D.J. and Stubbins, A. (2015) Marine Photochemistry of Organic Matter. In: Dennis A. Hansell and Craig A. Carlson (eds.). *Biogeochemistry of Marine Dissolved Organic Matter* 2nd Ed. Academic Press. pp. 389–450.

Moran, M.A., Sheldon, W.M. and Zepp, R.G. (2000) Carbon loss and optical property changes during long-term photochemical and biological degradation of estuarine dissolved organic matter. *Limnology and Oceanography*. 45 (August 1997), pp. 1254–1264.

Mostofa, K.M.G., Yoshioka, T., Mottaleb, A. and Vione, D. (2013) *Photobiogeochemistry of Organic Matter: Principles and Practices in Water Environments*. Springer.

Murphy, K.R., Butler, K.D., Spencer, R.G.M., Stedmon, C.A., Boehme, J.R. and Aiken, G.R. (2010) Measurement of Dissolved Organic Matter Fluorescence in Aquatic Environments: An Interlaboratory Comparison. *Environmental science & technology*. 44 pp. 9405–9412.

Murphy, K.R., Stedmon, C.A., Waite, T.D. and Ruiz, G.M. (2008) Distinguishing between terrestrial and autochthonous organic matter sources in marine environments using fluorescence spectroscopy. *Marine Chemistry*. 108 pp. 40–58.

Murphy, K.R., Stedmon, C.A., Wenig, P. and Bro, R. (2014) OpenFluor- an online spectral library of auto-fluorescence by organic compounds in the environment. *Analytical Methods*. 6 pp. 658–661.

Naden, P.S., Old, G.H., Eliot-Laize, C., Granger, S.J., Hawkins, J.M.B., Bol, R. and Haygarth, P. (2010) Assessment of natural fluorescence as a tracer of diffuse agricultural pollution from slurry spreading on intensely-farmed grasslands. *Water Research*. 44 (6), pp. 1701–1712.

Nelson, N.B. and Gauglitz, J.M. (2016) Optical Signatures of Dissolved Organic Matter Transformation in the Global Ocean. *Frontiers in Marine Science*. 2 (January), pp. 1–15.

Ogawa, H., Amagai, Y., Koike, I., Kaiser, K. and Benner, R. (2001) Production of Refractory Dissolved Organic Matter by Bakteria. *Science*. 292 (5518), pp. 917–920.

Omori, Y., Hama, T., Ishii, M. and Saito, S. (2011) Vertical change in the composition of marine humic-like fluorescent dissolved organic matter in the subtropical western North Pacific and its relation to photoreactivity. *Marine Chemistry*. 124 (1–4), pp. 38–47.

Para, J., Coble, P.G., Charrière, B., Tedetti, M., Fontana, C. and Sempéré, R. (2010) Fluorescence and absorption properties of chromophoric dissolved organic matter (CDOM) in coastal surface waters of the northwestern Mediterranean Sea, influence of the Rhône River. *Biogeosciences*. 7 (12), pp. 4083–4103.

Park, M. and Snyder, S.A. (2018) Sample handling and data processing for fluorescent excitation-emission matrix (EEM) of dissolved organic matter (DOM). *Chemosphere*. 193 pp. 530–537.

Parlanti, E., Wörz, K., Geoffroy, L. and Lamotte, M. (2000) Dissolved organic matter fluorescence spectroscopy as a tool to estimate biological activity in a coastal zone submitted to anthropogenic inputs. *Organic Geochemistry*. 31 pp. 1765–1781.

Patil, P., Sawant, D. and Deshmukh, R. (2012) Physico-Chemical Parameters for Testing of Water–a Review. *International Journal of Environmental Sciences*. 3 (3), pp. 1194–1207.

Peleato, N.M., Legge, R.L. and Andrews, R.C. (2017) Investigation of fluorescence methods for rapid detection of municipal wastewater impact on drinking water sources. *Spectrochimica Acta - Part A: Molecular and Biomolecular Spectroscopy*. 171 pp. 104–111.

Perminova, I. V., Frimmel, F.H., Kudryavtsev, A. V., Kulikova, N.A., Abbt-Braun, G., Hesse, S. and Petrosyan, V.S. (2003) Molecular weight characteristics of humic substances from different environments as determined by size exclusion

chromatography and their statistical evaluation. *Environmental Science and Technology*. 37 (11), pp. 2477–2485.

Persichetti, G., Testa, G. and Bernini, R. (2013) High sensitivity UV fluorescence spectroscopy based on an optofluidic jet waveguide. *Optics Express*. 21 (20), pp. 24219–24230.

Postel, S. (2015) Water for life *Frontiers in Ecology and the Environment* 7 (2).

Promega (2010) *Amino Acids: Technical Reference*.

Qian, C., Wang, L.F., Chen, W., Wang, Y.S., Liu, X.Y., Jiang, H. and Yu, H.Q. (2017) Fluorescence Approach for the Determination of Fluorescent Dissolved Organic Matter. *Analytical Chemistry*. 89 (7), pp. 4264–4271.

Repeta, D.J. (2015) Chemical Characterization and Cycling of Dissolved Organic Matter. In: Dennis A. Hansell and Craig A. Carlson (eds.). *Biogeochemistry of Marine Dissolved Organic Matter* 2nd Ed. Academic Press. pp. 21–63.

Reynolds, D.M. (2003) Rapid and direct determination of tryptophan in water using synchronous fluorescence spectroscopy. *Water Research*. 37 pp. 3055–3060.

Reynolds, D.M. (2002) The differentiation of biodegradable and non-biodegradable dissolved organic matter in wastewaters using fluorescence spectroscopy. *Journal of Chemical Technology and Biotechnology*. 77 (April), pp. 965–972.

Reynolds, D.M. (2014) The Principles of Fluorescence. In: Andy Baker, Darren M Reynolds, Jamie Lead, Paula G Coble, and Robert G M Spencer (eds.). *Aquatic Organic Matter Fluorescence* Cambridge Environmental Chemistry Series. Cambridge University Press. pp. 3–34.

Reynolds, D.M. and Ahmad, S.R. (1997) Rapid and direct determination of wastewater BOD values using a fluorescence technique. *Water Research*. 31 (8), pp. 2012–2018.

Reynolds, D.M. and Ahmad, S.R. (1995) The effect of metal ions on the fluorescence of sewage wastewater. *Water Research*. 29 (9), pp. 2214–2216.

Ridgwell, A. and Arndt, S. (2015) Why Dissolved Organics Matter: DOC in Ancient Oceans and Past Climate Change. In: Dennis A. Hansell and Craig A. Carlson (eds.). *Biogeochemistry of Marine Dissolved Organic Matter* 2nd Ed. Academic Press. pp. 1–20.

Roccaro, P., Vagliasindi, F.G.A. and Korshin, G. V. (2009) Changes in NOM fluorescence caused by chlorination and their associations with disinfection by-products formation. *Environmental Science and Technology*. 43 (3), pp. 724–729.

Romera-Castillo, C., Chen, M., Yamashita, Y. and Jaffé, R. (2014) Fluorescence characteristics of size-fractionated dissolved organic matter: Implications for a molecular assembly based structure? *Water Research*. 55 pp. 40–51.

Romera-Castillo, C., Sarmento, H., Alvarez-Salgado, X.A., Gasol, J.M. and Marrasé, C. (2011) Net Production and Consumption of Fluorescent Colored Dissolved Organic Matter by Natural Bacterial Assemblages Growing on Marine Phytoplankton Exudates. *Applied and Environmental Microbiology*. 77 (21), pp. 7490–7498.

Ruhala, S.S. and Zarnetske, J.P. (2017) Using *in-situ* optical sensors to study dissolved organic carbon dynamics of streams and watersheds: A review. *Science of the Total Environment*. 575 pp. 713–723.

Saraceno, J.F., Pellerin, B.A., Downing, B.D., Boss, E., Bachand, P.A.M. and Bergamaschi, B.A. (2009) High-frequency *in situ* optical measurements during a storm event: Assessing relationships between dissolved organic matter, sediment concentrations, and hydrologic processes. *Journal of Geophysical Research: Biogeosciences*. 114 pp. 1–11.

Saraceno, J.F., Shanley, J.B., Downing, B.D. and Pellerin, B.A. (2017) Clearing the waters: Evaluating the need for site-specific field fluorescence corrections based on

turbidity measurements. *Limnology and Oceanography: Methods*. 15 (4), pp. 408–416.

Schaeffer, A.B. and Fulton, M.D. (1933) A Simplified Method of Staining Endospores. *Science*. 77 (1990), pp. 194.

Shimotori, K., Omori, Y. and Hama, T. (2009) Bacterial production of marine humic-like fluorescent dissolved organic matter and its biogeochemical importance. *Aquatic Microbial Ecology*. 58 pp. 55–66.

Shimotori, K., Watanabe, K. and Hama, T. (2012) Fluorescence characteristics of humic-like fluorescent dissolved organic matter produced by various taxa of marine bacteria. *Aquatic Microbial Ecology*. 65 pp. 249–260.

Shubina, D., Fedoseeva, E., Gorshkova, O. and Patsaeva, S. (2010) the ' Blue Shift ' of Emission Maximum and the Fluorescence Quantum Yield As Quantitative Spectral Characteristics. *EARSeL eProceedings 9, 1/2010*. pp. 13–21.

Shutova, Y., Baker, A., Bridgeman, J. and Henderson, R.K. (2014) Spectroscopic characterisation of dissolved organic matter changes in drinking water treatment: From PARAFAC analysis to online monitoring wavelengths. *Water Research*. 54 pp. 159–169.

Sierra, M.M.D., Giovanela, M., Parlanti, E. and Soriano-Sierra, E.J. (2005) Fluorescence fingerprint of fulvic and humic acids from varied origins as viewed by single-scan and excitation/emission matrix techniques. *Chemosphere*. 58 pp. 715–733.

Sigee, D.C. (2004) *Freshwater Microbiology*. Wiley.

da Silva, G.A. and de Almeida, E.A. (2006) Production of Yellow-Green Fluorescent Pigment by *Pseudomonas fluorescens*. *Brazilian Archives of Biology and Technology*. 49 (3), pp. 411–419.

Singh, S., Inamdar, S. and Scott, D. (2013) Comparison of Two PARAFAC Models of

Dissolved Organic Matter Fluorescence for a Mid-Atlantic Forested Watershed in the USA. *Journal of Ecosystems*. 2013 pp. 1–16.

Smith, C.B., Anderson, J.E. and Webb, S.R. (2004) Detection of *Bacillus* endospores using total luminescence spectroscopy. *Spectrochimica Acta - Part A: Molecular and Biomolecular Spectroscopy*. 60 pp. 2517–2521.

Sohn, M., Himmelsbach, D.S., Barton, F.E.I. and Fedorka-Cray, P.J. (2009) Fluorescence Spectroscopy for Rapid Detection and Classification of Bacterial Pathogens. *Applied Spectroscopy*. 63 (11), pp. 1251–1255.

Somerville, G., Mikoryak, C.A., Reitzer, L. and Mikoryak, C.A.N.N. (1999) Physiological Characterization of *Pseudomonas aeruginosa* during Exotoxin A Synthesis: Glutamate, Iron Limitation, and Aconitase Activity. *Journal of Bacteriology*. 181 (4), pp. 1072–1078.

Sorensen, J.P.R., Baker, A., Cumberland, S.A., Lapworth, D.J., MacDonald, A.M., Pedley, S., Taylor, R.G. and Ward, J.S.T. (2018a) Real-time detection of faecally contaminated drinking water with tryptophan-like fluorescence: defining threshold values. *Science of the Total Environment*. 622–623 pp. 1250–1257.

Sorensen, J.P.R., Lapworth, D.J., Marchant, B.P., Nkhuwa, D.C.W., Pedley, S., Stuart, M.E., Bell, R.A., Chirwa, M., Kabika, J., Liemisa, M. and Chibesa, M. (2015a) *In situ* tryptophan-like fluorescence: A real-time indicator of faecal contamination in drinking water supplies. *Water Research*. 81 pp. 38–46.

Sorensen, J.P.R., Lapworth, D.J., Nkhuwa, D.C.W., Stuart, M.E., Gooddy, D.C., Bell, R.A., Chirwa, M., Kabika, J., Liemisa, M., Chibesa, M. and Pedley, S. (2015b) Emerging contaminants in urban groundwater sources in Africa. *Water Research*. 72 pp. 51–63.

Sorensen, J.P.R., Lapworth, D.J., Read, D.S., Nkhuwa, D.C.W., Bell, R.A., Chibesa, M., Chirwa, M., Kabika, J., Liemisa, M. and Pedley, S. (2015c) Tracing enteric pathogen contamination in sub-Saharan African groundwater. *Science of the Total*

Environment. 538 pp. 888–895.

Sorensen, J.P.R., Sadhu, A., Sampath, G., Sugden, S., Dutta Gupta, S., Lapworth, D.J., Marchant, B.P. and Pedley, S. (2016) Are sanitation interventions a threat to drinking water supplies in rural India? An application of tryptophan-like fluorescence. *Water Research*. 88 pp. 923–932.

Sorensen, J.P.R., Vivanco, A., Ascott, M.J., Gooddy, D.C., Lapworth, D.J., Read, D.S., Rushworth, C.M., Bucknall, J., Herbert, K., Karapanos, I., Gumm, L.P. and Taylor, R.G. (2018b) Online fluorescence spectroscopy for the real-time evaluation of the microbial quality of drinking water. *Water Research*.

Spencer, R.G.M., Aiken, G.R., Wickland, K.P., Striegl, R.G. and Hernes, P.J. (2008) Seasonal and spatial variability in dissolved organic matter quantity and composition from the Yukon River basin, Alaska. *Global Biogeochemical Cycles*. 22 pp. 1–13.

Spencer, R.G.M., Bolton, L. and Baker, A. (2007) Freeze/thaw and pH effects on freshwater dissolved organic matter fluorescence and absorbance properties from a number of UK locations. *Water Research*. 41 pp. 2941–2950.

Stedmon, C.A. and Bro, R. (2008) Characterizing dissolved organic matter fluorescence with parallel factor analysis : a tutorial. *Limnology and Oceanography: Methods*. 6 pp. 572–579.

Stedmon, C.A. and Markager, S. (2005) Resolving the variability of dissolved organic matter fluorescence in a temperate estuary and its catchment using PARAFAC analysis. *Limnology and Oceanography*. 50 (2), pp. 686–697.

Stedmon, C.A., Markager, S. and Bro, R. (2003) Tracing dissolved organic matter in aquatic environments using a new approach to fluorescence spectroscopy. *Marine Chemistry*. 82 pp. 239–254.

Stedmon, C.A., Seredyńska-Sobecka, B., Boe-Hansen, R., Le Tallec, N., Waul, C.K. and Arvin, E. (2011) A potential approach for monitoring drinking water quality from groundwater systems using organic matter fluorescence as an early warning for contamination events. *Water Research*. 45 pp. 6030–6038.

Stokes, G.G. (1852) On the Change of Refrangibility of Light. *Philosophical Transactions of the Royal Society of London*. 142 pp. 463–562.

Stubbins, A., Lapierre, J., Berggren, M., Prairie, Y.T., Dittmar, T. and del Giorgio, P.A. (2014) What's in an EEM? Molecular Signatures Associated with Dissolved Organic Fluorescence in Boreal Canada. *Environmental Science & Technology*. 48 pp. 105598–110606.

Suksomjit, M., Nagao, S., Ichimi, K., Yamada, T. and Tada, K. (2009) Variation of dissolved organic matter and fluorescence characteristics before, during and after phytoplankton bloom. *Journal of Oceanography*. 65 (6), pp. 835–846.

Tanaka, K., Kuma, K., Hamasaki, K. and Yamashita, Y. (2014) Accumulation of humic-like fluorescent dissolved organic matter in the Japan Sea. *Scientific reports*. 4 pp. 5292.

Tedetti, M., Joffre, P. and Goutx, M. (2013) Development of a field-portable fluorometer based on deep ultraviolet LEDs for the detection of phenanthrene- and tryptophan-like compounds in natural waters. *Sensors and Actuators, B: Chemical*. 182 pp. 416–423.

The Public Health Laboratory Service Water Sub-Committee (1953) The Effect of Sodium Thiosulphate on the Coliform and Bacterium coli Counts of Non-Chlorinated Water Samples. *The Journal of Hygiene*. 51 (4), pp. 572–577.

Thurman, E.M. (1985) *Organic geochemistry of natural waters.* M. A. Norwell (ed.). Springer.

Timko, S.A., Maydanov, A., Pittelli, S.L., Conte, M.H., Cooper, W.J., Koch, B.P., Schmitt-Kopplin, P. and Gonsior, M. (2015) Depth-dependent photodegradation of marine dissolved organic matter. *Frontiers in Marine Science*. 2 (September), pp. 1–13.

Tranvik, L.J. (1999) Photochemical effects on bacterial degradation of dissolved organic matter in lake water. *DOC Degradation in Freshwater and Marine Systems: Microbial versus Photochemical Processes*.

Valeur, B. and Berberan-Santos, M.N. (2011) A brief history of fluorescence and phosphorescence before the emergence of quantum theory. *Journal of Chemical Education*. 88 (6), pp. 731–738.

Wang, Z., Cao, J. and Meng, F. (2015) Interactions between protein-like and humic-like components in dissolved organic matter revealed by fluorescence quenching. *Water Research*. 68 pp. 404–413.

Wasserman, A.E. (1965) Absorption and Fluorescence of Water-Soluble Pigments Produced by Four Species of *Pseudomonas*. *Applied Microbiology*. 13 (2), pp. 175–180.

Watras, C.J., Hanson, P.C., Stacy, T.L., Morrison, K.M., Mather, J., Hu, Y.-H. and Milewski, P. (2011) A temperature compensation method for CDOM fluorescence sensors in freshwater. *Limnology and Oceanography: Methods*. 9 pp. 296–301.

Watras, C.J., Morrison, K.A., Mather, J., Milewski, P. and Hanson, P.C. (2014) Correcting CDOM fluorescence measurements for temperature effects under field conditions in freshwaters. *Limnology and Oceanography: Methods*. (7), pp. 23–24.

Westerhoff, P., Chao, P. and Mash, H. (2004) Reactivity of natural organic matter with aqueous chlorine and bromine. *Water Research*. 38 (6), pp. 1502–1513.

Winter, A.R., Fish, T.A.E., Playle, R.C., Smith, D.S. and Curtis, P.J. (2007) Photodegradation of natural organic matter from diverse freshwater sources. *Aquatic Toxicology*. 84 pp. 215–222.

Wünsch, U.J., Murphy, K.R. and Stedmon, C.A. (2015) Fluorescence Quantum Yields of Natural Organic Matter and Organic Compounds : Implications for the Fluorescence-based Interpretation of Organic Matter Composition. *Frontiers in Marine Science*. 2 (November), pp. 1–15.

Xiao, K., Liang, S., Xiao, A., Lei, T., Tan, J., Wang, X. and Huang, X. (2017) Fluorescence quotient of excitation–emission matrices as a potential indicator of organic matter behavior in membrane bioreactors. *Environmental Science: Water Research & Technology*. 4 pp. 281–290.

Xie, W., Zhang, S., Ruan, L., Yang, M., Shi, W., Zhang, H. and Li, W. (2017) Evaluating Soil Dissolved Organic Matter Extraction Using Three-Dimensional Excitation-Emission Matrix Fluorescence Spectroscopy. *Pedosphere*. 27 (5), pp. 968–973.

Yang, L., Kim, D., Uzun, H., Karanfil, T. and Hur, J. (2015) Assessing trihalomethanes (THMs) and N-nitrosodimethylamine (NDMA) formation potentials in drinking water treatment plants using fluorescence spectroscopy and parallel factor analysis. *Chemosphere*. 121 pp. 84–91.

Yang, L., Shin, H.S. and Hur, J. (2014) Estimating the concentration and biodegradability of organic matter in 22 wastewater treatment plants using fluorescence excitation emission matrices and parallel factor analysis. *Sensors*. 14 pp. 1771–1786.

Yu, H., Liang, H., Qu, F., Han, Z.S., Shao, S., Chang, H. and Li, G. (2015) Impact of dataset diversity on accuracy and sensitivity of parallel factor analysis model of dissolved organic matter fluorescence excitation-emission matrix. *Scientific Reports*. 5 (October 2014), pp. 1–11.

Zang, X., van Heemst, J.D., Dria, K.J. and Hatcher, P.G. (2000) Encapsulation of protein in humic acid from a histosol as an explanation for the occurrence of organic nitrogen in soil and sediment. *Organic Geochemistry*. 31 (7), pp. 679–695.

Zhao, W., Lv, L. and Miao, H. (2013) Tracing the Variability of Dissolved Organic Matter

Fluorescence in the East China Sea in the Red Tide Season with use of Excitation - emission Matrix Spectroscopy and Parallel Factor Analysis. *Marine Science Research and Development*. 4 (1), pp. 1–6, http://dx.doi.org/10.4172/2155–9910.1000144.

Zhi, E., Yu, H., Duan, L., Han, L., Liu, L. and Song, Y. (2015) Characterization of the composition of water DOM in a surface flow constructed wetland using fluorescence spectroscopy coupled with derivative and PARAFAC. *Environmental Earth Sciences*. 73 (9), pp. 5153–5161.

Zhou, Y., Jeppesen, E., Zhang, Y., Shi, K., Liu, X. and Zhu, G. (2016) Dissolved organic matter fluorescence at wavelength 275/342 nm as a key indicator for detection of point-source contamination in a large Chinese drinking water lake. *Chemosphere*. 144 pp. 503–509.

Zhou, Y., Shi, K., Zhang, Y., Jeppesen, E., Liu, X., Zhou, Q., Wu, H., Tang, X. and Zhu, G. (2017) Fluorescence peak integration ratio IC:ITas a new potential indicator tracing the compositional changes in chromophoric dissolved organic matter. *Science of the Total Environment*. 574 pp. 1588–1598.

Zhu, G., Bian, Y., Hursthouse, A.S., Wan, P., Szymanska, K., Ma, J., Wang, X. and Zhao, Z. (2017) Application of 3-D Fluorescence: Characterization of Natural Organic Matter in Natural Water and Water Purification Systems. *Journal of Fluorescence*. 27 (6), pp. 2069–2094.

Ziervogel, K., Osburn, C., Brym, A., Battles, J., Joye, S., D'souza, N., Montoya, J., Passow, U. and Arnosti, C. (2016) Linking Heterotrophic Microbial Activities with Particle Characteristics in Waters of the Mississippi River Delta in the Aftermath of Hurricane Isaac. *Frontiers in Marine Science*. 3 (February), pp. 1–12.

Appendix I: Published material

Fox, B.G., Thorn, R.M.S., Anesio, A.M. and Reynolds, D.M. (2017) The *in situ* bacterial production of fluorescent organic matter; an investigation at a species level. *Water Research*. 125 pp. 350–359.

Water Research 125 (2017) 350–359

Contents lists available at ScienceDirect

Water Research

journal homepage: www.elsevier.com/locate/watres

The *in situ* bacterial production of fluorescent organic matter; an investigation at a species level

B.G. Fox [a], R.M.S. Thorn [a], A.M. Anesio [b], D.M. Reynolds [a, *]

[a] Centre for Research in Biosciences, University of the West of England, Bristol, BS16 1QY, UK
[b] School of Geographical Sciences, University of Bristol, Bristol, BS8 1SS, UK

ARTICLE INFO

Article history:
Received 21 April 2017
Received in revised form
31 July 2017
Accepted 17 August 2017
Available online 18 August 2017

Keywords:
Dissolved organic matter
In situ microbial processing
Excitation-emission matrix fluorescence spectroscopy
Fluorescent organic matter
Autochthonous
Allochthonous

ABSTRACT

Aquatic dissolved organic matter (DOM) plays an essential role in biogeochemical cycling and transport of organic matter throughout the hydrological continuum. To characterise microbially-derived organic matter (OM) from common environmental microorganisms (*Escherichia coli, Bacillus subtilis* and *Pseudomonas aeruginosa)*, excitation-emission matrix (EEM) fluorescence spectroscopy was employed. This work shows that bacterial organisms can produce fluorescent organic matter (FOM) *in situ* and, furthermore, that the production of FOM differs at a bacterial species level. This production can be attributed to structural biological compounds, specific functional proteins (e.g. pyoverdine production by *P. aeruginosa*), and/or metabolic by-products. Bacterial growth curve data demonstrates that the production of FOM is fundamentally related to microbial metabolism. For example, the majority of Peak T fluorescence (> 75%) is shown to be intracellular in origin, as a result of the building of proteins for growth and metabolism. This underpins the use of Peak T as a measure of microbial activity, as opposed to bacterial enumeration as has been previously suggested. This study shows that different bacterial species produce a range of FOM that has historically been attributed to high molecular weight allochthonous material or the degradation of terrestrial FOM. We provide definitive evidence that, in fact, it can be produced by microbes within a model system (autochthonous), providing new insights into the possible origin of allochthonous and autochthonous organic material present in aquatic systems.

1. Introduction

Dissolved organic matter (DOM) in aquatic systems plays an essential role in global biogeochemical cycling (Bieroza and Heathwaite, 2016; Hudson et al., 2007). It is generally accepted that the majority of DOM found in freshwaters is allochthonous, with a proportion of the DOM considered to be produced *in situ*, i.e. autochthonous material (Coble et al., 2014). Fluorescence excitation-emission matrix (EEM) spectroscopy has been increasingly employed in recent research to characterise aquatic fluorescent organic matter (FOM) and fluorescent dissolved organic matter (FDOM) (Baker, 2005; Bridgeman et al., 2015). The use of this technique has advanced our understanding of FDOM, its classification, transformation and potential origin (Hudson et al., 2007; Stedmon and Bro, 2008).

Aquatic FDOM has been characterised as consisting of humic-like material considered to be of allochthonous origin of terrestrial input (Coble et al., 2014). The compounds associated with terrestrially derived FDOM are known to be stable higher molecular weight aromatic compounds, generally considered non-labile (Cooper et al., 2016). However, recent work concerning the marine environment has suggested that humic-like FDOM could be a consequence of bacterial metabolism (Guillemette and del Giorgio, 2012; Kramer and Herndl, 2004; Romera-Castillo et al., 2011; Shimotori et al., 2012). Recent findings by Kallenbach et al. (2016) have shown the production of extracellular humic material by bacteria within soil organic matter. There is no direct evidence that the production of humic-like FDOM in freshwaters is the result of bacterial processing. However, Elliott et al. (2006) attributed the presence of this FOM in laboratory samples to stress as opposed to a

Abbreviations: OM, organic matter; DOM, dissolved organic matter; EEM, excitation-emission matrix; FOM, fluorescent organic matter; FDOM, fluorescent dissolved organic matter; QSU, quinine sulphate units; PARAFAC, parallel factor analysis; OD, optical density; *E. coli*, *Escherichia coli*; *B. subtilis*, *Bacillus subtilis*; *P. aeruginosa*, *Pseudomonas aeruginosa*.

* Corresponding author.
E-mail address: darren.reynolds@uwe.ac.uk (D.M. Reynolds).

http://dx.doi.org/10.1016/j.watres.2017.08.040

function that may inherently occur within aquatic systems. What is clear from the literature is that a more detailed understanding of microbial/OM interactions in freshwater systems is needed.

Autochthonous and allochthonous FDOM can be associated with protein-like fluorescence ($\lambda_{ex}/\lambda_{em}$ 230–280/330–360 nm) specifically referred to as Peak T, $\lambda_{ex}/\lambda_{em}$ 275/340 nm, (tryptophan-like) and Peak A_T, $\lambda_{ex}/\lambda_{em}$ 230/305 nm, (tyrosine-like) (Coble et al., 2014). This protein-like FDOM is attributed and assumed to be of microbial origin (Cammack et al., 2004; Coble et al., 2014; Hambly et al., 2015; Smith et al., 2004). Recent literature suggests that Peak T fluorescence may act as a surrogate for microbial and bacterial activity (Baker et al., 2015; Cumberland et al., 2012), as first highlighted by Hudson et al. (2008). Recent surface freshwater research has also attempted to use Peak T fluorescence to determine enumeration of specific species. For example, Baker et al. (2015) observed a log correlation R = 0.74 across a 7-log range in *Escherichia coli* enumeration for sewage impacted rivers. Using Peak T fluorescence to infer microbial enumeration, and activity, has been further suggested for groundwater systems, where there is little background fluorescence interference (Sorensen et al., 2016, 2015). Sorensen et al. (2015) investigated low levels of microbial contamination in drinking water supplies, reporting linear correlations, R^2 = 0.57 from < 2 to 700 cfu 100 ml^{-1}. Although relationships have been demonstrated for protein-like fluorescence and the presence of bacteria in freshwater systems, the research reported thus far does not take into account the implication and impact of microbial activity at an individual species level.

The study aim was to further our understanding of the role aquatic microbes play in the production of both protein-like and humic-like FOM in freshwaters. For this, we focus on the development of FOM in a model system using a simplified microbial community, thus removing the background complexities observed in environmental samples. Using this approach, we also determine the intracellular and extracellular fluorescence signatures of common freshwater bacterial species.

2. Methods

2.1. Bacterial species

Three bacterial species were cultured for analysis; *Escherichia coli* (ATCC 10536) was used as its presence in freshwaters can indicate sewage contamination (Sigee, 2004); *Bacillus subtilis* (ATCC 6633) was used as it is a ubiquitous soil bacterium (Graumann, 2007) that may be transferred into freshwater systems; and *Pseudomonas aeruginosa* (NCIMB 8295) as it is ubiquitous in freshwater systems (Elliott et al., 2006; Sigee, 2004).

2.2. Media

A non-fluorescent minimal media was developed to promote growth within our model system whilst excluding the presence of proteinaceous material. The basal medium consisted of a final concentration of 0.2% v/v glucose solution, as the sole carbon source, and a solution containing a source of phosphate, nitrogen, sodium and magnesium. The basal medium was adopted from the ATCC® medium 778 Davis and Mingioli minimal medium (Davis and Mingioli, 1950), but without the addition of amino acids and agar. All elements of the basal medium were filter sterilised using a Minisart® 0.2 μm cellulose filter (Sartorius Stedim Biotech, Germany). $CaCl_2$ (final concentration 0.035% v/v) and a trace element solution (final concentration 0.1% v/v), obtained from Kragelund and Nybroe (1994), were added to the sterile basal medium prior to inoculation. These chemicals were sterilised by autoclaving at 121 °C for 15 min.

2.3. Fluorescence measurements

Fluorescence excitation-emission matrices (EEMs) were collected using an Aqualog® (Horiba Ltd., Japan). Samples were not filtered prior to fluorescence spectroscopic analysis (except for bacterial supernatant samples, section 2.6). The scan parameters employed were; excitation wavelengths from 200 to 500 nm via 1 nm steps, and emission wavelengths of 247.88–829.85 nm in 1.16 nm steps using an integration time of 500 ms. A micro quartz cuvette (1400 μL) with a 10 mm path-length was used throughout. Spectra were blank subtracted, corrected for inner filter effects (for both excitation and emission wavelengths) and first and second order Rayleigh Scattering masked (±10 nm at $\lambda_{ex} = \lambda_{em}$ and $2\lambda_{ex} = \lambda_{em}$) (Coble et al., 2014; McKnight et al., 2001). Fluorescence data is reported in quinine sulphate units (QSU), determined from normalising data to the fluorescence from 1 μg L^{-1} quinine sulphate at λ_{ex} = 347.5 nm and λ_{em} = 450 nm (Kramer and Herndl, 2004; Mostofa et al., 2013; Shimotori et al., 2012, 2009). Instrument validation was undertaken daily with a quinine sulphate standard (Starna Cells, USA), with CV being < 3% (n = 5) in all events.

2.4. Fluorescence data analysis

A custom script, written in Python™ (Python Software Foundation), was used to convert the data into QSU and create the EEM maps. The script crops the data window to λ_{ex} 240–490 nm, λ_{em} 250–550 nm to allow for the analysis of the UV spectra, the area of interest within FDOM work. Data λ_{ex} < 240 nm was discounted due to the data quality produced by the Aqualog® caused by the signal to noise ratio. The custom script was then used to undertake peak picking for specific fluorescence peaks. Some of the peak picked data was normalised to the maxima to provide a clear visual representation of the fluorescence development over time. The EEM data was also investigated by employing parallel factor (PARAFAC) analysis (Stedmon and Bro, 2008) in Solo (Eigenvector Research Inc., WA, USA) software, in conjunction with the MATLAB® PLS-Toolbox (Mathworks, USA).

2.5. Bacterial growth curves

Growth curves (n = 9 i.e. nine independent replicates) of each bacterial species were undertaken by inoculating 150 mL of the sterile medium (section 2.2) from a fresh overnight plate culture (< 24 h) and incubating the samples at 37 °C, shaking at 150 rpm. Aliquots were collected every 30 min for fluorescence measurements (section 2.3) and optical density (OD) measurements at 600 nm (WPA Spectrawave S1200, Biochrom, UK); OD, attenuation determined by absorbance and scattering, is routinely used to represent the relative increase in cell numbers within a sample when monitoring bacterial growth (Hall et al., 2014). OD data was also normalised to the maxima.

2.6. Bacterial culture analysis

Media was inoculated, from a fresh overnight plate culture (< 24 h), with each of the bacterial species and incubated overnight at 37 °C, shaking at 150 rpm throughout. Overnight cultures were centrifuged at 5000×*g* for 5 min (Allegra X-30R, Beckman Coulter™, USA) to form a bacterial pellet. The supernatant was pipetted off and filtered using a Minisart® 0.2 μm cellulose filter (Sartorius Stedim Biotech, Germany) to guarantee all cells were removed. The pellet was resuspended and washed 3 times in 5 mL of ¼ strength Ringer solution (Oxoid Ltd., UK) to ensure that any supernatant or media was no longer present. To physically lyse the cells, a 1 mL aliquot of the resuspended cells was sonicated

(Ultrasonic Processor XL 2020, Misonix Inc., US) in three 10 s pulses at a fixed frequency of 20 KHz, not exceeding 40% amplitude, and kept over ice throughout (Doron, 2009). Physical lysis was undertaken to ensure no extra chemicals were added to the cells that may alter the fluorescence properties of the sample (nine independent replicates). An endospore suspension for *B. subtilis* was prepared as described by Lawrence and Palombo (2009). To check for the presence of endospores and the removal of vegetative cells, an endospore stain was conducted using the Schaeffer-Fulton method (Schaeffer and Fulton, 1933).

3. Results and discussion

Filtering of samples was not performed prior to spectroscopic analysis to maintain sample integrity (Baker et al., 2007), since the focus of this study is on *in situ* bacterial production of FOM in a model system. Each individual bacterial species exhibited unique fluorescing signatures. Some FOM, specifically Peak T, was dominant in all samples exhibiting high fluorescence intensities. This limited the application of PARAFAC analysis, whereby no robust model, CORCONDIA > 90% (Bro and Kiers, 2003), that adequately

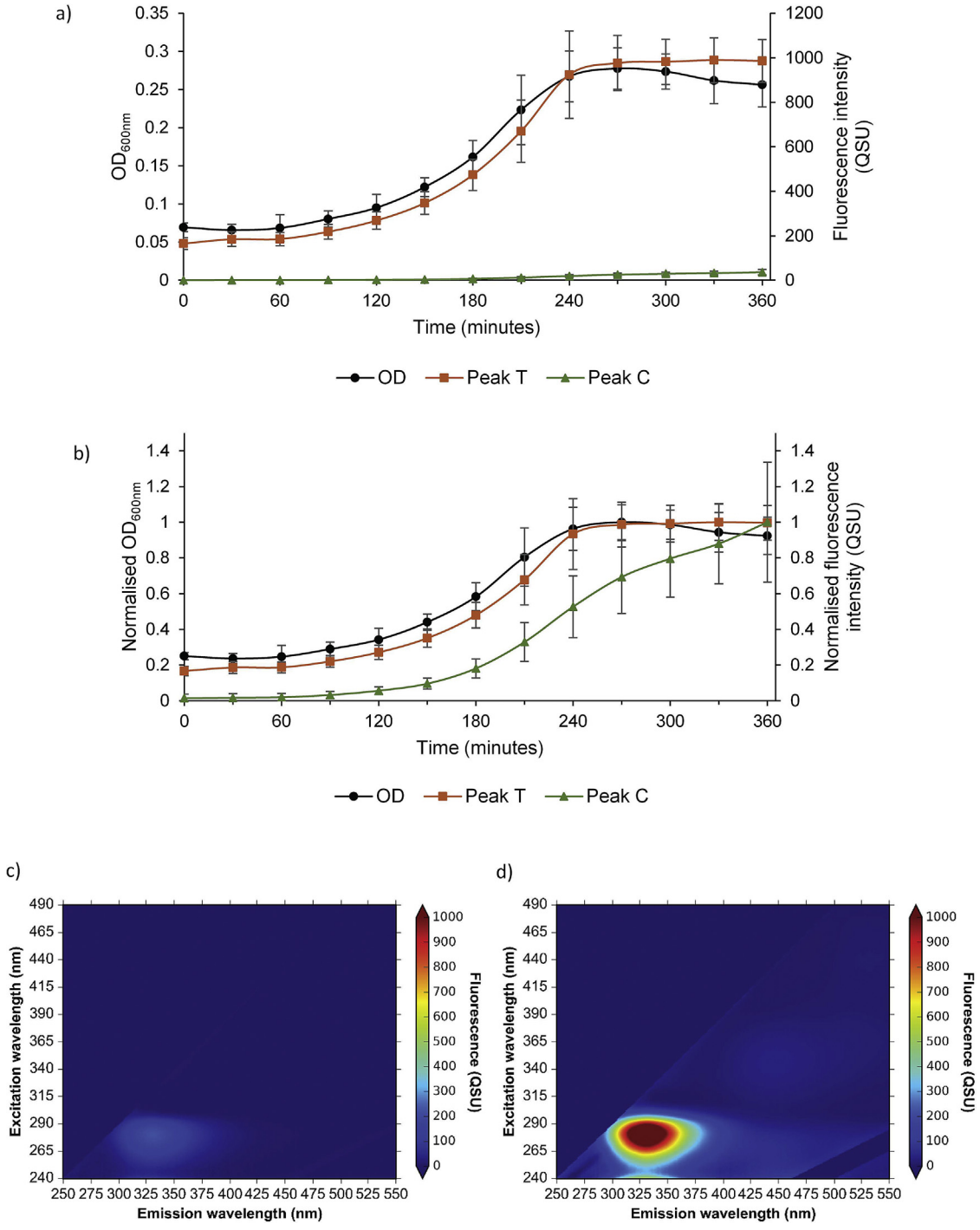

Fig. 1. Fluorescence and optical density (OD_{600nm}) data for *Escherichia coli* growth curve, showing: a) optical density and fluorescence (QSU, 1 QSU = 1 μg^{-1} quinine sulphate) ± 1 standard deviation (n = 9); b) optical density and fluorescence data normalised to the maximum value ±1 standard deviation (n = 9); c) excitation-emission matrix at time zero; and d) excitation-emission matrix at 360 min.

explained the dataset could be identified. Subsequently, peak picking (Asmala et al., 2016), an established method for spectral analysis, was applied to peaks identified within the EEMs.

3.1. Bacterial growth curves

3.1.1. Escherichia coli

The *E. coli* growth curve is shown in Fig. 1, whereby Peak T is the dominant fluorescence peak and is present at time zero, upon initial addition of the *E. coli* cells (Dartnell et al., 2013; Sohn et al., 2009). During the growth curve, the intensity of Peak T increases in line with the optical density (OD) of the sample (Fig. 1). During the exponential stage (growth phase after acclimatisation; Hogg, 2005) there is a log increase in the intensity of Peak T fluorescence. This, alongside the increase in OD, leads to a significant strong correlation between Peak T and OD, $R^2 = 0.9821$ ($p < 0.001$). This suggests that Peak T fluorescence intensity can be attributed to an increase in *E. coli* population size, in accordance with previous studies (Baker et al., 2015; Cumberland et al., 2012; Dartnell et al., 2013; Deepa and Ganesh, 2017; Sohn et al., 2009). However, as tryptophan is an essential amino acid, necessary for protein formation during growth and other metabolic pathways, it will be produced as a result of cell multiplication and metabolic processing (Coble et al., 2014; Hogg, 2005). As such, Peak T fluorescence can also be attributed to *E. coli* cell activity.

Fig. 1 shows that Peak C also develops during the exponential phase of the growth curve, exhibiting a lag in relation to the OD. The intensity of Peak C continues to increase even during stationary phase, in which cell deaths are equal to newly formed cells (Elliott et al., 2006; Hogg, 2005). Nevertheless a positive correlation between OD and Peak C fluorescence intensity is identified, $R^2 = 0.8624$ ($p < 0.001$), supporting the association of Peak C with bacterial numbers. However, the observed lag in conjunction with the continued increase in fluorescence intensity during the stationary phase strongly supports the idea that metabolic activity, and not bacterial numbers *per se*, may be the main driver for the creation and production of Peak C fluorophores. Notably, the observed maximum fluorescence intensity of Peak C is a factor of 10 lower than Peak T (Fig. 1a). It can, therefore, be suggested that Peak C may be derived as a metabolic by-product or a secondary metabolite produced mainly during the stationary phase (Fig. 1b). Peak X (Table 1) is only present within the stationary phase, albeit at comparatively low fluorescence intensities (~ 30 QSU). The microbial production of Peaks C and X demonstrates the ability of *E. coli* to rapidly produce (within 8 h), *in situ*, FOM associated with allochthonous high molecular weight FOM.

3.1.2. Bacillus subtilis

Fig. 2 highlights Peak T as the dominant fluorescence peak within the *B. subtilis* growth curve. Peak T intensity increases by an order of magnitude throughout the growth curve, in line with the increased OD (Fig. 2), demonstrating a strong significant correlation, $R^2 = 0.9879$ ($p < 0.005$). However, as Peak T fluorescence intensity increases during what appears to be early stationary phase (Fig. 2), it could be suggested that these fluorophores are produced by metabolically active cells. This emphasises the use of Peak T as an indicator of microbial activity rather than being attributed to cell enumeration, despite the significant correlation identified. The production of Peak T within the stationary phase (Fig. 2) could also be related to *B. subtilis* sporulation, demonstrated by the high intensity Peak T fluorescence obtained bacterial endospores analysed alone (Fig. 3). This suggests that some of the fluorophores attributable to Peak T fluorescence are related to structural proteins since endospores are not metabolically active, although this is species specific.

Within the *B. subtilis* growth curve, Peak C demonstrates a sudden rise, at 360 min, prior to OD and Peak T development (Fig. 2), with a strong positive correlation between Peak C fluorescence intensity and the OD being identified, $R^2 = 0.9465$ ($p < 0.005$). This further challenges our current understanding of Peak C being attributed to terrestrial allochthonous material (Coble et al., 2014). Smith et al. (2004) suggested that the Peak C fluorescence, identified in the presence of *Bacillus* sp., may be related to the fluorescence of endospores. However, Fig. 3 demonstrates the endospore suspension obtained from *B. subtilis* within our study as having high Peak T, and low Peak C, fluorescence intensity.

Florescence Peaks M and A_M are produced and observed at very low intensities within the early stationary phase of the growth curve. A possible explanation of this observation is the result of the biodegradation of OM responsible for Peak C fluorescence, a process that has been noted in the literature (Coble et al., 2014). Alternatively, this could indicate that Peaks M and A_M can be produced directly, *in situ*, by bacteria, as has been suggested to occur within marine environments (Coble, 1996; Shimotori et al., 2009).

3.1.3. Pseudomonas aeruginosa

Peak T is ubiquitous within the *P. aeruginosa* growth curve (Fig. 4), increasing by an order of magnitude within the exponential phase. A relatively weaker correlation, $R^2 = 0.7601$ ($p < 0.005$), is identified between Peak T and the OD, likely to be caused by the upregulation of Peak T independent of cell number which can be seen at 330 min, in the late exponential, early stationary phase (Fig. 4). Prior to this, the Peak T fluorescence development tracks the OD ($R^2 = 0.9674$, $p < 0.05$). One possible explanation for this sudden increase in Peak T fluorescence intensity is the production of exotoxin A; exotoxin A is an iron-scavenging enzyme that is produced by *P. aeruginosa* upon entry into stationary phase (Lory, 1986; Somerville et al., 1999). Previous studies have shown how Exotoxin A can be used to determine protein activity, by assessing tryptophan (Peak T) fluorescence quenching upon binding of NAD+ to the enzyme active site (Beattie and Merrill, 1999, 1996; Beattie et al., 1996). Therefore, the observed subsequent sudden

Table 1
Identification of the fluorescence peaks, generated via microbial processing, during bacterial growth curves and culturing experiments.

Named Fluorescence Peak	$\lambda_{ex}/\lambda_{em}$ (nm)	Peak Association
T	280/300–380	Attributed to amino acid (tryptophan) presence.
C	350/400–480	Common aquatic FDOM associated with humic substances.
A_C	250/400–460	Observed alongside Peak C but considered to be separate due to varying ratios between the two peaks. Excites in the UVC region.
C+	410/450–500	Typically associated with soils and freshwaters and attributed to terrestrially sourced CDOM.
M	240/370–430	Originally observed in marine environments but now associated with recent microbial activity in aquatic systems.
A_M	300/370–430	Associated with Peak M due to simultaneous occurrence, excites in the UVC region
X	440/510–550	Previously uncharacterised – likely to be a high molecular weight fluorophore

Nomenclature and association derived from Coble et al. (2014).

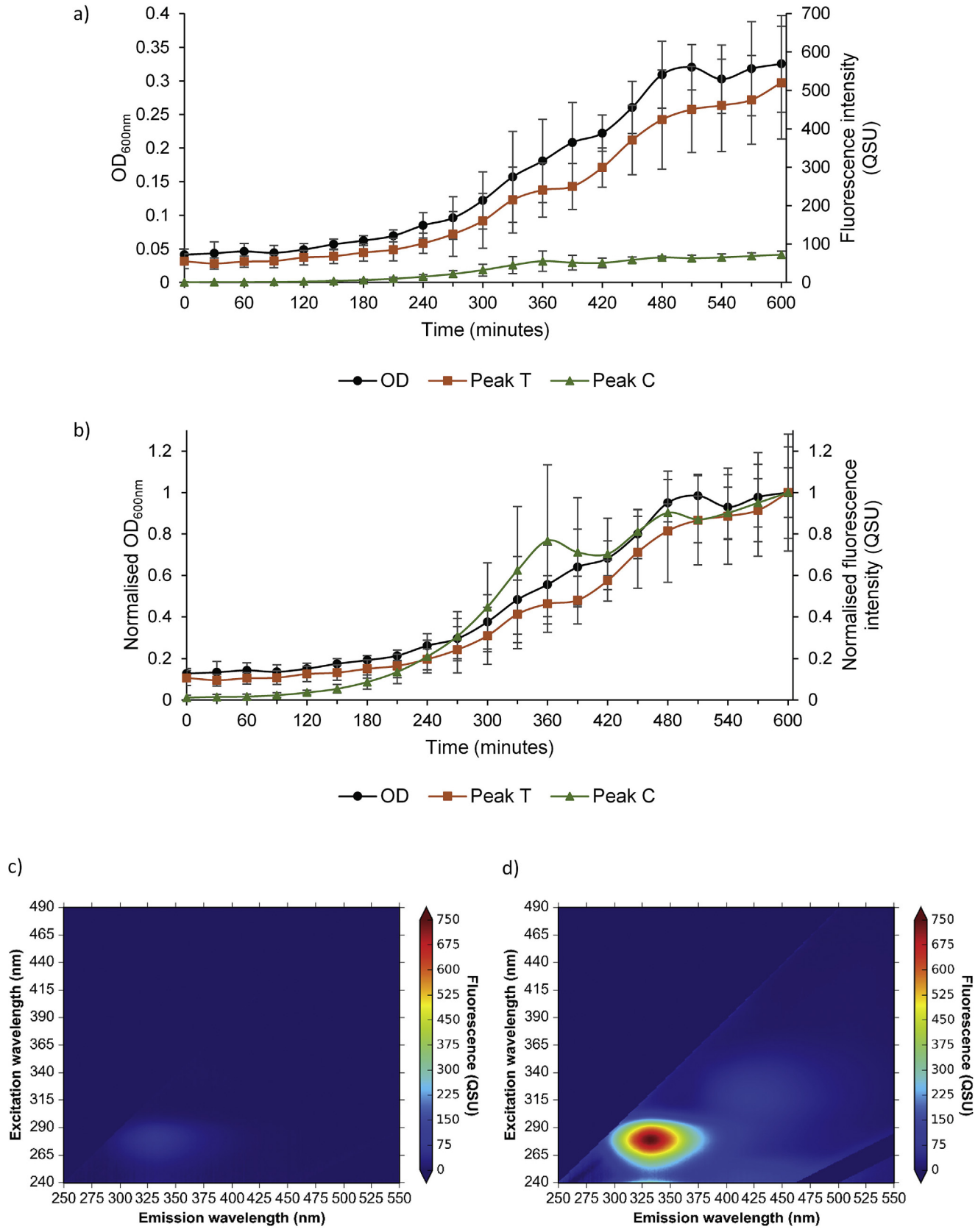

Fig. 2. Fluorescence and optical density (OD_{600nm}) data for *Bacillus subtilis* growth curve, showing: a) optical density and fluorescence (QSU, 1 QSU = 1 μg^{-1} quinine sulphate) ± 1 standard deviation (n = 9); b) optical density and fluorescence data normalised to the maximum value ± 1 standard deviation (n = 9); c) excitation-emission matrix at time zero; and d) excitation-emission matrix at 360 min.

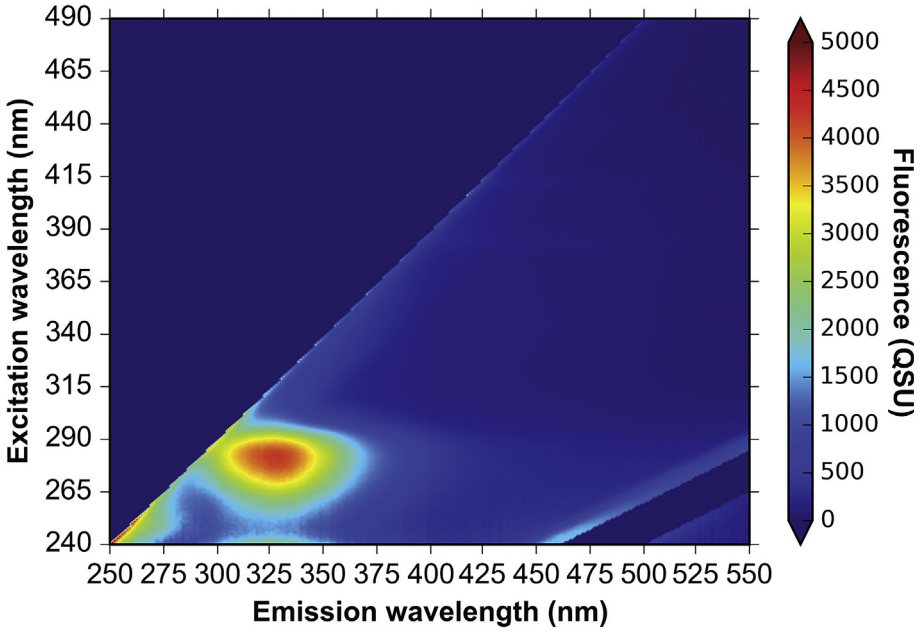

Fig. 3. Fluorescence excitation-emission matrix of *Bacillus subtilis* endospores (QSU, 1 QSU = 1 μg^{-1} quinine sulphate).

decline in Peak T fluorescence intensity at 450 min may be as a result of this quenching phenomena (Fig. 4).

P. aeruginosa has the most complex EEM spectra of the species analysed within this study (Dartnell et al., 2013; Elliott et al., 2006; Smith et al., 2004), with Peaks T, C and A_C all immediately identified upon inoculation and during the lag phase (a period of acclimatisation; Hogg, 2005). The occurrence of Peaks C and A_C at inoculation suggests it is likely that this FDOM is intracellular and produced within the cells during the initial overnight incubation; likely to be structural or functional proteins produced via microbial metabolic pathways, or potentially intracellular metabolic by-products. These peaks increase log-fold throughout the growth curve, with both Peaks C and A_C being correlated with, despite a lag in relation to, the OD; $R^2 = 0.7024$ ($p < 0.005$) and $R^2 = 0.7146$ ($p < 0.005$) respectively. The data indicates upregulation of these peaks during late exponential phase and stationary phase, suggesting that these peaks are a result of metabolic activity.

Peak C+ develops rapidly and to a high intensity during the stationary phase of *P. aeruginosa* growth (Fig. 4) and this fluorescent peak is associated with the siderophore pyoverdine (Dartnell et al., 2013; Wasserman, 1965). Pyoverdine is an extracellular iron-scavenging metabolite produced by *P. aeruginosa* and is associated with microbial virulence (da Silva and de Almeida, 2006). The fluorescence intensity of this high molecular weight OM within the *P. aeruginosa* growth curve, suggests that this Peak C+ fluorescence could be derived from the building and exporting of pyoverdine. Peak C+ has been seen in freshwater environments and is currently attributed to terrestrial allochthonous OM. However, our work proves that microbial compounds produced *in situ* (akin to autochthonous material) may contribute to this Peak C+ fluorescence. As such, Peak C+ may act as a biomarker for an active *P. aeruginosa* community, although further investigation within natural environmental systems is required.

3.2. Overnight culturing of bacterial species

From the microbial growth curve data it has been shown that all the fluorescence peaks identified (Table 1) are microbially produced *in situ*, with variations in peak occurrence between bacterial species. To further investigate the microbial source and origin of the OM, overnight cultures of each species were analysed to determine the presence of FDOM in the supernatant, OM within resuspended cells and lysed cells (see section 2.6). This provides a preliminary understanding of where the observed fluorescence is located post FOM production.

Peak T fluorescence is the only ubiquitous fluorescence peak common to all bacterial species cultured overnight (Table 2). This shows that the intensity of Peak T alone cannot be used to determine bacterial enumeration, especially in systems with complex microbial communities, but supports its use as a measure of microbial activity. The highest intensity for Peak T fluorescence is seen within the resuspended and lysed cells, suggesting that the majority of this material is intracellular, either as structural or functional biological molecules. This explains the presence of Peak T upon inoculation and the increase in intensity with cell multiplication (section 3.1). However, the presence of Peak T in the supernatant also indicates that some of this fluorescence signal is derived from extracellular FDOM, although the amount is species specific, varying from 5 to 25%. This material is possibly associated with metabolic by-products or extracellular proteins (many of which may be functional) that have been exported from the cells.

Peak C fluorescence was observed in both the supernatant and cell lysis fractions for *E. coli* and *B. subtilis* (shown in Table 2). Within the supernatant fraction, this can be attributed to either (1) material exported out of the cell (either functional proteins or metabolic by-products) or (2) cellular debris as a result of cell lysis during growth (prior to sampling). However, Peak C fluorescence may also be derived from compounds that fluoresce when not bound within a cell where the fluorescence signal is quenched or inhibited. Peak C is present in all elements of the *P. aeruginosa* culture, indicating that for this species this FOM is likely to be a functional protein that can be exported to become extracellular DOM. Collectively, this data indicates that the fluorophores that give rise to Peak C fluorescence may be derived from either cell lysis (Elliott et al., 2006) or attributed to microbial metabolic by-products or extracellular proteins (Guillemette and del Giorgio,

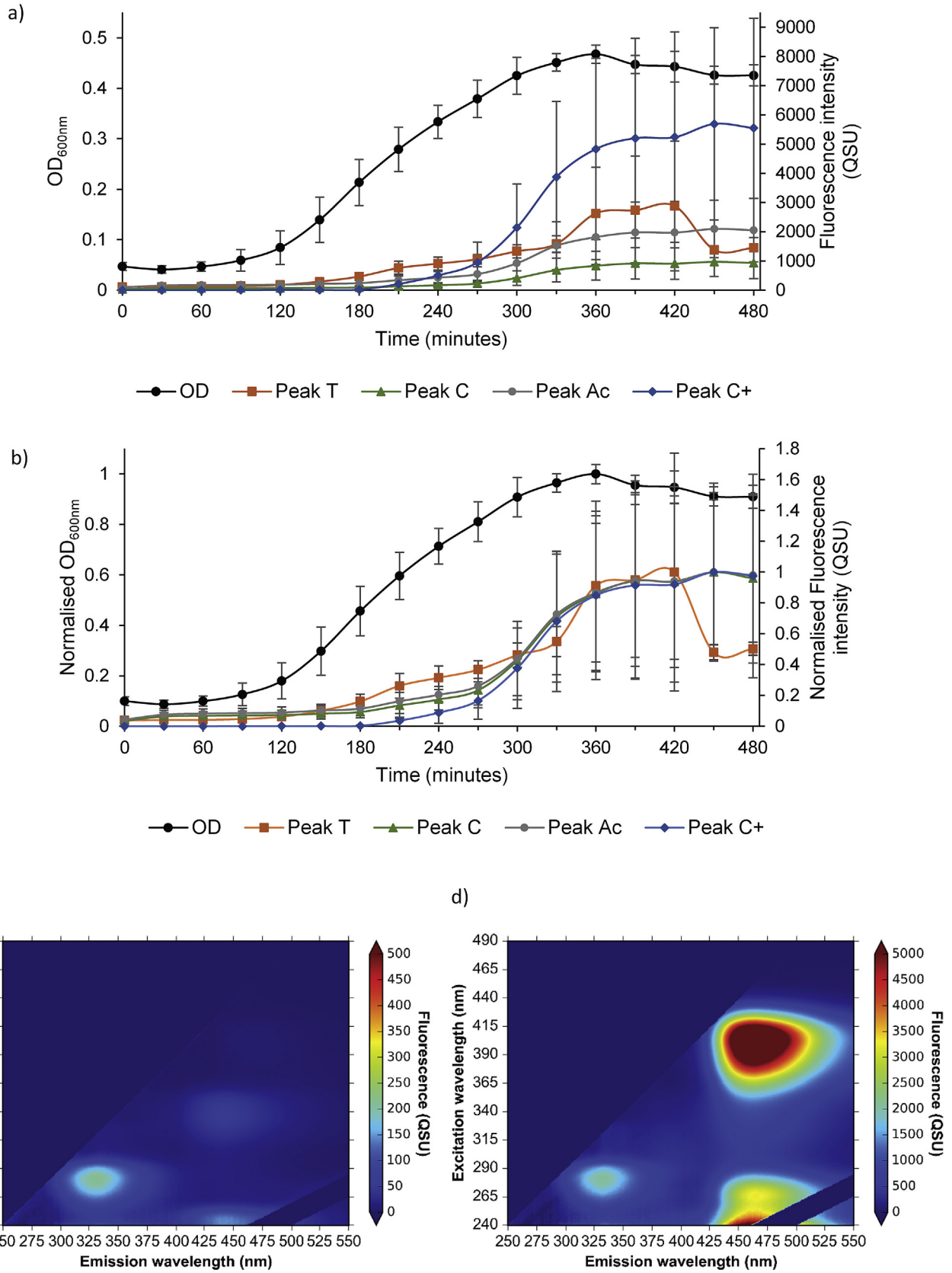

Fig. 4. Fluorescence and optical density (OD_{600nm}) data for *Pseudomonas aeruginosa* growth curve, showing: a) optical density and fluorescence (QSU, 1 QSU = 1 μg^{-1} quinine sulphate) ± 1 standard deviation (n = 9); b) optical density and fluorescence data normalised to the maximum value ± 1 standard deviation (n = 9); c) excitation-emission matrix at time zero; and d) excitation-emission matrix at 360 min.

Table 2
Identified peaks generated through microbial processing in the different fractions of the overnight cultures.

Named fluorescence Peak	*Escherichia coli*			*Bacillus subtilis*			*Pseudomonas aeruginosa*		
	Supernatant	Resuspended cells	Lysed cells	Supernatant	Resuspended cells	Lysed cells	Supernatant	Resuspended cells	Lysed cells
T	*	*	*	*	*	*	*	*	*
C	*		*	*		*	*	*	*
A_C	*						*	*	*
C+	*						*	*	*
M				*			*	*	*
A_M							*		
X	*			*			*		

* Indicates presence of fluorescence peak in sample fraction
Shaded regions indicate absence of fluorescence peak in sample fraction.

2012; Shimotori et al., 2009).

Peak A_C is also seen in all fractions of the *P. aeruginosa* culture and in the *E. coli* supernatant. This suggests that this FOM may be a function of a particular biological molecule(s) common to both *P. aeruginosa* and *E. coli*. Peak C+ was also observed in the *E. coli* supernatant, but at far lower levels compared to *P. aeruginosa*. The high fluorescence intensity of Peak C+ in all elements of the *P. aeruginosa* culture, and the association of this peak with pyoverdine (section 3.1), demonstrates the possible intracellular production and extracellular output of this FOM. Peak M is also observed within all fractions of the *P. aeruginosa* culture, but is only present in the *B. subtilis* supernatant. This suggests it may have a similar species specific function like Peak A_C, or be derived via the biodegradation of Peak C (Coble, 1996; Coble et al., 2014). As the fluorophores attributed to these peaks (T, C, A_C, C+ and M) can be exported from cells and are identified in cells, lysed cell material and supernatant, they are unlikely to represent cellular structural material. Whilst Peak M is identified in relation to both *B. subtilis* and *P. aeruginosa*, Peak A_M is only observed in the supernatant of *P. aeruginosa*, although these peaks have been seen to occur simultaneously in the environment (Coble et al., 2014). Therefore, Peak A_M could be attributed to either species specific proteins or bacterial metabolic by-products. From this, Peaks M and A_M must be considered separately as they are likely derived from different fluorophores.

Although noted in previous life science research (Smith et al., 2004), Peak X (Table 1) has not yet been reported or characterised in aquatic FDOM. However, it is identified at low fluorescence intensities in the supernatant for all species analysed within this study (Table 2). Based on our current understanding of fluorophore structures (Lakowicz, 2006), it is likely that this peak is derived from high molecular weight compounds (characterised as humic and fulvic acids), that would usually be attributed to terrestrial allochthonous material in the environment. Nevertheless, as it is only seen in the supernatant it is likely to be secreted from the cells and not related to cellular structure.

3.3. Future work

The protein-like fluorescence region has been the focus for research investigating microbially-derived, autochthonous dissolved organic matter. The data from this study furthers our current understanding of bacteria-OM interactions and highlights the importance of metabolic activity and bacterial population growth for driving the dynamics of microbially produced FOM and FDOM, albeit within a model system. Furthermore the bacterially derived FOM, exhibits the same fluorescent features as DOM observed in natural systems which has previously been attributed as being allochthonous in origin. This work raises questions regarding the extent to which bacterially produced FOM occurs in freshwater systems and the role that any production plays in the biogeochemical cycling throughout the hydrological continuum. Finally, further work should also explore the metabolic pathways responsible for the microbial production and transformation of FOM and FDOM, including optical regions that are limited by the instrumentation used in this study (e.g. λ_{ex} 200–240 nm).

4. Conclusions

- Peak T fluorescence correlates strongly with an increasing bacterial population, but is dependent on microbial metabolic activity. As such, we suggest Peak T as a proxy for microbial activity rather than enumeration.
- This work provides direct evidence that Peak T fluorescence is ubiquitous within the bacterial cells analysed within this study. It is mainly identified as intracellular material but also exists as extracellular FDOM.

- Peak C is produced *in situ* during the exponential stage of bacterial growth curves, likely to be produced via microbial metabolic pathways during microbial growth, or derived from metabolic by-products.
- FOM peaks can be partially attributed to microbial metabolic processing, through the production of biological molecules, some of which is exported from the cell. These FOM peaks include regions that are currently associated with allochthonous high molecular weight compounds, categorised as humic and fulvic acids.
- FOM production varies between bacterial species, with this work providing definitive evidence that freshwater FOM can be produced by microbes *in situ*. It can therefore be of autochthonous origin, altering and enhancing our understanding regarding the complexity of environmental OM origin.
- Extracellular organic matter contributes to FDOM and, as such, is available as an organic matter source for microorganisms, playing an essential role in nutrient exchange and global carbon cycling.

Acknowledgements

This work was funded by the Natural Environmental Research Council (NERC) and Chelsea Technologies Group Ltd as a CASE Award (NE/K007572/1).

References

Asmala, E., Kaartokallio, H., Carstensen, J., Thomas, D.N., 2016. Variation in riverine inputs affect dissolved organic matter characteristics throughout the estuarine gradient. Front. Mar. Sci. 2, 1–15. http://dx.doi.org/10.3389/fmars.2015.00125.

Baker, A., 2005. Thermal fluorescence quenching properties of dissolved organic matter. Water Res. 39, 4405–4412. http://dx.doi.org/10.1016/j.watres.2005.08.023.

Baker, A., Cumberland, S.A., Bradley, C., Buckley, C., Bridgeman, J., 2015. To what extent can portable fluorescence spectroscopy be used in the real-time assessment of microbial water quality? Sci. Total Environ. 532, 14–19. http://dx.doi.org/10.1016/j.scitotenv.2015.05.114.

Baker, A., Elliott, S., Lead, J.R., 2007. Effects of filtration and pH perturbation on freshwater organic matter fluorescence. Chemosphere 67, 2035–2043. http://dx.doi.org/10.1016/j.chemosphere.2006.11.024.

Beattie, B.K., Merrill, A.R., 1999. A fluorescence investigation of the active site of *Pseudomonas aeruginosa* exotoxin a. J. Biol. Chem. 274, 15646–15654. http://dx.doi.org/10.1074/jbc.274.22.15646.

Beattie, B.K., Merrill, A.R., 1996. *In vitro* enzyme activation and folded stability of *Pseudomonas aeruginosa* exotoxin a and its C-Terminal peptide. Biochemistry 35, 9042–9051. http://dx.doi.org/10.1021/bi960396k.

Beattie, B.K., Prentice, G.A., Merrill, A.R., 1996. Investigation into the catalytic role for the tryptophan residues within domain III of *Pseudomonas aeruginosa* exotoxin a. Biochemistry 35, 15134–15142. http://dx.doi.org/10.1021/bi961985t.

Bieroza, M.Z., Heathwaite, A.L., 2016. Unravelling organic matter and nutrient biogeochemistry in groundwater-fed rivers under baseflow conditions: uncertainty in *in situ* high-frequency analysis. Sci. Total Environ. http://dx.doi.org/10.1016/j.scitotenv.2016.02.046.

Bridgeman, J., Baker, A., Brown, D., Boxall, J.B., 2015. Portable LED fluorescence instrumentation for the rapid assessment of potable water quality. Sci. Total Environ. 524–525, 338–346. http://dx.doi.org/10.1016/j.scitotenv.2015.04.050.

Bro, R., Kiers, H.A.L., 2003. A new efficient method for determining the number of components in PARAFAC models. J. Chemom. 17, 274–286. http://dx.doi.org/10.1002/cem.801.

Cammack, W.K.L., Kalff, J., Prairie, Y.T., Smith, E.M., 2004. Fluorescent dissolved organic matter in lakes: relationships with heterotrophic metabolism. Limnol. Oceanogr. 49, 2034–2045. http://dx.doi.org/10.4319/lo.2004.49.6.2034.

Coble, P.G., 1996. Characterization of marine and terrestrial DOM in seawater using excitation-emission matrix spectroscopy. Mar. Chem. 51, 325–346. http://dx.doi.org/10.1016/0304-4203(95)00062-3.

Coble, P.G., Lead, J., Baker, A., Reynolds, D.M., Spencer, R.G.M., 2014. Aquatic Organic Matter Fluorescence. Cambridge University Press.

Cooper, K.J., Whitaker, F.F., Anesio, A.M., Naish, M., Reynolds, D.M., Evans, E.L., 2016. Dissolved organic carbon transformations and microbial community response to variations in recharge waters in a shallow carbonate aquifer. Biogeochemistry 129, 215–234. http://dx.doi.org/10.1007/s10533-016-0226-4.

Cumberland, S., Bridgeman, J., Baker, A., Sterling, M., Ward, D., 2012. Fluorescence spectroscopy as a tool for determining microbial quality in potable water applications. Environ. Technol. 33, 687–693. http://dx.doi.org/10.1080/09593330.2011.588401.

da Silva, G.A., de Almeida, E.A., 2006. Production of yellow-green fluorescent pigment by *Pseudomonas fluorescens*. Braz. Arch. Biol. Technol. 49, 411–419. http://dx.doi.org/10.1590/S1516-89132006000400009.

Dartnell, L.R., Roberts, T.A., Moore, G., Ward, J.M., Muller, J.P., 2013. Fluorescence characterization of clinically-important bacteria. PLoS One 8, 1–13. http://dx.doi.org/10.1371/journal.pone.0075270.

Davis, B.D., Mingioli, E.S., 1950. Mutants of Escherichia coli requiring methionine or vitamin B12. J. Bacteriol. 60, 17–28.

Deepa, N., Ganesh, A.B., 2017. Minimally invasive fluorescence sensing system for real-time monitoring of bacterial cell cultivation. Instrum. Sci. Technol. 45, 85–100. http://dx.doi.org/10.1080/10739149.2016.1198372.

Doron, N., 2009. Sonication of Bacterial Samples [WWW Document]. In: http://wolfson.huji.ac.il/expression/procedures/cell_lysis/Sonication_of_bacterial_samples.html.

Elliott, S., Lead, J.R., Baker, A., 2006. Characterisation of the fluorescence from freshwater, planktonic bacteria. Water Res. 40, 2075–2083. http://dx.doi.org/10.1016/j.watres.2006.03.017.

Graumann, P. (Ed.), 2007. Bacillus: Cellular and Molecular Biology. Caister Academic Press.

Guillemette, F., del Giorgio, P.A., 2012. Simultaneous consumption and production of fluorescent dissolved organic matter by lake bacterioplankton. Environ. Microbiol. 14, 1432–1443. http://dx.doi.org/10.1111/j.1462-2920.2012.02728.x.

Hall, B.G., Acar, H., Nandipati, A., Barlow, M., 2014. Growth rates made easy. Mol. Biol. Evol. 31, 232–238. http://dx.doi.org/10.1093/molbev/mst187.

Hambly, A.C., Arvin, E., Pedersen, L.F., Pedersen, P.B., Seredyńska-Sobecka, B., Stedmon, C.A., 2015. Characterising organic matter in recirculating aquaculture systems with fluorescence EEM spectroscopy. Water Res. 83, 112–120. http://dx.doi.org/10.1016/j.watres.2015.06.037.

Hogg, S., 2005. Essential Microbiology. Wiley.

Hudson, N., Baker, A., Reynolds, D.M., 2007. Fluorescence analysis of dissolved organic matter in natural, waste and polluted water - a review. River Res. Appl. 23, 631–649. http://dx.doi.org/10.1002/rra.1005.

Hudson, N., Baker, A., Ward, D., Reynolds, D.M., Brunsdon, C., Carliell-Marquet, C., Browning, S., 2008. Can fluorescence spectrometry be used as a surrogate for the Biochemical Oxygen Demand (BOD) test in water quality assessment? An example from South West England. Sci. Total Environ. 391, 149–158. http://dx.doi.org/10.1016/j.scitotenv.2007.10.054.

Kallenbach, C.M., Frey, S.D., Grandy, A.S., 2016. Direct evidence for microbial-derived soil organic matter formation and its ecophysiological controls. Nat. Commun. 7, 1–10. http://dx.doi.org/10.1038/ncomms13630.

Kragelund, L., Nybroe, O., 1994. Culturability and expression of outer membrane proteins during carbon, nitrogen, or phosphorus starvation of *Pseudomonas fluorescens* DF57 and *Pseudomonas putida* DF14. Appl. Environ. Microbiol. 60, 2944–2948.

Kramer, G.D., Herndl, G.J., 2004. Photo- and bioreactivity of chromophoric dissolved organic matter produced by marine bacterioplankton. Aquat. Microb. Ecol. 36, 239–246.

Lakowicz, J.R., 2006. Principles of Fluorescence Spectroscopy, third ed. Springer. http://dx.doi.org/10.1007/978-0-387-46312-4.

Lawrence, H.A., Palombo, E.A., 2009. Activity of essential oils against *Bacillus subtilis* spores. J. Microbiol. Biotechnol. 19, 1590–1595. http://dx.doi.org/10.4014/jmb.0904.04016.

Lory, S., 1986. Effect of iron on accumulation of exotoxin a-specific mRNA in *Pseudomonas aeruginosa*. J. Bacteriol. 168, 1451–1456.

McKnight, D.M., Boyer, E.W., Westerhoff, P.K., Doran, P.T., Kulbe, T., Anderson, D.T., 2001. Spectroflourometric characterization of dissolved organic matter for indication of precursor organic material and aromaticity. Limnol. Oceanogr. 46, 38–48.

Mostofa, K.M.G., Yoshioka, T., Mottaleb, A., Vione, D., 2013. Photobiogeochemistry of Organic Matter: Principles and Practices in Water Environments. Springer.

Romera-Castillo, C., Sarmento, H., Alvarez-Salgado, X.A., Gasol, J.M., Marrasé, C., 2011. Net production and consumption of fluorescent colored dissolved organic matter by natural bacterial assemblages growing on marine phytoplankton exudates. Appl. Environ. Microbiol. 77, 7490–7498. http://dx.doi.org/10.1128/AEM.00200-11.

Schaeffer, A.B., Fulton, M.D., 1933. A simplified method of staining endospores. Sci. (80) 77, 194. http://dx.doi.org/10.1126/science.77.1990.194.

Shimotori, K., Omori, Y., Hama, T., 2009. Bacterial production of marine humic-like fluorescent dissolved organic matter and its biogeochemical importance. Aquat. Microb. Ecol. 58, 55–66. http://dx.doi.org/10.3354/ame01350.

Shimotori, K., Watanabe, K., Hama, T., 2012. Fluorescence characteristics of humic-like fluorescent dissolved organic matter produced by various taxa of marine bacteria. Aquat. Microb. Ecol. 65, 249–260. http://dx.doi.org/10.3354/ame01552.

Sigee, D.C., 2004. Freshwater Microbiology. Wiley.

Smith, C.B., Anderson, J.E., Webb, S.R., 2004. Detection of *Bacillus* endospores using total luminescence spectroscopy. Spectrochim. Acta - Part A Mol. Biomol. Spectrosc. 60, 2517–2521. http://dx.doi.org/10.1016/j.saa.2003.12.030.

Sohn, M., Himmelsbach, D.S., Barton, F.E.I., Fedorka-Cray, P.J., 2009. Fluorescence spectroscopy for rapid detection and classification of bacterial pathogens. Appl. Spectrosc. 63, 1251–1255.

Somerville, G., Mikoryak, C.A., Reitzer, L., Mikoryak, C.A.N.N., 1999. Physiological characterization of *Pseudomonas aeruginosa* during exotoxin a synthesis: glutamate, iron limitation, and aconitase activity. J. Bacteriol. 181, 1072–1078.

Sorensen, J.P.R., Lapworth, D.J., Marchant, B.P., Nkhuwa, D.C.W., Pedley, S.,

Stuart, M.E., Bell, R.A., Chirwa, M., Kabika, J., Liemisa, M., Chibesa, M., 2015. *In situ* tryptophan-like fluorescence: a real-time indicator of faecal contamination in drinking water supplies. Water Res. 81, 38–46. http://dx.doi.org/10.1016/j.watres.2015.05.035.

Sorensen, J.P.R., Sadhu, A., Sampath, G., Sugden, S., Dutta Gupta, S., Lapworth, D.J., Marchant, B.P., Pedley, S., 2016. Are sanitation interventions a threat to drinking water supplies in rural India? An application of tryptophan-like fluorescence. Water Res. 88, 923–932. http://dx.doi.org/10.1016/j.watres.2015.11.006.

Stedmon, C.A., Bro, R., 2008. Characterizing dissolved organic matter fluorescence with parallel factor analysis: a tutorial. Limnol. Oceanogr. Methods 6, 572–579. http://dx.doi.org/10.4319/lom.2008.6.572.

Wasserman, A.E., 1965. Absorption and fluorescence of water-soluble pigments produced by four species of *Pseudomonas*. Appl. Microbiol. 13, 175–180.